

21008

NATIONAL LIBRARY  
OTTAWA



BIBLIOTHÈQUE NATIONALE  
OTTAWA

NAME OF AUTHOR... MICHAEL VICTOR FALK .....

TITLE OF THESIS... VIBRATIONAL SPECTRA OF  
SEVERAL ISOTOPIC FORMS OF ETHER-  
HYDROGEN CHLORIDE AND ETHYLENE SULPHIDE .....

UNIVERSITY... UNIVERSITY OF ALBERTA .....

DEGREE FOR WHICH THESIS WAS PRESENTED... P.H.D. ....

YEAR THIS DEGREE GRANTED... 1974 .....

Permission is hereby granted to THE NATIONAL LIBRARY  
OF CANADA to microfilm this thesis and to lend or sell copies  
of the film.

The author reserves other publication rights, and  
neither the thesis nor extensive extracts from it may be  
printed or otherwise reproduced without the author's  
written permission.

(Signed) ... *MV Falk* .....

PERMANENT ADDRESS:  
#402-11007-83 AVE  
EDMONTON, ALTA  
.....

DATED... Jan... 31..... 1974

THE UNIVERSITY OF ALBERTA

VIBRATIONAL SPECTRA OF SEVERAL ISOTOPIC FORMS OF  
DIMETHYL ETHER--HYDROGEN CHLORIDE AND ETHYLENE  
SULPHIDE

by

C

MICHAEL VICTOR FALK

A THESIS,

SUBMITTED TO THE FACULTY OF GRADUATE STUDIES AND RESEARCH  
IN PARTIAL FULFILMENT OF THE REQUIREMENTS FOR THE DEGREE

OF

DOCTOR OF PHILOSOPHY

DEPARTMENT OF CHEMISTRY

EDMONTON, ALBERTA

SPRING, 1974

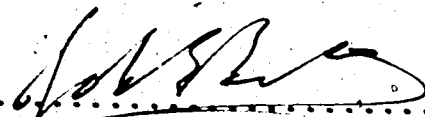
THE UNIVERSITY OF ALBERTA

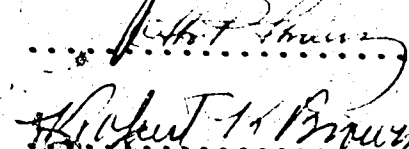
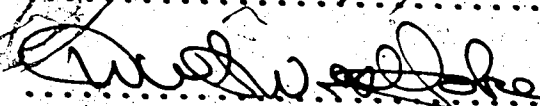
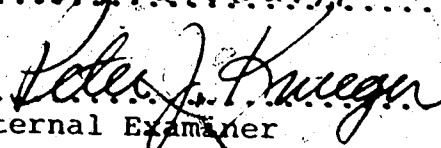
FACULTY OF GRADUATE STUDIES AND RESEARCH

The undersigned certify that they have read, and recommend to the Faculty of Graduate Studies and Research, for acceptance, a thesis entitled

"VIBRATIONAL SPECTRA OF SEVERAL ISOTOPIC FORMS OF DIMETHYL ETHER...HYDROGEN CHLORIDE AND ETHYLENE SULPHIDE"

submitted by MICHAEL VICTOR FALK in partial fulfilment of the requirements for the degree of Doctor of Philosophy.

  
.....  
Supervisor

  
.....  
  
.....  
B. J. Ratcliffe  
.....  
  
.....  
External Examiner

January 17, 1974  
.....

Date

## A B S T R A C T

Infrared spectra of the gaseous, hydrogen-bonded molecule formed from dimethyl ether and hydrogen chloride,  $(\text{CH}_3)_2\text{O} \cdots \text{HCl}$ , and its isotopic modifications  $(\text{CH}_3)_2\text{O} \cdots \text{DCl}$ ,  $(\text{CD}_3)_2\text{O} \cdots \text{HCl}$  and  $(\text{CD}_3)_2\text{O} \cdots \text{DCl}$ , have been studied in detail between 33 and  $4000 \text{ cm}^{-1}$ . The hydrogen bond stretching mode is assigned between 110 and  $120 \text{ cm}^{-1}$  for  $(\text{CH}_3)_2\text{O} \cdots \text{HCl}$ ,  $(\text{CH}_3)_2\text{O} \cdots \text{DCl}$  and  $(\text{CD}_3)_2\text{O} \cdots \text{HCl}$ . The two  $\text{O} \cdots \text{HCl}$  deformation modes yield a broad, complex absorption centered at  $470 \text{ cm}^{-1}$ . It is interpreted in terms of sum and difference transitions involving the  $\text{HCl}$  wagging modes, which are deduced to be at  $50 \text{ cm}^{-1}$ . The  $\text{O} \cdots \text{DCl}$  deformation modes yield a band centered at  $360 \text{ cm}^{-1}$ . Bands at  $790 \text{ cm}^{-1}$  and  $600 \text{ cm}^{-1}$  in the spectra of  $(\text{CH}_3)_2\text{O} \cdots \text{HCl}$  and  $(\text{CD}_3)_2\text{O} \cdots \text{DCl}$  are assigned to the overtones of the deformation modes. Many of the ethereal modes of  $(\text{CH}_3)_2\text{O} \cdots \text{HCl}$  and  $(\text{CD}_3)_2\text{O} \cdots \text{HCl}$  are assigned between 800 and  $1500 \text{ cm}^{-1}$ . The shape of the band assigned to the symmetric C-O stretching mode of  $(\text{CH}_3)_2\text{O} \cdots \text{HCl}$  does not resemble band shapes calculated for this absorption using two possible geometries of the molecule and does not, therefore, indicate which geometry is correct. The effect of sample temperature on the shape of the band due to the  $\text{HCl}$  stretching mode indicates that the fundamental transition is at  $2480 \text{ cm}^{-1}$ , not at  $2574 \text{ cm}^{-1}$  as previously postulated. The band due to the  $\text{DCl}$  stretching

mode of  $(\text{CH}_3)_2\text{O---DCl}$  has a different shape to that of  $(\text{CD}_3)_2\text{O---DCl}$ . The differences are attributed to combination transitions involving the ethereal modes. It is suggested that combination transitions involving the DCl or HCl stretching modes and the DCl or HCl wagging modes cause shoulders  $50\text{ cm}^{-1}$  away from the peak due to the DCl stretching mode and contribute to the general diffuseness of the band due to the HCl stretching mode. The relative intensities of all of the bands due to  $(\text{CH}_3)_2\text{O---HCl}$  are presented.

Infrared and Raman spectra of ethylene sulphide- $\text{h}_4$  and ethylene sulphide- $\text{d}_4$  and infrared spectra of cis and trans 1,2-dideuterioethylene sulphide have been recorded in this laboratory by D. A. Othen and are assigned in this work. Thirty-six frequencies from these spectra are assigned to fundamental vibrations and these frequencies are used in normal coordinate calculations. A force field containing sixteen force constants reproduces the thirty-six observed frequencies with an average error of 0.41%. The calculated frequencies allow many of the unassigned experimental frequencies to be assigned. The normal modes of each isotopic molecule are described in terms of the intramolecular displacements determined from the eigenvectors and potential energy distributions. Most of the methylenic modes of the dideuterated molecules cannot be described simply. The  $\text{A}_2$  methylenic rock is

calculated to be of a higher frequency than the  $A_2$  methylenic twist for both ethylene sulphide- $h_4$  and ethylene sulphide- $d_4$ .

## P R E F A C E

This thesis deals with the vibrational spectra of two unrelated molecular systems. In the first three chapters, the infrared spectra of several isotopic forms of the hydrogen-bonded molecule dimethyl ether---hydrogen chloride are presented and discussed. In Chapter 4, the normal vibrations of four isotopic forms of ethylene sulphide are analyzed.

## A C K N O W L E D G E M E N T S

I wish to express my deepest gratitude to Dr. J. E. Bertie for the privilege of working under his direction and for his guidance and encouragement during the course of this work.

I also wish to express my appreciation to the other members of this department with whom I have discussed parts of this work and to the members of the machine shop, glass shops and electronics shop who constructed and maintained much of the equipment used in this research.

I also wish to express thanks to Dr. O. P. Strausz and members of his research group for supplying and purifying the various isotopic forms of ethylene sulphide and to Dr. D. A. Othen for recording the spectra of these molecules.

Financial support by the National Research Council of Canada and the University of Alberta is gratefully acknowledged.



B L E O F C O N T E N T S

Page

CHAPTER 1

|   |    |
|---|----|
| INTRODUCTION . . . . .  | 1  |
| 1.1 General Introduction . . . . .                                  | 1  |
| 1.2 Hydrogen Bonding. . . . .                                       | 1  |
| 1.3 The Infrared Spectra of Hydrogen-Bonded Molecules . . . . .     | 5  |
| 1.4 Theories of Intensity Enhancement . . . . .                     | 14 |
| 1.5 Theories of Band Broadening . . . . .                           | 17 |
| 1.6 Infrared Spectra of Gaseous Hydrogen-Bonded Molecules . . . . . | 27 |
| 1.7 Aims of this Work . . . . .                                     | 32 |

CHAPTER 2

|   |    |
|---|----|
| EXPERIMENTAL TECHNIQUES . . . . .                       | 34 |
| 2.1 Preparation and Purification of Chemicals . . . . . | 34 |
| 2.2 Vacuum Lines and the Infrared Cell. . . . .         | 35 |
| 2.3 Infrared Spectrophotometers . . . . .               | 40 |

CHAPTER 3

|  |    |
|--|----|
| RESULTS AND DISCUSSION . . . . .                                     | 44 |
| 3.1 General . . . . .  | 44 |
| 3.2 Far Infrared Region . . . . .                                    | 46 |
| 3.3 Infrared Spectra Between 200 and 800 $\text{cm}^{-1}$ . . . . .  | 53 |
| 3.4 Infrared Spectra Between 800 and 1500 $\text{cm}^{-1}$ . . . . . | 71 |

|  | <u>Page</u> |
|--|-------------|
| 3.5 Infrared Spectra Above $1500\text{ cm}^{-1}$ . . . . . | 84          |
| 3.6 Relative Intensities of the Bands . . . . .            | 99          |
| 3.7 Summary . . . . .                                      | 102         |

CHAPTER 4

VIBRATIONAL ASSIGNMENT AND NORMAL COORDINATE  
CALCULATIONS FOR FOUR ISOTOPIC MODIFICATIONS  
OF ETHYLENE SULPHIDE . . . . . 103

|  |     |
|--|-----|
| 4.1 General Introduction . . . . .   | 103 |
| 4.2 Structure, Symmetry and Vibrational<br>Coordinates of Ethylene Sulphide . . . . .  | 104 |
| 4.3 Previous Studies of the Vibrations of<br>Ethylene Sulphide . . . . .   | 119 |
| 4.4 The Assignment of the Spectra of<br>$C_2H_4S$ , $C_2D_4S$ , <u>cis</u> - $C_2D_2H_2S$ and <u>trans</u> -<br>$C_2D_2H_2S$ . . . . . | 124 |
| 4.5 Computer Programs and the $G$ and $F$<br>Matrices . . . . .  | 140 |
| 4.6 Development of the Force Field . . . . .   | 144 |
| 4.7 Discussion . . . . .   | 156 |

REFERENCES . . . . . 169

APPENDIX I G MATRICES . . . . . 179

APPENDIX II EIGENVECTORS AND POTENTIAL ENERGY  
DISTRIBUTIONS . . . . . 183

APPENDIX III POTENTIAL ENERGY DISTRIBUTIONS AMONG  
THE DIAGONAL ELEMENTS OF THE  $F$   
MATRICES. . . . . 191

APPENDIX IV INFRARED SPECTRA OF GASEOUS  $C_2D_4S$ ,  
cis- $C_2D_2H_2S$  AND trans- $C_2D_2H_2S$  . . . . . 196

L I S T O F T A B L E S

| <u>Table</u> |  | <u>Page</u> |
|--------------|--|-------------|
| 1            | Frequencies and Assignments of Absorption Between 800 and 1500 $\text{cm}^{-1}$ by $(\text{CH}_3)_2\text{O}---\text{HCl}$ , $(\text{CD}_3)_2\text{O}---\text{HCl}$ and the Free Ethers | 77          |
| 2            | Frequencies and Relative Intensities of the Absorption Bands of $(\text{CH}_3)_2\text{O}---\text{HCl}$   | 100         |
| 3            | Molecular Parameters of Ethylene Sulphide  | 107         |
| 4            | Rotational Constants of Four Isotopic Forms of Ethylene Sulphide   | 108         |
| 5            | Internal Coordinates for Ethylene Sulphide   | 110         |
| 6            | Symmetry Coordinates for $\text{C}_2\text{H}_4\text{S}$ and $\text{C}_2\text{D}_4\text{S}$   | 112         |
| 7            | Symmetry Coordinates for <u>cis</u> - $\text{C}_2\text{D}_2\text{H}_2\text{S}$   | 114         |
| 8            | Symmetry Coordinates for <u>trans</u> - $\text{C}_2\text{D}_2\text{H}_2\text{S}$   | 116         |
| 9            | Previous Assignments of the Fundamental Frequencies of Liquid $\text{C}_2\text{H}_4\text{S}$   | 121         |
| 10           | Previous Assignments of the Fundamental Frequencies of Gaseous $\text{C}_2\text{H}_4\text{S}$  | 122         |
| 11           | Frequencies and Assignment of Features Observed in the Infrared and Raman Spectra of $\text{C}_2\text{H}_4\text{S}$  | 126         |
| 12           | Frequencies and Assignment of Features Observed in the Infrared and Raman Spectra of $\text{C}_2\text{D}_4\text{S}$  | 127         |

| <u>Table</u>   | <u>Page</u> |
|--|-------------|
| 13    Frequencies and Assignment of Features<br>Observed in the Infrared Spectrum of<br>Gaseous <u>cis</u> -C <sub>2</sub> D <sub>2</sub> H <sub>2</sub> S   | 128         |
| 14    Frequencies and Assignment of Features<br>Observed in the Infrared Spectrum of<br>Gaseous <u>trans</u> -C <sub>2</sub> D <sub>2</sub> H <sub>2</sub> S | 129         |
| 15    Various Force Fields of Ethylene Sulphide  | 145         |
| 16    Observed Frequencies and Those Calculated<br>from the Various Force Fields for C <sub>2</sub> H <sub>4</sub> S   | 146         |
| 17    Observed Frequencies and Those Calculated<br>from the Various Force Fields for C <sub>2</sub> D <sub>4</sub> S   | 148         |
| 18    Observed Frequencies and Those Calculated<br>from the Various Force Fields for <u>cis</u> -<br>C <sub>2</sub> D <sub>2</sub> H <sub>2</sub> S          | 151         |
| 19    Observed Frequencies and Those Calculated<br>from the Various Force Fields for <u>trans</u> -<br>C <sub>2</sub> D <sub>2</sub> H <sub>2</sub> S        | 152         |
| 20    The Assignment of the Fundamental<br>Frequencies of C <sub>2</sub> H <sub>4</sub> S  | 157         |
| 21    The Assignment of the Fundamental<br>Frequencies of C <sub>2</sub> D <sub>4</sub> S  | 158         |
| 22    The Assignment of the Fundamental<br>Frequencies of <u>cis</u> -C <sub>2</sub> D <sub>2</sub> H <sub>2</sub> S   | 160         |
| 23    The Assignment of the Fundamental<br>Frequencies of <u>trans</u> -C <sub>2</sub> D <sub>2</sub> H <sub>2</sub> S                                       | 162         |

| <u>Figure</u> | <u>L I S T   O F   F I G U R E S</u>   | <u>Page</u> |
|---------------|--|-------------|
| 1             | The Six Vibrational Modes of an A-H---B Molecule   | 7           |
| 2             | The Induced and A-H Dipoles of an A-H---B Molecule and Their Directions of Change During the $\nu_s$ and $\nu_b$ Vibrations                  | 16          |
| 3             | The Stepanov Energy Level Scheme for an (A-H---B) Molecule   | 21          |
| 4             | The Six Vibrational Modes of the O---HCl Part of $(\text{CH}_3)_2\text{O---HCl}$   | 29          |
| 5             | Stainless Steel Manifold for High Gas Pressures  | 37          |
| 6             | Cross-sectional View of the Infrared Gas Cell  | 39          |
| 7             | Absorption Between 90 and 140 $\text{cm}^{-1}$ by $(\text{CH}_3)_2\text{O---HCl}$ and the Free Components                                    | 47          |
| 8             | Absorption Between 90 and 140 $\text{cm}^{-1}$ by $(\text{CH}_3)_2\text{O---DCl}$ and the Free Components                                    | 50          |
| 9             | Absorption Between 90 and 140 $\text{cm}^{-1}$ by $(\text{CD}_3)_2\text{O---HCl}$ and the Free Components                                    | 51          |
| 10            | Absorption Between 200 and 600 $\text{cm}^{-1}$ by the Four Isotopic Forms of $(\text{CH}_3)_2\text{O---HCl}$ and the Free Ethers            | 54          |
| 11            | Absorption Between 700 and 875 $\text{cm}^{-1}$ by $(\text{CH}_3)_2\text{O---HCl}$ , $(\text{CH}_3)_2\text{O---DCl}$ and the Free Components | 63          |

| <u>Figure</u> |   | <u>Page</u> |
|---------------|---|-------------|
| 12            | Absorption Between 500 and 650 $\text{cm}^{-1}$ by<br>( $\text{CD}_3$ ) $_2\text{O}$ ---DCl and the Free Components                                   | 65          |
| 13            | Absorption Between 850 and 1525 $\text{cm}^{-1}$ by<br>the Ethereal Modes of ( $\text{CH}_3$ ) $_2\text{O}$ ---HCl and<br>the Free Ether              | 73          |
| 14            | Two Possible Geometries for ( $\text{CH}_3$ ) $_2\text{O}$ ---HCl   | 78          |
| 15            | Predicted Bandshapes for Absorption by<br>( $\text{CH}_3$ ) $_2\text{O}$ ---HCl   | 81          |
| 16            | Absorption Between 2300 and 2800 $\text{cm}^{-1}$ by<br>( $\text{CH}_3$ ) $_2\text{O}$ ---HCl at +35°C and -30°C                                      | 85          |
| 17            | Absorption Between 2300 and 2800 $\text{cm}^{-1}$ by<br>( $\text{CD}_3$ ) $_2\text{O}$ ---HCl at +35°C and -30°C                                      | 88          |
| 18            | The Stepanov Energy Level Scheme for<br>( $\text{CH}_3$ ) $_2\text{O}$ ---HCl   | 92          |
| 19            | Absorption Between 1500 and 2000 $\text{cm}^{-1}$ by<br>( $\text{CH}_3$ ) $_2\text{O}$ ---DCl at +30°C and -30°C                                      | 94          |
| 20            | Absorption Between 1500 and 2000 $\text{cm}^{-1}$ by<br>( $\text{CD}_3$ ) $_2\text{O}$ ---DCl at +30°C and -30°C                                      | 95          |
| 21            | The Structure of Ethylene Sulphide  | 105         |
| 22            | The Orientation of <u>cis</u> - $\text{C}_2\text{D}_2\text{H}_2\text{S}$ with Respect<br>to the Cartesian Axes and the Principal<br>Axes of Inertia   | 136         |
| 23            | The Orientation of <u>trans</u> - $\text{C}_2\text{D}_2\text{H}_2\text{S}$ with<br>Respect to the Cartesian Axes and the<br>Principal Axes of Inertia | 138         |

## CHAPTER 1

### I N T R O D U C T I O N

#### 1.1 General Introduction

The first three chapters of this thesis deal with the infrared spectra of the gas-phase, hydrogen-bonded molecules formed between dimethyl ether- $h_6$  and hydrogen chloride  $[(CH_3)_2O \cdots HCl]$ , dimethyl ether- $h_6$  and deuterium chloride  $[(CH_3)_2O \cdots DCl]$ , dimethyl ether- $d_6$  and hydrogen chloride,  $[(CD_3)_2O \cdots HCl]$ , and dimethyl ether- $d_6$  and deuterium chloride  $[(CD_3)_2O \cdots DCl]$ . In Section 1.2 a general discussion of the phenomenon of hydrogen bonding is presented. The normal modes of vibration of hydrogen-bonded molecules are defined and described in Section 1.3 and the current theories of intensity enhancement and broadening of the infrared absorption bands of these molecules are reviewed in Sections 1.4 and 1.5, respectively. The previous studies of the infrared spectra of the dimethyl ether-hydrogen chloride system and related hydrogen-bonded systems in the gas phase are reviewed in Section 1.6. The aims of the present study are presented in Section 1.7.

#### 1.2 Hydrogen Bonding

Since the concept of hydrogen bonding was first definitively introduced by Latimer and Rodebush (1) in 1920, thousands of articles have appeared in the literature to illustrate the broad occurrence of this,

phenomenon. In addition to its well known role in determining the properties and structures of many biologically important compounds, hydrogen bonding has been shown to be of great importance in most other fields of chemistry. Despite the vast number of studies of hydrogen-bonded systems, the theoretical understanding of hydrogen bonding is still only semi-quantitative in nature. Much of the knowledge of hydrogen-bonded systems has been reviewed in texts by Pimentel and McClellan (2), Vinogradov and Linnel (3) and Hamilton and Ibers (4). Also, the book by Hadzi and Thompson (5) and the review of the spectroscopic manifestations of hydrogen bonding by Murthy and Rao (6) are particularly useful in relation to the work presented in this thesis.

A hydrogen bond is said to exist when a hydrogen atom is bound simultaneously to two or more atoms (2). In this thesis the term 'hydrogen bond' refers to the weaker of the two bonds in the triatomic system  $A-H \cdots B$ , and is the  $H \cdots B$  bond. The energy of a hydrogen bond usually lies between 3 and 10 kcal/mole, with the average energy about 7 kcal/mole. These energies are intermediate between the energy of a normal covalent bond and those of the less specific van der Waals' interactions. The  $A-H$  bond in the  $A-H \cdots B$  system is considered to be a normal covalent bond, although somewhat weaker than it would be in the absence of hydrogen bonding.  $A-H$  is the proton



donor functional group and B is the proton acceptor atom or site of a molecule. Usually A is an electronegative atom such as O, N, F, S, Cl etc. and B is generally an atom or ion with one or more lone pairs of electrons, such as F, N, O, Cl, Cl<sup>-</sup> etc.

When a hydrogen bond is formed, it is found that, if A and B are atoms, the A---B and H---B distances are usually shorter than the sum of the van der Waals' radii (7) of the A and B atoms and the H and B atoms, respectively. In X-ray and neutron diffraction studies these observations are used as criteria for the presence of hydrogen bonding. The A---B distances found by these studies have been used in theoretical calculations of the energy of the hydrogen bond (8). However, a complete and rigorous quantum mechanical model which can predict this energy does not exist at present, since the approximations which must be used in the calculation limit the accuracy to the same order of magnitude as the energy itself. Qualitatively, it is believed (9) that the energy of the hydrogen bond arises principally from four distinct interactions. Firstly, electrostatic interactions, predominantly Coulombic in nature, arise from attraction between the positive charge on the H atom and the negative charge on B. Secondly, the approach of the A-H group towards B causes distortions in the negative charge distributions on A-H and B and leads to delocalization

effects in which part of the charge of B resides at A or H. Thirdly, the motion of the electrons in A-H and B gives rise to a dispersion interaction between a fluctuating dipole in A-H and the fluctuating dipole that it induces in B. Finally, a repulsive interaction results from the overlap of the electron charge clouds of the A, H and B atoms.

When A-H and B are portions of the same molecule, the interaction A-H---B is termed intramolecular hydrogen bonding. An example of this type of interaction is that which can occur in ortho-halophenols (10). Since intramolecular hydrogen bonds affect mainly the electronic structures on the proton donor and acceptor groups, the physical behaviour of systems with these types of hydrogen bonds is close to that of normal, non-hydrogen-bonded substances. When A-H and B are located in two separate molecules, the interaction is termed intermolecular hydrogen bonding. This thesis deals with intermolecular hydrogen bonding and specifically with that which occurs between the hydrogen atom of a hydrogen chloride molecule and one of the lone pairs of electrons on the oxygen atom of a dimethyl ether molecule. Since these types of hydrogen bonds change the number, mass, shape and electronic structure of the interacting molecules, studies of the physical properties of an intermolecular hydrogen-bonded system often yield information about

these interactions. Non-spectroscopic methods (11,12) include studies of melting and boiling points, dielectric constants and dipole moments, viscosity, vapour pressure and molar volumes. Unfortunately, changes in these physical properties can also occur as a result of less specific interactions and, therefore, non-spectroscopic studies cannot provide unambiguous proof of hydrogen bonding. Spectroscopic techniques, however, are capable of providing evidence relating the involvement of a specific hydrogen atom and specific acceptor group in the formation of a weak bond. The most widely used techniques are infrared and Raman spectroscopy (13,14), nuclear magnetic resonance (15), and X-ray and neutron diffraction (16). Perhaps the most spectacular spectroscopic manifestation of hydrogen bonding occurs in the vibrational spectra of hydrogen-bonded molecules and, as a result, infrared and Raman studies provide the most commonly used criteria for the presence of hydrogen bonding.

### 1.3 The Infrared Spectra of Hydrogen-Bonded Molecules

In general, two effects of hydrogen bonding are observed in the infrared spectrum of a hydrogen-bonded molecule: 1) the frequencies, shapes and intensities of absorption bands that are present in the spectrum of the hydrogen-bonded molecule and in the spectra of the non-

bonded proton donor and acceptor molecules are different in the two cases; 2) new bands appear in the spectrum of the hydrogen-bonded molecule as a result of the loss of rotational and translational degrees of freedom of the component molecules. It is particularly useful to consider the six vibrations which occur in the A-H---B part of a hydrogen-bonded molecule (13). Figure 1 displays these vibrations where B is treated as a point mass and the proton donor is considered to be a bent, triatomic molecule, R-A-H. Each vibrational mode is denoted by the appropriately subscripted letter  $\nu$  (13), and may be described as shown in Figure 1, where the plane is that formed by the two bonds to atom A.

Of these modes, the A-H stretching mode,  $\nu_s$ , has received most attention since it usually absorbs between 2500 and 3500  $\text{cm}^{-1}$ , a region which is easily accessible to study. As far back as 1932 Freymann (17) observed that in the spectra of alcohols there are two regions of absorption by the O-H stretching mode, one due to the monomer at about 3700  $\text{cm}^{-1}$  and one due to associated molecules at about 3400  $\text{cm}^{-1}$ . Since then it has been shown that the A-H stretching mode in a hydrogen-bonded molecule is always lower in frequency than the corresponding mode in the absence of hydrogen bonding. Murthy and Rao (6) give an extensive list of these frequency shifts for a large number of hydrogen-bonded molecules.

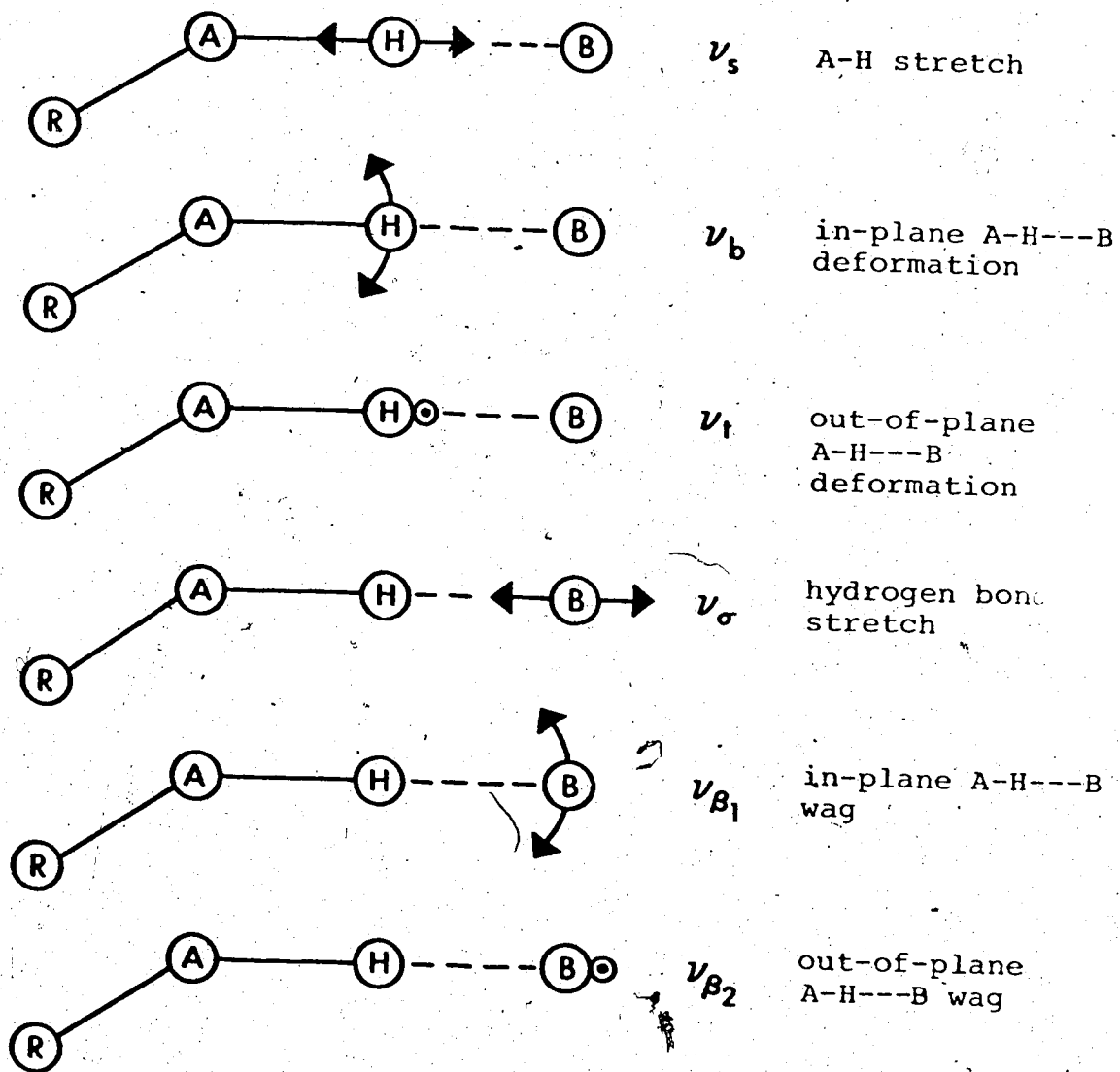


FIGURE 1. The six vibrational modes involving the A, H and B atoms of the non-linear, hydrogen-bonded molecule, R-A-H...B.

There are cases in which a decrease in the A-H stretching frequency,  $\Delta\nu_s$ , indicates the presence of a hydrogen bond, although the A---B distance is greater than the sum of the van der Waals' radii of the A and B atoms. For example, Holzbecher, Knop and Falk (18) have shown that the  $\nu_s$  absorption for the more weakly bound of the two hydroxyl groups in solid  $\text{Na}_2[\text{Fe}(\text{CN})_5\text{NO}]\cdot 2\text{H}_2\text{O}$  is about  $100\text{ cm}^{-1}$  below that expected for a non-hydrogen-bonded hydroxyl group, even though the nearest neighbour to the oxygen atom is a nitrogen atom  $3.63\text{ \AA}$  away. The sum of the van der Waals' radii for oxygen and nitrogen is  $2.9\text{ \AA}$  (7) and thus  $3.63\text{ \AA}$  is well outside the range predicted for the O---N distance when an O-H---N hydrogen bond is formed. Thus, the change in the A-H stretching frequency,  $\Delta\nu_s$ , clearly provides a very sensitive probe for detecting hydrogen bonding.

The decrease in frequency of the A-H stretching vibration when a hydrogen bond is formed must be brought about, at least in part, by a reduction of the A-H stretching force constant, caused by a redistribution of electron density of the A-H bond (19). Thus  $\Delta\nu_s$  must reflect many of the properties of the hydrogen bond. The most important correlation is the relationship between  $\Delta\nu_s$  and  $\Delta H$ , the energy of the hydrogen bond. Such a relationship was first proposed by Badger and Bauer in 1937 (20) and an approximate, linear relationship between  $\Delta\nu_s$  and  $\Delta H$  has been established by Drago et al (21,22) for molecules containing hydroxyl

groups. The negative slope of the straight line corresponds to a decrease in the O-H stretching frequency by about  $60 \text{ cm}^{-1}$  for each kcal/mole. Unfortunately, a simple relationship has not been established to cover all A-H---B systems, because the slope of the  $\Delta\nu_s$  vs  $\Delta H$  line depends upon the nature of the interacting molecules (13). Also, correlations between  $\Delta\nu_s$  and other properties of the hydrogen-bonded system, such as the A---B or H---B distance, or the base strength, depend largely upon the nature of the component molecules and only qualitative conclusions can usually be drawn from them (13).

In addition to decreasing the  $\nu_s$  frequency, the formation of a hydrogen bond also causes an extreme increase in the breadth of the bands associated with this mode. The intensity of the  $\nu_s$  fundamental absorption is also increased, usually by an order of magnitude (23), although the first overtone of  $\nu_s$  is usually less intense than in the absence of hydrogen bonding (24). These phenomena are unique to hydrogen-bonded systems and are observed for gases, liquids, solutions and solids. However, the increases in the breadth and intensity of the  $\nu_s$  absorption upon hydrogen bond formation are not well understood, and few correlations between these phenomena and properties of the hydrogen bond have been made. Because they are important in the interpretation of the spectrum of  $(\text{CH}_3)_2\text{O}---\text{HCl}$ , the theories of intensity enhancement and band-broadening in hydrogen-bonded systems

are reviewed in Sections 1.4 and 1.5, respectively.

In A-D---B systems  $\nu_s$  is found to absorb at a lower frequency than the corresponding mode in the non-associated deuterium donor molecule, and the ratio of the frequency  $\nu_s$  in A-H---B to that in A-D---B usually lies between 1.3 and 1.4. Although the intensity enhancement of the  $\nu_s$  fundamental absorption in A-D---B systems is usually as large as that in A-H---B systems, the increased breadth of the absorption is usually less pronounced for the deuterium bond (25).

The in-plane and out-of-plane A-H---B deformation modes,  $\nu_b$  and  $\nu_t$  respectively, are modes in which the hydrogen atom is displaced in directions perpendicular to the direction of the hydrogen bond. Unless the proton donating molecule is diatomic,  $\nu_b$  is present in the absence of hydrogen bonding as the in-plane R-A-H deformation mode. If the donor molecule contains more than three atoms,  $\nu_t$  is also present in the absence of hydrogen bonding as a torsional mode. When the proton donating molecule is diatomic, both  $\nu_b$  and  $\nu_t$  can be considered as new vibrational modes arising from the loss of two rotational degrees of freedom of the donor and acceptor molecules. This special case is discussed in Section 1.6 for the hydrogen halides hydrogen bonded to ethers and nitriles. In the most general case, when  $\nu_b$  and  $\nu_t$  are both present in the absence of hydrogen bonding, the hydro-



gen bond acts as a constraint to these vibrations and thus their force constants are increased, causing them to shift to higher frequencies. For example, it is known (26) that in unassociated alcohols  $\nu_b$  and  $\nu_t$  absorb between 1200 and 1300  $\text{cm}^{-1}$  and at about 225  $\text{cm}^{-1}$ , respectively, while in hydrogen-bonded alcohols they absorb between 1330 and 1410  $\text{cm}^{-1}$  and at about 650  $\text{cm}^{-1}$ , respectively. Usually, the infrared absorption bands due to  $\nu_b$  and  $\nu_t$  do not show any major intensity change when a hydrogen bond is formed but they do become somewhat broader (26,27).

Few successful correlations between the shifts in  $\nu_b$  or  $\nu_t$  with properties of the hydrogen bond have been made, although it has been shown that the absolute values of these shifts, as well as  $\Delta\nu_s$ , become larger as the strength of the hydrogen bond is increased (27,28). A major difficulty in correlating the shifts of  $\nu_b$  and  $\nu_t$  with properties of the hydrogen bond is that they often occur in the same spectral regions as many other transitions and cannot be definitively assigned, sometimes because they are coupled with some other vibrational mode. Since  $\nu_b$  and  $\nu_t$  are modes which involve the motion of the hydrogen atom to a large degree, they shift in frequency by a factor of about 0.7 when a deuterium atom is substituted for the hydrogen atom in A-H---B, and a study of the deuterium shift often leads to a definitive assignment. In cases where  $\nu_b$  and  $\nu_t$  mix with other modes,

however, a vibrational analysis is needed to assign them (29).

The last three modes shown in Figure 1 arise from the loss of three translational degrees of freedom of the interacting molecules. The  $\nu_{\sigma}$  mode involves motion of the interacting molecules against each other along the hydrogen bond and the  $\nu_{\beta_1}$  and  $\nu_{\beta_2}$  modes involve wagging motions of one molecule about the other, in directions perpendicular to the direction of the hydrogen bond. Because the hydrogen bond is very weak relative to normal covalent bonds, the force constants for  $\nu_{\sigma}$  and the  $\nu_{\beta}$  modes are very small and, thus, these modes absorb at low frequencies, usually below  $200 \text{ cm}^{-1}$ . This region also contains absorption by skeletal and torsional modes (30) which often complicate the assignment of  $\nu_{\sigma}$  and  $\nu_{\beta}$ . However, numerous studies have been made in which  $\nu_{\sigma}$  has been unequivocally assigned, usually in the region between  $100$  and  $200 \text{ cm}^{-1}$  (31). The few studies in which  $\nu_{\beta}$  modes have been successfully assigned indicate that these modes absorb weakly below  $100 \text{ cm}^{-1}$ . For example, Carlson, Witkowski and Fateley (32) assign a  $\nu_{\beta}$  mode at  $68 \text{ cm}^{-1}$  in formic acid dimer and at  $50 \text{ cm}^{-1}$  in acetic acid dimer.

Due to the lack of experimental data on the  $\nu_{\beta}$  modes no correlation has been made between their frequencies and properties of the hydrogen bond. However, it has been established that the frequency of the  $\nu_{\sigma}$  mode depends

upon the strength of the hydrogen bond in a similar manner to the magnitude of the shift of the A-H stretching frequency,  $\Delta\nu_s$ . For example, Brasch et al (33) have shown that in two different solid forms of phenol, the frequency of  $\nu_\sigma$  was higher in the form which had the larger  $\Delta\nu_s$  and, presumably, the stronger hydrogen bond.

No significant shift is observed in the frequency of  $\nu_\sigma$  or  $\nu_\beta$  when a deuterium atom is substituted for the hydrogen-bonded hydrogen atom (31). This arises from the fact that these modes involve the motion of whole molecules against each other and the substitution of one deuterium atom for a hydrogen atom causes little change in the vibrating masses.

In addition to the characteristic absorption by the six modes shown in Figure 1, the infrared spectra of hydrogen-bonded molecules show that the absorption by the other vibrational modes present in both the proton donor and acceptor molecules is influenced by the presence of the hydrogen bond. In particular, the frequencies of absorption of the modes involving the atoms participating directly in the hydrogen bond are shifted relative to their positions in the spectra of the non-associated molecules. This shift may be negative, as is found for the C=O stretching frequency of several carbonyl acceptor molecules (34), or positive, as is found for the skeletal vibrations of the pyridine-ethanol system (35). The

vibrational modes which do not involve atoms participating directly in the hydrogen bond show smaller shifts. No large changes in the intensities and widths of the bands due to these modes are generally observed when a hydrogen bond is formed.

#### 1.4 Theories of Intensity Enhancement

In general, the intensity of an infrared absorption band is proportional to the square of the dipole moment function,  $\mu$ , which can be expanded as a power series in the normal coordinates,  $Q_i$ , of the molecule (36):

$$\mu = \mu_0 + \sum_i \left( \frac{\partial \mu}{\partial Q_i} \right)_0 Q_i + \frac{1}{2} \sum_i \sum_j \left( \frac{\partial^2 \mu}{\partial Q_i \partial Q_j} \right)_0 Q_i Q_j + \dots \quad [1]$$

where  $\mu_0$  is the permanent dipole moment of the molecule. Only the first two terms on the right hand side of equation [1] are considered in the approximation of electrical harmonicity while the second and higher order derivatives are referred to as the electrical anharmonicity.

It has been stated (23) that the large increase in intensity of the  $\nu_s$  fundamental absorption and decrease in intensity of the first overtone arises from an increase in the absolute value of  $\partial \mu / \partial Q_s$  and a decrease in the absolute value of  $\partial^2 \mu / \partial Q_s^2$ , where  $Q_s$  is the normal coordinate of the  $\nu_s$  vibration. However the intensity of the overtone is also dependent upon the mechanical anharmonic-

icity (37) and this explanation can only be acceptable if the mechanical anharmonicity is small. Sandorfy et al (38, 39) have shown that, in a number of hydrogen-bonded alcohols, the mechanical anharmonicity is large and, therefore, should also contribute to the intensity of the overtone. Calculations (40) have shown that, if mechanical anharmonicity is taken into account, a large increase in  $\partial\mu/\partial Q_s$  is, by itself, sufficient to increase the intensity of the fundamental and to lower that of the overtone.

Huggins and Pimentel (41) have suggested that polarization of the lone pairs of electrons on the acceptor atom, B, accounts for the intensity increase of the  $\nu_s$  fundamental. Figure 2(a) shows that in an unperturbed A-H---B molecule, a dipole,  $\mu_i$ , is induced in the lone pairs of electrons on B by the highly polar A-H bond and that this induced dipole has the same direction as the A-H dipole,  $\mu_{AH}$ . During the  $\nu_s$  vibration, as shown in Figure 2(b),  $\mu_i$  vibrates in phase with  $\mu_{AH}$  and contributes an additional component to the overall change of dipole moment,  $\partial\mu/\partial Q_s$ . The lack of an intensity increase of the  $\nu_b$  (or  $\nu_t$ ) absorption upon formation of a hydrogen bond can also be explained using this model, since during the  $\nu_b$  vibration, as shown in Figure 2(c), the induced dipole vibrates exactly out-of-phase with the vibration of  $\mu_{AH}$ . Thus  $\partial\mu_i/\partial Q_b$  is opposite in sign to  $\partial\mu_{AH}/\partial Q_b$ , and  $\partial\mu/\partial Q_b$  is not in-

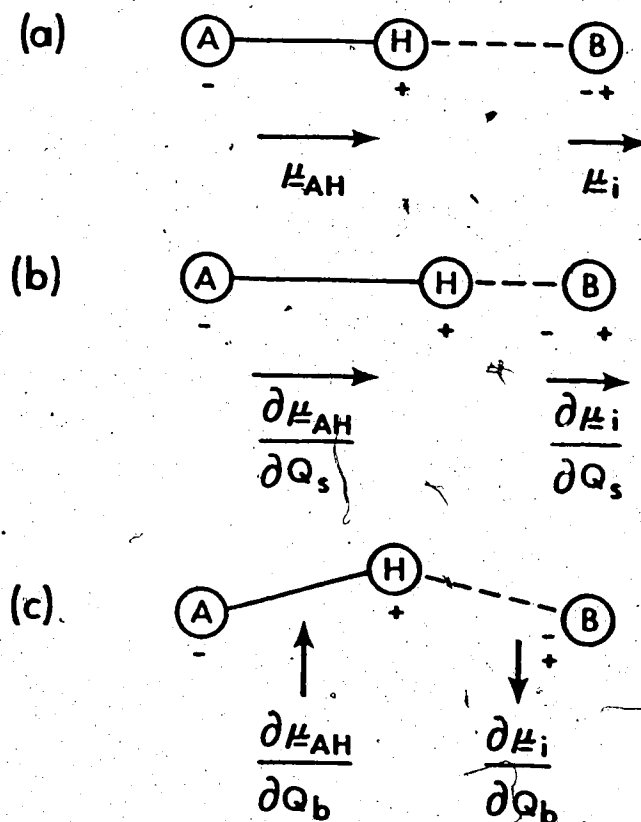


**FIGURE 2.** (a) The induced dipole,  $\mu_i$ , and the A-H dipole,  $\mu_{AH}$ , of an unperturbed A-H...B molecule. (b) Directions of the changes in dipole moments during the  $\nu_s$  vibration of an A-H...B molecule. (c) Directions of the changes in dipole moments during the  $\nu_b$  vibration of an A-H...B molecule.

creased. This is obviously an oversimplified picture but it does provide a useful model to qualitatively explain the intensity behaviours of the  $\nu_s$  and  $\nu_b$  modes.

### 1.5 Theories of Band Broadening

It is generally believed that at least one of the following two mechanisms plays a major role in determining the breadth of the  $\nu_s$  band of a hydrogen-bonded molecules.

[1] Interactions between  $\nu_s$  and the low frequency vibrations which involve the hydrogen bond,  $\nu_\sigma$  and  $\nu_\beta$ , give rise to a series of combination bands and hot bands (42), which distribute the intensity of  $\nu_s$  over a large frequency range.

[2] Overtone or summation bands of fundamentals other than  $\nu_s$  which are close in frequency to  $\nu_s$  are intensified through Fermi resonance (37) with  $\nu_s$ .

Neither of these mechanisms is dependent upon the physical state of the system but, while broad  $\nu_s$  absorptions are observed in the spectra of hydrogen-bonded molecules in all physical states, the bands are usually broader in the spectra of liquids and concentrated solutions (43). This additional broadening has been explained (43) by postulating the existence of a variety of hydrogen-bonded species,

each with a unique  $\nu_s$  frequency and corresponding absorption band which may be broadened through mechanisms 1 or 2.

Mechanisms 1 and 2 can only be operational if the potential energy surface for the hydrogen-bonded molecule is anharmonic in nature (44). The presence of anharmonicity is in itself a broadening mechanism, since it causes the frequency of a given vibrational mode,  $\nu_i$ , to be dependent on the degree of excitation of other vibrational modes,  $\nu_j$ ,  $\nu_k$ , etc. Consequently a band of frequencies results from each vibrational degree of freedom instead of the single, discrete frequency predicted for a harmonic oscillation (37). In addition, the presence of anharmonicity allows bands due to combinations of vibrations to appear in the spectrum. These bands are denoted by  $2\nu_i$  if they are due to the overtone of the  $\nu_i$  vibrational mode and by  $\nu_i + n\nu_j$  or  $\nu_i - n\nu_j$  if they are due to summation or difference transitions, respectively. A summation band,  $\nu_i + n\nu_j$ , arises from the simultaneous excitation of one quantum of the  $\nu_i$  vibrational mode and  $n$  quanta of the  $\nu_j$  vibrational mode. A difference band,  $\nu_i - n\nu_j$ , arises from the transition from a state in which  $n$  quanta of the  $\nu_j$  vibration have been excited, to a state which is one quantum of  $\nu_i$  above the ground state.

Mechanism 1 results from the anharmonic force field of a hydrogen-bonded molecule, which allows coupling between the A-H stretching mode,  $\nu_s$ , and the hydrogen bond stretching



mode,  $\nu_o$  (45). This coupling was described classically by the 'fluctuation' theory of Badger and Bauer (20), which is based on the observation that the A-H frequency decreases as the A---B distance,  $r_{AB}$ , decreases on hydrogen bond formation. The theory considers that the range of values of  $r_{AB}$ , which must exist due to the thermal vibrations of the relatively weak hydrogen bond, leads to a range of  $\nu_s$  frequencies. This should give rise to a broad absorption band for  $\nu_s$ , with the high frequency portion of the band arising from  $\nu_s$  vibrations occurring at larger-than-average values of  $r_{AB}$  and the low frequency portion of the band arising from  $\nu_s$  vibrations occurring at shorter-than-average  $r_{AB}$  values. For an isolated A-H---B system, however, the change in the  $r_{AB}$  distance occurs rhythmically with the frequency of the  $\nu_o$  vibration. In effect, the  $\nu_s$  vibration is frequency modulated by the  $\nu_o$  vibration and this idea allowed Batuev (46,47) to extend the fluctuation theory to become the frequency modulation theory, still framed in classical mechanics. Batuev showed that the broad band which results should consist of a series of sub-bands with frequencies  $\nu_s \pm n\nu_o$ , where  $n$  is integral. Since these bands must 'borrow' intensity from the fundamental  $\nu_s$  band, the total intensity is then spread out over a wide frequency range.

The quantum mechanical treatment of the anharmonic coupling between  $\nu_s$  and  $\nu_o$  also leads to the result that

transitions of the type  $\nu_S \pm n\nu_\sigma$ , where  $n$  is integral should be observed. In the absence of special conditions, the intensities of the transitions are expected to decrease in the order  $\nu_S$ ,  $\nu_S + \nu_\sigma$ ,  $\nu_S + 2\nu_\sigma$ ,  $\nu_S + 3\nu_\sigma$  . . . . ., and  $\nu_S + n\nu_\sigma$  is expected to be more intense than  $\nu_S - n\nu_\sigma$  by the Boltzmann factor,  $\exp(-nhc\nu_\sigma/kT)$ .

A quantum mechanical treatment of the interaction between  $\nu_S$  and  $\nu_\sigma$  was first discussed by Stepanov (48) and later modified by Sheppard (45). It is necessary to outline its main features in some detail, because it leads to the possibility that the normal intensity distribution presented above may not apply. Stepanov argued that, because  $\nu_\sigma$  is usually about ten times lower in frequency than  $\nu_S$ , separate potential energy curves can be drawn for  $\nu_\sigma$  in the  $V_S = 0$  and  $V_S = 1$  vibrational states. This separation is analogous to the separation of electronic and nuclear motion in the quantum mechanical treatment of molecules (49). The energy levels of  $\nu_\sigma$  can then be drawn on these curves for each state of  $V_S$ , as shown in Figure 3 for an A-H---B molecule. At large A---B distances, no hydrogen bond is present and the curves are separated by the vibrational energy of the non-hydrogen-bonded A-H stretching mode,  $\nu_{AH}(\text{free})$ . The separation of the curves close to their minima is approximately equal to the vibrational energy of  $\nu_S$  in the hydrogen-bonded molecule. Thus the curve for the  $V_S = 1$  state has a deeper minimum than that

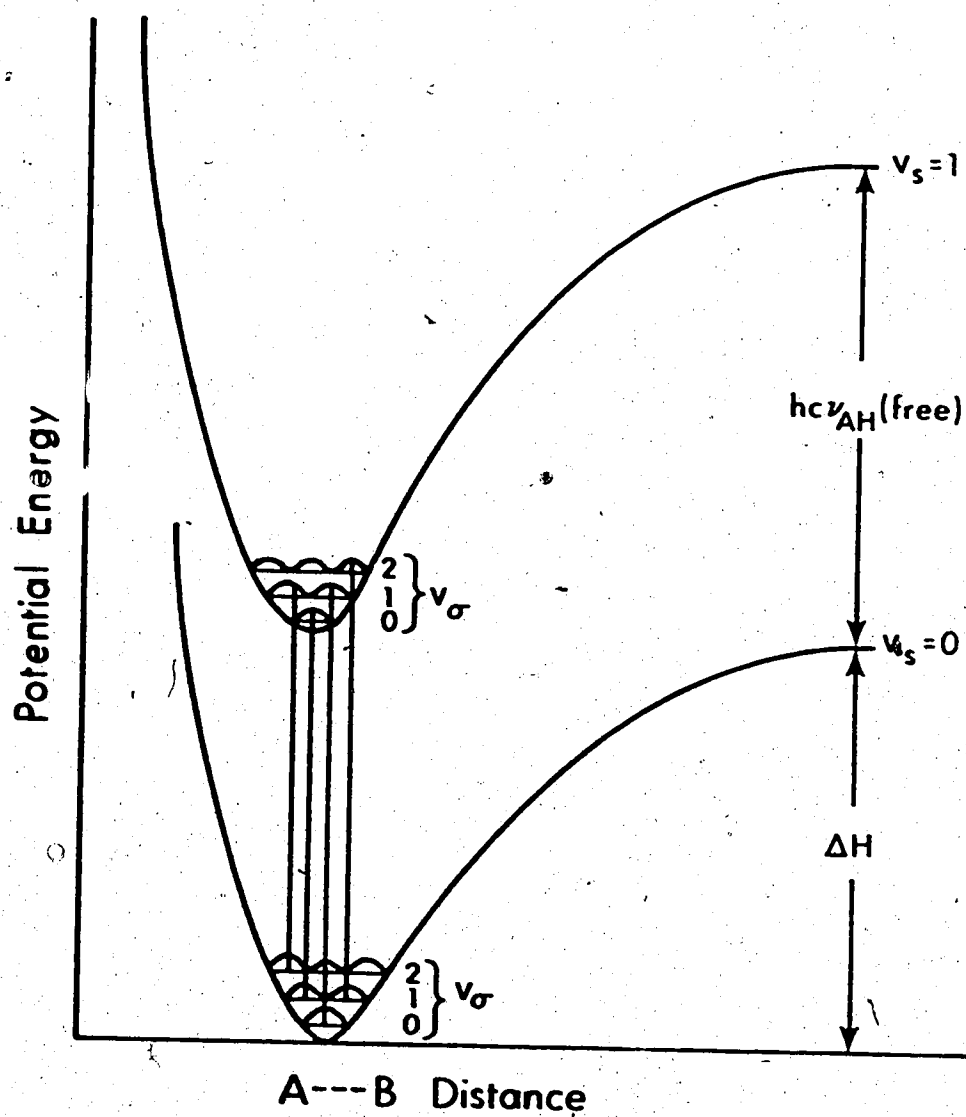


**FIGURE 3.** The Stepanov energy level scheme for the interaction of  $\nu_s$  and  $\nu_\sigma$  vibrations in the hydrogen-bonded molecule, A-H...B.  $\nu_s$  and  $\nu_\sigma$  are the quantum numbers for the A-H and H...B stretching vibrations, respectively, and the curves drawn on the energy levels are the squares of the wavefunctions.

for the  $V_s = 0$  state. Sheppard (45) has argued that since the hydrogen atom moves on the average closer to the center of the bond when  $V_s = 1$ , the hydrogen bond is stronger when  $V_s = 1$  than when  $V_s = 0$  and the potential energy minimum occurs at a shorter A---B distance when  $V_s = 1$ , as shown in Figure 3. Because the A---B motion during the  $\nu_\sigma$  vibration is, classically, so much slower than the A-H motion during  $\nu_s$ , Stepanov argued that the transitions from  $V_s = 0$  to  $V_s = 1$  occur at constant A---B distance and, therefore, the more probable transitions occur at A---B distances which are more probably occupied in the various  $\nu_\sigma$  levels. The probability of occupancy of each  $\nu_\sigma$  level, that is the square of the wave function (50), is sketched in Figure 3 and the most probable transitions are believed to originate and terminate at the maxima in these probability curves. This effect may be referred to as the vibrational Franck-Condon (51) effect, and it manifests itself in the case depicted in Figure 3 by allowing the summation band,  $\nu_s + \nu_\sigma$  [ $V_s = 0 \rightarrow 1$ ,  $V_\sigma = 0 \rightarrow 1$ ], to be more intense than the fundamental band,  $\nu_s$  [ $V_s = 0 \rightarrow 1$ ,  $V_\sigma = 0 \rightarrow 0$ ]. These arguments, therefore, predict that combination bands of the type  $\nu_s \pm n\nu_\sigma$  may appear in the spectrum with an unusual intensity distribution. They also predict that hot bands, from transitions of the type  $\nu_s + n\nu_\sigma - n\nu_\sigma$ ,  $\nu_s + (n+1)\nu_\sigma - n\nu_\sigma$  or  $\nu_s + n\nu_\sigma - (n+1)\nu_\sigma$  (42), may appear in the spectrum with unusually high intensities. Due to the

mechanical anharmonicity, these hot transitions can absorb at frequencies significantly different from those of their corresponding ground state transitions and, thus, they can contribute to the general background of the  $\nu_s$  band and, in some cases, lead to a diffuse band structure. However, hot transitions can contribute to a large degree only if the temperature is high enough to produce a large population in the excited  $V_\sigma$  states when  $V_s = 0$ , and at very low temperatures the band should be resolved into features separated by about the frequency of  $\nu_\sigma$ .

Perhaps the best proof to date that combination bands involving  $\nu_s$  and  $\nu_\sigma$  and other low-lying vibrational modes, along with the hot bands associated with these transitions, can be responsible for the broad, diffuse band seen for some hydrogen-bonded systems is given by the studies by Evans and Lo (52, 53) of the dibromide ion,  $\text{BrHBr}^-$ . This ion has two stretching modes, a symmetric mode which is analogous to  $\nu_\sigma$ , and an asymmetric mode which is analogous to  $\nu_s$ . An extremely broad, diffuse band between 500 and  $1300 \text{ cm}^{-1}$  in the spectra of  $\text{BrHBr}^-$  at temperatures greater than  $100^\circ\text{K}$  has been assigned to the asymmetric stretch. In spectra of  $\text{BrHBr}^-$  at about  $20^\circ\text{K}$  this band is resolved into well defined peaks which may be identified as bands of the type  $\nu_s + n\nu_\sigma$ , as well as sum bands involving  $\nu_s$  and a lattice mode. The difference bands were not present

in the spectra of  $\text{BrHBr}^-$  at  $20^\circ\text{K}$  but were evident in spectra of  $\text{BrHBr}^-$  at  $100^\circ\text{K}$ .

The importance of interactions between  $\nu_s$  and the hydrogen-bond wagging modes,  $\nu_\beta$ , has been pointed out by Thomas and coworkers (54,55), who have provided convincing evidence that hot bands of the hydrogen halide stretching vibration in  $\text{CH}_3\text{CN}---\text{HCl}$  and  $\text{CH}_3\text{CN}---\text{HF}$  from excited states of  $\nu_\beta$  contribute significantly to the breadth of the observed band.

Mechanism 2 is the only other mechanism of band broadening which has received widespread attention. In a polyatomic molecule, if two vibrational levels belonging to two different vibrations or combinations of vibrations are nearly degenerate and are of the same symmetry, a perturbation of these levels can result from a resonance interaction (37). Thus, the two energy levels are split, causing the frequency of one vibration to be higher than expected and the frequency of the other to be lower than expected. In addition, the intensities of the bands due to transitions to these energy levels are mixed. Thus the intensity of an overtone or combination band, which is usually much weaker than that of a fundamental band, can appear to be much greater than expected. In other words, it is possible for the weaker band to borrow intensity from the stronger one. This has the effect of distributing the intensity of the stronger band over a larger frequency range than in

the absence of an interaction. In the cases where the interaction occurs through anharmonic terms in the potential energy function, as must be the case if a combination level interacts with a fundamental level, this effect is known as Fermi resonance, and is well documented (37) in the spectra of non-hydrogen-bonded molecules. Bratož, Hadži and Sheppard (56) pointed out that interactions between  $\nu_s$  and overtone or combination transitions which absorb close to  $\nu_s$  could account for the broad  $\nu_s$  band in the spectra of hydrogen-bonded molecules. In particular, these authors were able to assign much of the complicated structure on the broad  $\nu_s$  band observed in many carboxylic acid dimers (56) to summation transitions which involve vibrations of the COOH groups, and which are enhanced in intensity by Fermi resonance with the O-H stretching vibration. In addition, Haurie and Novak (57) have shown that many of the features on the  $\nu_s$  band of acetic acid dimer can be assigned to summation transitions which involve vibrations in the aliphatic part of the acid and which are enhanced in intensity by Fermi resonance with  $\nu_s$ . Clearly, thus, if the hydrogen-bonded molecule is large and many combination transitions have frequencies which are close to  $\nu_s$ , this mechanism of band broadening can be very important. It is also clear that, since the enhancement of intensity of overtone or combination bands occurs to a greater degree as the frequency difference between these bands and  $\nu_s$

becomes smaller, these bands can be intensified over a larger range of frequencies if  $\nu_s$  is not a single band but is instead a progression of bands of the type  $\nu_s \pm n\nu_\sigma$ . Thus mechanism 2 becomes a more powerful broadening mechanism when considered in conjunction with mechanism 1.

Witkowski (58) and Marechal et al (59-62) have had significant success in attempting to account for the complex spectra (56) of the carboxylic acid dimers without invoking Fermi resonance. While details of their theory are not completely clear, they consider the anharmonic coupling between  $\nu_s$  and  $\nu_\sigma$  and the interaction between the two hydrogen bonds in the molecule. Because of the interaction between the two hydrogen bonds in each dimer, the transitions that they calculate cannot be all clearly related to those in a simple sum and difference band series of the type  $\nu_s \pm n\nu_\sigma$ , although all of their transitions are of this type. The only system that they treat that does not contain the complications of two interacting hydrogen bonds is that of the N-H---N bond in solid imidazole (59). In this case their calculated transitions are simply those expected from the most elementary considerations of sum and difference bands of the type  $\nu_s \pm n\nu_\sigma$ , that is, an equi-spaced series of bands with relative intensities in the order  $\nu_s > \nu_s + \nu_\sigma > \nu_s + 2\nu_\sigma > \nu_s + 3\nu_\sigma$ , and  $\nu_s + n\nu_\sigma$  being more intense than  $\nu_s - n\nu_\sigma$  by the Boltzmann factor for the level  $n\nu_\sigma$ . Thus the details



of their apparent success in explaining the spectra of the carboxylic acid dimers are obscure at present.

### 1.6 Infrared Spectra of Gaseous Hydrogen-Bonded Molecules

In order to develop the vibrational theory of hydrogen-bonded molecules, more vibrational data on isolated A-H---B systems are highly desirable. These data are best obtained through infrared studies of gaseous systems containing one hydrogen bond per molecule. Unfortunately, the number of systems which can be successfully studied in the gas phase is limited since a significant partial pressure of the hydrogen-bonded molecule is needed to obtain a good spectrum. The formation of a hydrogen-bonded molecule is controlled by the equilibrium



and relatively few systems have sufficiently large equilibrium constants to produce enough of the hydrogen-bonded molecule. The carboxylic acids are perhaps the easiest to study in the gas phase since, even at room temperature, the majority of the molecules exist as hydrogen-bonded dimers (63). Unfortunately, each dimer has a cyclic structure containing two hydrogen bonds and infrared studies of these acids do not yield direct information about isolated hydrogen bonds. The most extensively

studied gaseous molecules which contain one hydrogen bond are those formed between alcohols and amines (64-68), ethers and inorganic acids (25,68-79), and between cyanides and hydrogen halides (54,55,80,81). Of particular interest are studies of hydrogen-bonded molecules in which the proton donors are hydrogen halides (25,54,55,72-81). Since the proton donors are diatomic in these molecules, the forms of the vibrations involving the hydrogen bond, shown in Figure 4 for  $(\text{CH}_3)_2\text{O}---\text{HCl}$ , are slightly different from those presented earlier in Section 1.3. In particular, the  $\nu_b$  and  $\nu_t$  modes in  $(\text{CH}_3)_2\text{O}---\text{HCl}$  would correspond to pure rotations of the hydrogen chloride molecule in the absence of a hydrogen bond. Also, the  $\nu_\beta$  modes in  $(\text{CH}_3)_2\text{O}---\text{HCl}$  are represented as wagging motion of the hydrogen chloride molecule in directions perpendicular to the direction of the hydrogen bond.

Arnold, Bertie and Millen (72) first reported that the infrared spectra of mixtures of gaseous hydrogen halides with aliphatic ethers contained the broad association band which is characteristic of hydrogen-bonded molecules. In particular, the spectra of mixtures of hydrogen chloride with various ethers (73) each revealed an intense band which was about  $400\text{ cm}^{-1}$  wide and had its absorption maximum at about  $2570\text{ cm}^{-1}$ . The absorption maximum was assigned to  $\nu_s$ , the HCl stretching mode in  $\text{R}_2\text{O}---\text{HCl}$ , and two shoulders which were displaced by about  $100\text{ cm}^{-1}$  to either

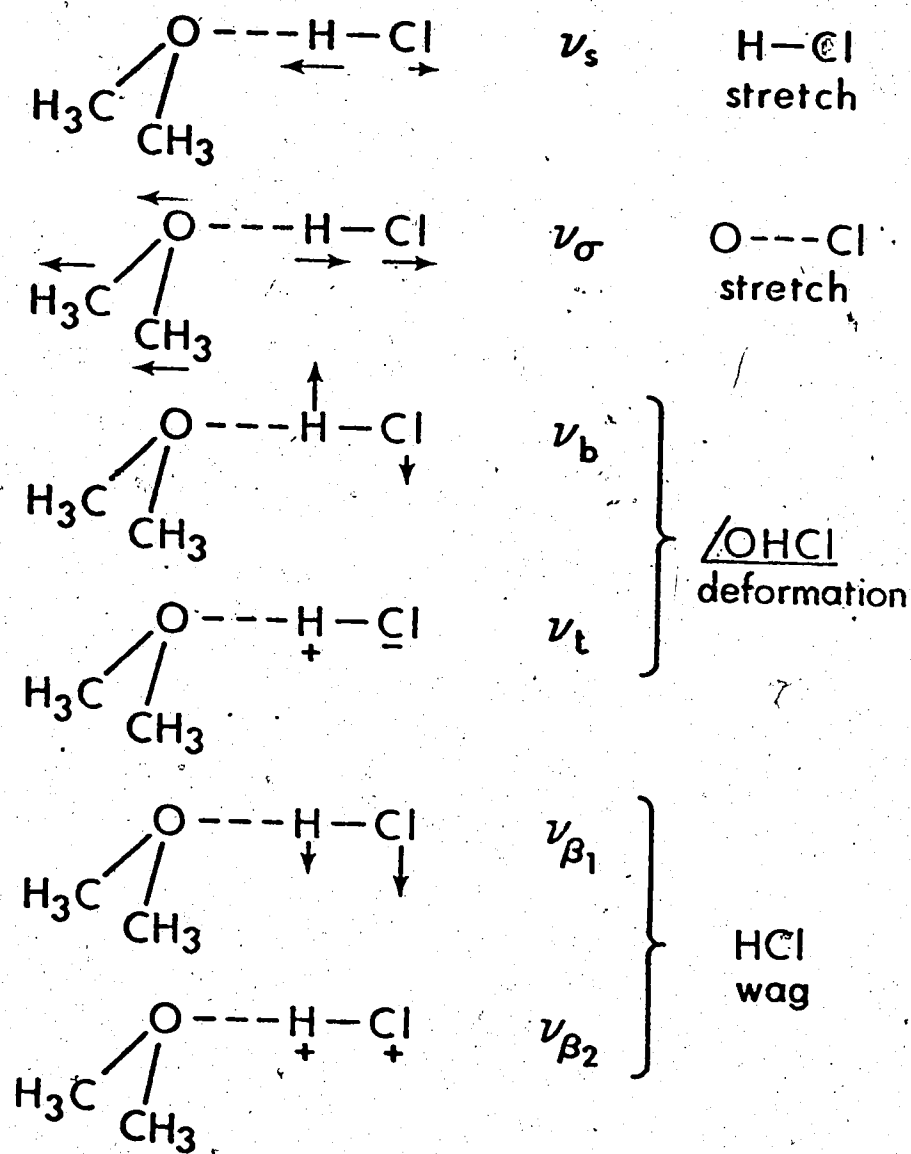


FIGURE 4. The six vibrational modes involving the O---HCl part of the hydrogen-bonded molecule,  $(\text{CH}_3)_2\text{O}\cdots\text{HCl}$ .

side of the maximum were assigned to the sum and difference bands  $\nu_s \pm \nu_\sigma$ . Broad bands observed in the spectra of  $(\text{CH}_3)_2\text{O}---\text{DCl}$  (25) and  $(\text{CH}_3)_2\text{O}---\text{HF}$  (77) were also interpreted in this manner. From these assignments the frequency of  $\nu_\sigma$  was predicted to be about  $100 \text{ cm}^{-1}$  in  $(\text{CH}_3)_2\text{O}---\text{HCl}$  and  $(\text{CH}_3)_2\text{O}---\text{DCl}$  and about  $170 \text{ cm}^{-1}$  in  $(\text{CH}_3)_2\text{O}---\text{HF}$ . These frequencies are reasonably close to the observed values of  $117 \text{ cm}^{-1}$  (75) for  $\nu_\sigma$  in  $(\text{CH}_3)_2\text{O}---\text{HCl}$  and  $180 \text{ cm}^{-1}$  (79) for  $\nu_\sigma$  in  $(\text{CH}_3)_2\text{O}---\text{HF}$ . The  $\nu_b$  and  $\nu_t$  modes have been reported (78) to lie at  $755$  and  $665 \text{ cm}^{-1}$  in  $(\text{CH}_3)_2\text{O}---\text{HF}$  and at  $550$  and  $490 \text{ cm}^{-1}$  in  $(\text{CH}_3)_2\text{O}---\text{DF}$ , although it is not known which mode has the higher frequency. These modes have not been observed in the spectra of gaseous  $(\text{CH}_3)_2\text{O}---\text{HCl}$  and  $(\text{CH}_3)_2\text{O}---\text{DCl}$ .

At room temperature the equilibrium constant for formation of gaseous  $(\text{CH}_3)_2\text{O}---\text{HCl}$  is small (82-84) and therefore a large proportion of the component molecules is not hydrogen bonded. However, since the heat of formation of  $(\text{CH}_3)_2\text{O}---\text{HCl}$  from its component molecules is negative, having been reported to lie between  $-5.6$  and  $-7.6 \text{ kcal/mole}$  (75,82-84), a decrease in temperature of the system causes the equilibrium constant to become larger. Thus, by recording spectra of gaseous mixtures of dimethyl ether- $\text{h}_6$  with large excesses of hydrogen chloride at low temperatures, Le Calvé, Grange and Lascombe (76) were able to observe the bands due to the

ethereal modes in  $(\text{CH}_3)_2\text{O}^{\text{---}}\text{HCl}$  between 800 and  $1300\text{ cm}^{-1}$ . Shchepkin and Belozerskaya (74) have suggested that a band shape analysis of the band due to the symmetric C-O stretching mode in  $(\text{CH}_3)_2\text{O}^{\text{---}}\text{HCl}$  leads to the conclusion that this molecule has  $C_s$  symmetry (Section 3.4).

Studies of dimethyl ether and hydrogen chloride mixtures have also been made for the liquid (85) and solid (86,87) phases. It seems clear that a variety of hydrogen-bonded species in which the oxygen atom is protonated can exist in these phases in addition to the  $(\text{CH}_3)_2\text{O}^{\text{---}}\text{HCl}$  molecule. There is, however, no evidence that any species other than  $(\text{CH}_3)_2\text{O}^{\text{---}}\text{HCl}$  is formed in the gas phase.

The hydrogen-bonded molecules formed between the cyanides and hydrogen fluoride (55,80,81) or hydrogen chloride (54) give rise to  $\nu_s$  bands which exhibit fine structures separated by about 2 or  $3\text{ cm}^{-1}$  (54,55) which is in sharp contrast to the broad, diffuse bands usually observed for the  $\nu_s$  vibration in other hydrogen-bonded molecules. Thomas et al (54,55) have interpreted this fine structure as due to hot transitions of the  $\nu_s$  vibration arising from excited  $\nu_g$  states. Similar fine structure was observed (55,81) on the band at  $585\text{ cm}^{-1}$  due to the degenerate F-H---N deformation modes,  $\nu_b = \nu_t$ , in acetonitrile-hydrogen fluoride. Thomas (55) interpreted this fine structure as due to hot transitions of these modes arising from excited  $\nu_g$  levels, but Huang and Couzi

(81) have assigned it to the normal fine structure of a perpendicular band of a symmetric top (88).

In his treatment of the anharmonic interaction between the A-H and hydrogen bond stretching modes,  $\nu_s$  and  $\nu_\sigma$ , Stepanov pointed out that the energy absorbed during the excitation of  $\nu_s$  often exceeds the dissociation energy of the hydrogen-bonded molecule. If the excitation energy is transferred to the  $\nu_\sigma$  mode, it could cause the molecule to predissociate\* (89) and this could cause the absorption bands due to the excitation of  $\nu_s$  to be broad. The fine structure separated by 2 or 3  $\text{cm}^{-1}$  on the  $\nu_s$  bands in acetonitrile---hydrogen chloride and acetonitrile---hydrogen fluoride (54,55) proves that these molecules must have lifetimes greater than about  $10^{-11}$  seconds and that broadening by predissociation cannot be of importance in these systems. The shift of  $\nu_s$  on formation of the hydrogen bond in  $\text{CH}_3\text{CN}---\text{HCl}$  (54) is smaller than that when  $(\text{CH}_3)_2\text{O}---\text{HCl}$  (73) is formed, and this suggests (13) that the hydrogen bond in  $(\text{CH}_3)_2\text{O}---\text{HCl}$  is the stronger of the two. It is, therefore, very improbable that predissociation causes significant broadening of the band due to  $\nu_s$  in  $(\text{CH}_3)_2\text{O}---\text{HCl}$ .

### 1.7 Aims of this Work

The initial aim of this work was to obtain the infrared spectra of the gaseous, hydrogen-bonded molecules

$(\text{CH}_3)_2\text{O}---\text{HCl}$ ,  $(\text{CD}_3)_2\text{O}---\text{HCl}$ ,  $(\text{CH}_3)_2\text{O}---\text{DCl}$  and  $(\text{CD}_3)_2\text{O}---\text{DCl}$  in as much detail as possible, and, in particular, to locate the  $\nu_b$ ,  $\nu_t$  and  $\nu_\beta$  modes (Figure 4). A second aim was to study the temperature dependence of the shape of the  $\nu_s$  bands in the spectra of these four molecules to test the proposed influence of difference bands (25,73). Further aims were to confirm the isotope shift of the  $117\text{ cm}^{-1}$  band reported by Belozerskaya and Shchepkin (75) and to extend the work of LeCalvé et al (76) to determine the shapes of the remaining bands due to modes of the ethereal part of  $(\text{CH}_3)_2\text{O}---\text{HCl}$ .

## CHAPTER 2

### EXPERIMENTAL TECHNIQUES

#### 2.1 Preparation and Purification of Chemicals

The dimethyl ether- $\text{h}_6$  was obtained from Matheson, the dimethyl ether- $\text{d}_6$  and deuterium chloride from Merck, Sharpe and Dohme and the argon from Linde. Each gas except argon was dried by repeated distillations from a methanol-dry ice bath until no water absorption could be detected in the infrared spectrum of about one-half an atmosphere of the gas. The argon was boiled from a cold trap at well below  $-100^\circ\text{C}$  and no further purification was found necessary. The deuterium chloride always contained at least 10% hydrogen chloride in spite of repeatedly flushing the vacuum lines and the cell with the deuterated acid prior to use. Both the deuterium chloride and the commercially available hydrogen chloride contained traces of carbon dioxide which could not be readily removed. Its presence was unimportant in the deuterium chloride but its infrared spectrum interfered with a region of interest in the spectra of hydrogen chloride-ether mixtures. For this reason, hydrogen chloride free from carbon dioxide was prepared in vacuo by the hydrolysis of phosphorous pentachloride to phosphoric acid and gaseous hydrogen chloride (90). The reaction vessel was a one litre triple-neck flask fitted with a 250 ml. vented dropping funnel in one neck



and connected to a conventional glass vacuum rack. The dropping funnel was modified by the inclusion of a stopcock on the venting tube. Distilled water was first introduced into the dropping funnel and degassed by direct pumping through the venting tube until freezing occurred. The ice was then allowed to melt and the water was degassed again. The evacuated funnel was then isolated from the apparatus while the phosphorous pentachloride was put into the reaction vessel and degassed by direct pumping for several hours. The pump was then isolated from the apparatus and water was added drop-by-drop to the phosphorous pentachloride. The wet hydrogen chloride distilled in vacuum to a flask cooled with liquid nitrogen. The hydrogen chloride was then dried by repeated distillations from a methanol-dry ice bath.

## 2.2 Vacuum Lines and the Infrared Cell

When the total gas pressure required did not exceed one atmosphere, the infrared cell was connected to the manifold of a conventional glass vacuum rack. Gas pressures were measured to  $\pm 1$  Torr with the cell at room temperature using a mercury-filled U-tube manometer. When spectra of mixtures of gases were required, the cell was first filled to the desired pressure of one component and then isolated from the manifold. The manifold was evacuated to a pressure of at least  $10^{-2}$  Torr and the second

component was then introduced into the manifold at a pressure slightly above the desired total pressure. The cell valve was then quickly opened and closed repeatedly, allowing the two gases to mix within the cell but minimizing diffusion out of the cell, until the pressure in the manifold stopped decreasing. The final pressure minus the pressure of the first component was assumed to give the pressure of the second component.

When the total gas pressure did exceed one atmosphere, the gases were handled in the  $7\frac{1}{2}$  inch long, 1 inch i.d. and  $1\frac{1}{2}$  inch o.d. stainless steel manifold shown in Figure 5. Matheson type 32R stainless steel gas valves were screwed into  $5/16$  inch threaded sockets in the manifold and served to isolate the various parts of the system. To ensure a vacuum-tight system, the valve threads were taped with Teflon and each valve was screwed tightly against a lead washer between the manifold and the valve. The standard Teflon O-rings usually used in the valves were replaced by lightly greased  $1/4$ " x  $3/8$ " Buna N rubber O-rings. The manifold was connected to a glass vacuum rack by a rubber vacuum hose and to the infrared cell by a  $1/4$  inch Mason-Renshaw Industries 'compress-o-coupling' O-ring connector welded to a gas valve. Two stainless steel test tubes welded to the gas valves served as 'cold fingers'. Pressures of greater than one atmosphere in the manifold were measured by a Marsh Mastergauge type

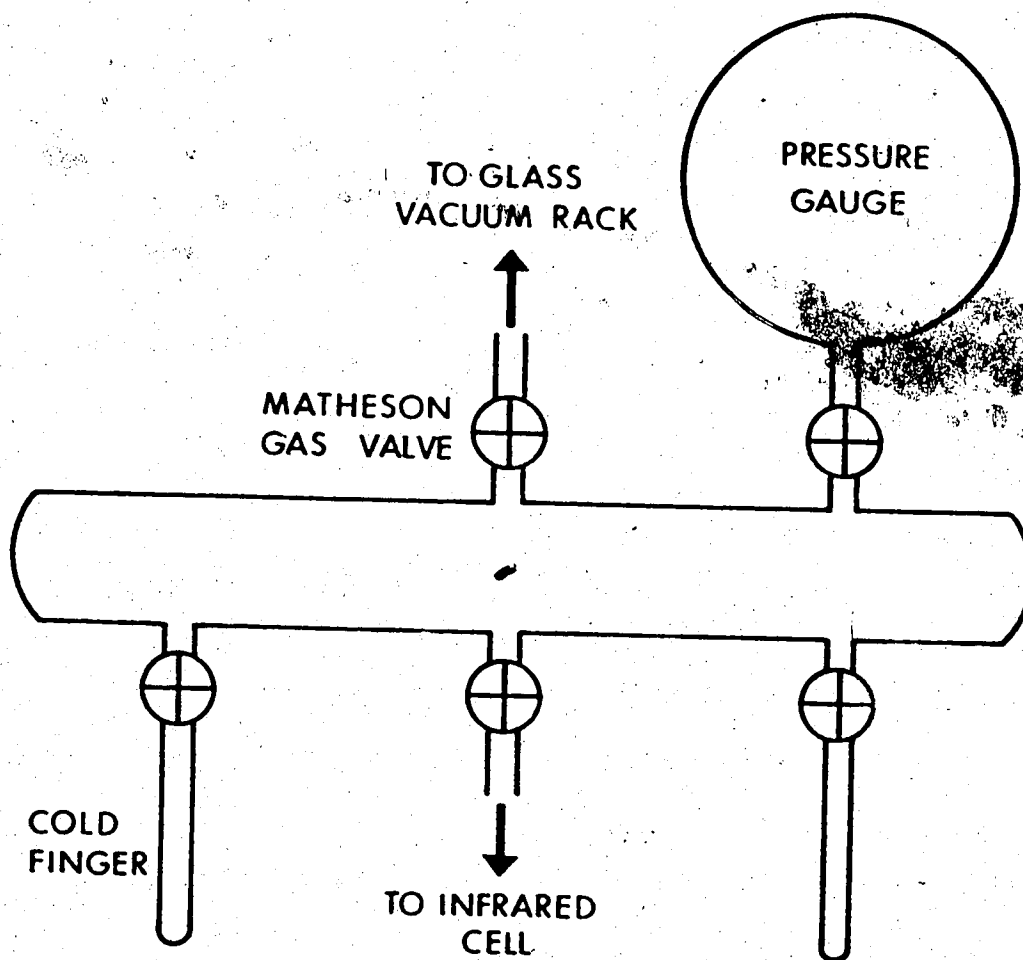


FIGURE 5. Stainless steel manifold used to handle gases at pressures exceeding one atmosphere (not drawn to scale).

100 M compound gauge, capable of measuring pressures up to 100 PSIG (5870 Torr) with an accuracy of  $\pm 0.5$  PSIG (26 Torr). Pressures of less than one atmosphere in the metal manifold and cell were measured by the U-tube manometer in the glass vacuum system. All pressures were measured with the cell at room temperature. To achieve pressures of greater than one atmosphere, the gas of interest was first condensed into one of the two cold fingers of the stainless steel manifold. The manifold was then isolated from the glass system and the condensate allowed to warm up until the vapour pressure reached the desired level. Mixtures of gases were prepared in a manner analogous to that used when the total pressure of gas did not exceed one atmosphere. The pressure of the component present in the least quantity was always known most accurately as it was measured by the U-tube manometer.

The cell used for the infrared measurements was cylindrical with a one inch internal diameter and ten centimeter path length and is shown in Figure 6. The windows were held in place against greased Buna N rubber O-rings by circular end caps which were screwed to the body of the cell. A coaxial, stainless steel jacket permitted the cell to be cooled with a stream of cold nitrogen gas. The cell was made of copper tube, with a 0.1 inch wall thickness, for optimum heat transfer. Without insulation of the outside of the coaxial jacket, tempera-

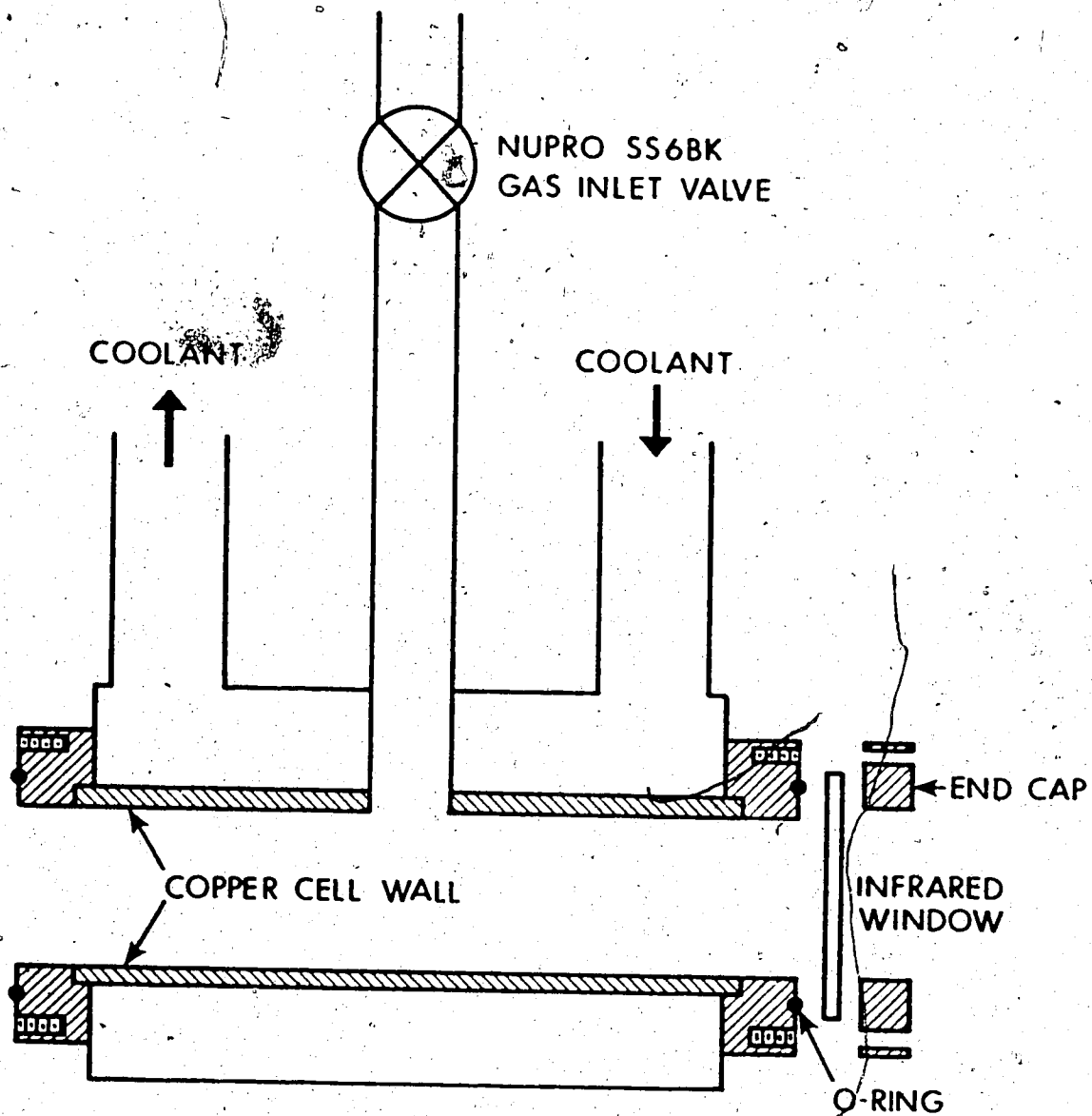


FIGURE 6. Cross-sectional view of the infrared gas cell. All parts other than the copper cell wall are stainless steel.

tures down to  $-40^{\circ}\text{C}$  could be maintained by regulating the flow rate of the nitrogen. The temperature of the cell wall was measured to  $\pm 1^{\circ}\text{C}$  by a calibrated thermometer or sometimes was measured by copper-constantan thermocouples in contact with the cell wall.

High density polyethylene,  $1/16''$  thick, was used for windows in the range  $20-400\text{ cm}^{-1}$  and 6 mm. thick potassium chloride windows were used for the  $500 - 4000\text{ cm}^{-1}$  range. Six mm. thick cesium iodide windows were also used in the range  $200-650\text{ cm}^{-1}$  but these had to be coated with a thin film of paraffin to prevent attack by hydrogen chloride. This film was applied by wetting the window on one side with a solution of paraffin wax in petroleum ether and allowing the ether to evaporate. These windows were less desirable than potassium chloride in the region above  $650\text{ cm}^{-1}$  because the paraffin coating sometimes affected the infrared transmission. The infrared cell and high pressure manifold were tested for safety at high pressures by filling both with 100 PSIG (5870 Torr) of argon. No loss in pressure was noted over a period of at least ten hours with any of the above windows.

### 2.3 Infrared Spectrophotometers

The infrared spectra in the range  $200-4000\text{ cm}^{-1}$  were recorded on a Beckman IR-12 spectrophotometer. A slit program was used such that the resolution was about  $2\text{ cm}^{-1}$

between 650 and 4000  $\text{cm}^{-1}$  and about 4  $\text{cm}^{-1}$  between 200 and 650  $\text{cm}^{-1}$ . Scanning speeds of 20  $\text{cm}^{-1}/\text{min.}$  between 200 and 2000  $\text{cm}^{-1}$  and 40  $\text{cm}^{-1}/\text{min.}$  between 2000 and 4000  $\text{cm}^{-1}$  were used with a pen period of 2 seconds. The instrument was operated under double beam conditions with the reference beam either empty or containing enough ether in a gas cell at room temperature to cancel the absorption due to uncomplexed ether in the sample (Section 3.1). When water vapour was to be removed from the instrument it was purged with air which was dried using a Puregas model HR-211-112-9 dryer. If both water and carbon dioxide were to be removed, the instrument was purged with nitrogen gas, boiled from a liquid nitrogen storage dewar and warmed to room temperature. The infrared cell fitted into the spectrophotometer with the gas valve and the inlet and outlet tubes of the cooling jacket protruding from the sample compartment cover. This cover was made from two plexiglass plates and masking tape, and the cracks between the cover and the tubes passing through it were filled with plasticine. This allowed the instrument purge to be maintained so efficiently that no condensation on the cell was observed, even at  $-40^{\circ}\text{C.}$  The frequencies between 200 and 1700  $\text{cm}^{-1}$  were measured with respect to a fiducial marker, programmed to produce a mark on the spectrum at 25  $\text{cm}^{-1}$  intervals and calibrated against the spectrum of water vapour and the standard gases (91). The frequencies

between 1700 and 3000  $\text{cm}^{-1}$  were measured with respect to the rotational fine structure of the fundamental vibrational band of either hydrogen chloride or deuterium chloride (91).

The far infrared spectra were recorded on a Beckman IR-11 spectrophotometer and also by using a Beckman R.I.I.C. FS 720 interferometer. Both instruments were calibrated using the hydrogen chloride pure rotation lines (92) and spectra were run at about 1  $\text{cm}^{-1}$  resolution. The Beckman-IR 11 was used in the range 80-150  $\text{cm}^{-1}$  with a scanning speed of 10  $\text{cm}^{-1}/\text{min}$ . and a pen period of 8 seconds. The instrument was purged with dry nitrogen, and the cell was sealed into it in the same way as for the IR-12. The interferometer was fitted with a step-drive for the moving mirror and the standard Analogue-Digital converter plus paper tape output was replaced by a Hewlett-Packard model 2401C integrating Digital Voltmeter and an IBM model 026 card punch. The interferograms were recorded both sides of zero path and the spectra were calculated using the Cooley-Tukey, sine plus cosine, Fourier Transform subroutine, RHARM (93), called by a data manipulation program written in this laboratory. The spectra were plotted on an off-line Calcomp plotter. The gas cell used for the interferometer was identical to the one described above except that a metal plate was fixed to the cell, below the gas-inlet valve and the ends of the cooling tubes. An O-ring seal



43.

between the plate and cell compartment allowed the interferometer to be evacuated.

## CHAPTER 3

### R E S U L T S   A N D   D I S C U S S I O N

#### 3.1 General

In this chapter the infrared absorption spectra of  $(\text{CH}_3)_2\text{O}---\text{HCl}$  and its isotopic modifications are presented and discussed. Section 3.2 deals with the far infrared region of the spectrum, where the hydrogen bond stretching vibration absorbs, and Section 3.3 deals with the region between 200 and  $800 \text{ cm}^{-1}$ , where absorptions are assigned to the  $\text{O}---\text{HCl}$  deformation vibrations. In Section 3.4 the absorption by the ethereal modes is presented and discussed in terms of the geometry of the hydrogen-bonded molecule. In Section 3.5 a study of the effect of temperature on the shapes of the bands due to the hydrogen chloride stretching vibrations in the various isotopic modifications of  $(\text{CH}_3)_2\text{O}---\text{HCl}$  is presented and the features on these bands are assigned. The relative intensities of the absorption bands in the spectrum of  $(\text{CH}_3)_2\text{O}---\text{HCl}$  are presented in Section 3.6.

In many of the spectral regions described in this chapter the absorption by the hydrogen-bonded molecule was complicated by overlapping absorption by the free components. Absorption by free hydrogen chloride was significant only in the  $3000 \text{ cm}^{-1}$  and far infrared regions but absorption by free ether occurred in most regions of interest. Attempts were made to minimize the amount of free ether present by

cooling the cell and/or by preparing mixtures of high pressures of hydrogen chloride with low pressures of ether, thereby forcing a larger percentage of the ether present to become hydrogen bonded. Unfortunately, in many cases the onset of condensation occurred before the absorption by the free ether became insignificant and it was necessary to subtract this absorption from that by the mixture to obtain the absorption by the hydrogen-bonded molecule. This was done by placing an appropriate pressure of ether in a 10 cm. long gas cell at ambient temperature in the reference beam of the spectrophotometer, or by obtaining the absorbance spectrum of an appropriate pressure of ether in a 10 cm. path length and subtracting it from the absorbance spectrum of the mixture. The latter method proved to be the more advantageous in regions of strong free ether absorption. An uncertainty always existed in choosing the correct amount of ether absorption to subtract, but it was found that the resultant spectra were not critically dependent upon this amount, and in most cases the absorbance subtracted was that due to the same pressure of ether as was used in the mixtures. The absorption by the free ether was not found to be significantly affected by temperature or by pressure-broadening by an inert gas and thus the temperature of, and the total pressure within the reference ether cell was not important.

In addition to bands which could be assigned to either the hydrogen-bonded molecule or to the free components, the infrared spectra of mixtures of the components often contained

bands which grew in intensity with time. To confirm that none of the bands assigned to the hydrogen-bonded molecule in fact arose from some reaction product, spectra of various mixtures of the components were recorded at various intervals over a period of twenty-four hours. Any band which grew in intensity could not then be assigned to some mode of the hydrogen-bonded molecule. The main reaction products were found to be methyl chloride, which formed fairly rapidly when the partial pressure of each component was large, and a thin yellow film, probably copper (II) chloride, which was slowly deposited throughout the cell and on the cell windows, causing a decrease in the infrared transparency of the cell.

### 3.2 Far Infrared Region

In the region below  $200 \text{ cm}^{-1}$  only one band which was not present in the spectra of the free components was observed. In Figure 7, curves A, B, and C show the spectra between  $90$  and  $150 \text{ cm}^{-1}$  of a mixture of 325 Torr of dimethyl ether- $\text{h}_6$  with 325 Torr of hydrogen chloride at  $0^\circ\text{C}$ ,  $10^\circ\text{C}$  and  $20^\circ\text{C}$  respectively. A band which is not present in the spectrum of pressure-broadened hydrogen chloride (curve D) or pressure-broadened dimethyl ether- $\text{h}_6$  (curve E) is clearly visible close to the  $J = 5 \rightarrow 6$  pure rotation line of the free hydrogen chloride. The absence of an absorption at this frequency in the spectra of the pressure-broadened unmixed components indicates that the absorption present in

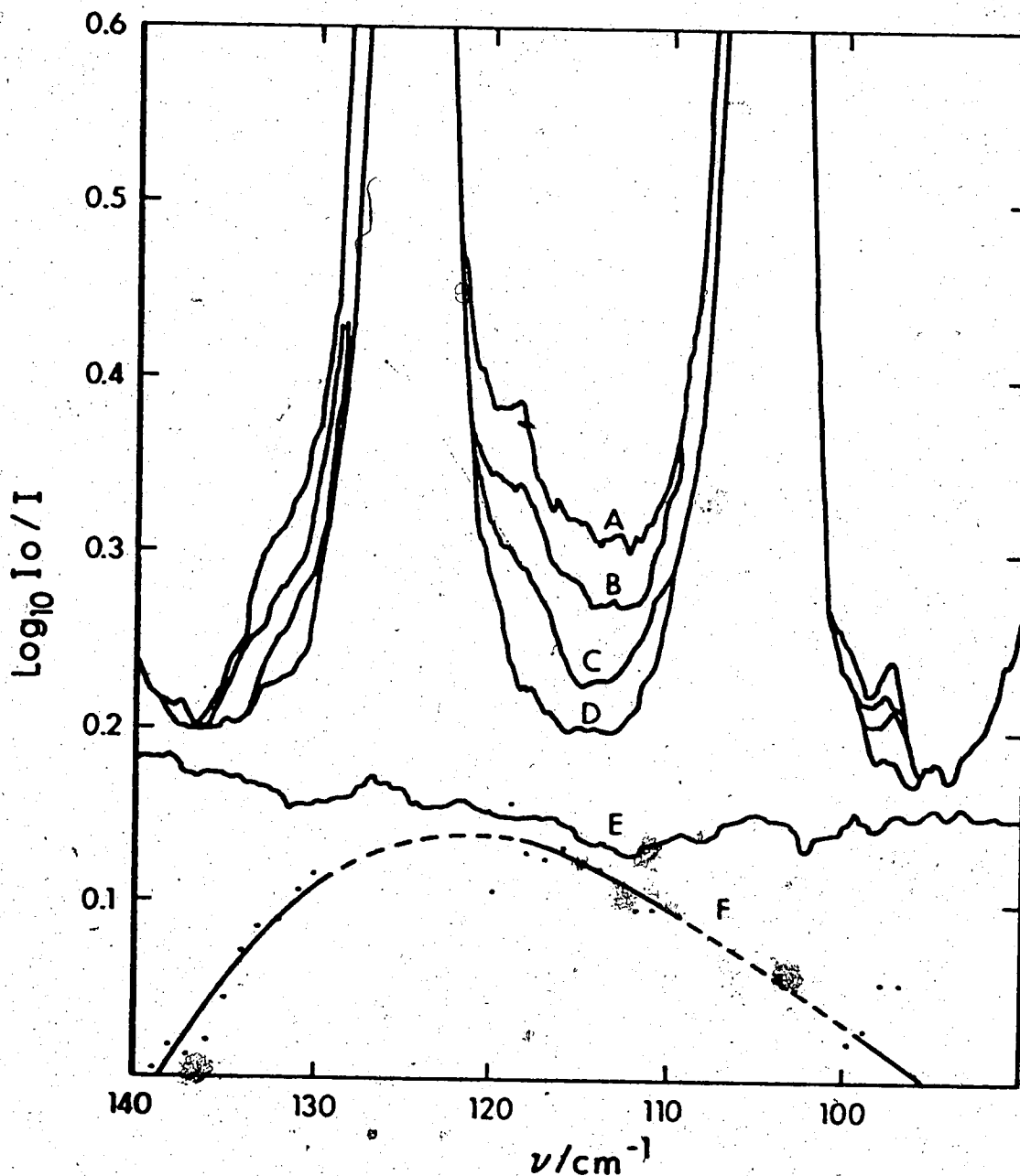


**FIGURE 7.** Curves A, B and C show absorption by 325 Torr of dimethyl ether- $\text{h}_6$  plus 325 Torr of hydrogen chloride at  $0^\circ\text{C}$ ,  $10^\circ\text{C}$  and  $20^\circ\text{C}$ , respectively. Curves D and E show absorption at  $0^\circ\text{C}$  by 325 Torr of hydrogen chloride and 325 Torr of dimethyl ether- $\text{h}_6$ , respectively, each pressure broadened with 325 Torr of air. Curve F was obtained by subtracting the absorption in curves D and E from that in curve A.

spectra of the mixtures arises from a specific interaction between the components rather than from a pressure-broadening effect such as is observed for the trimethylamine-methanol system (67,68). The intensity of the band increases reversibly as the sample temperature is lowered from 20°C to 0°C and is the kind of temperature dependence which is expected for an absorption by a hydrogen-bonded molecule in dynamic equilibrium with its component molecules. Curve F in Figure 7 shows the spectrum obtained by subtracting the absorption due to the unmixed gases from that of the mixture at 0°C. Due to the strong absorption by free hydrogen chloride, the resultant band in curve F is poorly defined but it has a half-width of about 25-30  $\text{cm}^{-1}$  and its maximum is at  $119 \pm 4 \text{ cm}^{-1}$ .

Spectra of 440 Torr of dimethyl ether- $\text{h}_6$  mixed with 220 Torr of hydrogen chloride and 220 Torr of dimethyl ether- $\text{h}_6$  mixed with 440 Torr of hydrogen chloride, both at 0°C, showed the same absorption as that shown in Figure 7. The intensity of the absorption by the 2:1 mixture was the same as that by the 1:2 mixture, but was slightly less intense than the absorption by the 1:1 mixture. This behavior can be predicted from a simple calculation of the equilibrium concentration of the hydrogen-bonded molecule if one assumes that the molecule is composed of dimethyl ether- $\text{h}_6$  and hydrogen chloride in equal proportions. Further, the 25-30  $\text{cm}^{-1}$  half-width of the band is consistent with that calcu-

lated for the rotational envelope of a vibrational transition in the molecule  $(\text{CH}_3)_2\text{O}---\text{HCl}$  (Section 3.4), so the band can confidently be assigned to this molecule.

In Figure 8, curve A shows the spectrum of a mixture of 325 Torr of dimethyl ether- $\text{h}_6$  with 325 Torr of deuterium chloride at  $0^\circ\text{C}$  and curves B and C, respectively, show the spectra of free deuterium chloride and free dimethyl ether- $\text{h}_6$ , both pressure-broadened with dry air at  $0^\circ\text{C}$ . In spite of the very strong absorption by the free deuterium chloride, a band close to  $120\text{ cm}^{-1}$  is clearly visible in the spectrum of the mixture. The intensity of this band was found to decrease, reversibly, as the temperature was raised from  $0^\circ\text{C}$ . Curve D shows the spectrum obtained by subtracting the absorption by the unmixed gases from that by the mixture and, although curve D is poorly defined, it shows that the band is very similar in frequency and half-width to the band displayed in curve F of Figure 7. It follows, from the assignment of the latter band to  $(\text{CH}_3)_2\text{O}---\text{HCl}$ , that the band displayed in curve D of Figure 8 arises from  $(\text{CH}_3)_2\text{O}---\text{DCl}$ .

In Figure 9, curve A shows the spectrum of a mixture of 325 Torr of dimethyl ether- $\text{d}_6$  with 325 Torr of hydrogen chloride at  $0^\circ\text{C}$  and curves B and C show the spectra of the pressure-broadened unmixed gases at  $0^\circ\text{C}$ . The spectrum obtained by subtracting the absorption by the unmixed gases from that of the mixture is shown in curve D and reveals a band with a half-width which is comparable to the half-widths of the bands shown in Figures 7 and 8. The band shown in

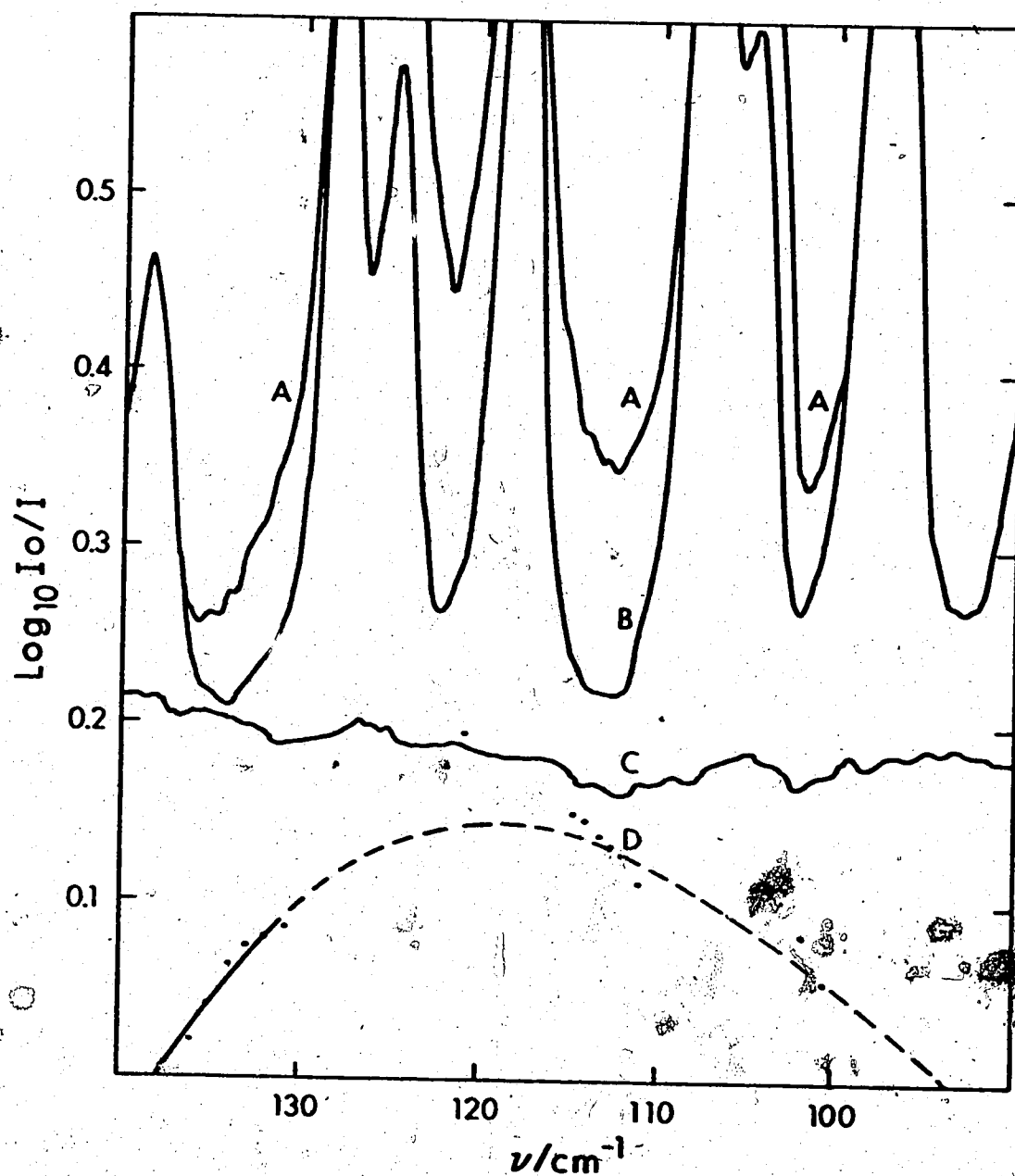


FIGURE 8. Infrared absorption by mixtures at  $0^\circ\text{C}$  of 325 Torr of dimethyl ether- $\text{h}_6$  plus 325 Torr of deuterium chloride (curve A); 325 Torr of deuterium chloride plus 325 Torr of dry air (curve B); 325 Torr of dimethyl ether- $\text{h}_6$  plus 325 Torr of dry air (curve C). Curve D was obtained by subtracting the absorption in curves B and C from that in curve A.



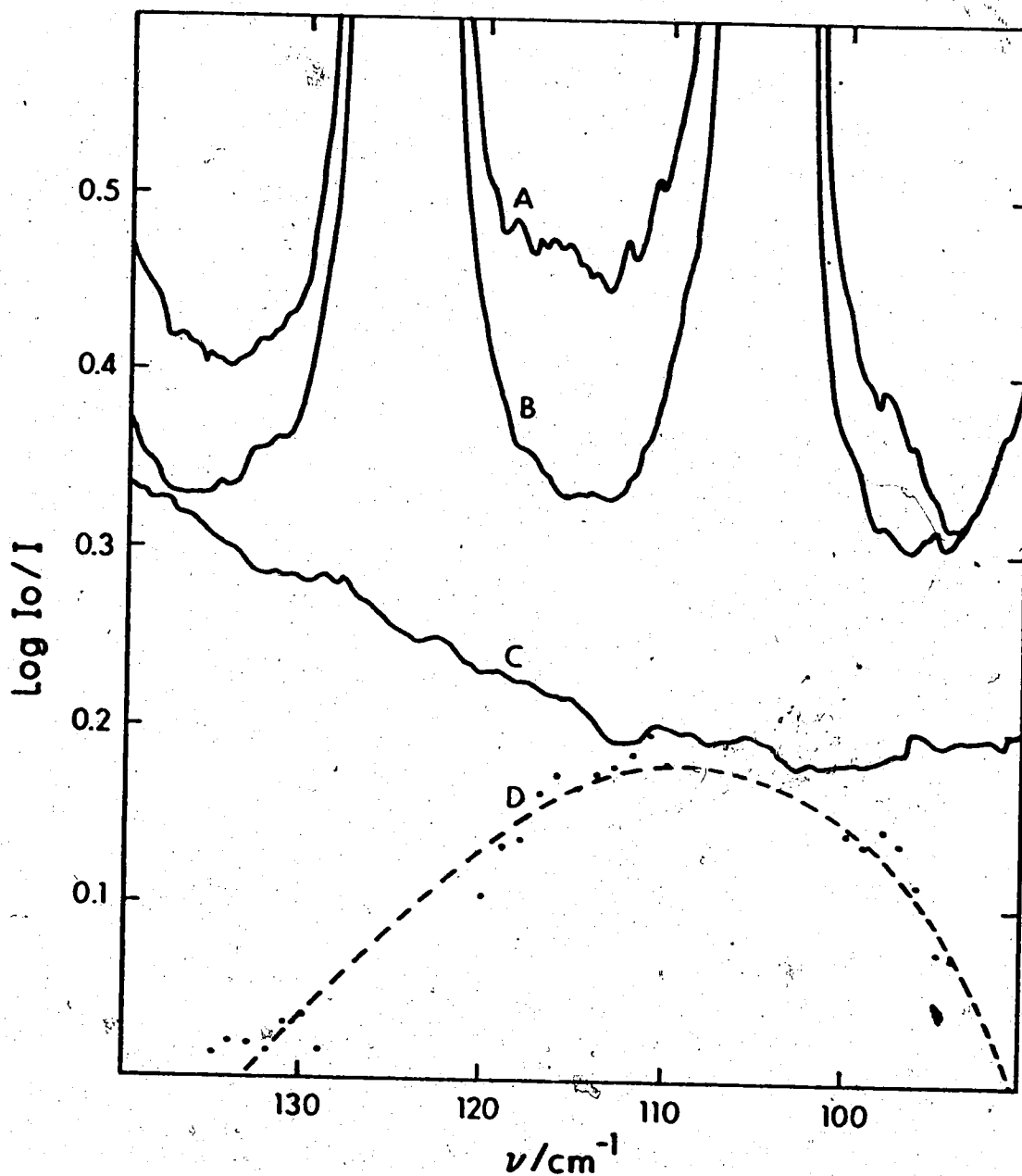


FIGURE 9. Infrared absorption by mixtures at  $0^\circ\text{C}$  of: 325 Torr of dimethyl ether- $\text{d}_6$  plus 325 Torr of hydrogen chloride (curve A); 325 Torr of hydrogen chloride plus 325 Torr of dry air (curve B); 325 Torr of dimethyl ether- $\text{d}_6$  plus 325 Torr of dry air (curve C). Curve D was obtained by subtracting the absorption in curves B and C from that in curve A.

curve D of Figure 9 lies about  $5 - 10 \text{ cm}^{-1}$  to low frequency of those shown in Figures 7 and 8 although this frequency shift may appear to be much larger than it really is due to errors in subtracting the absorption due to the unmixed gases. This band was found to decrease in intensity as the temperature was raised from  $0^\circ\text{C}$  and it is clear that the bands observed in all three mixtures arise from either the  $\nu_\sigma$  or  $\nu_\beta$  modes of the hydrogen-bonded molecule. In general, an angle bending or torsional mode is expected to absorb at a lower frequency than a stretching mode involving the same atoms (94), but no other band which could be assigned to one of these three modes was found above or below the band close to  $119 \text{ cm}^{-1}$ . The HCl wagging modes, however, are expected to absorb very weakly and below  $100 \text{ cm}^{-1}$  (13) and probably interact with the rotation of the molecule. Indirect evidence is also given in Section 3.3 that these modes absorb at about  $50 \text{ cm}^{-1}$ . Thus the band at  $119 \text{ cm}^{-1}$  is assigned to the hydrogen bond stretching mode,  $\nu_\sigma$ , in agreement with Belozerskaya and Shchepkin (75). This frequency is close to the frequency predicted for  $\nu_\sigma$  in  $(\text{CH}_3)_2\text{O} \cdots \text{HCl}$  by Bertie and Millen (73).

A knowledge of the anharmonicity of the hydrogen bond stretching mode is important to the theoretical understanding of hydrogen-bonded systems. A study of the contribution of the hot bands of the fundamental (42) to the structure of the  $119 \text{ cm}^{-1}$  band could lead to a semi-quantitative evaluation of the anharmonicity of this mode in the ether-hydrogen

chloride molecule, and attempts were made to obtain a clearer view of the band for this purpose. Calculations indicated that much of the interfering absorption due to free hydrogen chloride could be removed by simply increasing the partial pressure of the ether while decreasing the partial pressure of the hydrogen chloride. Spectra of mixtures of 50 to 100 Torr of hydrogen chloride with up to 1500 Torr of dimethyl ether-h<sub>6</sub> were recorded but the absorption by the ether in this region, which is not a problem at a pressure of 440 Torr, was sufficiently strong at the higher pressures to prevent better spectra from being obtained.

### 3.3 Infrared Spectra Between 200 and 800 cm<sup>-1</sup>

In box I of Figure 10, curve A shows the spectrum between 300 and 600 cm<sup>-1</sup> of a mixture at -30°C of 880 Torr of hydrogen chloride with 110 Torr of dimethyl ether-h<sub>6</sub>. Curve B shows the spectrum of 110 Torr of dimethyl ether-h<sub>6</sub> at -30°C and curve C shows the spectrum obtained by subtracting the absorption due to the ether from the absorption due to the mixture. Hydrogen chloride does not absorb in this region and its spectrum is not shown. Curve C displays a broad absorption extending from about 325 to 590 cm<sup>-1</sup> which has a half-width of about 150 cm<sup>-1</sup> and is not present in the spectrum of the free ether. Superimposed on the band are several sub-bands, the most prominent of

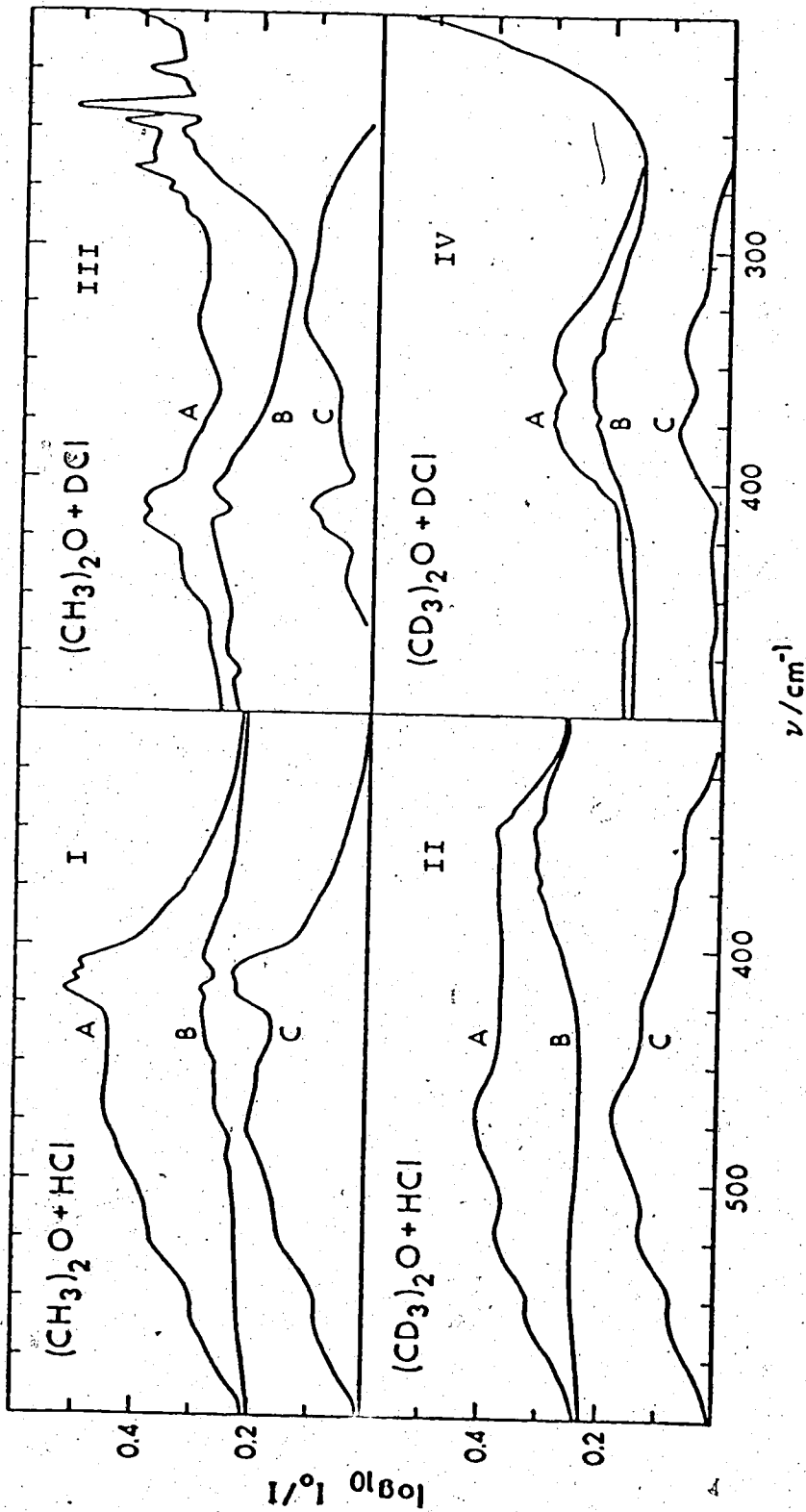


FIGURE 10 Curves A: Infrared absorption by mixtures of 110 Torr of dimethyl ether-h<sub>6</sub> or dimethyl ether-d<sub>6</sub> plus 880 Torr of hydrogen chloride or deuterium chloride, as indicated, at -30°C. Curves B: infrared absorption by 110 Torr of dimethyl ether-h<sub>6</sub> (boxes I and III) or dimethyl ether-d<sub>6</sub> (boxes II and IV) at -30°C. In each box curve C was obtained by subtracting curve B from curve A.

which is a peak with a half-width of about 20 centered at  $415 \text{ cm}^{-1}$ . In addition, three relatively strong features, at 480, 525 and  $570 \text{ cm}^{-1}$ , are evident as well as weak shoulders at about 440 and  $380 \text{ cm}^{-1}$ . Due to uncertainties in the appropriate amount of free ether absorption to subtract, these latter two features, as well as the doublet character of the peak at  $415 \text{ cm}^{-1}$  and the rather sharp top to the feature at  $480 \text{ cm}^{-1}$ , may not be real.

Spectra of samples at 30, -10 and  $-30^\circ\text{C}$  showed that the intensity of the band increased with decreasing temperature in spite of some condensation occurring at  $-30^\circ\text{C}$ . This temperature dependence of the intensity of the band and the absence of the absorption in spectra of the unmixed gases are consistent with the assignment of the band to a hydrogen-bonded product molecule. Further, spectra of 440 Torr of hydrogen chloride with 220 Torr of dimethyl ether- $\text{h}_6$  at  $-30^\circ\text{C}$  showed the same absorption as shown in box I in Figure 10 and revealed that the relative intensities of the features at 570, 525, 480,  $415 \text{ cm}^{-1}$  did not depend upon whether the ratio of acid to ether was 2:1 or 8:1. This is consistent with the assignment of the whole band to the 1:1 hydrogen-bonded molecule,  $(\text{CH}_3)_2\text{O}---\text{HCl}$ .

In box II of Figure 10, curve A shows the spectrum between 300 and  $600 \text{ cm}^{-1}$  of a mixture at  $-30^\circ\text{C}$  of 880 Torr of hydrogen chloride with 110 Torr of dimethyl ether- $\text{d}_6$  and curve B shows the spectrum of 110 Torr of dimethyl

ether-d<sub>6</sub> at -30°C. The subtraction spectrum, shown in curve C, displays an absorption with a half-width of about 150 cm<sup>-1</sup> between 325 and 590 cm<sup>-1</sup> that is very similar to the absorption shown in curve C of box I. A study of the effect of temperature on the intensity of the band and of the effect of changing the acid to ether ratio showed that the absorption arises from the 1:1 hydrogen-bonded molecule, (CD<sub>3</sub>)<sub>2</sub>O---HCl.

The main differences between the bands displayed in curves C of boxes I and II occur below 450 cm<sup>-1</sup>. Most striking is the absence, in box II, of a peak at 415 cm<sup>-1</sup>. Since this peak is present only in spectra of mixtures containing dimethyl ether-h<sub>6</sub> it must arise from a vibrational mode in the ethereal part of the (CH<sub>3</sub>)<sub>2</sub>O---HCl molecule. The absorption by the free dimethyl ether-h<sub>6</sub> between 375 and 500 cm<sup>-1</sup> has been assigned to the C-O-C deformation mode (95,96) and the 415 cm<sup>-1</sup> absorption by (CH<sub>3</sub>)<sub>2</sub>O---HCl is clearly due to the analogous mode in the ethereal part of the molecule. Curve C of box II displays a weak feature at about 340 cm<sup>-1</sup> which is not present in curve C of box I and which falls in the region of absorption by the C-O-C deformation mode of dimethyl ether-d<sub>6</sub> (95). By analogy with the argument used for the assignment of the 415 cm<sup>-1</sup> peak in the spectrum of (CH<sub>3</sub>)<sub>2</sub>O---HCl, the feature at 340 cm<sup>-1</sup> may be assigned to the C-O-C deformation mode in (CD<sub>3</sub>)<sub>2</sub>O---HCl. The very weak feature at about 370 cm<sup>-1</sup> in the spectrum of (CD<sub>3</sub>)<sub>2</sub>O---HCl is probably spurious.

Above  $450\text{ cm}^{-1}$  the absorption does not depend significantly upon which ether is present in the mixture. The shoulders at  $570$  and  $525\text{ cm}^{-1}$  on the band displayed in box II coincide almost exactly with similar features in box I. The absorption maximum in  $(\text{CD}_3)_2\text{O}---\text{HCl}$  is a smooth feature centered at  $470\text{ cm}^{-1}$  and coincides closely with the feature at  $480\text{ cm}^{-1}$  on the absorption by  $(\text{CH}_3)_2\text{O}---\text{HCl}$  (this feature may be slightly higher in frequency than it should be due to poor cancellation of the free ether absorption). This series of sub-bands, at  $570$ ,  $525$  and  $470\text{ cm}^{-1}$ , has a spacing of about  $50\text{ cm}^{-1}$  and leads to the conclusion that the shoulder at  $425\text{ cm}^{-1}$  in the spectrum of  $(\text{CD}_3)_2\text{O}---\text{HCl}$  is also a member of the group, but due to overlapping absorption is not seen in the spectrum of  $(\text{CH}_3)_2\text{O}---\text{HCl}$ .

The features which are common to the spectra of  $(\text{CH}_3)_2\text{O}---\text{HCl}$  and  $(\text{CD}_3)_2\text{O}---\text{HCl}$  in this frequency region must have their origin in the  $\text{O}---\text{H}-\text{Cl}$  part of the molecules. Of the six vibrational modes confined to this part of the molecule (Figure 4), only  $\nu_b$  or  $\nu_t$ , the  $\text{O}---\text{H}-\text{Cl}$  deformation modes, can reasonably be expected to give rise to absorption in this region. Proof that this absorption is due to  $\nu_b$  and/or  $\nu_t$  was obtained by recording spectra analogous to those shown in boxes I and II of Figure 10, but with deuterium chloride in place of hydrogen chloride. In box III, curve A shows the spectrum of a mixture at  $-30^\circ\text{C}$  of 880 Torr of deuterium chloride with 110 Torr of dimethyl

ether-h<sub>6</sub> and curve B shows that of 110 Torr of dimethyl ether-h<sub>6</sub> at -30°C. The subtraction spectrum, shown in curve C, reveals that, except for the peak at 415 cm<sup>-1</sup>, the absorption by (CH<sub>3</sub>)<sub>2</sub>O---DCl is centered at a lower frequency than that by (CH<sub>3</sub>)<sub>2</sub>O---HCl and thus can only arise from a vibrational mode involving the motion of the hydrogen-bonded hydrogen atom. Of the vibrational modes confined to the O---H-Cl part of the molecule, other than ν<sub>b</sub> or ν<sub>t</sub>, only ν<sub>s</sub>, the H-Cl stretching mode, involves this motion. This mode, however, is known to absorb close to 2500 cm<sup>-1</sup> (73) and therefore cannot give rise to absorption in the 450 cm<sup>-1</sup> region.

The peak at 415 cm<sup>-1</sup> in the spectrum of (CH<sub>3</sub>)<sub>2</sub>O---HCl was assigned above to the C-O-C deformation mode and is not expected to shift in frequency by isotopic substitution of an atom outside the ethereal part of the molecule. Thus the peak at 415 cm<sup>-1</sup> in the spectrum of (CH<sub>3</sub>)<sub>2</sub>O---DCl clearly arises from this mode. The remainder of the absorption shown in curve C of box III is rather weak but features at 440, 375, 330 and 285 cm<sup>-1</sup> are evident. These features are nearly coincident with features at about 430, 380, 340 and 290 cm<sup>-1</sup> seen on curve C in box IV, which shows the analogous subtraction spectrum of (CD<sub>3</sub>)<sub>2</sub>O---DCl. Although vibrational modes in the ethereal parts of the (CH<sub>3</sub>)<sub>2</sub>O---DCl and (CD<sub>3</sub>)<sub>2</sub>O---DCl molecules clearly influence the relative intensities and, to a lesser extent, the frequencies of the features, the major portion of these absorptions must be



assigned to modes in the O---D-Cl part of the molecules. The feature at  $340\text{ cm}^{-1}$  in the spectrum of  $(\text{CD}_3)_2\text{O---DCl}$  must include absorption by the C-O-C deformation mode as this mode absorbs at  $340\text{ cm}^{-1}$  in  $(\text{CD}_3)_2\text{O---HCl}$  and is not expected to shift in frequency in  $(\text{CD}_3)_2\text{O---DCl}$ .

Some of the differences between the spectra of  $(\text{CH}_3)_2\text{O---DCl}$  and  $(\text{CD}_3)_2\text{O---DCl}$  may arise from errors in the subtraction of the free ether absorption from that of the mixture since the absorption by the ether is of the same order of magnitude as that by the hydrogen-bonded molecule. However, spectra of other mixtures with the same partial pressures of components contained features at the same frequencies although their relative intensities varied somewhat in different spectra. Attempts were made to obtain more intense absorption by all four isotopic modifications of  $(\text{CH}_3)_2\text{O---HCl}$  by increasing the partial pressure of the acid in the mixtures and by cooling the gas cell below  $-30^\circ\text{C}$ . Unfortunately, the onset of condensation and the rapid formation of reaction products under these conditions prevented better spectra than those presented from being obtained.

The bands assigned above to the O---H-Cl deformation modes,  $\nu_b$  and/or  $\nu_t$ , have many of the characteristics of those due to the H-Cl stretching mode,  $\nu_s$  (Section 3.5). In each case the bands are extremely broad, with a half-width about five to ten times that expected for a band due

to a single fundamental transition in  $(\text{CH}_3)_2\text{O}---\text{HCl}$  or  $(\text{CD}_3)_2\text{O}---\text{HCl}$ , and complex, with four equally-spaced features. The breadth and complexity of the band due to the  $\nu_s$  mode has been attributed (73) to interactions between  $\nu_s$  and  $\nu_\sigma$ , the hydrogen bond stretching mode. By analogy, the breadth and complexity of the bands due to  $\nu_b$  and/or  $\nu_t$  probably arise from interaction of these modes with the HCl wagging modes,  $\nu_{\beta_1}$ , and  $\nu_{\beta_2}$ . Thus the observed features on these bands may be assigned to transitions of the type  $\nu_b$ , or  $\nu_t$ ,  $\pm n\nu_\beta$ , where  $n$  is integral or zero. From the separation of the features the fundamental frequency of the  $\nu_\beta$  modes must be about  $50 \text{ cm}^{-1}$ . The frequency of the  $\nu_\beta$  modes is not expected to be significantly different in the DCl complexes and thus the observation that the features on the bands due to the O---D-Cl deformation modes are separated by about  $50 \text{ cm}^{-1}$  leads to the conclusion that these features also are due to transitions of the type  $\nu_b$ , or  $\nu_t$ ,  $\pm n\nu_\beta$ .

If the hydrogen chloride molecule attaches itself to one of the lone pairs of electrons on the oxygen atom of the ether molecule, the hydrogen-bonded molecule belongs to the point group  $C_s$  (Section 3.4). The only element of symmetry is a mirror plane which contains the hydrogen chloride molecule and the oxygen atom of the ether and which bisects the C-O-C bond angle.  $\nu_b$  is defined as the in-plane O---H-Cl deformation mode in which motion of the hydrogen-bonded hydrogen atom is parallel to this plane and  $\nu_t$  is the out-of-

plane mode and involves motion of the hydrogen atom perpendicular to this plane. Thus  $\nu_b$  and  $\nu_t$  have different symmetries and cannot interact with each other. Symmetry arguments, however, permit any sum or difference band of  $\nu_b$  or  $\nu_t$  with either  $\nu_{\beta_1}$  the in-plane HCl wagging mode, or  $\nu_{\beta_2}$  the out-of-plane HCl wagging mode. Thus, the bands of the type  $\nu_b \pm n\nu_{\beta_2}$  and  $\nu_t \pm n\nu_{\beta_1}$  are as probable as those of the type  $\nu_b \pm n\nu_{\beta_1}$  and  $\nu_t \pm n\nu_{\beta_2}$ , although the modes in the former combinations do not take place in the same plane while those in the latter combinations do. Thus no distinction between the  $\nu_{\beta}$  modes in the combinations with  $\nu_b$  and  $\nu_t$  can be made on symmetry grounds, although intuitively one would expect combinations of modes in which atomic displacements take place in the same plane to be more likely to occur than those in which the atomic displacements are perpendicular to each other.

Since a difference transition originates in an excited vibrational energy level, a difference band must decrease in intensity as the temperature is lowered due to depopulation of molecules of that level. However, calculations showed that the Boltzmann distribution of molecules between the ground state and levels up to  $100 \text{ cm}^{-1}$  above it was not significantly dependent upon the temperature between  $+30^\circ\text{C}$  and  $-30^\circ\text{C}$ , and a change in intensity of a difference band such as  $\nu_b - \nu_{\beta}$  would not be detected in this temperature range. Thus the observed constancy of the bandshape with temperature does not rule out the contribution of such difference bands

to the structure of the O---H-Cl and O---D-Cl deformation bands.

Before the assignment of the features of these bands is discussed in more detail, the spectra shown in Figure 11 must be presented. Curves A and B, respectively, show the absorption between 700 and 875  $\text{cm}^{-1}$  by a mixture of one atmosphere of dimethyl ether- $\text{h}_6$  with two atmospheres of hydrogen chloride, and by a mixture of two atmospheres of dimethyl ether- $\text{h}_6$  with one atmosphere of hydrogen chloride, both at +35°C. A broad band, centered at about 790  $\text{cm}^{-1}$ , is clearly evident in both curves, but is not present in the spectra of the free ether (curve D) or the free hydrogen chloride (curve E). The absorption is overlapped above 825  $\text{cm}^{-1}$  by a strong band due to the symmetric C-O stretching mode of dimethyl ether- $\text{h}_6$  (95,96) and thus no reliable measurement of its half-width can be made. Its intensity, which is about one-sixth of that of the band centered at 470  $\text{cm}^{-1}$  in  $(\text{CH}_3)_2\text{O---HCl}$ , is the same for dimethyl ether- $\text{h}_6$  : hydrogen chloride ratios of 1:2 and 2:1. In the spectra of mixtures with a total pressure of one atmosphere the intensity at 790  $\text{cm}^{-1}$  was found to increase reversibly as the temperature was lowered to the onset of condensation. Thus the band is assigned to the  $(\text{CH}_3)_2\text{O---HCl}$  molecule. Curve C shows the spectrum of a mixture of two atmospheres of dimethyl ether- $\text{h}_6$  with one atmosphere of deuterium chloride at +35°C. Comparison of curves B and C shows that

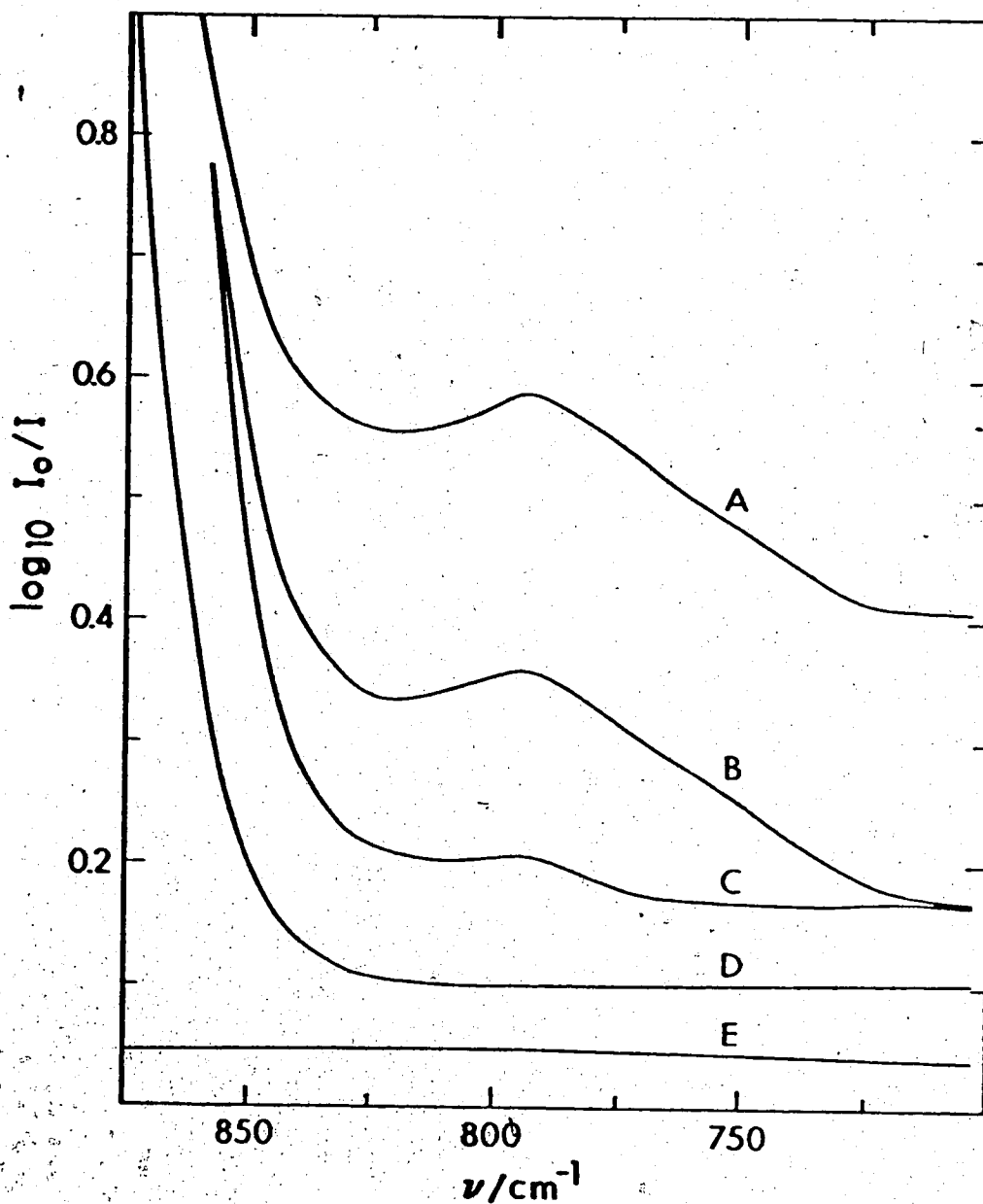


FIGURE 11. Infrared absorption at +35°C by: 1 atm of dimethyl ether- $\text{h}_6$  mixed with 2 atm of hydrogen chloride (curve A); 2 atm of dimethyl ether- $\text{h}_6$  mixed with 1 atm of hydrogen chloride (curve B); 2 atm of dimethyl ether- $\text{h}_6$  mixed with 1 atm of deuterium chloride (curve C); 1 atm of dimethyl ether- $\text{h}_6$  (curve D); 1 atm of hydrogen chloride (curve E).

the broad absorption at  $790\text{ cm}^{-1}$  has almost completely disappeared in the latter case, leaving only a weak feature about one-twentieth as intense as that in curve B. The deuterium chloride contained at least 5% hydrogen chloride as an impurity and the residual band may be assigned to  $(\text{CH}_3)_2\text{O}---\text{HCl}$  rather than  $(\text{CH}_3)_2\text{O}---\text{DCl}$ .

Since the band is not present at  $790\text{ cm}^{-1}$  in the spectrum of  $(\text{CH}_3)_2\text{O}---\text{DCl}$ , it must arise from a mode in which the motion of the hydrogen-bonded hydrogen atom is important. Only two assignments appear to be possible for this feature. Either it is due to one of the  $\text{O}---\text{H}-\text{Cl}$  deformation modes or to the first overtone of one of these modes. In either case a band should be present at  $790\text{ cm}^{-1}$  in the spectrum of  $(\text{CD}_3)_2\text{O}---\text{HCl}$  and one at a lower frequency in the spectrum of  $(\text{CD}_3)_2\text{O}---\text{DCl}$  or  $(\text{CH}_3)_2\text{O}---\text{DCl}$ . The spectrum of  $(\text{CD}_3)_2\text{O}---\text{HCl}$  in the  $790\text{ cm}^{-1}$  region could not be obtained because of a strong overlapping absorption due to the symmetric C-O stretching mode of the dimethyl ether- $\text{d}_6$  (95) but the spectrum between  $500$  and  $650\text{ cm}^{-1}$  of  $(\text{CD}_3)_2\text{O}---\text{DCl}$  is presented in Figure 12. Curve A shows the absorption by a mixture of two atmospheres of dimethyl ether- $\text{d}_6$  with one atmosphere of deuterium chloride at  $+35^\circ\text{C}$ . A very weak, broad absorption extending from about  $550$  to  $620\text{ cm}^{-1}$  is just visible in the spectrum of the mixture but is not present in the spectrum of the free ether (curve B) or free deuterium chloride (curve C). The weak absorption

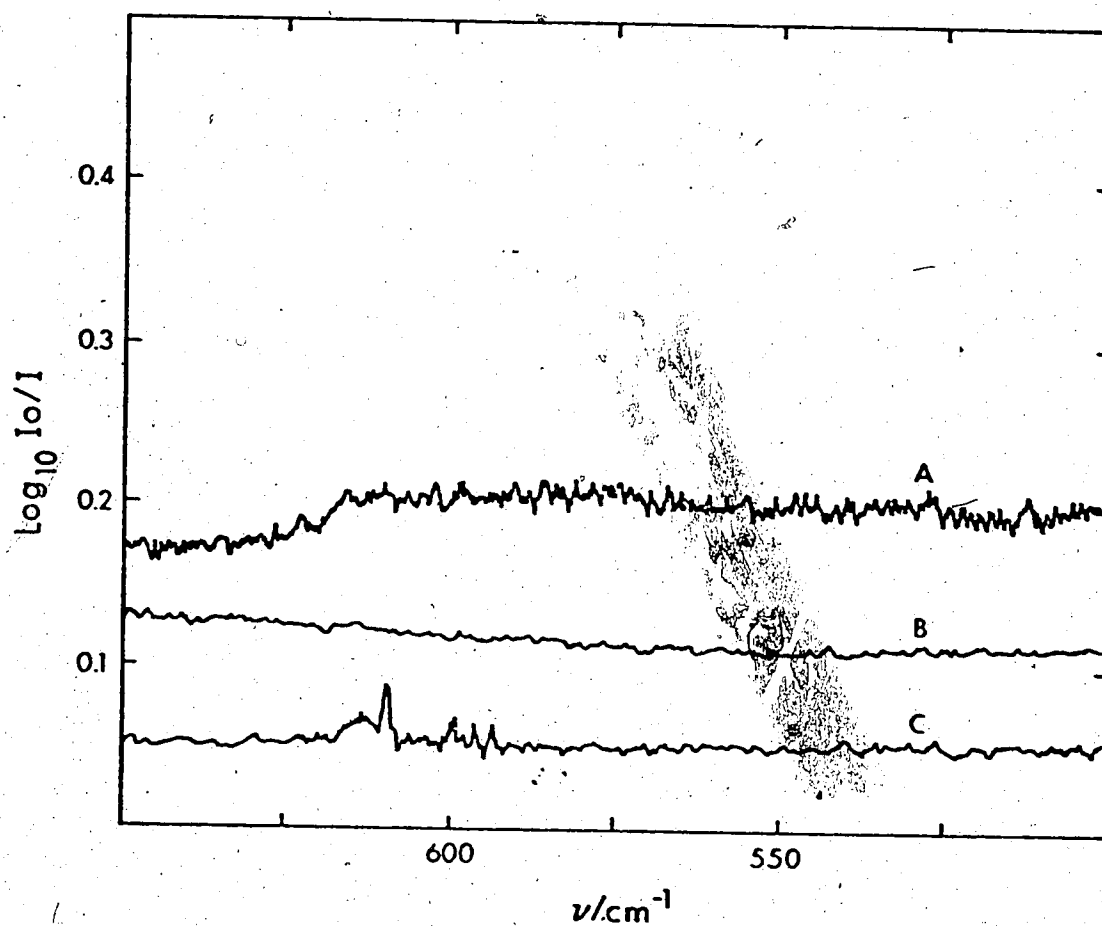


FIGURE 12. Infrared absorption at +35°C by: 2 atm of dimethyl ether-d<sub>6</sub> mixed with 1 atm of deuterium chloride (curve A); 2 atm of dimethyl ether-d<sub>6</sub> (curve B); 1 atm of deuterium chloride (curve C).

close to  $600\text{ cm}^{-1}$  shown in curve C arises from a thin yellow film which was present as an impurity on the cell windows (Section 3.1). To show that the weak feature shown in curve A actually arose from  $(\text{CD}_3)_2\text{O} \cdots \text{DCl}$  rather than from this film, the infrared cell was evacuated immediately after recording the spectrum of the mixture and the spectrum of the cell was recorded. The feature was not observed in this spectrum and therefore cannot arise from absorption by the cell. Attempts to observe this band with greater intensity, by cooling the cell and increasing the pressures of the components, resulted in either condensation of the complex or rapid formation of methyl chloride and were not successful.

The assignment of the  $790\text{ cm}^{-1}$  absorption by  $(\text{CH}_3)_2\text{O} \cdots \text{HCl}$  and the  $600\text{ cm}^{-1}$  absorption by  $(\text{CD}_3)_2\text{O} \cdots \text{DCl}$  to analogous modes necessitates a discussion of the relative intensities of the bands. It has been shown (97) that the intensity of  $\nu_s$  in free deuterium chloride is about one half of that in free hydrogen chloride. Since  $\nu_b$  and  $\nu_t$  involve primarily the motion of the hydrogen-bonded hydrogen atom, one would expect the intensity of  $\nu_b$  or  $\nu_t$  in the deuterium chloride complexes to be about one-half of that in the hydrogen chloride ones. Clearly the intensity of the absorption by  $(\text{CD}_3)_2\text{O} \cdots \text{DCl}$  is much less than one-half of that by  $(\text{CH}_3)_2\text{O} \cdots \text{HCl}$ . However, the absorption at  $790\text{ cm}^{-1}$  is not far removed from an extremely strong absorption due to the C=O symmetric stretching mode of the ether.



If the  $790\text{ cm}^{-1}$  absorption is due to a mode which has the same symmetry as the ethereal mode, it is possible for the weaker absorption to gain intensity through Fermi resonance (Section 1.6). The symmetric C-O stretching mode belongs to the  $A'$  symmetry species under the point group  $C_s$ , allowing such an interaction to take place if the  $790\text{ cm}^{-1}$  band were due to either  $\nu_b$  or to the first overtone of either  $\nu_b$  or  $\nu_t$ . In  $(\text{CD}_3)_2\text{O}---\text{DCl}$  there is no strong absorption close to  $600\text{ cm}^{-1}$  and thus no intensity enhancement through Fermi resonance is possible.

The  $\nu_b$  and  $\nu_t$  modes have been assigned to features of approximately the same intensity at  $755$  and  $655\text{ cm}^{-1}$  in the spectrum of  $(\text{CH}_3)_2\text{O}---\text{HF}$  (78) and at  $550$  and  $490\text{ cm}^{-1}$  in the spectrum of  $(\text{CH}_3)_2\text{O}---\text{DF}$  (78). As is the case for  $(\text{CH}_3)_2\text{O}---\text{HCl}$  and  $(\text{CH}_3)_2\text{O}---\text{DCl}$ , it is impossible to determine which mode has the higher frequency as both  $\nu_b$  and  $\nu_t$  show similar isotopic shifts and neither exists in the absence of the hydrogen bond. The separation of  $90\text{ cm}^{-1}$  between the modes in  $(\text{CH}_3)_2\text{O}---\text{HF}$  makes it very difficult to justify the assignment of one of these modes in  $(\text{CH}_3)_2\text{O}---\text{HCl}$  at  $790\text{ cm}^{-1}$  and the other near to  $470\text{ cm}^{-1}$ . It is probable, therefore, that  $\nu_b$  and  $\nu_t$  are both contained in the  $470\text{ cm}^{-1}$  band and that the  $790\text{ cm}^{-1}$  band is the absorption by  $2\nu_b$  or  $2\nu_t$ . The  $600\text{ cm}^{-1}$  absorption by  $(\text{CD}_3)_2\text{O}---\text{DCl}$  must then be assigned to  $2\nu_b$  or  $2\nu_t$ , with the fundamentals absorbing below  $400\text{ cm}^{-1}$ .

Unfortunately, the  $\nu_b$  and  $\nu_t$  modes cannot be uniquely assigned. If the ratio of the frequencies of  $\nu_b$  and  $\nu_t$  is the same for the HCl and DCl complexes as for the HF and DF ones, respectively, then  $\nu_b$  and  $\nu_t$  must be separated by about  $60 \text{ cm}^{-1}$  close to  $500 \text{ cm}^{-1}$  and by about  $40 \text{ cm}^{-1}$  close to  $350 \text{ cm}^{-1}$ . Since features were observed at 340 and  $380 \text{ cm}^{-1}$  in the spectrum of  $(\text{CD}_3)_2\text{O} \cdots \text{DCl}$ , they may be assigned to  $\nu_b$  and  $\nu_t$ . Their assignment at 470 and  $525 \text{ cm}^{-1}$  for the HCl complexes yields an isotopic ratio of 1.38 for both bands, compared to 1.40 under the harmonic approximation, if it is assumed that  $\nu_b$  is higher (or lower) than  $\nu_t$  in both the HCl and DCl complexes. This assignment, however, suggests that  $790 \text{ cm}^{-1}$  is a very low frequency for the first overtone of  $\nu_b$  or  $\nu_t$ . It is possible that this feature is at the low frequency end of a broad absorption, most of which is hidden by the much stronger band above  $850 \text{ cm}^{-1}$ . It is also possible that, because of the vibrational Franck-Condon effect (Section 1.6), the most intense transition in the overtone band is not the overtone of the most intense transition in the fundamental band. An alternative assignment which uses this feature is to assign  $\nu_b$  and  $\nu_t$  at 470 and  $420 \text{ cm}^{-1}$  in the HCl complexes and at 340 and  $290 \text{ cm}^{-1}$  in the DCl complexes but the isotopic ratio,  $420/290 = 1.45$ , is somewhat large.

It is useful to use these frequencies to calculate  $\omega_e$  and  $\omega_e x_e$  where

$$G(v) = \omega_e(v + 1/2) - \omega_e x_e (v + 1/2)^2 \quad (1)$$

as defined by Herzberg (98).  $G(v)$  is the energy term of the  $v^{\text{th}}$  vibrational energy level,  $\omega_e$  is the harmonic contribution to  $G(v)$ , and  $\omega_e x_e$  is the anharmonic constant. From this equation the following expressions are obtained for the fundamental and first overtone frequencies of the  $\nu_b$  (or  $\nu_t$ ) mode:

$$\nu_b = \omega_e - 2\omega_e x_e \quad (2a)$$

$$2\nu_b = 2\omega_e - 6\omega_e x_e \quad (2b)$$

Once  $\omega_e$  and  $\omega_e x_e$  for the HCl complexes have been calculated from these expressions, those for the DCl complexes, denoted by  $\omega_e^D$  and  $\omega_e x_e^D$ , may be computed (99) from the following formulae:

$$\omega_e^D = \rho \omega_e \quad (3a)$$

$$\omega_e x_e^D = \rho^2 \omega_e x_e \quad (3b)$$

where  $\rho^2 = G_D/G_H$ , where  $G_D$  and  $G_H$  are the G matrix elements (100) for the O---D-Cl and O---H-Cl deformation coordinates, respectively. These elements correspond to the element  $G_{\phi\phi}^3$ , defined in appendix VI of reference 36. If oxygen, hydrogen and chlorine atoms are taken to be collinear with  $r_{O-H} = r_{O-D} = 1.7 \text{ \AA}$  and  $r_{HCl} = r_{DCl} = 1.4 \text{ \AA}$  and  $G_D$

are 1.7193 and 0.8786 amu<sup>-1</sup> Å<sup>-2</sup>, respectively. The masses of the atoms used in the calculation were taken from reference 101. The values of  $G_D$  and  $G_H$  yield  $\rho^2 = 0.5111$  and  $\rho = 0.7149$ .

For the sake of simplicity in the following discussion the 790 cm<sup>-1</sup> band is assumed to arise from  $2\nu_b$ , the first overtone of the  $\nu_b$  mode, although it is impossible to determine whether it arises from  $2\nu_b$  or  $2\nu_t$ . The most reasonable agreement with this overtone frequency is obtained if  $\nu_b$  is assigned at 420 or 470 cm<sup>-1</sup>. To assign  $\nu_b$  at 570 or 525 cm<sup>-1</sup> leads to unreasonably large positive anharmonic terms, but one of these features may well be due to the other deformation mode,  $\nu_t$ . If  $\nu_b$  is assigned at 470 cm<sup>-1</sup> then  $\omega_e = 620$  cm<sup>-1</sup>,  $\omega_e x_e = 75$  cm<sup>-1</sup>,  $\omega_e^D = 443$  cm<sup>-1</sup> and  $\omega_e x_e^D = 38.3$  cm<sup>-1</sup>. Substitution of these values into equations 2a and 2b predicts  $\nu_b = 367$  cm<sup>-1</sup> and  $2\nu_b = 657$  cm<sup>-1</sup> in the DCl complexes. The weak feature observed in the spectrum of (CD<sub>3</sub>)<sub>2</sub>O---DCl (Figure 12) was definitely at a lower frequency than 657 cm<sup>-1</sup>, but 367 cm<sup>-1</sup> is close to an observed feature at 380 cm<sup>-1</sup>. The pairing of 470 and 380 cm<sup>-1</sup> indicates that 525 and 340 cm<sup>-1</sup> must correspond to the same vibration. Thus, this assignment requires that the anharmonicities be very large indeed, and does not agree well with the overtone frequency for (CD<sub>3</sub>)<sub>2</sub>O---DCl. The second assignment, in which 790 cm<sup>-1</sup> is taken to be the first overtone of 420 cm<sup>-1</sup>, yields

$\omega_e = 470 \text{ cm}^{-1}$ ,  $\omega_e x_e = 25 \text{ cm}^{-1}$ ,  $\omega_e^D = 336 \text{ cm}^{-1}$ , and  $\omega_e x_e^D = 12.8 \text{ cm}^{-1}$ , and predicts the corresponding frequencies for the DC1 complex to be 595 and  $310 \text{ cm}^{-1}$ . The former agrees well with the observed overtone absorption in the DC1 complex but  $310 \text{ cm}^{-1}$  does not correspond to any obvious feature in the observed spectrum. Thus, with the present data no unique assignment can be made, although of the two discussed, the second one is to be preferred on the basis of the smaller anharmonicity that it implies for this mode.

#### 3.4 Infrared Spectra Between 800 and $1500 \text{ cm}^{-1}$

Because absorption by the free ether is very strong in this region, it was necessary to record spectra of mixtures containing very high partial pressures of hydrogen chloride and low partial pressures of ether. The large excesses of hydrogen chloride in the mixtures caused most of the ether to become hydrogen bonded, even at ambient temperature. To further increase the percentage of ether present in the hydrogen-bonded form, the infrared cell was cooled. At  $-10^\circ\text{C}$  the equilibrium constant for the formation of  $(\text{CH}_3)_2\text{O} \cdots \text{HCl}$  is computed from the mean enthalpy and entropy reported by Govil, Clague and Bernstein (84) to be 1.86, standard state one atmosphere. Substitution of this value into the equilibrium expression for formation of  $(\text{CH}_3)_2\text{O} \cdots \text{HCl}$  reveals that at  $-10^\circ\text{C}$  only

six percent of the ether present in a mixture of 5860 Torr of hydrogen chloride with 10 Torr of dimethyl ether- $h_6$  remains uncomplexed. Under these conditions some condensation of the hydrogen-bonded complex undoubtedly occurs, but this has no effect upon the shapes and frequencies of the bands reported in this section. Due to the very large hydrogen chloride to ether ratios there exists a possibility that hydrogen-bonded species other than a 1:1 complex are present in these mixtures. However, the hydrogen chloride stretching mode,  $\nu_s$ , in the 1:1 complex is known to give rise to a band close to  $2500 \text{ cm}^{-1}$  (73) and a comparison of this band with the absorption by the high pressure mixtures in this region did not reveal any differences which could be attributed to other complexes.

In Figure 13, boxes II and III show spectra of 10 Torr of dimethyl ether- $h_6$  mixed with 5860 Torr of argon at  $+35^\circ\text{C}$  (curves A), and of 10 Torr of dimethyl ether- $h_6$  mixed with 5860 Torr of hydrogen chloride at  $+35^\circ\text{C}$ ,  $+10^\circ\text{C}$ ,  $0^\circ\text{C}$  and  $-10^\circ\text{C}$  (curves B, C, D and E, respectively). The intensities of the spectra shown in the latter four curves become progressively weaker as the temperature is lowered as a result of condensation of  $(\text{CH}_3)_2\text{O} \cdots \text{HCl}$ . In box II, curve A shows two bands with PQR structures, one at  $1102 \text{ cm}^{-1}$  with a half-width of about  $45 \text{ cm}^{-1}$  and PR separation of  $26.1 \text{ cm}^{-1}$ , and one at  $1179 \text{ cm}^{-1}$  with a half-width of about  $40 \text{ cm}^{-1}$  and a PR separation of  $22.0 \text{ cm}^{-1}$ .

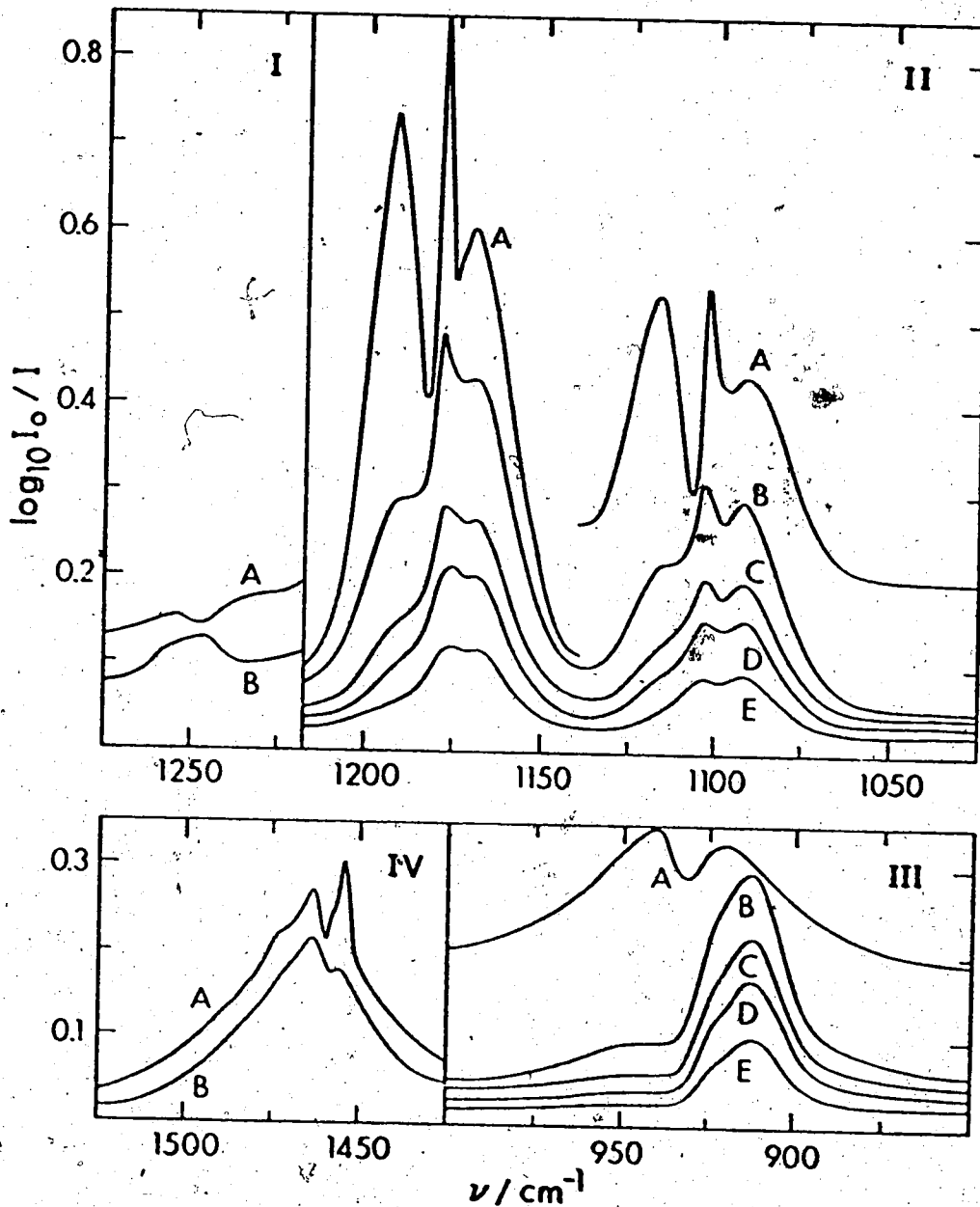


FIGURE 13. Infrared absorption spectra of: boxes I and IV, 20 Torr of dimethyl ether- $\text{h}_6$  mixed with 5850 Torr of Argon (curves A) or with 5850 Torr of hydrogen chloride (curves B), at  $0^\circ\text{C}$ ; boxes II and III, 10 Torr of dimethyl ether- $\text{h}_6$  mixed with 5860 Torr of Argon at  $+35^\circ\text{C}$  (curves A), or with 5860 Torr of hydrogen chloride at  $+35^\circ\text{C}$  (curves B),  $+10^\circ\text{C}$  (curves C),  $0^\circ\text{C}$  (curves D), or  $+10^\circ\text{C}$  (curves E).

Curves B through E show that, as the temperature is lowered and the absorption by free ether is decreased, the spectrum approaches a limit of two bands with half-widths of 25-30  $\text{cm}^{-1}$  and PR type structures. One band is centered at 1097  $\text{cm}^{-1}$  and has a PR separation of 11  $\text{cm}^{-1}$  and the other is centered at 1171  $\text{cm}^{-1}$  and has a PR separation of 9  $\text{cm}^{-1}$ . The bands at 1102 and 1179  $\text{cm}^{-1}$  in the spectrum of dimethyl ether- $\text{h}_6$  have been assigned (95,96) to mixtures of the asymmetric C-O stretching and  $\text{CH}_3$  rocking modes and thus the bands at 1097 and 1171  $\text{cm}^{-1}$  in the spectrum of  $(\text{CH}_3)_2\text{O}---\text{HCl}$  must arise from analogous modes. In box III, curve A displays a band centered at 934  $\text{cm}^{-1}$  with P and R branches separated by about 24  $\text{cm}^{-1}$ . Curves B through E show that the corresponding band in the spectrum of  $(\text{CH}_3)_2\text{O}---\text{HCl}$  has a halfwidth of about 20  $\text{cm}^{-1}$ , its absorption maximum at 912  $\text{cm}^{-1}$ , and a weak shoulder at about 925  $\text{cm}^{-1}$ . The band at 934  $\text{cm}^{-1}$  in the free ether has been assigned (95,96) to the symmetric C-O stretching mode, which must therefore be assigned at 912  $\text{cm}^{-1}$  in  $(\text{CH}_3)_2\text{O}---\text{HCl}$ .

Boxes I and IV of Figure 13 show spectra of 20 Torr of dimethyl ether- $\text{h}_6$  mixed with 5850 Torr of argon at 0°C (curves A) and of 20 Torr of dimethyl ether- $\text{h}_6$  mixed with 5850 Torr of hydrogen-chloride at 0°C (curves B). The shapes of the bands shown in curves B did not change as the temperature of the mixtures was lowered below 0°C and therefore these bands must arise almost completely



from  $(\text{CH}_3)_2\text{O}---\text{HCl}$ . In box I, curve A displays a weak band, centered at  $1245\text{ cm}^{-1}$ , with P and R branches separated by about  $20\text{ cm}^{-1}$ . This band has been assigned (95, 96) to the totally symmetric  $\text{CH}_3$  rocking mode of dimethyl ether- $\text{h}_6$ . The weak, slightly asymmetric band shown in curve B is centered at  $1248\text{ cm}^{-1}$  and undoubtedly arises from the analogous mode in the ethereal part of  $(\text{CH}_3)_2\text{O}---\text{HCl}$ . In box IV, curve A displays a band with a half-width of about  $35\text{ cm}^{-1}$  and with sharp features at  $1454$  and  $1462\text{ cm}^{-1}$  and a shoulder at about  $1475\text{ cm}^{-1}$ . This band has been assigned (95,96) to the five infrared active  $\text{CH}_3$  deformation modes in dimethyl ether- $\text{h}_6$ . Curve B shows that the band due to these modes in  $(\text{CH}_3)_2\text{O}---\text{HCl}$  has a half-width of about  $25\text{ cm}^{-1}$  and is centered at  $1465\text{ cm}^{-1}$ , although the absorption maximum is at  $1462\text{ cm}^{-1}$ .

The region between  $900$  and  $1200\text{ cm}^{-1}$  has been studied by Le Calvé, Grange, and Lascombe (76). The temperatures and the acid to ether ratios were higher in the present work, but the limiting band shapes reached as the temperature was lowered are essentially the same in both studies, except that the shoulder at  $925\text{ cm}^{-1}$  is less pronounced in this work than in reference 76. The bands at  $1248$  and  $1465\text{ cm}^{-1}$  in the spectrum of  $(\text{CH}_3)_2\text{O}---\text{HCl}$  are reported here for the first time. All of the bands between  $900$  and  $1500\text{ cm}^{-1}$  appeared unshifted in frequency in the spectrum of  $(\text{CH}_3)_2\text{O}---\text{DCl}$ , so there cannot be any

significant coupling between the ethereal modes and the modes involving primarily motion of the hydrogen-bonded hydrogen atom. The spectrum between 800 and 1500  $\text{cm}^{-1}$  of  $(\text{CD}_3)_2\text{O}---\text{HCl}$  was not studied in as much detail as that of  $(\text{CH}_3)_2\text{O}---\text{HCl}$  but four bands, centered at 816, 925, 1057, and 1160  $\text{cm}^{-1}$ , with approximate half-widths of 20, 40, 25, and 30  $\text{cm}^{-1}$ , respectively, were clearly evident and were close in frequency to four corresponding bands in the spectrum of dimethyl ether- $\text{d}_6$ . The frequencies of the bands in the spectra of  $(\text{CH}_3)_2\text{O}---\text{HCl}$ ,  $(\text{CD}_3)_2\text{O}---\text{HCl}$  and the ethers are presented in Table 1, along with their assignment (95,96).

Figure 14 shows two possible geometries for  $(\text{CH}_3)_2\text{O}---\text{HCl}$ . In structure I the hydrogen chloride molecule bonds to one of the lone pairs of electrons on the oxygen atom. The only element of symmetry in structure I is a mirror in the plane of the a- and c-principal axes of inertia and thus structure I has  $\text{C}_s$  symmetry. In structure II the hydrogen chloride molecule bonds simultaneously to both lone pairs of electrons on the oxygen atom and lies in the C-O-C plane of the ether molecule, forming a hydrogen-bonded molecule of  $\text{C}_{2v}$  symmetry. It has been suggested (74) that an analysis of the shape of the band due to the symmetric C-O stretching mode at 912  $\text{cm}^{-1}$  proves that the complex has  $\text{C}_s$  symmetry. To test the conclusion of reference 74, calculations were

TABLE 1

Frequencies <sup>a</sup> and Assignments <sup>b</sup> of Absorptions Between  
800 and 1500  $\text{cm}^{-1}$  in  $(\text{CH}_3)_2\text{O}---\text{HCl}$ ,  $(\text{CD}_3)_2\text{O}---\text{HCl}$  and  
the Free Ethers

| $(\text{CH}_3)_2\text{O}$ | $(\text{CH}_3)_2\text{O}---\text{HCl}$ | Assignment                                     |
|---------------------------|--|--|
| 934                       | 912                                    | Symmetric C-O<br>Stretch                       |
| 1102                      | 1097                                   | } $\text{CH}_3$ Rock + Asym-<br>metric Stretch |
| 1179                      | 1171                                   |  |
| 1245                      | 1248                                   | $\text{CH}_3$ Rock                             |
| 1462                      | 1465                                   | $\text{CH}_3$ Deformations                     |
| $(\text{CD}_3)_2\text{O}$ | $(\text{CD}_3)_2\text{O}---\text{HCl}$ | Assignment                                     |
| 829                       | 816                                    | Symmetric C-O<br>Stretch                       |
| 931                       | 925                                    | $\text{CD}_3$ Rock                             |
| ~1060                     | 1057                                   | $\text{CD}_3$ Deformations                     |
| 1163                      | 1160                                   | Asymmetric C-O<br>Stretch                      |

a) Frequencies are reported in  $\text{cm}^{-1}$ .

b) References 95 and 96.

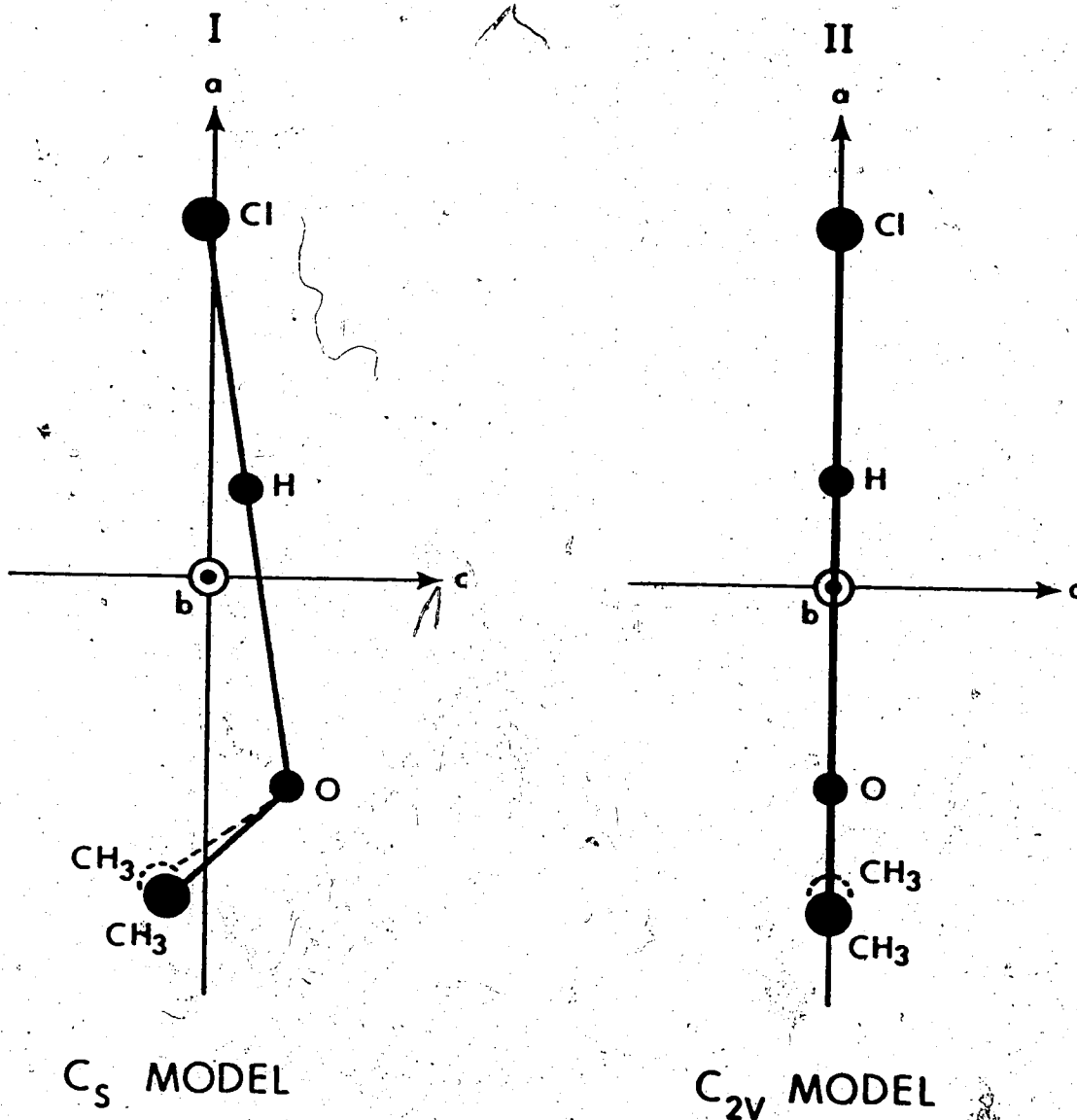


FIGURE 14. The two possible geometries for the  $(\text{CH}_3)_2\text{O}\cdots\text{HCl}$  molecule. The axes marked a, b and c are the principal axes of inertia.

made to determine the band shapes of the C-O symmetric stretching mode using both the  $C_s$  and  $C_{2v}$  models. For each model the geometry of the ether part of  $(CH_3)_2O\cdots HCl$  was assumed to be that reported by Buikis *et al* (102) for free dimethyl ether- $h_6$ , and the O $\cdots$ H and O $\cdots$ Cl distances were assumed to be 1.7 Å and 3.1 Å, respectively. The Schachtschneider program, 'CART' (103), and values of the atomic masses tabled in reference 101 were used to calculate the rotational constants (104) for each model. These constants, A, B, and C, respectively, are proportional to the inverse of the moments of inertia about the a-, b-, and c- principal axes of rotation which are defined in Figure 14 for each model. For the  $C_s$  model the values of the constants are  $A = 0.316$ ,  $B = 0.068$ ,  $C = 0.058 \text{ cm}^{-1}$  and for the  $C_{2v}$  model the constants are  $A = 0.337$ ,  $B = 0.061$ ,  $C = 0.053 \text{ cm}^{-1}$ . Thus both models are asymmetric rotors but closely approximate prolate symmetric top molecules.

For the  $C_{2v}$  model, the C-O symmetric stretching vibration would cause a dipole moment change along the a- principal axis of rotation and hence an A-type infrared absorption band (104) is predicted. The analogous mode for the  $C_s$  model would cause a dipole moment change in the ac plane, with almost equal components along the a- and c- axes, and hence an AC hybrid band (104,105) is predicted. Ueda and Shimanouchi (105) have calculated the shapes of A-, B-, and C-type infrared absorption

bands for forty different asymmetric rotors which are characterized according to their molecular shape by two parameters, X and Y, where

$$X = 2C/B \quad (1)$$

$$\text{and } Y = 1 - (C/A) - (C/B). \quad (2)$$

Substitution of the appropriate rotational constants into these equations yields  $X = 1.74$  and  $Y = -0.026$  for the  $C_{2v}$  model and  $X = 1.72$  and  $Y = -0.036$  for the  $C_s$  model. The values of these parameters in each case most closely approximate those of rotor number 8 of reference 105. The A-, B-, and C-type infrared absorption bands predicted for this rotor are shown in box I of Figure 15, as reproduced from reference 105. The A-type band, predicted for the  $C_{2v}$  model, has a PQR structure with a prominent Q branch. An AC hybrid band, such as that predicted for the  $C_s$  model, can be constructed by the superposition of A- and C-type bands. Since both the A- and C-type bands have PQR structures, the AC hybrid band will also have P, Q and R branches, and no distinction between the  $C_s$  and  $C_{2v}$  models can be made on the basis of band shape.

A more detailed look at the shapes of the bands predicted for the two models of  $(CH_3)_2O---HCl$  is warranted because the bands shown in box I of Figure 15 were calculated with the assumption that the sum of the rotational

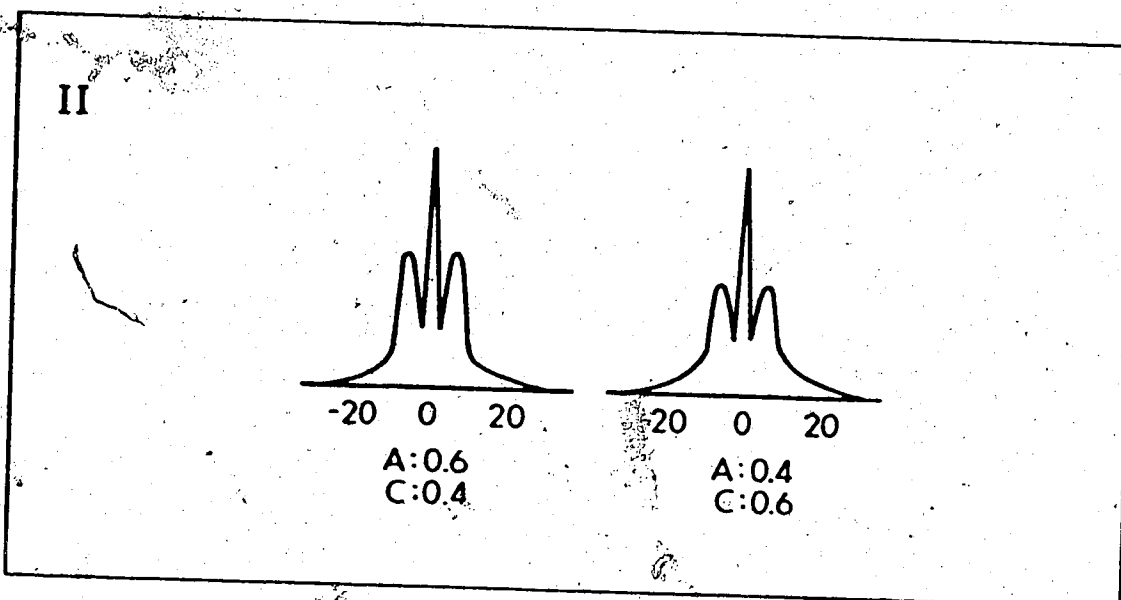
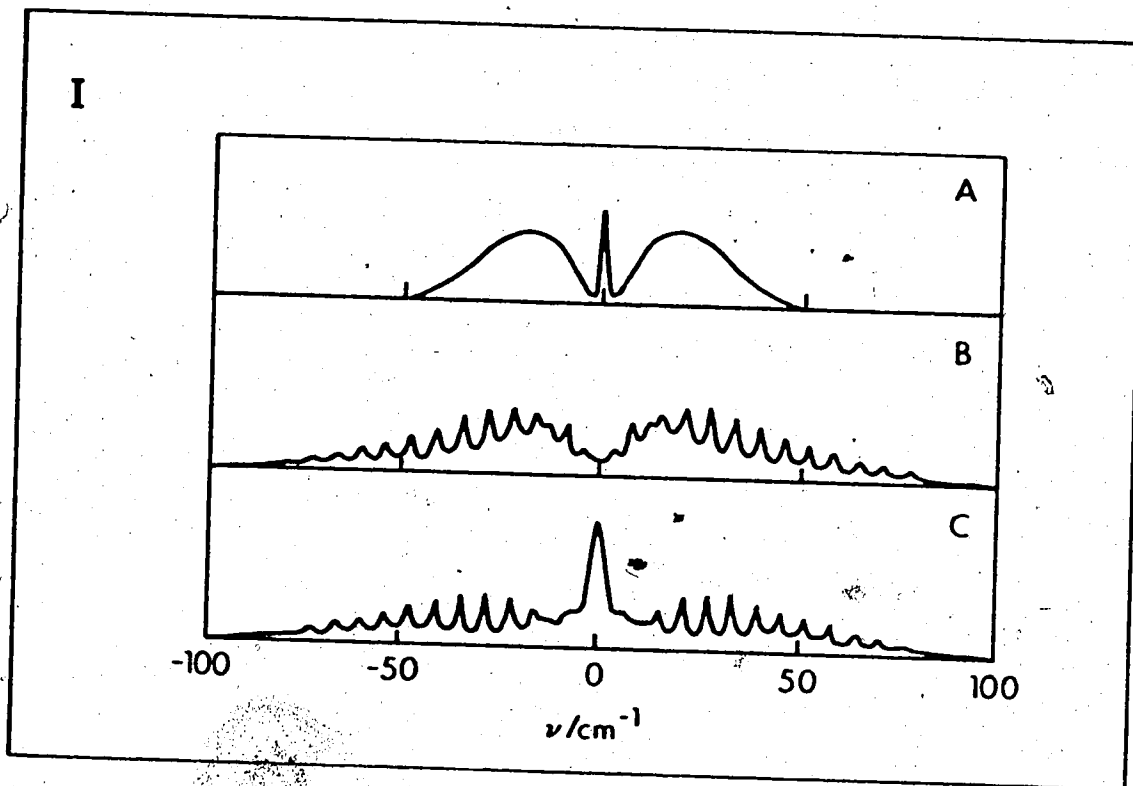


FIGURE 15. Box I, A-, B- and C- type bandshapes predicted for  $(\text{CH}_3)_2\text{O} \cdots \text{HCl}$ ; box II, typical AC hybrid bands of gauche-1,2-dichloroethane. These bands have been reproduced from reference 105.

constants,  $A + B + C$ , was  $5 \text{ cm}^{-1}$ , which is of the order of ten times the sum calculated for either model of  $(\text{CH}_3)_2\text{O}---\text{HCl}$ . As a result, the bands shown in box I of Figure 15 have much larger PR separations and therefore larger half-widths than would be expected for bands in the spectrum of  $(\text{CH}_3)_2\text{O}---\text{HCl}$ . The PR separations and half-widths of bands due to  $(\text{CH}_3)_2\text{O}---\text{HCl}$  can be calculated since, at a given temperature,  $T$ , they are approximately proportional to  $\sqrt{(A + B + C)/T}$ . Therefore, the PR separation of an A-type band in the spectrum of the  $C_{2v}$  model, for which  $A + B + C = 0.451 \text{ cm}^{-1}$ , would be that measured from the A-type band in box I of Figure 15, which is about  $40 \text{ cm}^{-1}$ , multiplied by  $\sqrt{0.451/5}$ . This yields a value of about  $12 \text{ cm}^{-1}$  and thus the separation of the Q branch from either the P or R branch should ideally be one half of this value, or about  $6 \text{ cm}^{-1}$ . The half-width of the A-type band shown in box I of Figure 15 is about  $70 \text{ cm}^{-1}$  and therefore the half-width of an A-type band in the spectrum of the  $C_{2v}$  model of  $(\text{CH}_3)_2\text{O}---\text{HCl}$  would be about  $20 \text{ cm}^{-1}$ . The AC hybrid band predicted for the C-O symmetric stretching mode of the  $C_s$  model should correspond closely to the AC hybrid band calculated in reference 105 for gauche-1,2-dichloroethane. This molecule has the rotational constants  $A = 0.3169 \text{ cm}^{-1}$ ,  $B = 0.0784 \text{ cm}^{-1}$  and  $C = 0.0675 \text{ cm}^{-1}$ , which yield  $X = 1.72$  and  $Y = -0.074$ . These values are



very close to those calculated for the  $C_s$  model of  $(CH_3)_2O---HCl$  and the sum of the rotational constants of gauche -1,2-dichloroethane is very close to the sum of the rotational constants of the  $C_s$  model, being 0.4628 and  $0.442 \text{ cm}^{-1}$ , respectively. Box II of Figure 15 displays two AC hybrid bands of gauche 1,2-dichloroethane with A:C ratios of 6:4 and 4:6. The AC hybrid band due to the symmetric C-O stretching mode in the  $C_s$  model is predicted to have an A:C ratio of approximately unity and should, therefore, correspond closely to the bands shown in box II of Figure 15. Each of these bands has a prominent Q branch, a PR separation of about  $10 \text{ cm}^{-1}$  and a half-width of about  $25 \text{ cm}^{-1}$ .

The half-widths of the bands predicted for both the  $C_s$  and  $C_{2v}$  models are close to the observed value of  $20 \text{ cm}^{-1}$ , but neither model predicts band shapes which correspond at all to the shape of the band at  $912 \text{ cm}^{-1}$ , for which no P, Q or R branches are resolved. The failure to predict the observed band shape must be influenced by the rather high population of the excited states of the  $\nu_o$  and  $\nu_\beta$  modes which must exist in the temperature range studied. Thus, excitation of the symmetric C-O stretching vibration must take place simultaneously from a large number of vibrational states which differ only in the number of quanta of the  $\nu_o$  or  $\nu_\beta$  modes which have been excited. The  $\nu_o$  and  $\nu_\beta$  modes involve motion

of the hydrogen chloride molecule; large deviations from the equilibrium molecular geometry probably exist in these states. Transitions from these excited states should, then, give rise to significantly different band shapes from those predicted from the equilibrium geometry, and since the observed band is a superposition of the bands due to these transitions, any PQR structure may well be lost.

### 3.5 Infrared Spectra above $1500\text{ cm}^{-1}$

In Figure 16, curve A shows the spectrum between  $2200$  and  $2800\text{ cm}^{-1}$  of a mixture of 250 Torr of dimethyl ether- $\text{h}_6$  with 250 Torr of hydrogen chloride at  $+35^\circ\text{C}$  and curve B shows the spectrum of a mixture of 100 Torr of dimethyl ether- $\text{h}_6$  with 100 Torr of hydrogen chloride at  $-30^\circ\text{C}$ . Each spectrum was recorded with enough ether, at  $+35^\circ\text{C}$  in the reference beam of the spectrophotometer to cancel the free ether absorption, which is shown in curve C. The sharp lines visible on the high frequency sides of the bands in curves A and B arise from free hydrogen chloride. The pressures of the components in the mixture at  $-30^\circ\text{C}$  were smaller than in the mixture at  $+35^\circ\text{C}$  but, as a result of the larger equilibrium constant for formation of  $(\text{CH}_3)_2\text{O}\cdots\text{HCl}$  at the lower temperature, the concentration of  $(\text{CH}_3)_2\text{O}\cdots\text{HCl}$  was approximately the same in both mixtures. Curve A displays a broad band with a half-width of about  $250\text{ cm}^{-1}$  and its absorption

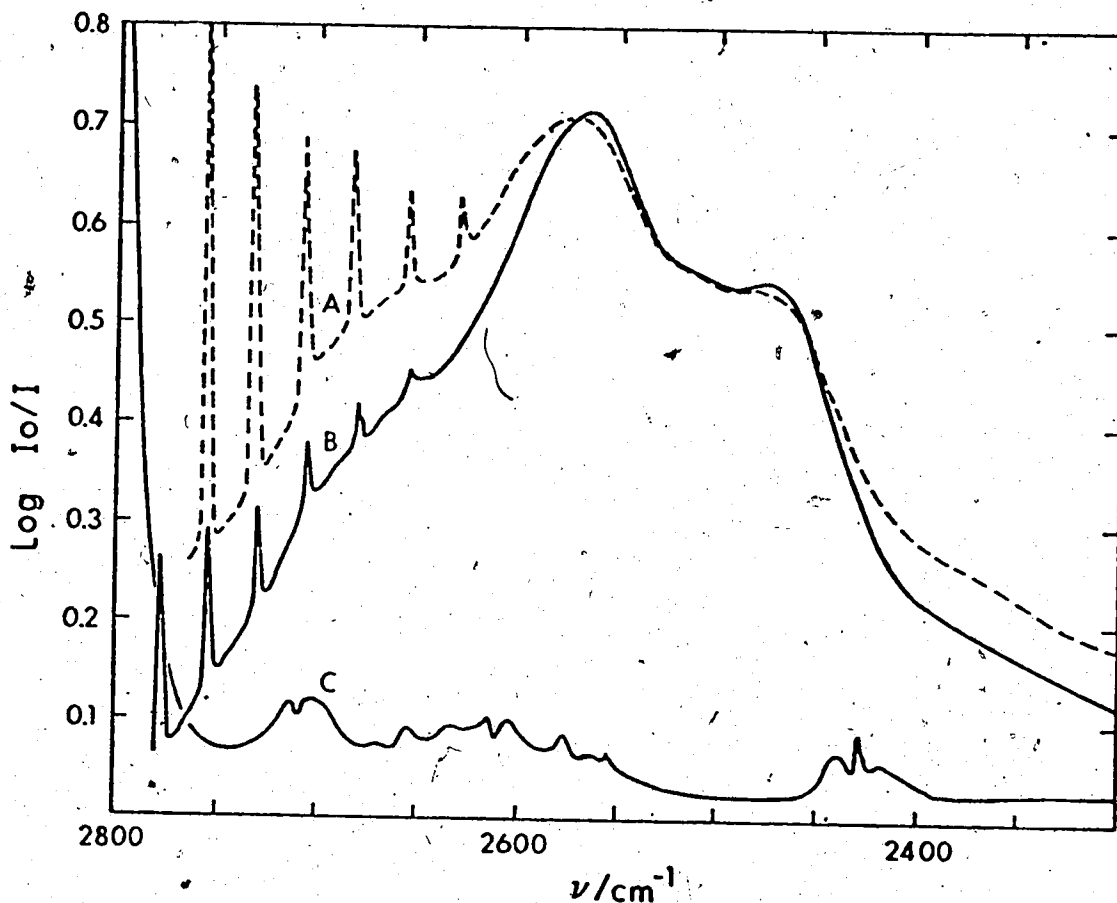


FIGURE 16. Infrared absorption by: 250 Torr of dimethyl ether-h<sub>6</sub> plus 250 Torr of hydrogen chloride at +35°C (curve A); 100 Torr of dimethyl ether-h<sub>6</sub> plus 100 Torr of hydrogen chloride at -30°C (curve B); 100 Torr of dimethyl ether-h<sub>6</sub> at +35°C (curve C). Curves A and B were recorded with 250 and 100 Torr, respectively, of dimethyl ether-h<sub>6</sub> at +35°C in a 10 cm. long cell in the reference beam.

maximum at  $2574 \text{ cm}^{-1}$ . Also evident are shoulders of approximately equal intensity at about  $2680$  and  $2480 \text{ cm}^{-1}$ , as well as a third, weak shoulder at about  $2360 \text{ cm}^{-1}$ . The shape of the band is identical to that reported by Bertie and Millen (73), who assigned the absorption maximum to the HCl stretching mode,  $\nu_s$ , and the three shoulders to various combination transitions of  $\nu_s$  with the hydrogen bond stretching mode,  $\nu_\sigma$ . Thus the shoulder at  $2680 \text{ cm}^{-1}$  was assigned to the sum band,  $\nu_s + \nu_\sigma$ , which represents the vibrational transition,  $[V_s = 0 \rightarrow 1, V_\sigma = 0 \rightarrow 1]$ . The shoulders at  $2480$  and  $2360 \text{ cm}^{-1}$  were assigned to the difference bands  $\nu_s - \nu_\sigma$ , i.e. the transition  $[V_s = 0 \rightarrow 1, V_\sigma = 1 \rightarrow 0]$ , and  $\nu_s - 2\nu_\sigma$ , the transition  $[V_s = 0 \rightarrow 1, V_\sigma = 2 \rightarrow 0]$ , respectively. On the basis of this assignment one expects the intensities of the features at  $2480$  and  $2360 \text{ cm}^{-1}$  to decrease relative to the absorption maximum as the sample temperature is lowered, since difference transitions originate in excited vibrational energy levels (42). The relative intensities of the features at  $2574$  and  $2680 \text{ cm}^{-1}$  should show little temperature dependence if the above assignment is correct, since both features are assigned to transitions originating in the vibrational ground state. Comparison of curves A and B shows that the weak feature at  $2360 \text{ cm}^{-1}$  is less intense relative to the absorption maximum at  $-30^\circ\text{C}$  than at  $+35^\circ\text{C}$ , which is consistent with its assignment to a difference

band. However, the intensity of the shoulder at  $2480\text{ cm}^{-1}$  does not appear to be dependent upon the temperature although the entire portion of the band to high frequency of the absorption maximum has lower intensity relative to that of the maximum at  $-30^\circ\text{C}$  than at  $+35^\circ\text{C}$ . These observations contradict the assignment of the  $2680\text{ cm}^{-1}$  feature to a simple sum band and the  $2480\text{ cm}^{-1}$  feature to a difference band.

In Figure 17, curve A shows the spectrum between  $2200$  and  $2800\text{ cm}^{-1}$  of a mixture of 250 Torr of dimethyl ether- $\text{d}_6$  with 250 Torr of hydrogen chloride at  $+35^\circ\text{C}$  and curve B shows the spectrum of a mixture of 100 Torr of dimethyl ether- $\text{d}_6$  with 100 Torr of hydrogen chloride at  $-30^\circ\text{C}$ . The absorption shown in curve A is identical to that reported by Bertie and Millen (73) for  $(\text{CD}_3)_2\text{O}---\text{HCl}$ . Comparison of curves A and B shows that the effect of sample temperature on the absorption by  $(\text{CD}_3)_2\text{O}---\text{HCl}$  is the same as that observed for  $(\text{CH}_3)_2\text{O}---\text{HCl}$ . The only differences between these spectra and those shown in Figure 16 are that for  $(\text{CD}_3)_2\text{O}---\text{HCl}$  the  $2480\text{ cm}^{-1}$  feature is slightly better resolved as a peak at the lower temperature, the absorption maximum is slightly narrower than for  $(\text{CH}_3)_2\text{O}---\text{HCl}$  and an absorption corresponding to the weak feature at  $2360\text{ cm}^{-1}$  in  $(\text{CH}_3)_2\text{O}---\text{HCl}$  is not visible. The latter difference is due to overlapping absorption by the C-D stretching modes (95,96) in both the free dimethyl ether- $\text{d}_6$  (curve C) and  $(\text{CD}_3)_2\text{O}---\text{HCl}$ . The

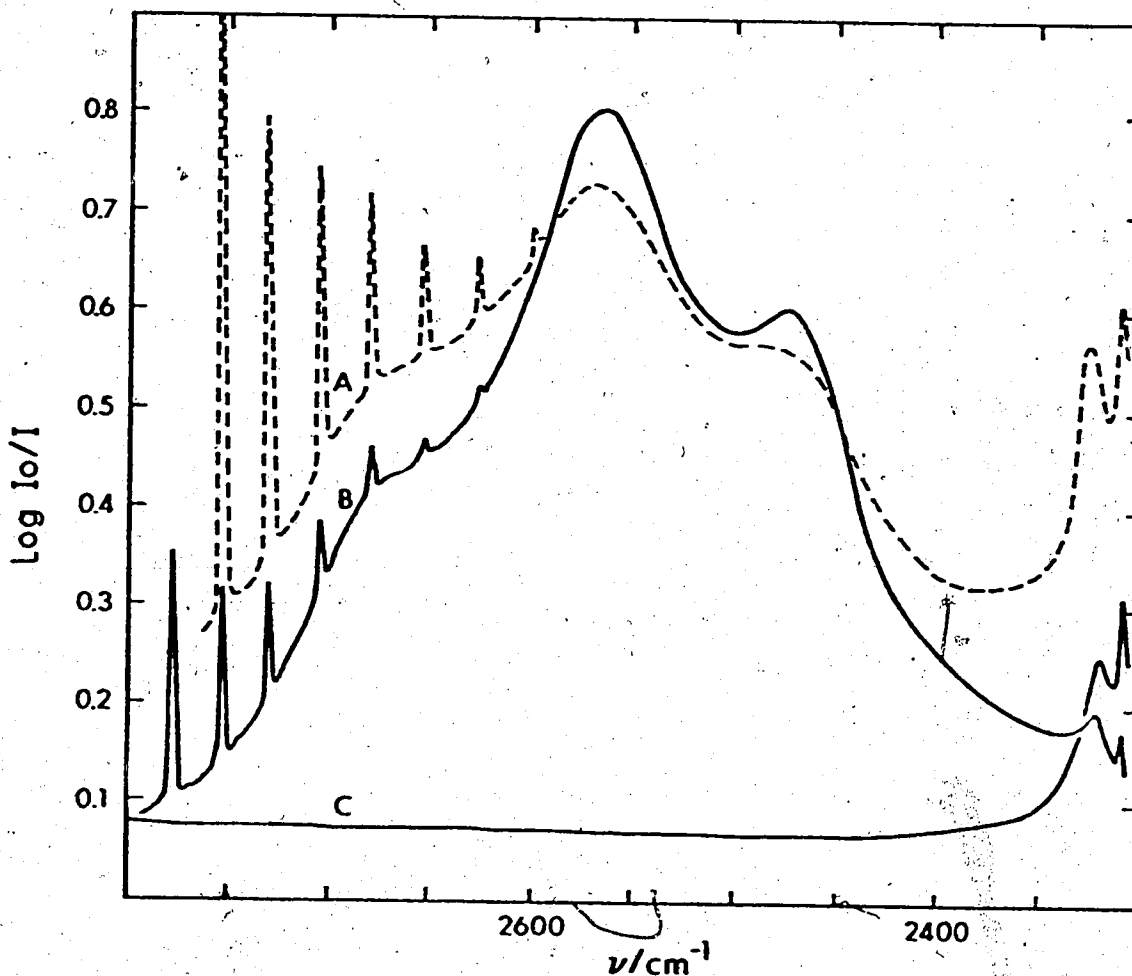


FIGURE 17. Infrared absorption by: 250 Torr of dimethyl ether- $d_6$  plus 250 Torr of hydrogen chloride at  $+35^\circ\text{C}$  (curve A); 100 Torr of dimethyl ether- $d_6$  plus 100 Torr of hydrogen chloride at  $-30^\circ\text{C}$  (curve B); 50 Torr of dimethyl ether- $d_6$  at  $+35^\circ\text{C}$  (curve C). Curves A and B were recorded with 250 and 100 Torr, respectively of dimethyl ether- $d_6$  at  $+35^\circ\text{C}$  in a 10 cm. long cell in the reference beam.

smaller width of the absorption maximum of  $(\text{CD}_3)_2\text{O}---\text{HCl}$  may well be due to the moments of inertia of this molecule being larger than those of  $(\text{CH}_3)_2\text{O}---\text{HCl}$ , and causing a narrower rotational envelope for each vibrational transition.

Since the shape of the band at the two temperatures is independent of the ether used, the general interpretation of the structure of the band given by Bertie and Millen (73), that it is due to sum and difference bands of the type  $\nu_s \pm n\nu_\sigma$  with no influence from Fermi resonance, must be correct. However, on the basis of the experimental evidence presented above, it is more reasonable to assign the  $2480 \text{ cm}^{-1}$  feature to  $\nu_s$  and the absorption maximum at  $2574 \text{ cm}^{-1}$  to  $\nu_s + \nu_\sigma$ . Thus the sum band,  $\nu_s + 2\nu_\sigma$ , must contribute to the intensity at  $2680 \text{ cm}^{-1}$  and the difference band,  $\nu_s - \nu_\sigma$ , must contribute to the  $2360 \text{ cm}^{-1}$  absorption. The observed decrease in intensity at  $2680 \text{ cm}^{-1}$  with decrease in temperature can be explained by postulating that hot transitions of  $\nu_s + 2\nu_\sigma$  of the type  $[\nu_s = 0 \rightarrow 1, \nu_\sigma = n \rightarrow n + 2]$ , where  $n$  is a non-zero integer, make an unusually large contribution to the intensity. In a study concurrent with but independent of this work, Lassegues, Huong and Lascombe (106,107) have quantitatively studied the  $\nu_s$  band in  $(\text{CH}_3)_2\text{O}---\text{HCl}$  between  $-50^\circ\text{C}$  and  $+90^\circ\text{C}$ , and have shown that the temperature dependence requires an assignment of this sort. These authors

observed that the intensities of the features at 2360 and 2680  $\text{cm}^{-1}$  show temperature dependencies which are compatible with transitions starting in levels which are higher in energy by approximately 1.8 quanta of  $\nu_{\sigma}$  than the starting levels for the transitions associated with the 2480 and 2574  $\text{cm}^{-1}$  features. This implies that, if the transitions [ $V_s = 0 \rightarrow 1, V_{\sigma} = 0 \rightarrow 0$ ] and [ $V_s = 0 \rightarrow 1, V_{\sigma} = 0 \rightarrow 1$ ] make the major contribution to the intensity at 2480 and 2574  $\text{cm}^{-1}$ , respectively, the hot transitions [ $V_s = 0 \rightarrow 1, V_{\sigma} = 2 \rightarrow 4$ ] and [ $V_s = 0 \rightarrow 1, V_{\sigma} = 2 \rightarrow 1$ ], must make the major contribution to the intensity at 2680 and 2360  $\text{cm}^{-1}$ , respectively.

It seems clear, however, that these four transitions, each of which should have a rotational envelope of about 25-30  $\text{cm}^{-1}$  (Section 3.4), cannot account for the diffuseness of the entire band unless some special mechanism, such as an abnormally large effect of centrifugal distortion (106), broadens the rotational envelope of each transition. Any such effect can only be operative in the  $V_s = 1$  (and possibly  $V_b = 1$  and  $V_t = 1$ ) states, because the half-widths of the bands due to the ethereal modes and  $\nu_{\sigma}$ , for which  $V_s = 0$  (and  $V_b = V_t = 0$ ), can be explained without invoking it. It seems more likely that, in addition to the four transitions proposed above, transitions starting in different  $V_{\sigma}$  levels also contribute significantly to the intensity of each sub-band and, due to mechanical anharmonicity, the intensity can be



spread out over a large frequency range. It is also possible that hot transitions of the  $\nu_s$  vibration from excited  $\nu_\beta$  states, which have been shown to be important in the interpretation of the spectra of  $\text{CH}_3\text{CN}---\text{HCl}$  (54) and  $\text{CH}_3\text{CN}---\text{HF}$  (55), contribute to the diffuseness of the  $\nu_s$  band in  $(\text{CH}_3)_2\text{O}---\text{HCl}$ . It is probable that these hot transitions are responsible for the slight shift of the  $\nu_s$  band and sharpening of the  $2480\text{ cm}^{-1}$  feature at the lower temperature.

The assignment of the absorption maximum to  $\nu_s + \nu_\sigma$  rather than to  $\nu_s$  and the implication that hot transitions contribute significantly to the intensity of the whole band can be rationalized in terms of the vibrational Franck-Condon effect (Section 1.6). From a consideration of the observed band and its assignment, reasonable potential energy curves, such as those shown in Figure 18, can be drawn to illustrate this effect in  $(\text{CH}_3)_2\text{O}---\text{HCl}$ . The energy separation of the curves, given in  $\text{cm}^{-1}$  for easy comparison with vibrational frequencies, is about  $2500\text{ cm}^{-1}$  close to the minima and  $2886\text{ cm}^{-1}$ , equal to the vibrational frequency of free hydrogen chloride (91), at large O---Cl distances. The dissociation energy of  $2485\text{ cm}^{-1}$  is the equivalent of the mean value of 7.1 kcal/mole reported by Govil, Clague and Bernstein (84). The assignment of  $\nu_s$  at  $2480\text{ cm}^{-1}$  and of  $\nu_s - \nu_\sigma$  at  $2360\text{ cm}^{-1}$  yields a value of  $120\text{ cm}^{-1}$  for the separation of the  $\nu_\sigma = 0$  and

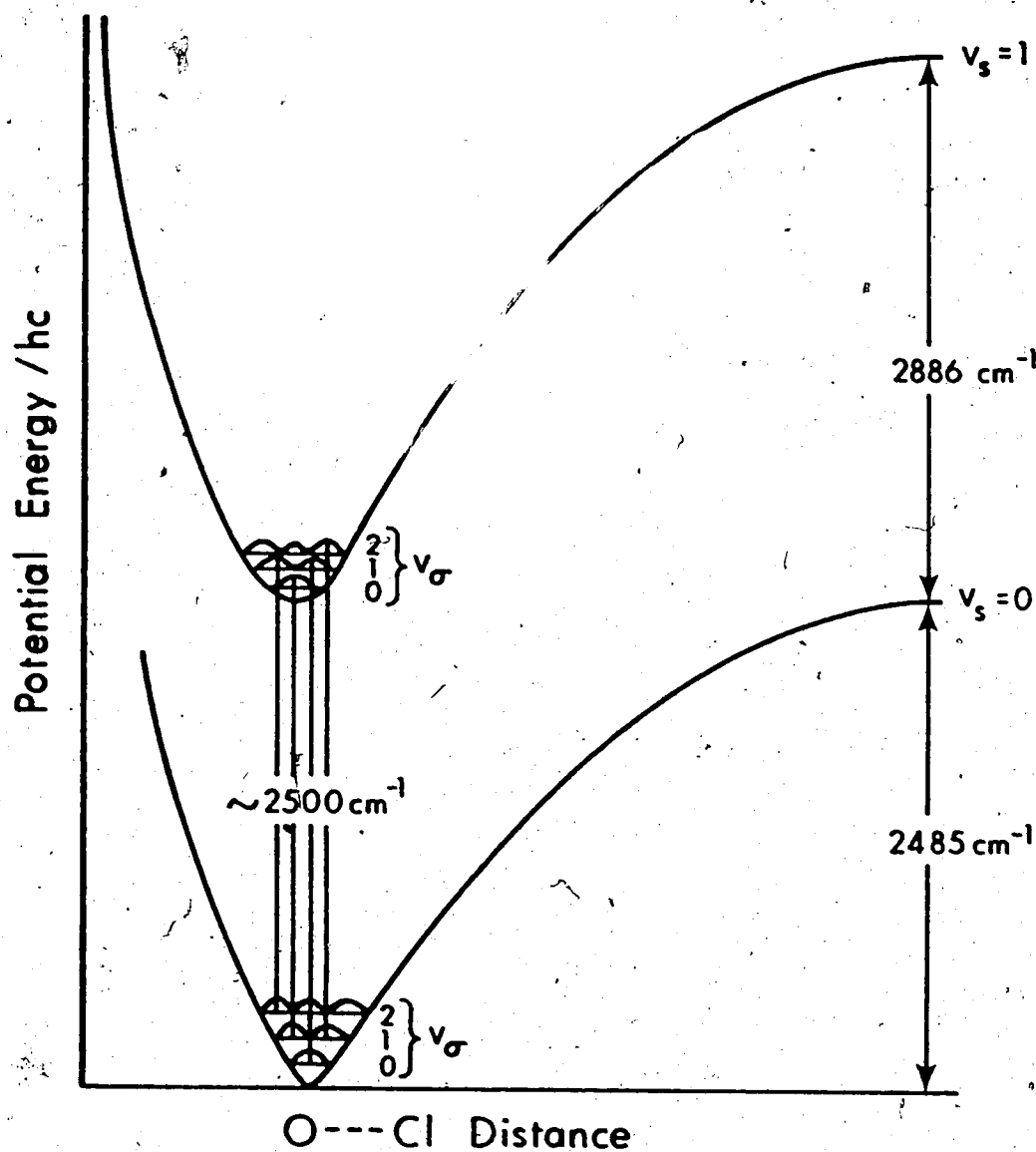


**FIGURE 18.** The Stepanov energy level scheme for the interaction of the  $v_s$  and  $v_\sigma$  modes in  $(\text{CH}_3)_2\text{O}\cdots\text{HCl}$ .  $v_s$  and  $v_\sigma$  are the quantum numbers for the HCl and hydrogen bond stretching vibrations, respectively, and the curves drawn on the energy levels are the squares of the wave functions.

$V_{\sigma} = 1$  levels when  $V_s = 0$ , which agrees very well with the observed frequency at  $119 \text{ cm}^{-1}$ . When  $V_s = 1$ , the separation is  $94 \text{ cm}^{-1}$  if the assignment of the  $2574 \text{ cm}^{-1}$  feature is correct. Thus the force constant for the  $\nu_{\sigma}$  mode must be smaller when  $V_s = 1$  than when  $V_s = 0$ , which implies that, although the potential curve for the  $V_s = 1$  state has a deeper minimum than that for the  $V_s = 0$  state, the minimum for the  $V_s = 1$  state is broader, so that the curvature is less. Since the intensity of  $\nu_s + \nu_{\sigma}$  is greater than that of  $\nu_s$ , the upper minimum must occur at a different O---Cl distance than the lower minimum, causing the transition [ $V_s = 0 \rightarrow 1$ ,  $V_{\sigma} = 0 \rightarrow 1$ ] to be more probable than the transition [ $V_s = 0 \rightarrow 1$ ,  $V_{\sigma} = 0 \rightarrow 0$ ]. The different equilibrium distances for the two  $V_s$  states can also cause transitions starting in excited  $V_{\sigma}$  levels to be more probable than the corresponding transition from the ground state.

Figures 19 and 20 show spectra between  $1500$  and  $2000 \text{ cm}^{-1}$  of 1:1 mixtures of deuterium chloride with dimethyl ether- $\text{h}_6$  and with dimethyl ether- $\text{d}_6$ , respectively, at  $-30^{\circ}\text{C}$  (curves A) and at  $+30^{\circ}\text{C}$  (curves B). The spectra were recorded with enough of the appropriate free ether in the reference beam of the spectrometer to cancel the absorption by the free ether, which is shown in curves C. Absorption by free deuterium chloride was not subtracted from these spectra and appears as the rather sharp lines on the portion of the bands above  $1850 \text{ cm}^{-1}$ . The broad

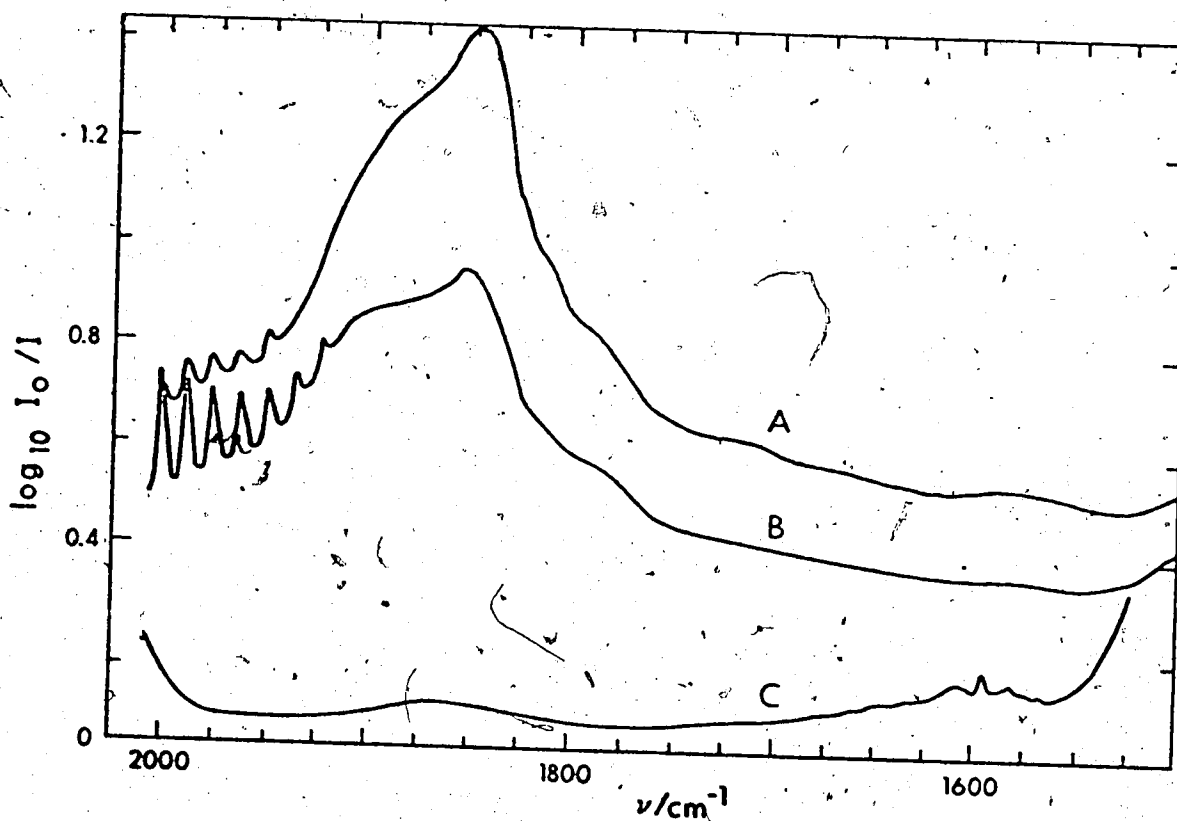
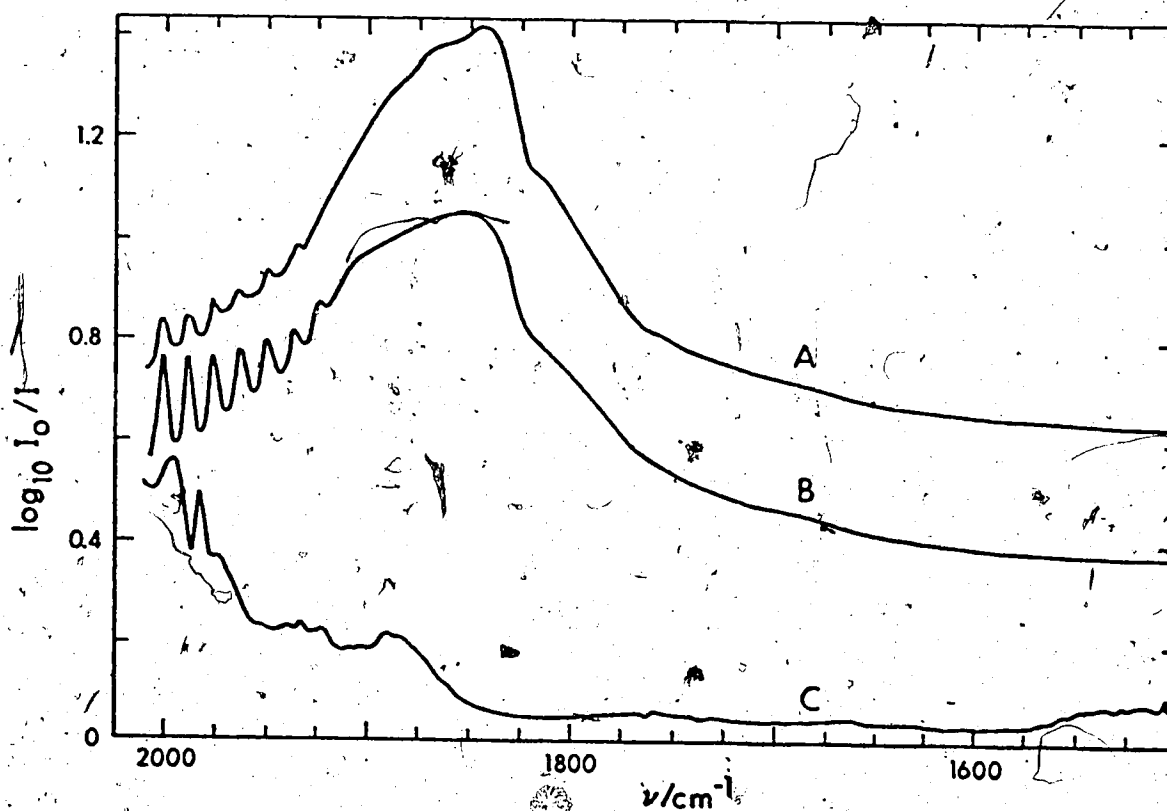


FIGURE 19. Infrared absorption by: 100 Torr of dimethyl ether- $\text{h}_6$  plus 100 Torr of deuterium chloride at  $-30^\circ\text{C}$  (curve A); 250 Torr of dimethyl ether- $\text{h}_6$  plus 250 Torr of deuterium chloride at  $+30^\circ\text{C}$  (curve B); 250 Torr of dimethyl ether- $\text{h}_6$  at  $+30^\circ\text{C}$  (curve C). Curves A and B were recorded with 100 and 250 Torr, respectively, of dimethyl ether- $\text{h}_6$  at  $+30^\circ\text{C}$  in a 10 cm. long cell in the reference beam.



**FIGURE 20.** Infrared absorption by: 100 Torr of dimethyl ether-d<sub>6</sub> plus 100 Torr of deuterium chloride at -30°C (curve A); 250 Torr of dimethyl ether-d<sub>6</sub> plus 250 Torr of deuterium chloride at +30°C (curve B); 250 Torr of dimethyl ether-d<sub>6</sub> at +30°C (curve C). Curves A and B were recorded with 100 and 250 Torr, respectively, of dimethyl ether-d<sub>6</sub> at +30°C in a 10 cm. long cell in the reference beam.

bands which are evident in curves B of Figures 19 and 20 have half-widths of about  $100 \text{ cm}^{-1}$  and their absorption maxima at  $1850 \text{ cm}^{-1}$  but display considerably different features. In  $(\text{CH}_3)_2\text{O} \cdots \text{DCl}$  (Figure 19) this band has shoulders at 1905, 1810 and  $1785 \text{ cm}^{-1}$  in addition to weak absorptions at 1700 and  $1580 \text{ cm}^{-1}$ . In  $(\text{CD}_3)_2\text{O} \cdots \text{DCl}$  (Figure 20) the band has shoulders at 1900, 1800 and  $1680 \text{ cm}^{-1}$ . Curves A of Figures 19 and 20 show that, although at the lower temperature the absorption bands shift to lower frequency by about  $5 \text{ cm}^{-1}$ , all of the features present at  $+30^\circ\text{C}$  are also present at  $-30^\circ\text{C}$ . These features are, however, less intense relative to the absorption maximum at  $-30^\circ\text{C}$  than at  $+30^\circ\text{C}$ . Curve A in Figure 20 also shows that the band in  $(\text{CD}_3)_2\text{O} \cdots \text{DCl}$  at  $-30^\circ\text{C}$  has an additional shoulder at about  $1870 \text{ cm}^{-1}$ .

The absorptions between  $1700$  and  $2000 \text{ cm}^{-1}$  in the spectra of mixtures of deuterium chloride and ethers have been assigned by Bertie and Millen (25) to the DCl stretching mode,  $\nu_s$ , in the 1:1 complex of deuterium chloride with the appropriate ether. These authors noted that the  $\nu_s$  bands of several ether-deuterium chloride hydrogen-bonded molecules are similar to those of the ether-hydrogen chloride molecules, with the side bands due to combinations of  $\nu_s$  with  $\nu_0$  weaker for the deuterated acid. However, the details of these bands in  $(\text{CH}_3)_2\text{O} \cdots \text{DCl}$  and  $(\text{CD}_3)_2\text{O} \cdots \text{DCl}$  cannot be entirely explained in this way

and there are differences between these two bands which must be explained. The feature at  $1870\text{ cm}^{-1}$  is present only in the spectrum of  $(\text{CD}_3)_2\text{O}---\text{DCl}$  (Figure 20) and must, therefore, arise from an ethereal mode. It can be attributed to the summation transition due to the combination of the symmetric C-O stretching mode at  $816\text{ cm}^{-1}$  with a  $\text{CD}_3$  deformation mode at  $1057\text{ cm}^{-1}$  (Table 1). This transition absorbs weakly in the spectrum of the pure ether and is, therefore, probably enhanced in intensity in the spectrum of  $(\text{CD}_3)_2\text{O}---\text{DCl}$  by a Fermi resonance interaction (Section 1.6) with the  $\nu_s$  mode. The shoulder close to  $1800\text{ cm}^{-1}$  appears as a single feature in the spectrum of  $(\text{CD}_3)_2\text{O}---\text{DCl}$  but as a doublet in the spectrum of  $(\text{CH}_3)_2\text{O}---\text{DCl}$ . This doublet may be due to a Fermi resonance type of interaction between the first overtone of the symmetric C-O stretching mode at  $912\text{ cm}^{-1}$  (Table 1), and the mode giving rise to the absorption close to  $1800\text{ cm}^{-1}$ , causing the single shoulder to split into two. No overtone or combination transition in  $(\text{CD}_3)_2\text{O}---\text{DCl}$  is available for such an interaction close to  $1800\text{ cm}^{-1}$  and thus no splitting of this shoulder occurs in the spectrum of this molecule. The final difference between the spectra of  $(\text{CH}_3)_2\text{O}---\text{DCl}$  and  $(\text{CD}_3)_2\text{O}---\text{DCl}$  is the presence of a feature at  $1580\text{ cm}^{-1}$  in the spectrum of the former molecule. A band at this frequency is also evident in the spectrum of  $(\text{CH}_3)_2\text{O}---\text{HCl}$  and undoubtedly corres-

ponds to a weak band at essentially the same frequency in the spectrum of dimethyl ether- $h_6$  (Figure 19, curve C). This band must also have enhanced intensity in the spectra of the hydrogen-bonded molecules as it would otherwise not have been observed because of the ether in the reference beam.

It is clear that the  $\nu_s$  bands in the spectra of the deuterium chloride complexes differ significantly from those in the spectra of the hydrogen chloride complexes in a way which is not simply due to the combination bands,  $\nu_s \pm n\nu_o$ , being weaker for the deuterated acids (25). The absorption maximum in the spectrum of  $(CH_3)_2O \cdots DCl$  or  $(CD_3)_2O \cdots DCl$  is accompanied by shoulders about  $50 \text{ cm}^{-1}$  to either side and, in view of the assignment of the  $\nu_\beta$  modes at about  $50 \text{ cm}^{-1}$  (Section 3.3), it is natural to assign the maximum to  $\nu_s$  and the shoulders to sum and difference transitions of the type  $\nu_s \pm \nu_\beta$ . The observed decrease in intensity with decreasing temperature of the feature at  $1900 \text{ cm}^{-1}$ , assigned to  $\nu_s + \nu_\beta$ , is explained by assuming that transitions of the type  $\nu_s + (n+1)\nu_\beta - n\nu_\beta$  contribute significantly to this intensity through the vibrational Franck-Condon effect. The assignment of  $\nu_s$  at  $1850 \text{ cm}^{-1}$  yields 1.340 for the ratio of the frequencies of  $\nu_s$  in the hydrogen chloride and deuterium chloride complexes. This value indicates that the anharmonicity of  $\nu_s$  in these complexes is greater than that of the cor-



responding mode in the ices, where the ratio is 1.354 (108), but is not extraordinarily large.

It is noteworthy that 1:1 mixtures of ether and hydrogen chloride at  $-30^{\circ}\text{C}$ , with a total pressure of 200 Torr, and at  $+35^{\circ}\text{C}$ , with a total pressure of 500 Torr, gave rise to  $\nu_s$  bands with approximately the same integrated absorbances but identical mixtures of ether with deuterium chloride always gave rise to  $\nu_s$  bands which were more intense at the lower temperature. This suggests that there is a slight increase in the temperature dependence of the equilibrium constant for formation of the hydrogen-bonded molecule when deuterium chloride is used in place of hydrogen chloride in the mixtures, and therefore, that  $\Delta H$ , the enthalpy change for formation of the hydrogen bond, is larger for  $(\text{CH}_3)_2\text{O}---\text{DCl}$  than for  $(\text{CH}_3)_2\text{O}---\text{HCl}$ . Unfortunately, no accurate computations of the heats of formation of these molecules are possible from the spectra presented above since neither the amounts of the free components in the mixtures nor the intensities are known accurately.

### 3.6 Relative Intensities of the Bands

In Table 2 the frequencies and approximate relative intensities of the bands in the spectrum of  $(\text{CH}_3)_2\text{O}---\text{HCl}$  are presented. Since the most intense band is that due to  $\nu_s$ , its intensity is given an arbitrary value of 100, so that the values for the intensities of the other bands

TABLE 2

Frequencies and Relative Intensities of  
Absorption Bands in  $(\text{CH}_3)_2\text{O}\cdots\text{HCl}$

| $\nu/\text{cm}^{-1}$ | Assignment                               | Intensity<br>(Arbitrary Units) |
|----------------------|--|--------------------------------|
| 2675                 | HCl stretch,<br>$\nu_s$                  | 100.0                          |
| 2574                 |  |                                |
| 2480                 |  |                                |
| ~2360                |  |                                |
| 1465                 | $\text{CH}_3$ deformation                | 5.8                            |
| 1248                 | $\text{CH}_3$ rock                       | 0.5                            |
| 1171                 | $\text{CH}_3$ rock<br>+ asym. CO stretch | 18.0                           |
| 1097                 |  |                                |
| 912                  | Symm. CO stretch                         | 10.0                           |
| 790                  | $2\nu_b, 2\nu_t$                         | 0.5                            |
| 570                  | O---H-Cl deformation $\nu_b, \nu_t$      | 3.0 <sup>a</sup>               |
| 525                  |  |                                |
| 470                  |  |                                |
| 415                  | C-O-C deformation                        |                                |
| 119                  | O--H stretch $\nu_\sigma$                | 0.3                            |

a) The intensity was measured for  $(\text{CD}_3)_2\text{O}\cdots\text{HCl}$

can be regarded as percentages of this intensity. The relative intensities of the bands above  $850\text{ cm}^{-1}$  should be quite reliable because they were all measured, with aid of a planimeter, from a single absorbance spectrum of a mixture of 20 Torr of dimethyl ether- $\text{h}_6$  with 5850 Torr of hydrogen chloride at  $10^\circ\text{C}$ . However, the relative intensities of the bands below  $850\text{ cm}^{-1}$  must be regarded as approximate as they were determined by calculating the integrated absorbance per atmosphere of complex (25) for each of these bands and comparing this value with that calculated for the  $\nu_s$  band. The equilibrium constant used to calculate the amount of complex present was computed from the mean enthalpy and entropy of formation reported by Govil, Clague and Bernstein (84). However, the errors on their values of the enthalpy and entropy of formation allow the equilibrium constant at  $0^\circ\text{C}$  to lie between 0.15 and 9.5, standard state 1 atmosphere. Thus, the relative intensities quoted for the bands below  $850\text{ cm}^{-1}$  may be considerably in error because widely differing pressures and temperatures of the component gases were required for the different bands and the intensities obtained markedly reflect the value of the equilibrium constant that was used. It should be noted that the relative intensity of the O---H-Cl deformation modes was determined for  $(\text{CD}_3)_2\text{O---HCl}$ . The limited portion of the band that was observable in  $(\text{CH}_3)_2\text{O---HCl}$  indicated that the intensity was approximately the same in the two

systems.

### 3.7 Summary

The most significant results of this study are that: 1) the assignment of the  $\nu_{\sigma}$  mode of  $(\text{CH}_3)_2\text{O} \cdots \text{HCl}$  near to  $120 \text{ cm}^{-1}$  is confirmed by the observation of absorption in this region in the spectra of  $(\text{CH}_3)_2\text{O} \cdots \text{DCl}$  and  $(\text{CD}_3)_2\text{O} \cdots \text{HCl}$ ; 2) the  $\nu_{\text{b}}$  and  $\nu_{\text{t}}$  modes give rise to absorption near to  $470 \text{ cm}^{-1}$  for the HCl complexes and near to  $360 \text{ cm}^{-1}$  for the DCl complexes. These absorptions are complicated, probably due to interaction with the  $\nu_{\beta}$  modes, which are deduced to be at about  $50 \text{ cm}^{-1}$ ; 3) an analysis of the shape of the band due to the C-O symmetric stretching mode of  $(\text{CH}_3)_2\text{O} \cdots \text{HCl}$  does not indicate the geometry of the molecule, as previously suggested; 4) the fundamental  $\nu_{\text{s}}$  absorption by  $(\text{CH}_3)_2\text{O} \cdots \text{HCl}$  is at  $2480 \text{ cm}^{-1}$  and not at  $2574 \text{ cm}^{-1}$  as previously postulated; and 5) combination transitions of the type  $\nu_{\text{s}} \pm n\nu_{\beta}$  cause shoulders  $50 \text{ cm}^{-1}$  away from the peak due to  $\nu_{\text{s}}$  in the DCl complexes.

## CHAPTER 4

### VIBRATIONAL ASSIGNMENT AND NORMAL COORDINATE CALCULATIONS FOR FOUR ISOTOPIC MODIFICATIONS OF ETHYLENE SULPHIDE

#### 4.1 General Introduction

The infrared spectra of ethylene sulphide- $h_4$ , ethylene sulphide- $d_4$ , cis-1,2-dideuterioethylene sulphide and trans-1,2-dideuterioethylene sulphide have been measured in this laboratory by D. A. Othen (109). Hereafter in this thesis these compounds will be referred to as  $C_2H_4S$ ,  $C_2D_4S$ , cis- $C_2D_2H_2S$  and trans- $C_2D_2H_2S$ , respectively. Raman spectra of liquid  $C_2H_4S$  and  $C_2D_4S$  were also recorded by D. A. Othen (109).

These spectra were assigned as part of the present work and normal coordinate calculations were carried out to determine how well a harmonic valence-force field containing selected force constants could reproduce the frequencies of the fundamental vibrations of all four isotopic modifications of ethylene sulphide. The calculations were also desired to assist the assignment of the spectrum of trans- $C_2D_2H_2S$ , to check the mutual compatibility of the assignments of the four molecules, and to determine the form of the methylenic vibrations for the HCD groups.

The structure, symmetry and vibrational coordinates of ethylene sulphide are given in Section 4.2 and the previous studies of the vibrations of ethylene sulfide are reviewed

in Section 4.3. The frequencies of the features observed in the spectra of the four isotopic molecules are presented and assigned in Section 4.4. The computer programs used in the normal coordinate calculations and various input data are described in Section 4.5 and the development of the force field is summarized in Section 4.6. The results of the calculations are discussed in Section 4.7.

#### 4.2 Structure, Symmetry and Vibrational Coordinates of Ethylene Sulphide

The structure of  $C_2H_4S$  has been investigated by Cunningham et al (110) by means of microwave spectroscopy. This molecule was found to have  $C_{2v}$  symmetry and the structure shown in Figure 21. In this work the atomic sites are referred to by the numbers which appear in Figure 21 as subscripts to the atomic symbols, and the bonds are referred to by the numbers which appear in parentheses beside them. In each of the four isotopic modifications of ethylene sulphide discussed in this chapter, atoms 1, 2 and 3 refer to  $^{32}S$ ,  $^{12}C$  and  $^{12}C$  atoms, respectively. In  $C_2D_4S$ , which has  $C_{2v}$  symmetry, atoms 4, 5, 6 and 7 are deuterium atoms. In cis- $C_2D_2H_2S$ , which is assumed to have  $C_s$  symmetry, atoms 5 and 7 are deuterium atoms, and in trans- $C_2D_2H_2S$ , which is assumed to have  $C_2$  symmetry, atoms 4 and 7 are deuterium atoms.

Also shown in Figure 21 is the orientation of the

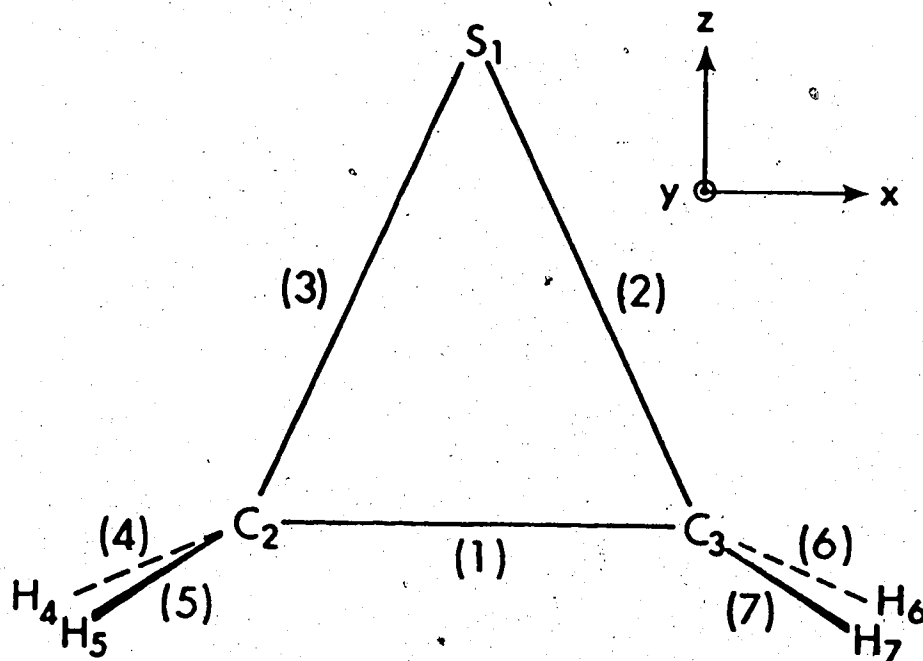


FIGURE 21. The structure of ethylene sulphide. In this drawing H<sub>4</sub> and H<sub>6</sub>, which should lie directly under H<sub>5</sub> and H<sub>7</sub>, respectively, have been offset for clarity. The number in parentheses beside each bond is used to designate that bond.

ethylene sulphide molecule with respect to the three Cartesian axes, and this orientation is the same for all four isotopic modifications. The x-Cartesian axis is parallel to the C-C bond, and the plane formed by atoms 1, 2 and 3 is the  $zx$  plane.

The bond angles and bond lengths in  $C_2D_4S$ , cis- $C_2D_2H_2S$  and trans- $C_2D_2H_2S$  are assumed to be the same as those in  $C_2H_4S$  (110), and are shown in Table 3. The rotational constants, A, B and C (Section 3.4), were calculated for each isotopic modification using these parameters and the appropriate atomic masses (101), and are presented in Table 4. The rotational constants are used in Section 4.4 to predict the rotational envelopes of the various vibrational transitions.

The fifteen fundamental vibrations of  $C_2H_4S$  form the representation (111)  $5A_1 + 3A_2 + 4B_1 + 3B_2$  under the point group  $C_{2v}$ , and since  $C_2D_4S$  also has  $C_{2v}$  symmetry, its vibrations also form this representation. The vibrations of cis- $C_2D_2H_2S$  form the representation  $8A' + 7A''$  under the point group  $C_s$  and those of trans- $C_2D_2H_2S$  form the representation  $8A + 7B$  under the point group  $C_2$ . In this work, the fundamental vibrations are numbered in the order of decreasing frequency within each symmetry class, following the convention introduced by Herzberg (112). Thus in  $C_2H_4S$  and  $C_2D_4S$ ,  $\nu_1$  through  $\nu_5$  refer to the five  $A_1$  vibrations,  $\nu_6$  through  $\nu_8$  refer to the three  $A_2$  vibrations,  $\nu_9$  through  $\nu_{12}$



TABLE 3

Molecular Parameters<sup>a</sup> of Ethylene Sulphide

|               |          |
|---------------|----------|
| $d_{C-C}$     | 1.4716 Å |
| $d_{C-S}$     | 1.8155 Å |
| $d_{C-H}$     | 1.0771 Å |
| $C-\hat{C}-S$ | 66.091°  |
| $C-\hat{S}-C$ | 47.818°  |
| $H-\hat{C}-H$ | 115.900° |
| $H-\hat{C}-C$ | 117.835° |
| $H-\hat{C}-S$ | 119.570° |
| $\alpha^b$    | 106.567° |

a) From reference 110.

b)  $\alpha$  is the angle between the  $C\hat{C}H$  and  $C\hat{S}C$  planes.

TABLE 4

Rotational Constants<sup>a</sup> of Four Isotopic Modifications  
of Ethylene Sulphide

| <u>Molecule</u>             | <u>A</u> | <u>B</u> | <u>C</u> |
|-----------------------------|----------|----------|----------|
| $C_2H_4S$                   | 0.7479   | 0.3608   | 0.2696   |
| $C_2D_4S$                   | 0.5256   | 0.3068   | 0.2291   |
| <u>cis</u> - $C_2D_2H_2S$   | 0.6209   | 0.3314   | 0.2470   |
| <u>trans</u> - $C_2D_2H_2S$ | 0.6174   | 0.3330   | 0.2463   |

---

a) Units are  $cm^{-1}$ .

refer to the four  $B_1$  vibrations and  $\nu_{13}$  through  $\nu_{15}$  refer to the three  $B_2$  vibrations. In cis- $C_2D_2H_2S$  or trans- $C_2D_2H_2S$ ,  $\nu_1$  through  $\nu_8$  refer to the eight  $A'$  or  $A$  vibrations, respectively, and  $\nu_9$  through  $\nu_{15}$  refer to the seven  $A''$  or  $B$  vibrations, respectively.

The internal coordinates (100) of ethylene sulphide, which are used in the normal coordinate calculations (Section 4.6), are listed in Table 5 and are defined with respect to Figure 21. The coordinates which describe the stretching of valence bonds are denoted  $R_i$ , where  $i$  refers to the bond number shown in Figure 21. Thus  $R_4$  is the coordinate which describes the stretching of a C-H bond at carbon atom 2 in  $C_2H_4S$  and cis- $C_2D_2H_2S$ . In  $C_2D_4S$  and trans- $C_2D_2H_2S$ ,  $R_4$  describes the stretching of a C-D bond at carbon atom 2. The coordinates which describe changes in valence angles are denoted  $\alpha_{jk}$ , where  $j$  and  $k$  indicate the two bonds forming the angle. Thus  $\alpha_{45}$  is the coordinate which describes the change in the  $\widehat{HCH}$  angle at carbon atom 2 in  $C_2H_4S$  and the changes in the  $\widehat{DCD}$  and  $\widehat{HCD}$  angles at carbon atom 2 in  $C_2D_4S$  and cis- or trans- $C_2D_2H_2S$ , respectively.

Five of the twenty internal coordinates defined in Table 5 must be redundant since there are only fifteen genuine vibrations in each isotopic modification of ethylene sulphide. Three of these redundancies arise since six internal coordinates,  $R_1$ ,  $R_2$ ,  $R_3$ ,  $\alpha_{13}$ ,  $\alpha_{12}$  and  $\alpha_{23}$ , are defined in the CSC ring, which has only three degrees of vibrational

TABLE 5

Internal Coordinates<sup>a</sup> for Ethylene Sulphide<sup>A</sup>

| <u>Coordinate Number</u> | <u>Notation</u> | <u>Description</u>                   |
|--------------------------|-----------------|--------------------------------------|
| 1                        | $R_1$           | $C_2-C_3$ Stretch                    |
| 2                        | $R_2$           | $C_3-S_1$ Stretch                    |
| 3                        | $R_3$           | $C_2-S_1$ Stretch                    |
| 4                        | $R_4$           | $C_2-H_4$ Stretch                    |
| 5                        | $R_5$           | $C_2-H_5$ Stretch                    |
| 6                        | $R_6$           | $C_3-H_6$ Stretch                    |
| 7                        | $R_7$           | $C_3-H_7$ Stretch                    |
| 8                        | $\alpha_{45}$   | $H_4-\overset{\wedge}{C}_2-H_5$ Bend |
| 9                        | $\alpha_{67}$   | $H_6-\overset{\wedge}{C}_3-H_7$ Bend |
| 10                       | $\alpha_{34}$   | $S_1-\overset{\wedge}{C}_2-H_4$ Bend |
| 11                       | $\alpha_{35}$   | $S_1-\overset{\wedge}{C}_2-H_5$ Bend |
| 12                       | $\alpha_{26}$   | $S_1-\overset{\wedge}{C}_3-H_6$ Bend |
| 13                       | $\alpha_{27}$   | $S_1-\overset{\wedge}{C}_3-H_7$ Bend |
| 14                       | $\alpha_{14}$   | $C_3-\overset{\wedge}{C}_2-H_4$ Bend |
| 15                       | $\alpha_{15}$   | $C_3-\overset{\wedge}{C}_2-H_5$ Bend |
| 16                       | $\alpha_{16}$   | $C_2-\overset{\wedge}{C}_3-H_6$ Bend |
| 17                       | $\alpha_{17}$   | $C_2-\overset{\wedge}{C}_3-H_7$ Bend |
| 18                       | $\alpha_{13}$   | $S_1-\overset{\wedge}{C}_2-C_3$ Bend |
| 19                       | $\alpha_{12}$   | $S_1-\overset{\wedge}{C}_3-C_2$ Bend |
| 20                       | $\alpha_{23}$   | $C_2-\overset{\wedge}{S}_1-C_3$ Bend |

a) Defined with respect to Figure 1.

freedom. The other two redundancies arise since only five of the six angle bending coordinates defined about each carbon atom are independent. In order to take full advantage of the symmetry of each isotopic modification, it was necessary to use all twenty internal coordinates to construct symmetry coordinates (111). The symmetry coordinates for  $C_2H_4S$  are the same as those for  $C_2D_4S$  and are presented in Table 6. These coordinates form the representation  $8A_1 + 3A_2 + 6B_1 + 3B_2$  under the point group  $C_{2v}$ , and a comparison of this representation with the vibrational representation of  $C_2H_4S$  or  $C_2D_4S$  shows that three  $A_1$  and two  $B_1$  symmetry coordinates are redundant. The symmetry coordinates for cis- $C_2D_2H_2S$ , which are presented in Table 7, form the representation  $11A' + 9A''$  under the point group  $C_s$  and, thus, three  $A'$  and two  $A''$  symmetry coordinates are redundant. The symmetry coordinates for trans- $C_2D_2H_2S$ , which are presented in Table 8, form the representation  $11A + 9B$  under the point group  $C_2$  and, thus, three  $A$  and two  $B$  symmetry coordinates are redundant. All redundant coordinates were included in the calculations and yielded zero roots upon solving the secular equation (100).

It is usual (113-116) to describe the vibrations of  $C_2H_4S$  as either 1) a C-H stretching mode, 2) a ring deformation mode, or 3) a methylenic angle bending mode. In certain cases the description (or form, or normal coordinate) of the vibrations is approximately given by the appropriate

TABLE 6

Symmetry Coordinates<sup>a</sup> for C<sub>2</sub>H<sub>4</sub>S and C<sub>2</sub>D<sub>4</sub>S

| Coordinate Number | Description   | Symmetry       |
|-------------------|---|----------------|
| S <sub>1</sub>    | R <sub>1</sub>  | A <sub>1</sub> |
| S <sub>2</sub>    | $\frac{1}{\sqrt{2}} \{ R_2 + R_3 \}$                                      | A <sub>1</sub> |
| S <sub>3</sub>    | $\frac{1}{2} \{ R_4 + R_5 + R_6 + R_7 \}$                                 | A <sub>1</sub> |
| S <sub>4</sub>    | $\frac{1}{\sqrt{2}} \{ \alpha_{45} + \alpha_{67} \}$                      | A <sub>1</sub> |
| S <sub>5</sub>    | $\frac{1}{2} \{ \alpha_{34} + \alpha_{35} + \alpha_{26} + \alpha_{27} \}$ | A <sub>1</sub> |
| S <sub>6</sub>    | $\frac{1}{2} \{ \alpha_{14} + \alpha_{15} + \alpha_{16} + \alpha_{17} \}$ | A <sub>1</sub> |
| S <sub>7</sub>    | $\frac{1}{\sqrt{2}} \{ \alpha_{13} + \alpha_{12} \}$                      | A <sub>1</sub> |
| S <sub>8</sub>    | α <sub>23</sub>   | A <sub>1</sub> |
| S <sub>9</sub>    | $\frac{1}{2} \{ R_4 - R_5 - R_6 + R_7 \}$                                 | A <sub>2</sub> |
| S <sub>10</sub>   | $\frac{1}{2} \{ \alpha_{34} - \alpha_{35} - \alpha_{26} + \alpha_{27} \}$ | A <sub>2</sub> |
| S <sub>11</sub>   | $\frac{1}{2} \{ \alpha_{14} - \alpha_{15} - \alpha_{16} + \alpha_{17} \}$ | A <sub>2</sub> |
| S <sub>12</sub>   | $\frac{1}{\sqrt{2}} \{ R_2 - R_3 \}$                                      | B <sub>1</sub> |
| S <sub>13</sub>   | $\frac{1}{2} \{ R_4 + R_5 - R_6 - R_7 \}$                                 | B <sub>1</sub> |
| S <sub>14</sub>   | $\frac{1}{\sqrt{2}} \{ \alpha_{45} - \alpha_{67} \}$                      | B <sub>1</sub> |
| S <sub>15</sub>   | $\frac{1}{2} \{ \alpha_{34} + \alpha_{35} - \alpha_{26} - \alpha_{27} \}$ | B <sub>1</sub> |

TABLE 6 (continued)

| <u>Coordinate Number</u> | <u>Description</u>   | <u>Symmetry</u> |
|--------------------------|--|-----------------|
| S <sub>16</sub>          | $\frac{1}{2} \left\{ \alpha_{14} + \alpha_{15} - \alpha_{16} - \alpha_{17} \right\}$ | B <sub>1</sub>  |
| S <sub>17</sub>          | $\frac{1}{\sqrt{2}} \left\{ \alpha_{13} - \alpha_{12} \right\}$                      | B <sub>1</sub>  |
| S <sub>18</sub>          | $\frac{1}{2} \left\{ R_4 - R_5 + R_6 - R_7 \right\}$                                 | B <sub>2</sub>  |
| S <sub>19</sub>          | $\frac{1}{2} \left\{ \alpha_{34} - \alpha_{35} + \alpha_{26} - \alpha_{27} \right\}$ | B <sub>2</sub>  |
| S <sub>20</sub>          | $\frac{1}{2} \left\{ \alpha_{14} - \alpha_{15} + \alpha_{16} - \alpha_{17} \right\}$ | B <sub>2</sub>  |

a) Defined with respect to the internal coordinates in Table 5.

TABLE 7

Symmetry Coordinates<sup>a</sup> for cis-C<sub>2</sub>D<sub>2</sub>H<sub>2</sub>S

| Coordinate Number | Description  | Symmetry |
|-------------------|--|----------|
| S <sub>1</sub>    | R <sub>1</sub>                                     | A'       |
| S <sub>2</sub>    | $\frac{1}{\sqrt{2}} \{R_2 + R_3\}$                 | A'       |
| S <sub>3</sub>    | $\frac{1}{\sqrt{2}} \{R_4 + R_6\}$                 | A'       |
| S <sub>4</sub>    | $\frac{1}{\sqrt{2}} \{R_5 + R_7\}$                 | A'       |
| S <sub>5</sub>    | $\frac{1}{\sqrt{2}} \{\alpha_{45} + \alpha_{67}\}$ | A'       |
| S <sub>6</sub>    | $\frac{1}{\sqrt{2}} \{\alpha_{34} + \alpha_{26}\}$ | A'       |
| S <sub>7</sub>    | $\frac{1}{\sqrt{2}} \{\alpha_{35} + \alpha_{27}\}$ | A'       |
| S <sub>8</sub>    | $\frac{1}{\sqrt{2}} \{\alpha_{14} + \alpha_{16}\}$ | A'       |
| S <sub>9</sub>    | $\frac{1}{\sqrt{2}} \{\alpha_{15} + \alpha_{17}\}$ | A'       |
| S <sub>10</sub>   | $\frac{1}{\sqrt{2}} \{\alpha_{13} + \alpha_{12}\}$ | A'       |
| S <sub>11</sub>   | $\alpha_{23}$                                      | A'       |
| S <sub>12</sub>   | $\frac{1}{\sqrt{2}} \{R_2 - R_3\}$                 | A''      |
| S <sub>13</sub>   | $\frac{1}{\sqrt{2}} \{R_4 - R_6\}$                 | A''      |
| S <sub>14</sub>   | $\frac{1}{\sqrt{2}} \{R_5 - R_7\}$                 | A''      |
| S <sub>15</sub>   | $\frac{1}{\sqrt{2}} \{\alpha_{45} - \alpha_{67}\}$ | A''      |



Table 7 (continued)

| <u>Coordinate Number</u> | <u>Description</u>                                   | <u>Symmetry</u> |
|--------------------------|--|-----------------|
| S <sub>16</sub>          | $\frac{1}{\sqrt{2}} \{ \alpha_{34} - \alpha_{26} \}$ | A''             |
| S <sub>17</sub>          | $\frac{1}{\sqrt{2}} \{ \alpha_{35} - \alpha_{27} \}$ | A''             |
| S <sub>18</sub>          | $\frac{1}{\sqrt{2}} \{ \alpha_{14} - \alpha_{16} \}$ | A''             |
| S <sub>19</sub>          | $\frac{1}{\sqrt{2}} \{ \alpha_{15} - \alpha_{17} \}$ | A''             |
| S <sub>20</sub>          | $\frac{1}{\sqrt{2}} \{ \alpha_{13} - \alpha_{12} \}$ | A''             |

a) Defined with respect to the internal coordinates in Table 5.

TABLE 8

Symmetry Coordinates<sup>a</sup> for trans-C<sub>2</sub>D<sub>2</sub>H<sub>2</sub>S

| Coordinate Number | Description  | Symmetry |
|-------------------|--|----------|
| S <sub>1</sub>    | R <sub>1</sub>                                       | A        |
| S <sub>2</sub>    | $\frac{1}{\sqrt{2}} \{ R_2 + R_3 \}$                 | A        |
| S <sub>3</sub>    | $\frac{1}{\sqrt{2}} \{ R_4 + R_7 \}$                 | A        |
| S <sub>4</sub>    | $\frac{1}{\sqrt{2}} \{ R_5 + R_6 \}$                 | A        |
| S <sub>5</sub>    | $\frac{1}{\sqrt{2}} \{ \alpha_{45} + \alpha_{67} \}$ | A        |
| S <sub>6</sub>    | $\frac{1}{\sqrt{2}} \{ \alpha_{34} + \alpha_{27} \}$ | A        |
| S <sub>7</sub>    | $\frac{1}{\sqrt{2}} \{ \alpha_{35} + \alpha_{26} \}$ | A        |
| S <sub>8</sub>    | $\frac{1}{\sqrt{2}} \{ \alpha_{14} + \alpha_{17} \}$ | A        |
| S <sub>9</sub>    | $\frac{1}{\sqrt{2}} \{ \alpha_{15} + \alpha_{16} \}$ | A        |
| S <sub>10</sub>   | $\frac{1}{\sqrt{2}} \{ \alpha_{13} + \alpha_{12} \}$ | A        |
| S <sub>11</sub>   | $\alpha_{23}$  | A        |
| S <sub>12</sub>   | $\frac{1}{\sqrt{2}} \{ R_2 - R_3 \}$                 | B        |
| S <sub>13</sub>   | $\frac{1}{\sqrt{2}} \{ R_4 - R_7 \}$                 | B        |
| S <sub>14</sub>   | $\frac{1}{\sqrt{2}} \{ R_5 - R_6 \}$                 | B        |
| S <sub>15</sub>   | $\frac{1}{\sqrt{2}} \{ \alpha_{45} - \alpha_{67} \}$ | B        |

TABLE 8 (continued)

| <u>Coordinate<br/>Number</u> | <u>Description</u>                                   | <u>Symmetry</u> |
|------------------------------|--|-----------------|
| S <sub>16</sub>              | $\frac{1}{\sqrt{2}} \{ \alpha_{34} - \alpha_{27} \}$ | B               |
| S <sub>17</sub>              | $\frac{1}{\sqrt{2}} \{ \alpha_{35} - \alpha_{26} \}$ | B               |
| S <sub>18</sub>              | $\frac{1}{\sqrt{2}} \{ \alpha_{14} - \alpha_{17} \}$ | B               |
| S <sub>19</sub>              | $\frac{1}{\sqrt{2}} \{ \alpha_{15} - \alpha_{16} \}$ | B               |
| S <sub>20</sub>              | $\frac{1}{\sqrt{2}} \{ \alpha_{13} - \alpha_{12} \}$ | B               |

a) Defined with respect to the internal coordinates in Table 5.

symmetry coordinate. Thus, because the C-H stretching vibrations have much different frequencies from those of the other modes, their forms can be expected to be closely approximated by the symmetry coordinates  $S_3$ ,  $S_9$ ,  $S_{13}$  and  $S_{18}$  (Table 6). Those vibrations approximated by  $S_3$  and  $S_{13}$  are called symmetric  $\text{CH}_2$  stretching modes while the other two are called asymmetric (or antisymmetric)  $\text{CH}_2$  stretching modes. There are three vibrational modes which involve deformation of the CSC ring. Since there are six symmetry coordinates in Table 6 which describe ring deformations ( $S_1$ ,  $S_2$ ,  $S_7$ ,  $S_8$ ,  $S_{12}$  and  $S_{17}$ ), three of these coordinates must be redundant. Although all coordinates are included in the calculation, the ring deformation modes will be qualitatively described by the symmetry coordinates,  $S_1$ ,  $S_2$  and  $S_{12}$ , which correspond to the C-C stretching mode, the symmetric C-S stretching mode and the asymmetric C-S stretching mode, respectively.

The remaining eight vibrations in  $\text{C}_2\text{H}_4\text{S}$  are usually classified as deformations, wags, twists and rocks (117) of the methylenic groups. Each of these terms describes displacements which are defined by linear combinations of the symmetry coordinates in Table 6 which involve the  $\hat{\text{SCH}}$  and  $\hat{\text{CCH}}$  angle bending coordinates. The methylenic deformations are described by  $S_5 + S_6$  and  $S_{15} + S_{16}$  and refer to the symmetrical 'scissors-like' bending of the  $\hat{\text{HCH}}$  angles. Because of redundancies, the methylenic deformations can also be

described by the symmetry coordinates  $S_4$  and  $S_{14}$  of Table 6. The term 'methylenic wags' refers to the 'fan-like' motions of the methylenic groups perpendicular to their own planes, and are defined by  $S_5 - S_6$  and  $S_{15} - S_{16}$ . The methylenic twists are defined by  $S_{10} - S_{11}$  and  $S_{19} - S_{20}$ , and refer to restricted rotation of the hydrogen atoms about the bisector of each  $\widehat{HCH}$  angle. The methylenic rocks are defined by  $S_{10} + S_{11}$  and  $S_{19} + S_{20}$ , and refer to the rotary motion of each methylenic group about an axis perpendicular to its plane. It must be emphasized that these terms are only approximate descriptions of the vibrations and normal coordinate calculations indicate that many vibrations are much more complicated than these simple terms imply. Nevertheless, this terminology is useful, and has been applied by others (113-116) to ethylene sulphide, and is used in this work.

The terminology given above can also be used to describe the vibrations of  $C_2D_4S$ . There is, however, no analogous terminology to describe the methylenic vibrations of cis- and trans- $C_2D_2H_2S$ . For simplicity, the vibrations which involve changes in the  $\widehat{CCH}$  and  $\widehat{SCH}$  angles (or  $\widehat{CCD}$  and  $\widehat{SCD}$  angles) will be referred to as  $\widehat{CCH}$  (or  $\widehat{CCD}$ ) deformations until the calculated form of these vibrations is presented.

#### 4.3 Previous Studies of the Vibrations of Ethylene Sulphide

The vibrational spectra of ethylene sulphide- $h_4$  have been studied several times. In 1940, Thompson and Dupré (113)

reported the infrared spectrum of the gas and the Raman spectrum of the liquid, with the unavoidably low frequency accuracy and resolution available at that time. In 1951, Thompson and Cave (114) repeated the work of Thompson and Dupré with better resolution and frequency accuracy, and showed that the earlier work was suspect. The following year, Guthrie, Scott and Waddington (115) reported the infrared spectrum of the liquid for the first time. More recently, LeBrumant (116) has studied the infrared and Raman spectra of the liquid and the infrared spectrum of the solid, and Aleksanyan and Kuz'yants (118) have reported the infrared spectra of the gas, liquid and solid and the Raman spectrum of the liquid.

The assignments of the fundamental frequencies which have resulted from these studies are shown in Tables 9 and 10 for the liquid and the gas, respectively. The assignment of the fundamental frequencies of the liquid (Table 9) by LeBrumant (116) was not modified from that of Guthrie, Scott and Waddington (115) apart from a more precise determination of the frequencies, but Aleksanyan and Kuz'yants (118,119) have assigned the  $A_1$   $CH_2$  wag at a higher frequency than either of the  $A_1$  ring deformation modes. There has been no experimental evidence to indicate the relative frequencies of the  $CH_2$  wag and the C-C stretching mode, and the isotopic derivatives studied in the present work should resolve this problem. The  $A_2$  modes appear very weakly in

TABLE 9

Previous Assignments of the Fundamental Frequencies<sup>a</sup>of Liquid C<sub>2</sub>H<sub>4</sub>S

|                 | Description                                | Guthrie<br>et al    | LeBrumant <sup>b</sup> | Aleksanyan<br>et al | Othen               |
|-----------------|--|---------------------|------------------------|---------------------|---------------------|
| v <sub>1</sub>  | A <sub>1</sub> C-H stretch                 | 3000                | 2994                   | 2993                | 2995                |
| v <sub>2</sub>  | A <sub>1</sub> CH <sub>2</sub> deformation | 1446                | 1446                   | 1445                | 1450                |
| v <sub>3</sub>  | A <sub>1</sub> ring mode                   | 1112                | 1111                   | 1024                | 1112                |
| v <sub>4</sub>  | A <sub>1</sub> CH <sub>2</sub> wag         | 1025                | 1024                   | 1112                | 1025                |
| v <sub>5</sub>  | A <sub>1</sub> ring mode                   | 625                 | 616                    | 613                 | 611                 |
| v <sub>6</sub>  | A <sub>2</sub> C-H stretch                 | 3080 <sup>c</sup>   | 3071                   | 3071                | 3072                |
| v <sub>7</sub>  | A <sub>2</sub> CH <sub>2</sub> twist       | 1100 <sup>c</sup>   | 1172                   | —                   | —                   |
| v <sub>8</sub>  | A <sub>2</sub> CH <sub>2</sub> rock        | 875 <sup>c</sup>    | 900                    | 895                 | (895) <sup>d</sup>  |
| v <sub>9</sub>  | B <sub>1</sub> C-H stretch                 | (3000) <sup>e</sup> | (2994) <sup>e</sup>    | (2993) <sup>e</sup> | (2995) <sup>e</sup> |
| v <sub>10</sub> | B <sub>1</sub> CH <sub>2</sub> deformation | 1427                | 1426                   | 1425                | 1431                |
| v <sub>11</sub> | B <sub>1</sub> CH <sub>2</sub> wag         | 1051                | 1050                   | 1052                | —                   |
| v <sub>12</sub> | B <sub>1</sub> ring mode                   | 660                 | 657                    | 650                 | (651) <sup>d</sup>  |
| v <sub>13</sub> | B <sub>2</sub> C-H stretch                 | 3080                | 3071                   | 3071                | 3072                |
| v <sub>14</sub> | B <sub>2</sub> CH <sub>2</sub> twist       | 943                 | 942                    | 943                 | 944                 |
| v <sub>15</sub> | B <sub>2</sub> CH <sub>2</sub> rock        | 824                 | 823                    | 823                 | 822                 |

a) In cm<sup>-1</sup>

b) LeBrumant accepted the assignment of Guthrie et al.

c) Values calculated from the frequencies of the corresponding B<sub>2</sub> modes.

d) Assignment of these features is not certain.

e) Assumed to be nearly degenerate with v<sub>1</sub>.

TABLE 10

Previous Assignments of the Fundamental Frequencies<sup>a</sup>

|                    |  | of Gaseous C <sub>2</sub> H <sub>4</sub> S |                                     |                     |
|--------------------|--|--|-------------------------------------|---------------------|
| <u>Description</u> |  | <u>Thompson and<br/>Cave</u>               | <u>Aleksanyan and<br/>Kuz'yants</u> | <u>Othen</u>        |
| v <sub>1</sub>     | A <sub>1</sub> C-H stretch                 | 3017                                       | 3013.5                              | 3013.5              |
| v <sub>2</sub>     | A <sub>1</sub> CH <sub>2</sub> deformation | 1471                                       | 1456                                | 1456.8              |
| v <sub>3</sub>     | A <sub>1</sub> ring mode                   | —  | 1033                                | 1109.9              |
| v <sub>4</sub>     | A <sub>1</sub> CH <sub>2</sub> wag         | 1107                                       | 1109.5                              | 1024.0              |
| v <sub>5</sub>     | A <sub>1</sub> ring mode                   | 626  | 627.4                               | 627.3               |
| v <sub>6</sub>     | A <sub>2</sub> C-H stretch                 | —  | —                                   | —                   |
| v <sub>7</sub>     | A <sub>2</sub> CH <sub>2</sub> twist       | —  | —                                   | —                   |
| v <sub>8</sub>     | CH <sub>2</sub> rock                       | —  | —                                   | —                   |
| v <sub>9</sub>     | B <sub>1</sub> C-H stretch                 | (3017) <sup>b</sup>                        | (3013.5) <sup>b</sup>               | (3013) <sup>b</sup> |
| v <sub>10</sub>    | B <sub>1</sub> CH <sub>2</sub> deformation | 1440                                       | 1435                                | 1435.9              |
| v <sub>11</sub>    | B <sub>1</sub> CH <sub>2</sub> wag         | 1050                                       | 1050                                | 1050.8              |
| v <sub>12</sub>    | B <sub>1</sub> ring mode                   | 685  | 668                                 | —                   |
| v <sub>13</sub>    | B <sub>2</sub> C-H stretch                 | 3089                                       | 3084                                | 3088.0              |
| v <sub>14</sub>    | B <sub>2</sub> CH <sub>2</sub> twist       | 825  | 944.0                               | 945.2               |
| v <sub>15</sub>    | B <sub>2</sub> CH <sub>2</sub> rock        | 945  | 824.0                               | 824.3               |

a) In cm<sup>-1</sup>b) Assumed to be nearly degenerate with v<sub>1</sub>.



the Raman spectrum and are inactive in the infrared spectrum, and their frequencies cannot be regarded as well determined. For completeness, the fundamental frequencies, obtained by Othen (109) from the Raman spectrum of the liquid, which are used in this work, are also presented in Table 9. These frequencies do not differ significantly from those reported by Le Brumant (116) and by Aleksanyan and Kuz'yants (118).

For the gas (Table 10), the fundamental frequencies of Aleksanyan and Kuz'yants (118) are consistent with those of Thompson and Cave (114) apart from the addition of  $1033 \text{ cm}^{-1}$  as the frequency of an  $A_1$  fundamental and the improved precision with which the frequencies were determined.

Aleksanyan and Kuz'yants have assigned (118,119) their frequencies of the gas following their assignment of the frequencies of the liquid (Table 9). This assignment disagrees with the earlier one of Thompson and Cave (114) in that the latter authors assigned the methylenic rocking mode to high frequency of the methylenic twisting mode. In recent years it has become accepted that methylenic twisting modes lie to high frequency of the rocking modes. This conclusion is based on the spectra of cyclobutane (120), cyclopropane (117,121-123), and hexamethylene tetramine (124-127), in which at least one methylenic twisting mode has a different symmetry from a methylenic rocking mode. In all cases, the methylenic twist was assigned a frequency comparable with that of the methylenic wag and considerably higher than that

of the rock. Consequently, this order has been accepted for ethylene oxide (128) and methylene cyclopropane (129,130), and is adopted in this work. For completeness, the fundamental frequencies of gaseous  $C_2H_4S$  which are used in this work (109) are included in Table 10; their assignment is discussed in Section 4.4. The vibrational spectra of  $C_2D_4S$  and cis- and trans- $C_2D_2H_2S$  have not been previously reported.

The observed frequencies listed in Tables 9 and 10 have been used (131-133) to calculate various force constants of  $C_2H_4S$ . In each case, however, the number of force constants required to reasonably reproduce the observed frequencies exceeded the number of frequencies, so these calculations are suspect. Further, Venkateswarlu et al (131,132) included frequencies from Thompson and Dupré's (113) early work which have since been shown to arise from impurities.

#### 4.4 The Assignment of the Spectra of $C_2H_4S$ , $C_2D_4S$ and cis- and trans- $C_2D_2H_2S$

The infrared spectra of gaseous  $C_2D_4S$ , cis- $C_2D_2H_2S$  and trans- $C_2D_2H_2S$  are presented in Appendix IV. The vibrational spectra of  $C_2H_4S$  are published (116,118) so those recorded by Othen (109) are not reproduced in this thesis. The frequencies of the features observed between 200 and  $1500\text{ cm}^{-1}$  and between 2000 and  $4000\text{ cm}^{-1}$  in the infrared spectrum of the gas and the Raman spectrum of the liquid are

presented in Table 11 for  $C_2H_4S$  and Table 12 for  $C_2D_4S$ . Tables 13 and 14 present the frequencies of all features consistently observed between 200 and  $4000\text{ cm}^{-1}$  in the infrared spectra of gaseous cis- $C_2D_2H_2S$  and trans- $C_2D_2H_2S$ , respectively. In Tables 11-14, the infrared absorption band associated with each frequency is described by the letters 'PR' if only P and R branches (134) were observed and by the letters 'PQR' if P, Q and R branches (134) were observed. The letter 'P' beside a frequency in Tables 11 and 12 indicates that the Raman band at this frequency has a depolarization ratio (135) which is less than 0.75. The assignments presented in Tables 11-14 were determined as part of the present work and are discussed below.

The first stage in the assignment of the peaks observed in the spectra to particular vibrations is to determine, as far as possible, the symmetry of the transition causing each peak. Two pieces of evidence give this information: 1) a Raman depolarization ratio of less than 0.75 can only arise from a totally symmetric mode (135), so the frequencies marked P in Tables 11 and 12 must arise from  $A_1$  transitions; 2) the shapes of the infrared absorption bands of gaseous molecules vary with the symmetry of the transition causing the absorption.

The shapes of the infrared absorption bands of the gaseous ethylene sulphide molecules can be predicted using the method outlined in Section 3.4. In both  $C_2H_4S$  and  $C_2D_4S$ ,

TABLE 11

Frequencies<sup>a</sup> and Assignment of Features Observed in the Infrared and

Raman Spectra of C<sub>2</sub>H<sub>4</sub>S

| <u>Infrared (gas)<sup>b</sup></u> | <u>Raman (liquid)<sup>b</sup></u> | <u>Assignment</u>   |
|-----------------------------------|-----------------------------------|---|
| 3088.0 m, PQR                     | 3071.7 m                          | $\nu_{13} B_2$ C-H stretch  |
| 3084.2 w, Q                       |                                   | hot band  |
| 3013.5 vs, PQR                    | 2994.7 vs, P                      | $\left\{ \begin{array}{l} \nu_1 A_1 \text{ C-H stretch} \\ \nu_9 B_1 \text{ C-H stretch} \end{array} \right.$ |
| 2903.6 w, PQR                     |                                   | $2\nu_2 A_1$  |
| 2863.5 w, PQR                     |                                   | $2\nu_{10} A_1$   |
| 1456.8 m, PQR                     | 1450 m, P                         | $\nu_2 A_1$ CH <sub>2</sub> deformation   |
| 1435.9 m, PR                      | 1431 m                            | $\nu_{10} B_1$ CH <sub>2</sub> deformation  |
| 1255 vw, PQR                      | 1230 vw                           | $2\nu_5 A_1$  |
| 1173.3 vw, Q                      |                                   |   |
| 1109.9 m, PQR                     | 1112 s, P                         | $\nu_3 A_1$ C-C stretch   |
| 1050.8 s, PR                      |                                   | $\nu_{11} B_1$ CH <sub>2</sub> wag  |
| 1024.0 m, PQR                     | 1025 s, P                         | $\nu_4 A_1$ CH <sub>2</sub> wag   |
| 945.2 m, PQR                      | 944 w                             | $\nu_{14} B_2$ CH <sub>2</sub> twist  |
|                                   | 895 vw                            | A <sub>2</sub> ?  |
| 824.3 w, PQR                      | 822 w                             | $\nu_{15} B_2$ CH <sub>2</sub> rock   |
| 688.1 m, bd                       |                                   |   |
|                                   | 650.8 m                           | $\nu_{12}^? B_1$ C-S stretch  |
| 627.3 vs, PQR                     | 627.3 vs, P                       | $\nu_5 A_1$ C-S stretch   |
| 623.0 w                           |                                   | hot band  |

a) In cm<sup>-1</sup>

b) Abbreviations: w = weak; m = medium; s = strong; v = very; bd = broad; P = polarized; Q = Q branch; PQR = P, Q and R branches were visible; PR = P and R branches only were visible.

TABLE 12

Frequencies<sup>a</sup> and Assignment of Features Observed in the Infrared and

Raman Spectra of C<sub>2</sub>D<sub>4</sub>S

| <u>Infrared (gas)<sup>b</sup></u> | <u>Raman (liquid)<sup>b</sup></u> | <u>Assignment</u>                                     |
|-----------------------------------|-----------------------------------|---|
|                                   | 2385 w                            |   |
| 2331.3 m, PQR                     | 2320 m                            | $\nu_{13}$ B <sub>2</sub> C-D stretch                 |
| 2215 w, Q                         |                                   | hot band  |
| 2212.5 m, PQR                     | 2201 s, P                         | $\nu_1$ A <sub>1</sub> C-D stretch                    |
| 2209 w, Q                         |                                   | hot band  |
| 2185.2 m, PR                      | 2177 w                            | $\nu_9$ B <sub>1</sub> C-D stretch                    |
| 2125 w, PQR                       | 2111 w, P                         | $2\nu_{10}$ A <sub>1</sub>                            |
| 1241.3 vw                         | 1222 m, P                         |   |
|                                   | 1180 m, P                         |   |
|                                   | 1168 m, P                         |   |
| 1064.2 m, PR                      | 1055 w                            | $\nu_{10}$ B <sub>1</sub> CD <sub>2</sub> deformation |
| 1027.8 w                          |                                   |   |
| 946.4 m, PQR                      | 940 s, P                          | $\nu_3$ A <sub>1</sub> C-C stretch                    |
| 830.7 s, PR                       | 829 w                             | $\nu_{11}$ B <sub>1</sub> CD <sub>2</sub> wag         |
| 766.5 m, PQR                      | 762 s, P                          | $\nu_4$ A <sub>1</sub> CD <sub>2</sub> wag            |
| 746.8 w                           |                                   |   |
| 710.8 m, PQR                      | 708 w                             | $\nu_{14}$ B <sub>2</sub> CD <sub>2</sub> twist       |
| 654 w, bd                         |                                   |   |
|                                   | 618 m                             | $\nu_{12}?$ B <sub>1</sub> C-S stretch                |
| 613.3 vs, PQR                     | 603 s, P                          | $\nu_5$ A <sub>1</sub> C-S stretch                    |
| 578.1 m, PQR                      | 579 w                             | $\nu_{15}$ B <sub>2</sub> CD <sub>2</sub> rock        |

a) In cm<sup>-1</sup>

b) The abbreviations are explained in Table 11.

TABLE 13

Frequencies and Assignment of Features Observed in the InfraredSpectrum of Gaseous *cis*-C<sub>2</sub>D<sub>2</sub>H<sub>2</sub>S

| $\nu/\text{cm}^{-1}$ | <sup>a</sup> | Assignment                     |
|----------------------|--------------|--------------------------------|
| 3052.0               | s, PQR       | $\nu_1$ A' C-H stretch         |
| 2272.4               | m, PQR       | $\nu_2$ A' C-D stretch         |
| 1332.6               | w, PQR       | $\nu_3$ A' HCD deformation     |
| 1310.0               | w, PR        | $\nu_4$ A'' HCD deformation    |
| 1083.7               | m, PQR?      |                                |
| 1068.5               | m, PR?       |                                |
| 971.9                | m, PQR       | $\nu_5$ A' CCH or CCD bend     |
| 921.3                | m, PR        | $\nu_{13}$ A'' CCH or CCD bend |
| 756.8                | m, PQR       | $\nu_6$ A' CCH or CCD bend     |
| 654.7                | m, PQR       | $\nu_7$ A' CCH or CCD bend     |
| 614.8                | s, PQR       | $\nu_8$ A' C-S stretch         |

a) The abbreviations are explained in Table 11

TABLE 14

Frequencies and Assignment of Features Observed in the InfraredSpectrum of Gaseous  $\text{trans-C}_2\text{D}_2\text{H}_2\text{S}$  A

| <u><math>\nu/\text{cm}^{-1}</math></u> a | <u>Assignment</u>                                |
|--|--|
| 3051.0 m, PQR                            | } C-H stretches                                  |
| 3044.2 m, PQR                            |  |
| 2272.2 m, PQR                            | } C-D stretches                                  |
| 2262.6 w, PQR                            |  |
| 1315.2 vw, Q                             | } $\hat{\text{HCD}}$ deformation                 |
| 1293.1 vw, Q                             |  |
| 1113.4 m, PQR                            | } $\nu_4$ A C-C stretch                          |
| 1002.8 s, PQR                            |  |
| 867.7 m, PQR                             | } $\hat{\text{CCH}}$ or $\hat{\text{CCD}}$ bends |
| 773.4 m, PQR                             |  |
| 704.5 m, PQR                             |  |
| 668.2 m, PQR                             | } $\nu_8$ A C-S stretch                          |
| 617.5 vs, PQR                            |  |
| 610 shoulder                             |  |

a) The abbreviations are explained in Table 11.

the principal axes of inertia, a-, b- and c-, are parallel to the z-, x- and y- Cartesian axes, respectively, which are defined in Figure 21. It can therefore be seen from the character table for the point group  $C_{2v}$  (136) that, in both  $C_2H_4S$  and  $C_2D_4S$ ,  $A_1$  vibrations cause dipole moment changes parallel to the a-axis, and therefore yield A-type (104,105) infrared absorption bands;  $B_1$  vibrations cause dipole moment changes parallel to the b-axis, and therefore yield B-type (104,105) infrared absorption bands; and  $B_2$  vibrations cause dipole moment changes parallel to the c-axis, and therefore yield C-type (104,105) infrared absorption bands. It is found, by substituting the values of the rotational constants of  $C_2H_4S$  and  $C_2D_4S$  given in Table 4 into equations 1 and 2 of Section 3.4, that  $X = 1.494$  and  $Y = -0.108$  for  $C_2H_4S$  and  $X = 1.493$  and  $Y = -0.183$  for  $C_2D_4S$ . These parameters indicate that  $C_2H_4S$  closely approximates rotor number 16 of reference 105 and  $C_2D_4S$  closely approximates rotor number 25. Therefore, for each molecule, a B-type band is predicted to have only P and R branches while A- and C- type bands are predicted to have P, Q and R branches (105).

The assignment of the  $A_1$  modes in  $C_2H_4S$  at 3013.5, 1456.8, 1109.9, 1024.0 and 627.3  $cm^{-1}$ , the  $B_1$  modes at 3013, 1435.9, and 1050.8  $cm^{-1}$ , and the  $B_2$  modes at 3088.0, 945.2 and 824.3  $cm^{-1}$  is consistent with previous assignments (Tables 9 and 10). The fourth  $B_1$  mode ( $\nu_{12}$ ) has been assigned between 650 and 685  $cm^{-1}$  by all previous authors



(113-116,118). The only band which is observed in this region in the infrared spectrum of gaseous  $C_2H_4S$  is a broad, featureless absorption at  $688.1\text{ cm}^{-1}$  whose shape is unlike any band shape predicted for  $C_2H_4S$  from reference 105. Since there is a band at  $650.8\text{ cm}^{-1}$  in the Raman spectrum of liquid  $C_2H_4S$  it has been argued (118) that the feature at  $688.1\text{ cm}^{-1}$  is the R branch of a band with PR structure whose P branch is hidden under the strong absorption at  $627.3\text{ cm}^{-1}$ . This implies that the separation between the P and R branches is at least  $35\text{ cm}^{-1}$ . However, the method of reference 105 (Section 3.4) predicts that the separation between the P and R branches of a B-type band in the infrared spectrum of gaseous  $C_2H_4S$  is about  $17\text{ cm}^{-1}$ . Because of this discrepancy between calculated and observed PR separations, the possibility that the  $688.1\text{ cm}^{-1}$  feature arises from an impurity cannot be ruled out, and the frequency of the fourth  $B_1$  mode of the gaseous molecule is left unassigned. In the liquid, this mode is probably at  $650.8\text{ cm}^{-1}$ .

The weak features with PQR structures at  $2903.6$ ,  $2863.5$  and  $1255\text{ cm}^{-1}$  in the infrared spectrum of  $C_2H_4S$  are assigned to the first overtones of the fundamental transitions at  $1456.8$ ,  $1435.9$  and  $627.3\text{ cm}^{-1}$ , respectively. The proximity of  $1255\text{ cm}^{-1}$  to twice  $627.3\text{ cm}^{-1}$  implies that this vibration is almost harmonic. The weak absorption at  $3084.2\text{ cm}^{-1}$  undoubtedly arises from a hot transition (42)

associated with the  $B_2$  mode assigned at  $3088.0 \text{ cm}^{-1}$ . A very weak feature at  $1173.3 \text{ cm}^{-1}$  cannot be assigned to an overtone or combination transition and its origin is not obvious. It does not have the characteristic PR structure of a  $B_1$  fundamental absorption, nor does it have a corresponding polarized Raman band which is characteristic of an  $A_1$  mode. Its assignment to a  $B_2$  mode would require that it shifts to  $710.8 \text{ cm}^{-1}$  or lower in  $C_2D_4S$ , which is most unlikely.

The assignment of the Raman spectrum of the liquid follows from the above assignment of the infrared spectrum of the gas. As is usual, the Raman spectrum does not provide good evidence of the location of the three  $A_2$  modes ( $\nu_6$ ,  $\nu_7$  and  $\nu_8$ ) and, thus, they are not assigned in Table 11. The weak feature at  $895 \text{ cm}^{-1}$  has been assigned by Le Brumant (116) to an  $A_2$  mode but was considered to be too weak to be confidently assigned in this work.

As is the case for  $C_2H_4S$ , the Raman spectrum of  $C_2D_4S$  (Table 12) does not provide a clear-cut indication of the frequencies of  $\nu_6$ ,  $\nu_7$  and  $\nu_8$ , so these modes are not assigned. Four strong Raman bands have depolarization ratios of less than 0.75. The corresponding infrared absorption bands, at  $2212.5$ ,  $946.4$ ,  $766.5$  and  $613.3 \text{ cm}^{-1}$ , show PQR structures and can be assigned to  $A_1$  modes. The product rule (137) can be used to predict the frequency of the fifth  $A_1$  mode. The theoretical value of the product of the  $A_1$  frequencies of  $C_2D_4S$  divided by the product of the  $A_1$  frequencies of

$C_2H_4S$  is given by:

$$\prod_{k=1}^5 \left( \frac{\nu_k'}{\nu_k} \right) = \left( \frac{m_H}{m_D} \right)^{3/2} \left( \frac{M'}{M} \right)^{1/2} = 0.3657 \quad (1)$$

where the primed symbols refer to properties of  $C_2D_4S$  and the corresponding unprimed ones refer to properties of  $C_2H_4S$ ,  $M$  is the molecular weight, the  $\nu_k$  are the frequencies and  $m_H$  and  $m_D$  are the masses (101) of the hydrogen and deuterium atoms, respectively. From the five  $A_1$  frequencies of  $C_2H_4S$  (Table 11) and the four  $A_1$  frequencies of  $C_2D_4S$  assigned above, the missing frequency is calculated to be  $1168 \text{ cm}^{-1}$ , which indicates that  $\nu_2$  is the missing fundamental.  $\nu_2$  of the gaseous molecule is left unassigned at present. There are three medium, polarized Raman bands of the liquid near to  $1168 \text{ cm}^{-1}$ , one of which could be due to  $\nu_2$ , or they could all be due to combination or overtone transitions.

The three strongest infrared bands with PQR structures which have corresponding depolarized Raman bands are assigned to the three  $B_2$  fundamentals. Thus  $\nu_{13}$  is assigned at  $2331.3 \text{ cm}^{-1}$ ,  $\nu_{14}$  at  $710.8 \text{ cm}^{-1}$  and  $\nu_{15}$  at  $578.1 \text{ cm}^{-1}$ . The theoretical value of the product rule for the  $B_2$  modes is given by:

$$\prod_{k=13}^{15} \left( \frac{\nu_k'}{\nu_k} \right) = \left( \frac{m_H}{m_D} \right)^{3/2} \left( \frac{M'}{M} \right)^{1/2} \left( \frac{C}{C'} \right)^{1/2} = 0.3967 \quad (2)$$

where  $C$  is the smallest rotational constant (Table 4), and the other symbols have been defined in equation 1. The value obtained from the three frequencies assigned above with those of  $C_2H_4S$  is 0.3988, which agrees well with the theoretical value.

Three of the  $B_1$  fundamentals can be readily assigned to the medium or strong bands at 2185.2, 1064.2 and 830.7  $cm^{-1}$ . These all have the PR structures expected for a  $B_1$  mode and corresponding depolarized bands appear weakly in the Raman spectrum. The situation concerning the fourth  $B_1$  mode is identical to that for  $C_2H_4S$ . The feature at 654  $cm^{-1}$  is too far away from the absorption at 613.3  $cm^{-1}$  for it to be the R branch of a B-type band whose P branch is buried under the absorption centered at 613.3  $cm^{-1}$ .  $\nu_{12}$  is, therefore, left unassigned for the gaseous molecule, although it probably appears as the medium band at 618  $cm^{-1}$  in the Raman spectrum of the liquid. The description of the fundamental vibrations of  $C_2D_4S$  given in Table 12 follows from the descriptions of the vibrations of  $C_2H_4S$  and the approximate frequency shifts expected to occur upon deuteration.

The weak features in the infrared spectrum of the gas at 654, 746.8, and 1027.8  $cm^{-1}$  cannot be assigned to combination or overtone transitions and they must be tentatively attributed to impurities. The weaker bands left unassigned above 1100  $cm^{-1}$  could all arise from hot, overtone, or combination transitions. The only one whose specific assign-

ment is clear from this data is at  $2125 \text{ cm}^{-1}$ , which is assigned to  $2\nu_{10}$ .

The assignment of the infrared spectrum of cis- $\text{C}_2\text{D}_2\text{H}_2\text{S}$  (Table 13) is also aided by considering the band shapes predicted for vibrational modes of the two symmetry classes,  $A'$  and  $A''$ . Figure 22 shows the relationship between the Cartesian axes, as defined in Figure 21, and the principal axes of inertia of cis- $\text{C}_2\text{D}_2\text{H}_2\text{S}$ . It can be seen that both z- and y-Cartesian axes lie in the ac plane of the molecule. The eight  $A'$  modes of cis- $\text{C}_2\text{D}_2\text{H}_2\text{S}$  cause dipole moment changes in this plane and, thus, lead to AC hybrid bands (104,105). The seven  $A''$  modes of cis- $\text{C}_2\text{D}_2\text{H}_2\text{S}$  cause dipole moment changes along the b-axis of inertia and give rise to B-type infrared absorption bands. It is found, by substituting the values of the rotational constants of cis- $\text{C}_2\text{D}_2\text{H}_2\text{S}$  (Table 4) into equations 1 and 2 of Section 3.4, that  $X = 1.491$  and  $Y = -0.143$ , which indicates that this molecule closely approximates the rotors numbered 16 and 25 in reference 105. The A- and C- type bands calculated for these rotors both have distinct P, Q and R branches, and therefore an AC hybrid band also has PQR structure. A B-type band, on the other hand, is predicted to have PR structure. Thus, the seven bands which clearly have PQR structures, at 3052.0, 2272.4, 1332.6, 971.9, 756.8, 654.7, and  $614.8 \text{ cm}^{-1}$  can confidently be assigned to  $A'$  modes, and the two bands which clearly have PR structures, at 1310.0 and  $921.3 \text{ cm}^{-1}$  can confidently

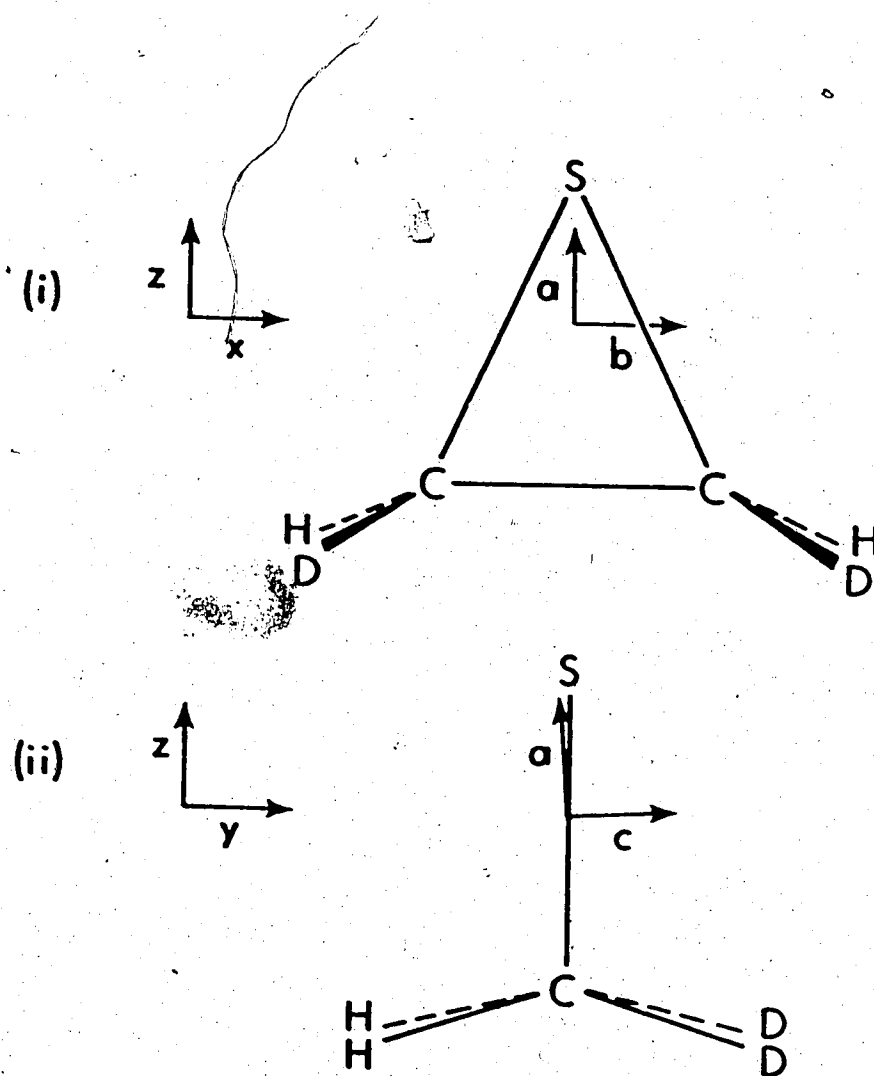


**FIGURE 22.** Projection of  $\text{cis-C}_2\text{D}_2\text{H}_2\text{S}$  on the  $zx$  (i) and  $zy$  (ii) Cartesian planes, showing the relationship between the Cartesian axes and the  $a$ -,  $b$ - and  $c$ - principal axes of inertia.

be assigned to A" modes. The absorption close to 1075 cm<sup>-1</sup> may be due to the superposition of absorptions by the eighth A' mode and a third A" mode, but, at this stage these modes cannot be confidently assigned.

The vibrations must be numbered in the order of decreasing frequency within each symmetry class. For the A' vibrations this is trivial since only one vibration is not assigned and that one undoubtedly is the A' C-C stretching mode,  $\nu_4$ , which should absorb somewhere between the A' frequencies 971.9 and 1332.6 cm<sup>-1</sup>. In addition, the bands at 3052.0, 2272.4, 1332.6 and 614.8 cm<sup>-1</sup> can be assigned to the A' C-H stretching vibration, the A' C-D stretching vibration, the A' HCD deformation, and the A' C-S stretching vibration, respectively. The other A' modes must be CCH or CCD deformations. The A" C-H and C-D stretching modes,  $\nu_9$  and  $\nu_{10}$ , must absorb above 2000 cm<sup>-1</sup> and are probably accidentally degenerate with the A' modes at 3052.0 and 2272.4 cm<sup>-1</sup>, respectively. The A" mode at 1310 cm<sup>-1</sup> is undoubtedly the HCD deformation  $\nu_{11}$ .  $\nu_{12}$  is probably at about 1075 cm<sup>-1</sup>, so 921.3 cm<sup>-1</sup> is probably due to  $\nu_{13}$ .  $\nu_{14}$  and  $\nu_{15}$  are not observed, but  $\nu_{15}$  is probably the A" C-S stretching mode and is, most likely, nearly coincident with the A' C-S stretching mode at 614.8 cm<sup>-1</sup>. Thus,  $\nu_{12}$  to  $\nu_{14}$  must be described as CCH or CCD bends.

Figure 23 shows the relationship between the Cartesian axes, as defined in Figure 21, and the principal axes of inertia of trans-C<sub>2</sub>D<sub>2</sub>H<sub>2</sub>S. It is seen that the x- and y-

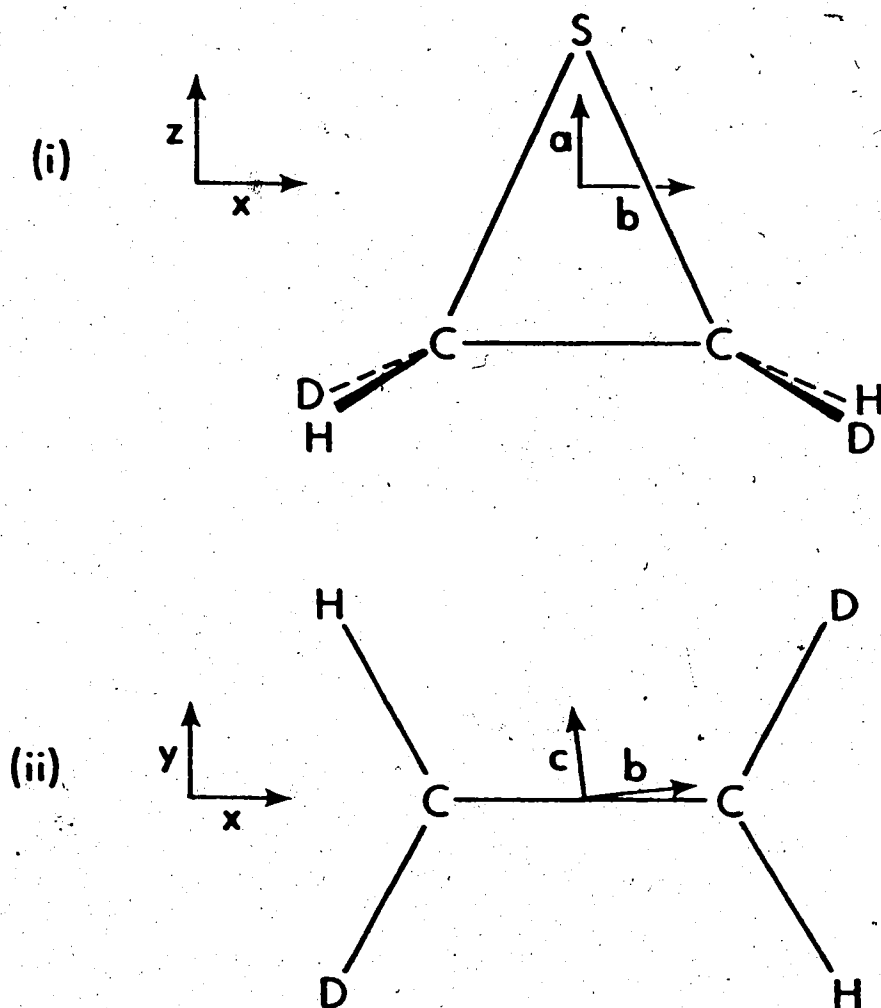


**FIGURE 23.** Projection of trans- $C_2D_2H_2S$  on the  $zx$  (i) and  $yx$  (ii) Cartesian planes, showing the relationship between the Cartesian axes and the  $a$ -,  $b$ - and  $c$ - principal axes of inertia.



Cartesian axes both lie in the bc plane of the molecule and the eight A vibrations give rise to A-type bands and the seven B vibrations give rise to BC hybrid bands (104, 105). The values of the rotational constants of trans- $C_2D_2H_2S$  substituted into equations 1 and 2 of Section 3.4 yield  $X = 1.479$  and  $Y = -0.139$ , which indicates that this molecule closely approximates the rotors numbered 16 and 25 of reference 105. Both A-type and BC hybrid bands for these rotors are predicted to have PQR structures, so no distinction between modes of A and B symmetry can be made on the basis of band shape alone.

Several frequencies in the spectrum of trans- $C_2D_2H_2S$  (Table 14) can be assigned in view of the assignments presented in Tables 11, 12 and 13. The bands at 1113.4 and 617.5  $cm^{-1}$  most probably arise from the A C-C stretching mode ( $\nu_4$ ) and the A C-S stretching mode ( $\nu_8$ ), respectively, and are assigned as such in Table 14. The bands at 3051.0 and 3044.2  $cm^{-1}$  obviously arise from C-H stretching modes and those at 2272.2 and 2262.6  $cm^{-1}$  from C-D stretching modes, although it is not known whether the A or B modes have the higher frequencies. Also, the two  $\widehat{HCD}$  deformations are expected to absorb close in frequency to the very weak features observed at 1315.2 and 1293.1  $cm^{-1}$ .

The assignment of the frequencies of the gaseous molecules which have been made in this section were used as data for the calculations which are described in the next two

sections. These calculations allowed further assignments to be made, as discussed later.

#### 4.5 Computer Programs and the $G$ and $F$ Matrices

The normal coordinate analysis was carried out with the aid of the programs VSEC and FPRT (138) which were written by Schachtschneider. These programs use the well-documented  $G$   $F$  matrix method (100) to calculate the vibrational frequencies,  $\nu_k$ , and the elements,  $l_{ik}$ , of the eigenvectors. The normal coordinates,  $Q_k$ , are related to the  $n$  internal coordinates,  $I_i$ , by  $n$  expressions of the type

$$I_i = \sum_{k=1}^{3N-6} l_{ik} Q_k \quad (1)$$

where  $N$  is the number of atoms in the molecule. Therefore the elements  $l_{ik}$  with  $k$  constant provide a description of the  $k^{\text{th}}$  normal vibration. VSEC and FPRT calculate the frequencies from the  $G$  and  $F$  matrices supplied and, in addition, FPRT compares the calculated frequencies with the observed ones, adjusts the force constants to improve the fit, and continues until a satisfactory solution is reached. If the  $G$  matrices, and observed frequencies of two or more isotopic molecules are supplied, the same force field can be refined to simultaneously fit the frequencies of all the mole-

cules. VSEC, which does not refine the force constants, was only used in the latter stages of the analysis to calculate the forms of the vibrations in terms of methylenic deformations, wags, etc.

The  $G$  matrix elements were calculated for each isotopic modification of ethylene sulphide from the molecular parameters listed in Table 3 and the atomic masses (101), using the programs CART and GMAT (103). The non-zero  $G$  matrix elements for each molecule are presented in Appendix I, where each element is identified by two integers,  $i$  and  $j$ , which refer to the internal coordinates,  $I_i$  and  $I_j$ , respectively, as defined in Table 5. Only the elements for which  $i \leq j$  are listed in Appendix I since the  $G$  matrices are symmetric.

The force constants which are described in this work are defined as the coefficients  $f_{ij}$  in the expression

$$V = \frac{1}{2} \sum_{i,j=1}^n f_{ij} I_i I_j \quad (2)$$

where  $V$  is the potential energy of a molecule in terms of the  $n$  internal coordinates under the harmonic approximation. The matrix formed by these coefficients is termed the  $F$  matrix. When  $i=j$  the coefficients,  $f_{ii}$ , are referred to as the diagonal force constants, and when  $i \neq j$  the coefficients,  $f_{ij}$ , are referred to as the

interaction constants.

The potential energy,  $V_k$ , of a particular vibration with normal coordinate  $Q_k$  and frequency  $\nu_k$  is given by (100):

$$V_k = 1/2 \lambda_k Q_k^2 \quad (3)$$

where  $\lambda_k = 4\pi^2 \nu_k^2$ , and is also given by

$$V_k = \sum_{i,j}^n (\text{PED})_{ijk} \quad (4)$$

where

$$(\text{PED})_{ijk} = \frac{f_{ij}}{\lambda_k} f_{ik} l_{jk} \quad (5)$$

Thus each term  $(\text{PED})_{ijk}$  with  $k$  constant describes the contribution to the potential energy of the  $k^{\text{th}}$  vibration from the force constant  $f_{ij}$ . The complete set of these terms with  $k$  constant is called the potential energy distribution for the  $k^{\text{th}}$  vibration, and provides a description of the vibration which supplements that given by the eigenvectors.

The general harmonic force field for  $\text{C}_2\text{H}_4\text{S}$  or  $\text{C}_2\text{D}_4\text{S}$  contains eight independent diagonal force constants and sixty-one independent interaction constants, and it is assumed that this force field is also valid for cis- and trans- $\text{C}_2\text{D}_2\text{H}_2\text{S}$ . The eight diagonal force constants in the general harmonic force field will be denoted by  $F(\text{CC})$ ,  $F(\text{CS})$ ,  $F(\text{CH})$ ,  $F(\text{HCH})$ ,  $F(\text{SCH})$ ,  $F(\text{CCH})$ ,

$F(\text{CCS})$  and  $F(\text{CSC})$ . The first three force constants are due to the forces which oppose the extension or contraction of the C-C, C-S and C-H bonds, respectively, and have units of  $\text{mdyne} / \text{\AA}$ . The latter five constants have units of  $\text{mdyne}-\text{\AA}$ , and are due to the forces which oppose the distortion of the  $\widehat{\text{HCH}}$ ,  $\widehat{\text{SCH}}$ ,  $\widehat{\text{CCH}}$ ,  $\widehat{\text{C\dot{C}S}}$  and  $\widehat{\text{C\dot{S}C}}$  bond angles, respectively.

The interaction constants account for the change in stiffness of a bond or bond angle as a result of the distortion of another bond or bond angle. The interaction constant between two bond-stretching coordinates,  $R_i$  and  $R_j$  (Table 5), is denoted by  $f(R_i, R_j)$  and has units of  $\text{mdyne} / \text{\AA}$ . The interaction constant between a bond-stretching coordinate,  $R_i$ , and an angle-bending coordinate,  $\alpha_{jk}$ , is denoted by  $f(R_i, \alpha_{jk})$  and has units of  $\text{mdyne}$ , while the interaction constant between two angle-bending coordinates,  $\alpha_{ij}$  and  $\alpha_{kl}$ , is denoted by  $f(\alpha_{ij}, \alpha_{kl})$  and has units of  $\text{mdyne}-\text{\AA}$ .

Because of symmetry, many of the force constants defined in equation 2 are equivalent and, for the sake of simplicity in this work, a reference to a particular force constant in an equivalent set will also implicitly refer to the other members of the set. Thus, for example, the diagonal constant  $F(\text{HCH})$  refers to both  $F(\text{H}_4\widehat{\text{C}}_2\text{H}_5)$  and  $F(\text{H}_6\widehat{\text{C}}_3\text{H}_7)$  (Figure 21), and reference to  $f(\alpha_{14}, \alpha_{34})$ , which describes the interaction between

the  $C_3\hat{C}_2H_4$  and  $S_1\hat{C}_2H_4$  angle-bending coordinates, also implies reference to  $f(\alpha_{15}, \alpha_{35})$ ,  $f(\alpha_{16}, \alpha_{26})$  and  $f(\alpha_{17}, \alpha_{27})$ .

#### 4.6 Development of the Force Field

Initially only the observed frequencies for  $C_2H_4S$  (Table 11) were used in the calculation. The initial values of the diagonal force constants are shown in column #1 of Table 15, the values of  $F(CC)$ ,  $F(CS)$ ,  $F(CCH)$  and  $F(SCH)$  having been taken from the force field for  $C_2H_4S$  reported by Freeman and Henshall (133). The values of  $F(CH)$ ,  $F(HCH)$ ,  $F(CCS)$  and  $F(CSC)$  are close to the values of analogous force constants in the force field of methylene cyclopropane reported by Bertie and Norton (130). The frequencies of  $C_2H_4S$  calculated with this initial force field are shown in column #1 of Table 16, which also contains the experimental frequencies. The differences between the calculated and observed frequencies are, on the average,  $84.0 \text{ cm}^{-1}$  or 6.99%, and were too large to allow FPRT to refine this force field. The potential energy distributions (Section 4.5) revealed that  $F(CCS)$  and  $F(CSC)$  did not contribute significantly to any of the normal modes. Thus these two diagonal force constants were constrained to zero and FPRT did then refine the remaining six constants. The fit between the eleven observed frequencies of  $C_2H_4S$  and the calculated ones did not im-

TABLE 15

Force Constants for Ethylene Sulphide<sup>a,b</sup>

| Constant   | #1   | #2     | #3     | #4     | Final  | Error <sup>c</sup> |
|--|------|--------|--------|--------|--------|--------------------|
| F(CC)  | 4.5  | 4.382  | 4.548  | 4.650  | 4.777  | 0.122              |
| F(CS)  | 2.8  | 2.937  | 2.399  | 2.404  | 2.492  | 0.107              |
| F(CH)  | 5.0  | 5.102  | 5.109  | 5.101  | 5.104  | 0.012              |
| F(HCH)   | 0.41 | 0.391  | 0.467  | 0.264  | 0.772  | 0.074              |
| F(SCH)   | 0.47 | 0.583  | 0.544  | 0.585  | 0.576  | 0.008              |
| F(CCH)   | 0.77 | 0.504  | 0.599  | 0.746  | 0.344  | 0.054              |
| F(CCS)   | 0.50 | 0.0    | 0.0    | 0.0    | 0.301  | 0.094              |
| F(CSC)   | 0.70 | 0.0    | 0.0    | 0.0    | 0.0    | —                  |
| F(R <sub>4</sub> , R <sub>5</sub> ) <sup>d</sup>   | —    | 0.014  | 0.019  | 0.029  | 0.019  | 0.014              |
| F(α <sub>14</sub> , α <sub>34</sub> ) <sup>d</sup> | —    | -0.182 | -0.252 | -0.193 | -0.348 | 0.035              |
| F(R <sub>1</sub> , α <sub>14</sub> ) <sup>d</sup>  | —    | —      | 0.275  | 0.254  | 0.293  | 0.046              |
| F(R <sub>2</sub> , α <sub>26</sub> ) <sup>d</sup>  | —    | —      | 0.227  | 0.243  | 0.373  | 0.065              |
| F(α <sub>45</sub> , α <sub>67</sub> ) <sup>d</sup> | —    | —      | 0.016  | 0.058  | 0.0    | —                  |
| F(α <sub>14</sub> , α <sub>15</sub> ) <sup>d</sup> | —    | —      | —      | 0.190  | -0.236 | 0.048              |
| F(α <sub>34</sub> , α <sub>35</sub> ) <sup>d</sup> | —    | —      | —      | 0.004  | 0.0    | —                  |
| F(α <sub>14</sub> , α <sub>16</sub> ) <sup>d</sup> | —    | —      | —      | -0.045 | -0.008 | 0.007              |
| F(α <sub>14</sub> , α <sub>17</sub> ) <sup>d</sup> | —    | —      | —      | —      | 0.072  | 0.008              |
| F(α <sub>14</sub> , α <sub>35</sub> ) <sup>d</sup> | —    | —      | —      | —      | -0.180 | 0.043              |
| F(R <sub>1</sub> , α <sub>34</sub> ) <sup>d</sup>  | —    | —      | —      | —      | -0.159 | 0.040              |

- a) The units are  $\text{mdyne}/\text{\AA}$  for bond-stretching force constants and stretch-stretch interaction constants,  $\text{mdyne}$  for bond stretch-angle bend interaction constants, and  $\text{mdyne}\text{-}\text{\AA}$  for angle-bending force constants and angle bend-angle bend interaction constants.
- b) Force constants which are shown as zero were constrained to zero during the refinement of that stage.
- c) Statistical error calculated by program (138) from relationship between force constants and frequencies.
- d) All force constants which are equivalent to this under  $C_{2v}$  symmetry had the same value.

TABLE 16

Observed Frequencies for Gaseous  $C_2H_4S$  and those Calculated with the Force Fields Shown in Table 15<sup>a</sup>

|                            | <u>OBS</u> | <u>#1</u>               | <u>#2</u>               | <u>#3</u>               | <u>#4</u>              | <u>Final</u>           |
|----------------------------|------------|-------------------------|-------------------------|-------------------------|------------------------|------------------------|
| $\nu_1$                    | 3013.5     | 2985.5                  | 3017.8                  | 3018.8                  | 3019.6                 | 3018.5                 |
| $\nu_2$                    | 1456.8     | 1684.6                  | 1486.7                  | 1452.1                  | 1463.9                 | 1466.0                 |
| $\nu_3$                    | 1109.9     | 1101.5                  | 1115.1                  | 1106.3                  | 1124.3                 | 1107.1                 |
| $\nu_4$                    | 1024.0     | 916.1                   | 952.7                   | 979.6                   | 999.1                  | 1023.5                 |
| $\nu_5$                    | 627.3      | 651.5                   | 657.2                   | 640.1                   | 640.8                  | 633.3                  |
| $\nu_6$                    |            | 3088.8                  | 3107.0                  | 3107.9                  | 3103.8                 | 3109.2                 |
| $\nu_7$                    |            | 1364.3                  | 992.4                   | 1051.9                  | 1083.4                 | 1160.3                 |
| $\nu_8$                    |            | 765.1                   | 894.5                   | 847.2                   | 896.5                  | 890.2                  |
| $\nu_9$                    | 3013       | 2975.3                  | 3008.5                  | 3011.2                  | 3011.2                 | 3010.4                 |
| $\nu_{10}$                 | 1435.9     | 1616.2                  | 1409.7                  | 1440.2                  | 1432.3                 | 1431.9                 |
| $\nu_{11}$                 | 1050.8     | 975.0                   | 1052.4                  | 1063.4                  | 1057.6                 | 1060.2                 |
| $\nu_{12}$                 |            | 653.3                   | 616.1                   | 586.8                   | 583.9                  | 645.9                  |
| $\nu_{13}$                 | 3088.0     | 3075.4                  | 3101.6                  | 3101.9                  | 3096.7                 | 3100.6                 |
| $\nu_{14}$                 | 945.2      | 1143.5                  | 951.3                   | 962.6                   | 950.5                  | 947.1                  |
| $\nu_{15}$                 | 824.3      | 801.6                   | 817.4                   | 811.1                   | 817.0                  | 820.5                  |
| Average Error <sup>b</sup> |            | 84.0 $cm^{-1}$<br>6.99% | 18.1 $cm^{-1}$<br>1.68% | 12.2 $cm^{-1}$<br>1.15% | 9.1 $cm^{-1}$<br>0.84% | 5.3 $cm^{-1}$<br>0.40% |

a) Observed and calculated frequencies in  $cm^{-1}$

b) Error in  $cm^{-1}$  calculated from  $\left[ \sum_k \left| \nu_k(\text{obs}) - \nu_k(\text{calc}) \right| \right] / n$  where  $n$

is the number of observed frequencies. Percent error calculated from

$$\left[ \sum_k \left| \frac{\nu_k(\text{obs}) - \nu_k(\text{calc})}{\nu_k(\text{obs})} \right| \times 100\% \right] / n.$$



prove after ten refinements by FPERT. At this point interaction constants were introduced into the force field and all constants, except  $F(\text{CCS})$  and  $F(\text{CSC})$  which were both constrained to zero, were refined after each addition.

The first interaction constant which was added to the diagonal field was  $f(R_4, R_5)$ , which takes into account the interaction between the two C-H stretching displacements on carbon atom 2 (Figure 21). Because of the symmetry of  $\text{C}_2\text{H}_4\text{S}$ , the interaction constant  $f(R_6, R_7)$  is equivalent to  $f(R_4, R_5)$ . These two equivalent constants improved the agreement between the observed and calculated C-H stretching frequencies,  $\nu_1$ ,  $\nu_9$  and  $\nu_{13}$ . A second interaction constant,  $f(\alpha_{14}, \alpha_{34})$ , which is equivalent to  $f(\alpha_{15}, \alpha_{35})$ ,  $f(\alpha_{16}, \alpha_{26})$  and  $f(\alpha_{17}, \alpha_{27})$ , takes into account the interaction between the  $\hat{\text{C}}\hat{\text{C}}\hat{\text{H}}$  and  $\hat{\text{S}}\hat{\text{C}}\hat{\text{H}}$  angle-bending coordinates which involve a common hydrogen atom, and improved the agreement between the observed and calculated methylenic frequencies,  $\nu_2$ ,  $\nu_4$ ,  $\nu_{10}$ ,  $\nu_{14}$  and  $\nu_{15}$ .

The frequencies of the ten fundamental vibrations assigned for  $\text{C}_2\text{D}_4\text{S}$  (Table 12) were then included in the calculation and the force field was refined to fit the frequencies of both  $\text{C}_2\text{H}_4\text{S}$  and  $\text{C}_2\text{D}_4\text{S}$ . The force constants and frequencies so obtained are shown in columns headed #2 in Tables 15, 16 and 17. Table 17 also contains the

TABLE 17

Observed Frequencies for Gaseous  $C_2D_4S$  and Those Calculated with the  
Force Fields Shown in Table 15<sup>a</sup>

|                    | <u>OBS</u> | <u>#2</u>      | <u>#3</u>      | <u>#4</u>      | <u>Final</u>  |
|--------------------|------------|----------------|----------------|----------------|---------------|
| $\nu_1$            | 2212.5     | 2214.1         | 2207.9         | 2209.5         | 2210.5        |
| $\nu_2$            |            | 1257.3         | 1151.1         | 1178.9         | 1186.8        |
| $\nu_3$            | 946.4      | 943.6          | 961.5          | 951.0          | 949.4         |
| $\nu_4$            | 766.5      | 796.8          | 766.4          | 783.1          | 764.3         |
| $\nu_5$            | 613.3      | 547.3          | 593.8          | 599.9          | 610.1         |
| $\nu_6$            |            | 2326.1         | 2327.3         | 2326.5         | 2333.4        |
| $\nu_7$            |            | 791.3          | 822.2          | 861.0          | 922.0         |
| $\nu_8$            |            | 632.8          | 611.3          | 635.6          | 630.3         |
| $\nu_9$            | 2185.2     | 2183.8         | 2184.1         | 2182.9         | 2184.8        |
| $\nu_{10}$         | 1064.2     | 1056.4         | 1059.5         | 1076.8         | 1066.6        |
| $\nu_{11}$         | 830.7      | 865.6          | 849.4          | 818.3          | 827.9         |
| $\nu_{12}$         |            | 546.3          | 546.2          | 549.3          | 607.0         |
| $\nu_{13}$         | 2331.3     | 2312.7         | 2312.3         | 2309.1         | 2312.1        |
| $\nu_{14}$         | 710.8      | 709.0          | 698.4          | 706.8          | 707.5         |
| $\nu_{15}$         | 578.1      | 583.4          | 594.8          | 584.5          | 584.3         |
| Average            |            | 16.9 $cm^{-1}$ | 11.6 $cm^{-1}$ | 10.2 $cm^{-1}$ | 4.9 $cm^{-1}$ |
| Error <sup>b</sup> |            | 2.19%          | 1.37%          | 1.08%          | 0.46%         |

a) Observed and calculated frequencies in  $cm^{-1}$ .

b) Defined in Table 16.

experimental frequencies for  $C_2D_4S$ . The frequencies of  $C_2H_4S$  were reproduced with an average error of  $18.1 \text{ cm}^{-1}$  or 1.68% and those of  $C_2D_4S$  with an average error of  $16.9 \text{ cm}^{-1}$  or 2.19%. The largest percent error occurred for the  $A_1$  C-S stretching vibration,  $\nu_5$ , in  $C_2D_4S$ , which was calculated at  $547.3 \text{ cm}^{-1}$  but assigned at  $613.3 \text{ cm}^{-1}$ . Attempts were made to improve this fit by allowing  $F(\text{CCS})$  and  $F(\text{CSC})$  to be refined but these attempts led to an unstable solution, no doubt due to the redundancies involved. Thus, these two force constants were reconstrained to zero.

No improvement in the overall fit was obtained by introducing any of the following interaction constants, one equivalent set at a time:  $f(R_1, R_2) = f(R_1, R_3)$ ;  $f(R_2, R_3)$ ;  $f(R_2, \alpha_{26}) = f(R_2, \alpha_{27}) = f(R_3, \alpha_{34}) = f(R_3, \alpha_{35})$ ;  $f(R_2, \alpha_{16}) = f(R_2, \alpha_{17}) = f(R_3, \alpha_{14}) = f(R_3, \alpha_{15})$ ; or  $f(R_1, \alpha_{14}) = f(R_1, \alpha_{15}) = f(R_1, \alpha_{16}) = f(R_1, \alpha_{17})$ . However, when  $f(R_1, \alpha_{14})$  and  $f(R_2, \alpha_{26})$  and their equivalents were added to the force field together, a solution was found which reproduced the observed frequencies of  $C_2H_4S$  and  $C_2D_4S$  with an average error of 1.30% in each case. However, the  $B_1$   $CH_2$  deformation,  $\nu_{10}$ , was calculated at a higher frequency than the  $A_1$   $CH_2$  deformation,  $\nu_2$ , in  $C_2H_4S$ . Thus the constant  $f(\alpha_{45}, \alpha_{67})$  was added to the force field and all force constants except  $F(\text{CCS})$  and  $F(\text{CSC})$  were refined to the values shown in column #3

of Table 15. The frequencies which were calculated for  $C_2H_4S$  and  $C_2D_4S$  with this force field are shown in the columns headed #3 in Tables 16 and 17, respectively, and the average difference between these frequencies and the experimental ones is  $12.2 \text{ cm}^{-1}$  (1.15%) for  $C_2H_4S$  and  $11.6 \text{ cm}^{-1}$  (1.37%) for  $C_2D_4S$ .

At this point, the frequencies of the normal modes of cis- $C_2D_2H_2S$  and trans- $C_2D_2H_2S$  were calculated using force field #3 and are shown in the columns headed #3 in Tables 18 and 19, respectively. The frequencies of the nine fundamentals of cis- $C_2D_2H_2S$  ( $\nu_1, \nu_2, \nu_3, \nu_5, \nu_6, \nu_7, \nu_8, \nu_{11}, \nu_{13}$ ) and the two fundamentals of trans- $C_2D_2H_2S$  ( $\nu_4$  and  $\nu_8$ ) which were assigned with confidence in Section 4.4 are also shown in these tables and the average difference between these frequencies and those calculated with force field #3 is  $17.1 \text{ cm}^{-1}$  (1.57%) for cis- $C_2D_2H_2S$  and  $22.6 \text{ cm}^{-1}$  (2.58%) for trans- $C_2D_2H_2S$ . However, this force field could not be further refined to a stable solution when these nine observed frequencies for cis- $C_2D_2H_2S$  and two observed frequencies for trans- $C_2D_2H_2S$  were included in the refinement process. Since the largest errors between the observed and calculated frequencies occurred for the methylenic modes, the interaction constants which involve the  $C\hat{C}H$  and  $S\hat{C}H$  angle-bending coordinates,  $f(\alpha_{14}, \alpha_{15}) = f(\alpha_{16}, \alpha_{17})$ ,  $f(\alpha_{34}, \alpha_{35}) = f(\alpha_{26}, \alpha_{27})$  and  $f(\alpha_{14}, \alpha_{16}) = f(\alpha_{15}, \alpha_{17})$ , were added to the

TABLE 18

Observed Frequencies for Gaseous  $\text{cis-C}_2\text{D}_2\text{H}_2\text{S}$  and Those Calculated  
with the Force Fields Shown in Table 15<sup>a</sup>

|                    | <u>OBS<sup>b</sup></u> | <u>#3</u>             | <u>#4</u>            | <u>Final</u>         |
|--------------------|------------------------|-----------------------|----------------------|----------------------|
| $\nu_1$            | 3052.0                 | 3063.0                | 3060.6               | 3062.2               |
| $\nu_2$            | 2272.4                 | 2257.5                | 2257.0               | 2259.1               |
| $\nu_3$            | 1332.6                 | 1303.3                | 1320.4               | 1329.2               |
| $\nu_4$            | (1083.7)               | 1078.3                | 1090.9               | 1080.0               |
| $\nu_5$            | 971.9                  | 969.4                 | 969.1                | 967.5                |
| $\nu_6$            | 756.8                  | 741.0                 | 753.2                | 760.2                |
| $\nu_7$            | 654.7                  | 659.4                 | 660.1                | 657.6                |
| $\nu_8$            | 614.8                  | 610.8                 | 609.4                | 608.2                |
| $\nu_9$            |                        | 3063.3                | 3061.0               | 3063.7               |
| $\nu_{10}$         |                        | 2253.4                | 2252.8               | 2257.4               |
| $\nu_{11}$         | 1310.0                 | 1292.3                | 1305.7               | 1302.7               |
| $\nu_{12}$         | (1068.5)               | 1028.5                | 1001.8               | 1068.1               |
| $\nu_{13}$         | 921.3                  | 867.5                 | 920.3                | 917.8                |
| $\nu_{14}$         |                        | 698.1                 | 712.1                | 719.2                |
| $\nu_{15}$         |                        | 556.7                 | 560.5                | 615.8                |
| Average            |                        |                       |                      |                      |
| Error <sup>c</sup> |                        | 17.1 $\text{cm}^{-1}$ | 6.5 $\text{cm}^{-1}$ | 5.4 $\text{cm}^{-1}$ |
|                    |                        | 1.57%                 | 0.53%                | 0.45%                |

- a) Observed and calculated frequencies in  $\text{cm}^{-1}$
- b) The frequencies in brackets could not be confidently assigned from the experimental data and were only included in the later stages of the refinement.
- c) Defined in Table 16. Frequencies in brackets were included in error calculations with final force field only.

TABLE 19

Observed Frequencies for Gaseous  $\text{trans-C}_2\text{D}_2\text{H}_2\text{S}$  and Those Calculated  
with the Force Fields Shown in Table 15<sup>a</sup>

|                               | <sup>b</sup><br>OBS | #3                               | #4                            | Final                         |
|-------------------------------|---------------------|----------------------------------|-------------------------------|-------------------------------|
| $\nu_1$                       | [3051.0]            | 3066.5                           | 3064.5                        | 3067.                         |
| $\nu_2$                       | [2272.2]            | 2265.2                           | 2266.2                        | 2270.2                        |
| $\nu_3$                       | [1315.2]            | 1306.1                           | 1330.2                        | 1338.3                        |
| $\nu_4$                       | 1113.4              | 1083.4                           | 1104.1                        | 1118.8                        |
| $\nu_5$                       |                     | 995.4                            | 984.8                         | 1026.1                        |
| $\nu_6$                       | [867.7]             | 814.2                            | 874.7                         | 876.5                         |
| $\nu_7$                       | [704.5]             | 695.5                            | 711.1                         | 698.7                         |
| $\nu_8$                       | 617.5               | 602.3                            | 608.2                         | 616.7                         |
| $\nu_9$                       | [3044.2]            | 3059.9                           | 3057.0                        | 3058.8                        |
| $\nu_{10}$                    | [2262.6]            | 2245.5                           | 2243.5                        | 2245.9                        |
| $\nu_{11}$                    | [1293.1]            | 1287.2                           | 1289.2                        | 1288.7                        |
| $\nu_{12}$                    | (1002.8)            | 1023.8                           | 1012.6                        | 1001.0                        |
| $\nu_{13}$                    | [773.4]             | 765.2                            | 759.6                         | 784.8                         |
| $\nu_{14}$                    | [668.2]             | 673.1                            | 666.4                         | 659.1                         |
| $\nu_{15}$                    | (618)               | 560.0                            | 563.1                         | 618.2                         |
| Average<br>Error <sup>c</sup> |                     | • 22.6 $\text{cm}^{-1}$<br>2.58% | 9.3 $\text{cm}^{-1}$<br>1.17% | 2.1 $\text{cm}^{-1}$<br>0.21% |

a) Observed and calculated frequencies in  $\text{cm}^{-1}$

b) The frequencies in brackets could not be confidently assigned from the experimental data. Those in round brackets were included in the late stages of the refinement, and those in square brackets were not included in the refinement.

c) Defined in Table 16. Frequencies in round brackets were included in error calculation with final force field only.

force field, one equivalent set at a time, and all force constants except  $F(\text{CCS})$  and  $F(\text{CSC})$  were refined after each addition. The force field and the calculated frequencies so obtained are presented in the columns headed #4 in Tables 15, 16, 17, 18, and 19. At this point in the calculation the average error between the observed and calculated frequencies of all four isotopic molecules was  $8.7 \text{ cm}^{-1}$  or 0.85%.

The calculations with force field #4 predicted that cis- $\text{C}_2\text{D}_2\text{H}_2\text{S}$  should have an  $A'$  mode ( $\nu_4$ ) at  $1090.9 \text{ cm}^{-1}$  and an  $A''$  mode ( $\nu_{12}$ ) at  $1001.8 \text{ cm}^{-1}$ . When the infrared spectrum of cis- $\text{C}_2\text{D}_2\text{H}_2\text{S}$  which was recorded by Othen (Table 13) was examined in greater detail, it was found that the broad, complicated absorption close to  $1075 \text{ cm}^{-1}$  could be reproduced by superimposing a band with PQB structure at  $1083.7 \text{ cm}^{-1}$  and a band with PR structure at  $1068.5 \text{ cm}^{-1}$ . In view of the band shapes (Section 4.4) and the predicted frequencies,  $1083.7 \text{ cm}^{-1}$  was assigned to  $\nu_4$  and  $1068.5 \text{ cm}^{-1}$  was assigned to  $\nu_{12}$ .

The shape of the absorption at  $1002.8 \text{ cm}^{-1}$  in the infrared spectrum of trans- $\text{C}_2\text{D}_2\text{H}_2\text{S}$  which was recorded by Othen (Table 14) was also examined in greater detail at this point. In Section 4.4 it was shown that modes of A symmetry in trans- $\text{C}_2\text{D}_2\text{H}_2\text{S}$  should give rise to A-type infrared absorption bands and modes of B symmetry should give rise to BC hybrid bands, and that the shapes of these

bands can be predicted by considering the shapes of the A-, B- and C-type bands for rotors numbered 16 or 25 of reference 105. It is found that a pure A-type band has PQR structure with the Q branch being more intense than either the P or R branches. A BC hybrid band also has PQR structure but whether or not the Q branch is more intense than the P and R branches depends upon the amount of C-type character (105). Since the Q branch of the band at  $1002.8 \text{ cm}^{-1}$  in the infrared spectrum of trans- $\text{C}_2\text{D}_2\text{H}_2\text{S}$  is less intense than the P and R branches, this band cannot arise from a mode of A symmetry and therefore it was assigned to a B mode. The calculations using force field #4 predict that the B mode  $\nu_{12}$  should absorb at  $1012.6 \text{ cm}^{-1}$  and thus  $\nu_{12}$  was assigned at  $1002.8 \text{ cm}^{-1}$ .

The inclusion of the two extra frequencies of cis- $\text{C}_2\text{D}_2\text{H}_2\text{S}$  and the extra one of trans- $\text{C}_2\text{D}_2\text{H}_2\text{S}$  in the calculations worsened the overall fit between the observed frequencies and those calculated with force field #4 and, even after several refinements of this force field, the average error was greater than 1.0%. Since force field #4 contained the interaction constants,  $f(\alpha_{14}, \alpha_{16}) = f(\alpha_{15}, \alpha_{17})$ , which take into account the interaction between CCH angle-bending coordinates which are 'cis' to each other, it seemed logical to add the 'trans' interaction constants,  $f(\alpha_{14}, \alpha_{17}) = f(\alpha_{15}, \alpha_{16})$ . However, when these force constants were added to the force field, an oscillatory



solution was obtained. Since  $f(\alpha_{45}, \alpha_{67})$  oscillated about zero, this constant was constrained to zero and the subsequent refinement of the remaining force constants gave a great improvement in the overall fit of the observed frequencies.

The frequencies which were most in error at this point were the symmetric C-S stretching frequencies,  $\nu_5$  in  $C_2H_4S$  and  $C_2D_4S$ , and  $\nu_8$  in cis and trans- $C_2D_2H_2S$ . Also, all of the asymmetric C-S stretching frequencies,  $\nu_{12}$  in  $C_2H_4S$  and  $C_2D_4S$ , and  $\nu_{15}$  in cis- and trans- $C_2D_2H_2S$ , were calculated below  $600\text{ cm}^{-1}$ . However, the only band observed below  $600\text{ cm}^{-1}$  in the spectra of the various isotopic modifications was at  $578.1\text{ cm}^{-1}$  in the spectrum of  $C_2D_4S$ , and this band was clearly due to a  $B_2$  mode (Table 12). A closer inspection of the band at  $617.5\text{ cm}^{-1}$  in the spectrum of trans- $C_2D_2H_2S$  revealed a shoulder at about  $610\text{ cm}^{-1}$  which can be assigned to the P branch of a weak band centered close to  $618\text{ cm}^{-1}$ . Thus the B C-S stretching mode was assigned at  $618\text{ cm}^{-1}$  in trans- $C_2D_2H_2S$  and this frequency was included in the refinement. A stable solution was obtained only after the diagonal force constant  $F(\text{CCS})$  was again included in the refinement. Then all asymmetric C-S stretching modes were calculated to absorb within  $6\text{ cm}^{-1}$  of the symmetric C-S stretching mode in the same molecule. This suggests that these modes are nearly degenerate in all four isotopic modifications.

The constraint on  $F(\text{CSC})$  was then released but a wildly oscillating solution was obtained so this constant was reconstrained to zero. The introduction of two additional sets of interaction constants,  $f(\alpha_{14}, \alpha_{35}) = f(\alpha_{15}, \alpha_{34}) = f(\alpha_{16}, \alpha_{27}) = f(\alpha_{17}, \alpha_{26})$  and  $f(R_1, \alpha_{34}) = f(R_1, \alpha_{35}) = F(R_1, \alpha_{26}) = f(R_1, \alpha_{27})$ , improved the overall fit of the frequencies to an average error of about 0.41%. The interaction constant,  $f(\alpha_{34}, \alpha_{35}) = f(\alpha_{26}, \alpha_{27})$ , was constrained to zero because the calculated uncertainty in this constant was larger than its value, but this caused no significant change in the fit of the observed frequencies. At this point no further improvement in the fit of the calculated frequencies to observed frequencies was considered justified since errors of 1% can easily arise from anharmonicity in the observed frequencies (139). The final force field is shown in Table 15 and the frequencies calculated with this force field are shown in Tables 16-19.

#### 4.7 Discussion

The comparison of the observed frequencies (Tables 11-14) with those calculated with the final force field (Tables 16-19) allows many of the remaining active fundamentals to be recognized in the spectra and assigned, as is summarized in Tables 20 to 23. In particular, the bands at 3051.0, 2272.2, 1315.2, 867.7 and 704.5  $\text{cm}^{-1}$  in

TABLE 20

The Assignment of the Fundamental Frequencies of  $C_2H_4S$ 

| Mode                           | Frequencies/cm <sup>-1</sup> |            | Description <sup>a</sup>                                |
|--------------------------------|------------------------------|------------|---|
|                                | Observed                     | Calculated |   |
| A <sub>1</sub> v <sub>1</sub>  | 3013.5                       | 3018.5     | Symmetric CH <sub>2</sub> stretch                       |
| A <sub>1</sub> v <sub>2</sub>  | 1456.8                       | 1466.0     | 90% CH <sub>2</sub> deformation +<br>10% C-C stretch    |
| A <sub>1</sub> v <sub>3</sub>  | 1109.9                       | 1107.1     | 90% C-C stretch +<br>10% C-S stretch                    |
| A <sub>1</sub> v <sub>4</sub>  | 1024.0                       | 1023.5     | CH <sub>2</sub> wag                                     |
| A <sub>1</sub> v <sub>5</sub>  | 627.3                        | 633.3      | 90% C-S stretch +<br>10% C-C stretch                    |
| A <sub>2</sub> v <sub>6</sub>  | —                            | 3109.2     | Asymmetric CH <sub>2</sub> stretch                      |
| A <sub>2</sub> v <sub>7</sub>  | —                            | 1160.2     | 75% CH <sub>2</sub> rock + 25%<br>CH <sub>2</sub> twist |
| A <sub>2</sub> v <sub>8</sub>  | —                            | 890.2      | 75% CH <sub>2</sub> twist + 25%<br>CH <sub>2</sub> rock |
| B <sub>1</sub> v <sub>9</sub>  | 3013                         | 3010.4     | Symmetric CH <sub>2</sub> stretch                       |
| B <sub>1</sub> v <sub>10</sub> | 1435.9                       | 1431.9     | CH <sub>2</sub> deformation                             |
| B <sub>1</sub> v <sub>11</sub> | 1050.8                       | 1060.2     | CH <sub>2</sub> wag                                     |
| B <sub>1</sub> v <sub>12</sub> | —                            | 645.9      | 85% C-S stretch +<br>15% C-C bend                       |
| B <sub>2</sub> v <sub>13</sub> | 3088.0                       | 3100.6     | Asymmetric CH <sub>2</sub> stretch                      |
| B <sub>2</sub> v <sub>14</sub> | 945.2                        | 947.1      | 55% CH <sub>2</sub> twist + 45%<br>CH <sub>2</sub> rock |
| B <sub>2</sub> v <sub>15</sub> | 824.3                        | 820.5      | 55% CH <sub>2</sub> rock +<br>45% CH <sub>2</sub> twist |

a) Determined from the potential energy distribution in Appendix III.

TABLE 21

The Assignment of the Fundamental Frequencies of  $C_2D_4S$ 

| Mode           | Frequencies/cm <sup>-1</sup> |            | Description <sup>a</sup>  |
|----------------|------------------------------|------------|---|
|                | Observed                     | Calculated |   |
| $A_1 \nu_1$    | 2212.5                       | 2210.5     | Symmetric $CD_2$ stretch  |
| $A_1 \nu_2$    | —                            | 1186.8     | 60% C-C stretch +<br>40% $CD_2$ deformation                     |
| $A_1 \nu_3$    | 946.4                        | 949.4      | 45% C-C stretch +<br>45% $CD_2$ deformation +<br>10% $CD_2$ wag |
| $A_1 \nu_4$    | 766.5                        | 764.3      | 80% $CD_2$ wag +<br>20% C-S stretch                             |
| $A_1 \nu_5$    | 613.3                        | 610.1      | 90% C-S stretch +<br>10% C-C stretch                            |
| $A_2 \nu_6$    | —                            | 2333.4     | Asymmetric $CD_2$ stretch                                       |
| $A_2 \nu_7$    | —                            | 922.0      | 80% $CD_2$ rock +<br>20% $CD_2$ twist                           |
| $A_2 \nu_8$    | —                            | 630.3      | 80% $CD_2$ twist +<br>20% $CD_2$ rock                           |
| $B_1 \nu_9$    | 2185.2                       | 2184.8     | Symmetric $CD_2$ stretch  |
| $B_1 \nu_{10}$ | 1064.2                       | 1066.6     | 80% $CD_2$ deformation +<br>10% $CD_2$ wag +<br>10% C-S stretch |
| $B_1 \nu_{11}$ | 830.7                        | 827.9      | 90% $CD_2$ wag +<br>10% $CD_2$ deformation                      |
| $B_1 \nu_{12}$ | —                            | 607.0      | 85% C-S stretch +<br>15% $\hat{C}CS$ bend                       |
| $B_2 \nu_{13}$ | 2331.3                       | 2312.1     | Asymmetric $CD_2$ stretch                                       |

TABLE 21 (continued)

|              |       |       |                                       |
|--------------|-------|-------|---------------------------------------|
| $B_2 v_{14}$ | 710.8 | 707.5 | 50% $CD_2$ twist +<br>50% $CD_2$ rock |
| $B_2 v_{15}$ | 578.1 | 584.3 | 50% $CD_2$ rock +<br>50% $CD_2$ twist |

a) Determined from the potential energy distribution in Appendix III.

TABLE 22

The Assignment of the Fundamental Frequencies of cis-C<sub>2</sub>D<sub>2</sub>H<sub>2</sub>S

| <u>Frequencies/cm<sup>-1</sup></u> |                 |                   |   |
|------------------------------------|-----------------|-------------------|---|
| <u>Mode</u>                        | <u>Observed</u> | <u>Calculated</u> | <u>Description<sup>a</sup></u>  |
| A' $\nu_1$                         | 3052.0          | 3062.2            | C-H stretch   |
| A' $\nu_2$                         | 2272.4          | 2259.1            | C-D stretch   |
| A' $\nu_3$                         | 1332.6          | 1329.2            | 65% $\hat{H}\hat{C}\hat{D}$ bend +<br>15% $\hat{S}\hat{C}\hat{H}$ bend +<br>10% $\hat{C}\hat{C}\hat{H}$ bend +<br>10% C-C stretch |
| A' $\nu_4$                         | 1083.7          | 1080.1            | 80% C-C stretch +<br>15% $\hat{S}\hat{C}\hat{H}$ bend +<br>5% C-S stretch   |
| A' $\nu_5$                         | 971.9           | 967.5             | 40% $\hat{C}\hat{C}\hat{H}$ bend +<br>40% $\hat{S}\hat{C}\hat{H}$ bend +<br>20% $\hat{H}\hat{C}\hat{D}$ bend                      |
| A' $\nu_6$                         | 756.8           | 760.2             | 85% $\hat{S}\hat{C}\hat{D}$ bend +<br>15% $\hat{S}\hat{C}\hat{H}$ bend  |
| A' $\nu_7$                         | 654.7           | 657.7             | 50% C-S stretch +<br>35% $\hat{C}\hat{C}\hat{D}$ bend +<br>15% $\hat{C}\hat{C}\hat{H}$ bend                                       |
| A' $\nu_8$                         | 614.8           | 608.2             | 75% C-S stretch +<br>25% $\hat{C}\hat{C}\hat{D}$ bend   |
| A'' $\nu_9$                        | 3052            | 3063.7            | C-H stretch   |
| A'' $\nu_{10}$                     | 2272            | 2257.4            | C-D stretch   |
| A'' $\nu_{11}$                     | 1310            | 1302.7            | 65% $\hat{H}\hat{C}\hat{D}$ bend +<br>25% $\hat{S}\hat{C}\hat{H}$ bend +<br>10% $\hat{C}\hat{C}\hat{H}$ bend                      |

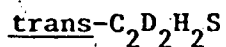
TABLE 22 (continued)

|                |        |        |  |
|----------------|--------|--------|--|
| $A'' \nu_{12}$ | 1068.5 | 1068.1 | 60% $\hat{C}CH$ bend +<br>20% $\hat{SCD}$ bend +<br>10% $\hat{SCH}$ bend +<br>10% $\hat{CCD}$ bend |
| $A'' \nu_{13}$ | 921.3  | 917.8  | 40% $\hat{CCD}$ bend +<br>35% $\hat{HCD}$ bend +<br>25% $\hat{SCH}$ bend                           |
| $A'' \nu_{14}$ | —      | 719.2  | 60% $\hat{SCD}$ bend +<br>15% $\hat{SCH}$ bend +<br>15% C-S stretch +<br>10% $\hat{CCD}$ bend      |
| $A'' \nu_{15}$ | —      | 615.8  | 70% C-S stretch +<br>15% $\hat{CCH}$ bend +<br>15% $\hat{SCD}$ bend                                |

a) Determined from the potential energy distributions and eigenvectors in Appendices II and III.

TABLE 23

## The Assignment of the Fundamental Frequencies of

Frequencies/cm<sup>-1</sup>

| Mode      | Observed | Calculated | Description <sup>a</sup>   |
|-----------|----------|------------|--|
| A $\nu_1$ | 3051.0   | 3067.0     | C-H stretch  |
| A $\nu_2$ | 2272.2   | 2270.2     | C-D stretch  |
| A $\nu_3$ | 1315.2   | 1338.4     | 65% $\hat{H}CD$ bend +<br>15% $\hat{SCH}$ bend +<br>10% $\hat{CCH}$ bend +<br>10% C-C stretch      |
| A $\nu_4$ | 1113.4   | 1118.8     | 60% C-C stretch +<br>20% $\hat{CCH}$ bend +<br>10% $\hat{CCD}$ bend +<br>10% C-S stretch           |
| A $\nu_5$ | —        | 1026.2     | 35% C-C stretch +<br>30% $\hat{CCH}$ bend +<br>25% $\hat{SCH}$ bend +<br>10% $\hat{SCD}$ bend      |
| A $\nu_6$ | 867.7    | 876.5      | 40% $\hat{CCD}$ bend +<br>25% $\hat{SCH}$ bend +<br>25% $\hat{HCD}$ bend +<br>10% $\hat{SCD}$ bend |
| A $\nu_7$ | 704.5    | 698.7      | 70% $\hat{SCD}$ bend +<br>20% C-S stretch +<br>10% $\hat{SCH}$ bend                                |
| A $\nu_8$ | 617.5    | 616.7      | 80% C-S stretch +<br>10% C-C stretch +<br>10% $\hat{SCH}$ bend                                     |
| B $\nu_9$ | 3044.2   | 3058.8     | C-H stretch  |



TABLE 2 (continued)

|              |        |        |   |
|--------------|--------|--------|---|
| $B \nu_{10}$ | 2262.2 | 2245.9 | C-D stretch   |
| $B \nu_{11}$ | 1293.1 | 1288.7 | 75% $\widehat{HCD}$ bend +<br>25% $\widehat{SCH}$ bend                                      |
| $B \nu_{12}$ | 1000.0 | 1000.9 | 40% $\widehat{CCH}$ bend +<br>30% $\widehat{HCD}$ bend +<br>30% $\widehat{SCH}$ bend        |
| $B \nu_{13}$ | 773.4  | 784.8  | 70% $\widehat{SCD}$ bend +<br>20% $\widehat{SCH}$ bend +<br>10% C-S stretch                 |
| $B \nu_{14}$ | 668.2  | 659.1  | 65% $\widehat{CCD}$ bend +<br>25% $\widehat{CCH}$ bend +<br>10% $\widehat{HCD}$ bend        |
| $B \nu_{15}$ | 618    | 618.2  | 70% C-S stretch +<br>15% $\widehat{CCS}$ bend +<br>15% $\widehat{CCD}, \widehat{SCD}$ bends |

- a) Determined from the potential energy distributions and eigenvectors in Appendices II and III

the infrared spectrum of trans-C<sub>2</sub>D<sub>2</sub>H<sub>2</sub>S can be assigned to modes of A symmetry and those at 3044.2, 2262.2, 1293.1, 773.4 and 668.2 cm<sup>-1</sup> can be assigned to modes of B symmetry. In addition, ν<sub>2</sub> of C<sub>2</sub>D<sub>4</sub>S is calculated to absorb at 1186.8 cm<sup>-1</sup>, which confirms its assignment in this region in the Raman spectrum of the liquid. The calculations also revealed several near-degeneracies which undoubtedly account for the failure to observe certain fundamentals in the spectra. First, for cis-C<sub>2</sub>D<sub>2</sub>H<sub>2</sub>S, the A' and A'' C-H stretching modes are calculated at 3062.2 and 3063.7 cm<sup>-1</sup>, respectively, and the A' and A'' C-D stretching modes are calculated at 2259.1 and 2257.4 cm<sup>-1</sup>, respectively. Second, the frequencies calculated for the symmetric and asymmetric C-S stretching modes differ by only 1.5 cm<sup>-1</sup> for trans-C<sub>2</sub>D<sub>2</sub>H<sub>2</sub>S, 3.1 cm<sup>-1</sup> for C<sub>2</sub>D<sub>4</sub>S, 7.6 cm<sup>-1</sup> for cis-C<sub>2</sub>D<sub>2</sub>H<sub>2</sub>S and 12.6 cm<sup>-1</sup> for C<sub>2</sub>H<sub>4</sub>S.

The forms of the normal vibrations in terms of the internal coordinates listed in Table 5 are given by the potential energy distributions and the eigenvectors (Section 4.5) which are presented in Appendix II for each isotopic molecule. In this Appendix, the elements of the potential energy distributions are listed, under each frequency, in the order of the sixteen non-zero force constants in the 'final' column of Table 15. The elements of the eigenvectors are listed, under each frequency, in the order of the internal coordinates in Table 5. From

Appendix II it is not easy to see which of the vibrations of  $C_2H_4S$  and  $C_2D_4S$  correspond to methylenic wags, deformations, rocks and twists. In order to describe the vibrations in terms of these motions, the calculations were repeated with the final force field for  $C_2H_4S$  and  $C_2D_4S$ , using VSEC (138). This program gives the potential energy distributions among the diagonal elements of the symmetrized force constant matrix,  $F_s$ , which is defined (138) as

$$\underline{F}_s = \underline{U} \underline{F} \underline{U}^t \quad (1)$$

where the elements of the  $\underline{U}$  matrix,  $U_{ij}$ , relate the symmetry coordinates,  $S_i$ , to the internal coordinates,  $I_j$ , through the matrix equation

$$\underline{S} = \underline{U} \underline{I} \quad (2)$$

For the calculation by VSEC, the symmetry coordinates shown in Table 6 were used except for  $S_4$ ,  $S_5$ ,  $S_6$ ,  $S_{10}$ ,  $S_{11}$ ,  $S_{14}$ ,  $S_{15}$ ,  $S_{16}$ ,  $S_{19}$  and  $S_{20}$ , which were rewritten as the linear combinations shown in Appendix III to describe the methylenic deformations, wags, rocks and twists. Appendix III also shows the potential energy distribution among the diagonal elements of the  $\underline{F}_s$  matrix which results from this calculation for  $C_2H_4S$  and  $C_2D_4S$ .

The calculated assignments of the normal modes of  $C_2H_4S$  and  $C_2D_4S$  as determined from Appendix III are summarized in Tables 20 and 21, respectively, along with the

observed and calculated frequencies. Most of the vibrations of  $C_2H_4S$  can be reasonably well described by a single type of displacement, e.g. methylenic wag, C-H stretch, etc. However, a significant amount of mixing occurs between the methylenic twisting and rocking vibrations. For  $C_2D_4S$ , all of the vibrations below  $2000\text{ cm}^{-1}$  involve several types of displacements, so the descriptions of the vibrations as twists, rocks, deformations or wags are less meaningful than for  $C_2H_4S$ . The calculations also show that, for both  $C_2H_4S$  and  $C_2D_4S$ , the  $A_2$  mode with the greater methylenic twisting character is to low frequency of the  $A_2$  mode with the greater methylenic rocking character, which is the reverse of the order accepted for other molecules (Section 4.3). This may indicate that the relative order of these modes depends upon the substituent in the ring, or might reflect a deficiency in the final force field, although the frequencies calculated for the  $A_2$  modes of  $C_2H_4S$  with this force field agree well with those reported by LeBrumant (Table 9). It is not surprising that these two modes mix since they have the same symmetry. The  $A_1$  methylenic wag of  $C_2H_4S$  is calculated at lower frequency than the C-C stretch, which suggests that the reverse order proposed by Aleksanyan and Kuz'yants (Tables 9 and 10) is wrong.

The vibrations of cis- $C_2D_2H_2S$  and trans- $C_2D_2H_2S$  cannot be conveniently described in the same way as those of  $C_2H_4S$  and  $C_2D_4S$ , so the potential energy distribution and

eigenvectors shown in Appendix II were used to indicate the form of these vibrations. It is more apparent which vibrations are  $\hat{S}\hat{C}\hat{H}$ ,  $\hat{C}\hat{C}\hat{H}$  bends and which are  $\hat{S}\hat{C}\hat{D}$ ,  $\hat{C}\hat{C}\hat{D}$  bends from the potential energy distribution among the diagonal elements of the F matrix symmetrized using the symmetry coordinates in Tables 7 and 8. Accordingly, these distributions are included in Appendix III. The information given in Appendices II and III is summarized in Tables 22 and 23 for cis- $C_2D_2H_2S$  and trans- $C_2D_2H_2S$ , respectively, by indicating the percentage contribution to the potential energy from the diagonal force constants for each equivalent set of internal coordinates. Except for the C-D and C-H stretching modes, most of the vibrations involve more than one type of displacement. Tables 22 and 23 also include the observed and calculated frequencies and, along with Tables 20 and 21, summarize the assignment of the fundamental frequencies in the spectra of the four molecules in the gas phase.

No further refinement of the force field shown in the 'final' column of Table 15 was attempted using all of the assigned frequencies in Tables 20-23. The sixteen force constants in this force field reproduced the thirty-six frequencies which were included in the final refinement with an average error of 0.41% and, thus, the force field appears to be quite reliable. The uncertainty in each force constant is calculated by FPERT from the relation-

ship between the frequencies and the force constants (138), and is given in Table 15. It can be seen that most of the force constants are well determined. It should be borne in mind, however, that many force constants in the general valence force field were not considered at all in this work. Further, those force constants that were tried and rejected because they did not improve the fit may well have had an influence if they had been tried at a different stage of the calculation. Therefore it is probable that the physical significance of the force constants obtained is not great, and further, that they should only be compared with those obtained for other molecules if the force fields for the other molecules contain similar interaction constants to those used in this work.

The most significant results obtained in this study are believed to be 1) that the potential energy distribution and the eigenvectors yielded descriptions of the various normal vibrations which were not greatly dependent on the force field, and 2) that the calculations indicate that the fundamental frequencies selected for the four isotopic modifications of ethylene sulphide are mutually consistent. It is believed, therefore, that the fundamental frequencies listed in Tables 20 - 23 and the descriptions of the vibrations in terms of the intramolecular displacements are reliable.

## R E F E R E N C E S

1. W. M. Latimer and W. H. Rodebush. J. Amer. Chem. Soc. 42, 1419 (1920).
2. G. C. Pimentel and A. L. McClellan. The Hydrogen Bond, W. H. Freeman and Co., San Francisco, 1960.
3. S. N. Vinogradov and R. H. Linnel. Hydrogen Bonding. D. Van Nostrand Reinhold Co., New York, 1971.
4. W. C. Hamilton and J. A. Ibers. Hydrogen Bonding in Solids. W. A. Benjamin Inc., New York, 1968.
5. D. Hadži and H. W. Thompson, editors. Hydrogen Bonding. Pergamon Press, London, 1959.
6. A. S. N. Murthy and C. N. R. Rao. Appl. Spec. Rev. 2, 69 (1968).
7. L. Pauling. The Nature of the Chemical Bond. Cornell University Press, Ithaca, N.Y., 1960, p.260.
8. Reference 3. Chapter 6.
9. C. A. Coulson. In reference 5. p.339.
10. D. A. K. Jones and J. G. Watkinson. Chem. Ind. 661 (1960).
11. Reference 2. Chapter 2. }
12. Reference 3. Chapter 2.
13. Reference 2. Chapter 3.
14. Reference 3. Chapter 3.
15. Reference 3. Chapter 4.
16. Reference 4. Chapter 2.

17. R. Freymann. *Comptes rendues Acad. Sci.* 195, 39 (1932).
18. M. Holzbecher, O. Knop, and M. Falk. *Can. J. Chem.* 49, 1413 (1971).
19. G. V. Yukhonevich. *Opt. Spect.* 2, 223 (1963).
20. R. M. Badger and S. H. Bauer. *J. Chem. Phys.* 5, 839 (1937).
21. M. D. Joesten and R. S. Drago. *J. Amer. Chem. Soc.* 84, 3817 (1962).
22. R. S. Drago, N. O'Bryan, and G. C. Vogel. *J. Amer. Chem. Soc.* 92, 3924 (1970).
23. Reference 3. P.65.
24. W. A. P. Luck and W. Ditter. *J. Mole. Struct.* 1, 261 (1967-68).
25. J. E. Bertie and D. J. Millen. *J. Chem. Soc.* 514 (1965).
26. A. V. Stuart and G. B. B. M. Sutherland. *J. Chem. Phys.* 24, 559 (1956).
27. P. V. Huong, M. Couzi, and J. Lascombe. *J. Chim. Phys.* 64, 1056 (1967).
28. E. Greinacher, W. Lüttke, and R. Mecke. *Z. Elektrochem.* 59, 23 (1955).
29. T. Miyazawa, T. Shimanouchi, and S. Mizushima. *J. Chem. Phys.* 24, 408 (1956).
30. J. W. Brasch, Y. Mikawa, and R. J. Jakobsen. *Appl. Spec. Rev.* 1, 187 (1968).



31. Reference 3. P.74.
32. G. L. Carlson, R. E. Witkowski, and W. G. Fateley. *Spectrochim. Acta.* 22, 1117 (1966).
33. J. W. Brasch, R. J. Jakobsen, W. G. Fateley, and N. T. McDevitt. *Spectrochim. Acta.* 24A, 203 (1968).
34. K. B. Whetsel and R. E. Kagarise. *Spectrochim. Acta.* 18, 315 (1962).
35. H. Takahashi, K. Mamola, and E. K. Plyler. *J. Mole. Spec.* 21, 217 (1966).
36. E. B. Wilson, J. C. Decius, and P. C. Cross. *Molecular Vibrations.* McGraw Hill Book Co., New York, 1955. P.41
37. G. Herzberg, *Molecular Spectra and Molecular Structure II. Infrared and Raman Spectra of Polyatomic Molecules.* D. Van Nostrand Co. Inc., Princeton, N. J., 1945. Chapter II. Section 5.
38. A. Foldes and C. Sandorfy. *J. Mole. Spec.* 20, 62 (1966).
39. M. Asselin and C. Sandorfy. *J. Mole. Struct.* 8, 145 (1971).
40. T. DiPaolo, C. Bourderson, and C. Sandorfy. *Can. J. Chem.* 50, 3161 (1972).
41. M. Huggins and G. C. Pimentel. *J. Phys. Chem.* 60, 1615 (1956).
42. Reference 37. Chapter III. Section 2.
43. Reference 2. Section 3.3.8.

44. S. Bratož and D. Hadži. *J. Chem. Phys.* 27, 991 (1957).
45. N. Sheppard. In reference 5. P.85.
46. M. I. Batuev. *Zhurn. Fiz. Khim.* 23, 1399 (1949).
47. M. I. Batuev. *Izvest. Akad. Nauk. SSSR. ser. Fiz.* 14, 429 (1950).
48. B. I. Stepanov. *Nature.* 157, 808 (1946).
49. L. Pauling and E. B. Wilson. *Introduction to Quantum Mechanics.* McGraw-Hill Book Co., New York, 1935. Chapter 10.
50. G. Herzberg. *Molecular Spectra and Molecular Structure I. Spectra of Diatomic Molecules.* D. Van Nostrand Co. Inc., Princeton, N.J., 1950. P.77.
51. Reference 50. Chapter 7.
52. J. C. Evans and G. Y-S. Lo. *J. Chem. Phys.* 71, 3942 (1967).
53. J. C. Evans and G. Y-S. Lo. *J. Chem. Phys.* 73, 448 (1969).
54. R. K. Thomas and H. Thompson. *Proc. Roy. Soc. Lond.* 316A, 303 (1970).
55. R. K. Thomas. *Proc. Roy. Soc. Lond.* 325A, 133 (1971).
56. S. Bratož, D. Hadži, and N. Sheppard. *Spectrochim. Acta.* 8, 249 (1956).
57. M. Haurie and A. Novak. *J. Chim. Phys.* 62, 146 (1965).

58. A. Witkowski. J. Chem. Phys. 47, 3645 (1967).
59. Y. Marechal and A. Witkowski. J. Chem. Phys. 48, 3697 (1968).
60. J.-L. Leviel and Y. Marechal. J. Chem. Phys. 54, 1104 (1971).
61. J. Bournay and Y. Marechal. J. Chem. Phys. 55, 1230 (1971).
62. P. Excoffon and Y. Marechal. Spectrochim. Acta. 28A, 269 (1972).
63. R. J. Jakobsen, Y. Mikawa, and J. W. Brasch. Spectrochim. Acta. 25A, 839 (1968).
64. D. J. Millen and J. Zabicky. Nature. 196, 889 (1962).
65. D. J. Millen and J. Zabicky. J. Chem. Soc. 3080 (1965).
66. S. A. Rice and J. L. Wood. J. Chem. Soc. Fara. Trans. II. 69, 87 (1973).
67. S. G. W. Ginn and J. L. Wood. Nature. 200, 467 (1963).
68. G. L. Carlson, R. E. Witkowski, and W. G. Fateley. Nature. 211, 1289 (1966).
69. D. J. Millen and O. A. Samsonov. J. Chem. Soc. 3085 (1965).
70. L. Al Adhami and D. J. Millen. Nature. 211, 1291 (1966).
71. R. M. Seel and N. Sheppard. Spectrochim. Acta. 25A, 1291 (1969).

72. J. Arnold, J. E. Bertie, and D. J. Millen. Proc. Chem. Soc. 121 (1961).
73. J. E. Bertie and D. J. Millen. J. Chem. Soc. 497 (1965).
74. D. N. Shchepkin and L. P. Belozerskaya. Optics and Spec. Suppl. 3, 101 (1968).
75. L. P. Belozerskaya and D. N. Shchepkin. Optics and Spec. Suppl. 3, 146 (1968).
76. J. LeCalvé, P. Grange, and J. Lascombe. Comptes rendues Acad. Sci. (Paris). 261, 2075 (1965).
77. J. Arnold and D. J. Millen. J. Chem. Soc. 503 (1965).
78. M. Couzi, J. LeCalvé, P. V. Huong, and J. Lascombe. J. Mole. Struct. 5, 363 (1970).
79. R. K. Thomas. Proc. Roy. Soc. Lond. 322A, 137 (1971).
80. J. Arnold and D. J. Millen. J. Chem. Soc. 510 (1965).
81. M. Couzi and P. V. Huong. Comptes rendues Acad. Sci. (Paris). 270B, 832 (1970).
82. T. Shidei. Mem. Coll. Sci. Kyoto Univ. 9A, 97 (1925).
83. A. T. Gladishev and Y. K. Syrkin. Comptes rendues Acad. Sci. URSS. 20, 45 (1938).
84. G. Govil, A. D. H. Clague, and H. J. Bernstein. J. Chem. Phys. 49, 2821 (1968).
85. G. L. Vidale and R. C. Taylor. J. Amer. Chem. Soc. 78, 294 (1956).
86. R. M. Seel and N. Sheppard. Spectrochim. Acta. 25A, 1287 (1969).

87. J. C. Lassegues, J. C. Cornut, P. V. Huong, and Y. Grenie. *Spectrochim. Acta.* 27A, 73 (1971).
88. Reference 37. P.428.
89. G. Herzberg. *Molecular Spectra and Molecular Structure III. Electronic Spectra and Electronic Structure of Polyatomic Molecules.* D. Van Nostrand Co. Inc., Princeton, N.J., 1966. P.455.
90. G. D. Parkes and J. W. Mellor. *Mellor's Modern Inorganic Chemistry.* Longmans, Green and Co., New York, 1939. P.736.
91. I.U.P.A.C. *Tables of Wavenumbers for the Calibration of Infrared Spectrometers.* Butterworths London, 1961.
92. R. L. Hansler and R. A. Oetjen. *J. Chem. Phys.* 21, 1340 (1953).
93. I.B.M. Scientific Subroutine Package.
94. Reference 36. P. 177.
95. Y. Kanazawa and K. Nukada. *Bull. Chem. Soc. Japan* 35, 612 (1962).
96. J. P. Perchard, M.-T. Forel, and M.-L. Josien. *J. Chim. Phys.* 61, 632 (1964).
97. W. S. Benedict, R. Herman, G. E. Moore and S. Silverman. *J. Chem. Phys.* 26, 1671 (1957).
98. Reference 50. P.92.
99. Reference 37. P.229.
100. Reference 36. Chapter 4.

101. R. C. Weast, editor. Handbook of Chemistry and Physics. The Chemical Rubber Co., Cleveland, Ohio, 1968. p.B-4.
102. U. Buikis, P. H. Kasai, and R. J. Myers. J. Chem. Phys. 48, 2753 (1963).
103. J. H. Schachtschneider. Technical Report No. 231-64. Project No. 31450. Shell Development Co., Emeryville, Cal., 1964.
104. Reference 37, Chapter IV, Section 4.
105. S. Ueda and T. Shimanouchi. J. Mole. Spec. 28, 350 (1968).
106. J. C. Lassegues, P. V. Huong, and J. Lascombe. Presented at the International Conference on Hydrogen Bonding. Ottawa, Ont., August, 1972.
107. J. C. Lassegues and P. V. Huong. Chem. Phys. Lett. 17, 444 (1972).
108. J. E. Bertie and E. Whalley. J. Chem. Phys. 40, 1646 (1964).
109. D. A. Othen and J. E. Bertie. Unpublished data.
110. G. L. Cunningham, A. W. Boyd, R. J. Myers, G. W. Gwinn, and W. J. LeVan. J. Chem. Phys. 19, 676 (1951).
111. Reference 36. Chapter 6.
112. Reference 37. p.271.
113. H. W. Thompson and J. Dupré. Trans. Fara. Soc. 36, 805 (1940).

114. H. W. Thompson and W. T. Cave. *Trans. Fara. Soc.* 47, 951 (1951).
115. G. B. Guthrie, D. W. Scott, and G. Waddington. *J. Amer. Chem. Soc.* 74, 2795 (1952).
116. J. LeBrumant. *Comptes rendues (Paris)* 266B, 283 (1968).
117. A. W. Baker and R. C. Lord. *J. Chem. Phys.* 23, 1636 (1955).
118. V. T. Aleksanyan and G. M. Kuz'yants. *Zh. Strukt. Khim.* 12, 266 (1971).
119. G. M. Kuz'yants and V. T. Aleksanyan. *Zh. Strukt. Khim.* 13, 617 (1972).
120. F. A. Miller, R. J. Capwell, R. C. Lord, and D. G. Rea. *Spectrochim. Acta.* 28A, 603 (1972).
121. Hs. W. Gunthard, R. C. Lord, and T. K. McCubbin Jr. *J. Chem. Phys.* 26, 768 (1956).
122. P. M. Mathai, G. G. Shepherd, and H. L. Welsh. *Can. J. Phys.* 34, 1448 (1956).
123. C. Brecher, E. Krikorian, J. Blanc, and R. S. Halford. *J. Chem. Phys.* 35, 1092 (1961).
124. M. Solinas. Ph.D. Thesis, University of Alberta, (1973).
125. R. Mecke and H. Spiesecke. *Spectrochim. Acta.* 7, 387 (1957).
126. A. Cheutin and J. P. Mathieu. *J. Chim. Phys.* 53, 106 (1956).

127. L. Couture-Mathieu, J. P. Mathieu, J. Cramer, and H. Poulet. *J. Chim. Phys.* 48, 1 (1951).
128. J. E. Bertie and D. A. Othen. *Can. J. Chem.* 51, 1155 (1973).
129. J. E. Bertie and M. G. Norton. *Can. J. Chem.* 48, 3889 (1970).
130. J. E. Bertie and M. G. Norton. *Can. J. Chem.* 49, 2229 (1971).
131. K. Venkateswarlu, S. Mariam, and M. P. Mathew. *Proc. Ind. Acad. Sci.* 62A, 159 (1965).
132. K. Venkateswarlu and P. A. Joseph. *J. Mole. Struct.* 6, 145 (1970).
133. J. M. Freeman and T. Henshall. *Can. J. Chem.* 46, 2135 (1968).
134. Reference 37. P.380.
135. Reference 36. Section 3.7.
136. Reference 36. Appendix X.
137. Reference 36. P.183.
138. J. H. Schachtschneider. Technical Report No. 57-65. Project No. 31450. Shell Development Co., Emeryville, Cal., 1965.
139. Reference 36. P.196.



A P P E N D I X I

G MATRIX ELEMENTS<sup>a</sup> FOR C<sub>2</sub>H<sub>4</sub>S, C<sub>2</sub>D<sub>4</sub>S, cis-C<sub>2</sub>D<sub>2</sub>H<sub>2</sub>S and

trans-C<sub>2</sub>D<sub>2</sub>H<sub>2</sub>S

(i) C<sub>2</sub>H<sub>4</sub>S

|       |           |       |           |       |           |       |           |
|-------|-----------|-------|-----------|-------|-----------|-------|-----------|
| 1 1   | 0.166667  | 1 2   | 0.033774  | 1 3   | 0.033774  | 1 4   | -0.038911 |
| 1 5   | -0.038911 | 1 6   | -0.038910 | 1 7   | -0.038910 | 1 8   | 0.115402  |
| 1 9   | 0.115402  | 1 10  | -0.002830 | 1 11  | -0.002830 | 1 12  | -0.002831 |
| 1 13  | -0.002831 | 1 14  | -0.068417 | 1 15  | -0.068417 | 1 16  | -0.068417 |
| 1 17  | -0.068417 | 1 18  | -0.041962 | 1 19  | -0.041962 | 1 20  | 0.083925  |
| 2 2   | 0.114611  | 2 3   | 0.021002  | 2 6   | -0.034979 | 2 7   | -0.034979 |
| 2 9   | 0.103741  | 2 10  | -0.004567 | 2 11  | -0.004567 | 2 12  | -0.070223 |
| 2 13  | -0.070223 | 2 14  | -0.014761 | 2 15  | -0.014761 | 2 16  | -0.003551 |
| 2 17  | -0.003551 | 2 18  | 0.064535  | 2 19  | -0.051769 | 2 20  | -0.012766 |
| 3 3   | 0.114611  | 3 4   | -0.034979 | 3 5   | -0.034979 | 3 8   | 0.103741  |
| 3 10  | -0.070223 | 3 11  | -0.070223 | 3 12  | -0.004567 | 3 13  | -0.004567 |
| 3 14  | -0.003550 | 3 15  | -0.003550 | 3 16  | -0.014761 | 3 17  | -0.014761 |
| 3 18  | -0.051769 | 3 19  | 0.064535  | 3 20  | -0.012766 | 4 4   | 1.075427  |
| 4 5   | -0.036401 | 4 8   | -0.069597 | 4 10  | -0.01662  | 4 11  | 0.082409  |
| 4 14  | -0.050076 | 4 15  | 0.100630  | 4 16  | 0.050076  | 4 17  | -0.041933 |
| 4 18  | 0.029181  | 4 19  | -0.014278 | 4 20  | -0.014903 | 5 5   | 1.075427  |
| 5 8   | -0.069597 | 5 10  | 0.082409  | 5 11  | -0.041662 | 5 14  | 0.100630  |
| 5 15  | -0.050076 | 5 16  | -0.041933 | 5 17  | 0.050076  | 5 18  | 0.029181  |
| 5 19  | -0.014278 | 5 20  | -0.014903 | 6 6   | 1.075427  | 6 7   | -0.036401 |
| 6 9   | -0.069597 | 6 12  | -0.041662 | 6 13  | 0.082409  | 6 14  | 0.050076  |
| 6 15  | -0.041933 | 6 16  | -0.050076 | 6 17  | 0.100630  | 6 18  | -0.014278 |
| 6 19  | 0.029181  | 6 20  | -0.014903 | 7 7   | 1.075427  | 7 9   | -0.069597 |
| 7 12  | 0.082409  | 7 13  | -0.041662 | 7 14  | -0.041933 | 7 15  | 0.050076  |
| 7 16  | 0.100630  | 7 17  | -0.050076 | 7 18  | -0.014278 | 7 19  | 0.029181  |
| 7 20  | -0.014903 | 8 8   | 1.916708  | 8 10  | -0.692087 | 8 11  | -0.692087 |
| 8 14  | -0.796177 | 8 15  | -0.796177 | 8 16  | -0.012075 | 8 17  | -0.012075 |
| 8 18  | -0.086546 | 8 19  | 0.042347  | 8 20  | 0.044199  | 9 9   | 1.916713  |
| 9 12  | -0.692089 | 9 13  | -0.692089 | 9 14  | -0.012075 | 9 15  | -0.012075 |
| 9 16  | -0.796181 | 9 17  | -0.796181 | 9 18  | 0.042347  | 9 19  | -0.086545 |
| 9 20  | 0.044199  | 10 10 | 0.997526  | 10 11 | -0.002737 | 10 12 | 0.007460  |
| 10 13 | -0.009091 | 10 14 | 0.279417  | 10 15 | -0.099738 | 10 16 | -0.033031 |
| 10 17 | 0.062311  | 10 18 | 0.032508  | 10 19 | -0.049056 | 10 20 | 0.016558  |
| 11 11 | 0.997526  | 11 12 | -0.009091 | 11 13 | 0.007460  | 11 14 | -0.099738 |
| 11 15 | 0.279417  | 11 16 | 0.062311  | 11 17 | -0.033031 | 11 18 | 0.032508  |
| 11 19 | -0.049066 | 11 20 | 0.016557  | 12 12 | 0.997528  | 12 13 | -0.002736 |
| 12 14 | -0.033030 | 12 15 | 0.062311  | 12 16 | 0.279422  | 12 17 | -0.099738 |
| 12 18 | -0.049066 | 12 19 | 0.032508  | 12 20 | 0.016557  | 13 13 | 0.997528  |
| 13 14 | 0.062311  | 13 15 | -0.033030 | 13 16 | -0.099738 | 13 17 | 0.279422  |
| 13 18 | -0.049066 | 13 19 | 0.032508  | 13 20 | 0.016557  | 14 14 | 1.053038  |
| 14 15 | -0.062504 | 14 16 | -0.126058 | 14 17 | 0.105560  | 14 18 | 0.011411  |
| 14 19 | 0.025339  | 14 20 | -0.036751 | 15 15 | 1.053038  | 15 16 | 0.105560  |
| 15 17 | -0.126058 | 15 18 | 0.011411  | 15 19 | 0.025339  | 15 20 | -0.036751 |
| 16 16 | 1.053039  | 16 17 | -0.062504 | 16 18 | 0.025339  | 16 19 | 0.011411  |
| 16 20 | -0.036750 | 17 17 | 1.053039  | 17 18 | 0.025339  | 17 19 | 0.011411  |
| 17 20 | -0.036750 | 18 18 | 0.086450  | 18 19 | -0.058050 | 18 20 | -0.028400 |
| 19 19 | 0.086450  | 19 20 | -0.028400 | 20 20 | 0.056801  | -1    |           |

(a) The integers before each entry refer to the internal coordinates in Table 5.

## APPENDIX I (continued)

(ii)  $C_{2D_4S}$ 

|       |           |       |           |       |           |       |           |
|-------|-----------|-------|-----------|-------|-----------|-------|-----------|
| 1 1   | 0.166667  | 1 2   | 0.033774  | 1 3   | 0.033774  | 1 4   | -0.038911 |
| 1 5   | -0.038911 | 1 6   | -0.038910 | 1 7   | -0.038910 | 1 8   | 0.115402  |
| 1 9   | 0.115402  | 1 10  | -0.002830 | 1 11  | -0.002830 | 1 12  | -0.002831 |
| 1 13  | -0.002831 | 1 14  | -0.068417 | 1 15  | -0.068417 | 1 16  | -0.068417 |
| 1 17  | -0.068417 | 1 18  | -0.041962 | 1 19  | -0.041962 | 1 20  | 0.083925  |
| 2 2   | 0.114611  | 2 3   | 0.021002  | 2 6   | -0.034979 | 2 7   | -0.034979 |
| 2 9   | 0.103741  | 2 10  | -0.004567 | 2 11  | -0.004567 | 2 12  | -0.070223 |
| 2 13  | -0.070223 | 2 14  | -0.014761 | 2 15  | -0.014761 | 2 16  | -0.003551 |
| 2 17  | -0.003551 | 2 18  | 0.064535  | 2 19  | -0.051769 | 2 20  | -0.012766 |
| 3 3   | 0.114611  | 3 4   | -0.034979 | 3 5   | -0.034979 | 3 8   | 0.103741  |
| 3 10  | -0.070223 | 3 11  | -0.070223 | 3 12  | -0.004567 | 3 13  | -0.004567 |
| 3 14  | -0.003550 | 3 15  | -0.003550 | 3 16  | -0.014761 | 3 17  | -0.014761 |
| 3 18  | -0.051769 | 3 19  | 0.064535  | 3 20  | -0.012766 | 4 4   | 0.579833  |
| 4 5   | -0.036401 | 4 8   | -0.069597 | 4 10  | -0.041662 | 4 11  | 0.082409  |
| 4 14  | -0.050076 | 4 15  | 0.100630  | 4 16  | 0.050076  | 4 17  | -0.041933 |
| 4 18  | 0.029181  | 4 19  | -0.014278 | 4 20  | -0.014903 | 5 5   | 0.579833  |
| 5 8   | -0.069597 | 5 10  | 0.082409  | 5 11  | -0.041662 | 5 14  | 0.100630  |
| 5 15  | -0.050076 | 5 16  | -0.041933 | 5 17  | 0.050076  | 5 18  | 0.029181  |
| 5 19  | -0.014278 | 5 20  | -0.014903 | 6 6   | 0.579833  | 6 7   | -0.036401 |
| 6 9   | -0.069597 | 6 12  | -0.041662 | 6 13  | 0.082409  | 6 14  | 0.050076  |
| 6 15  | -0.041933 | 6 16  | -0.050076 | 6 17  | 0.100630  | 6 18  | -0.014278 |
| 6 19  | 0.029181  | 6 20  | -0.014903 | 7 7   | 0.579833  | 7 9   | -0.069597 |
| 7 12  | 0.082409  | 7 13  | -0.041662 | 7 14  | -0.041933 | 7 15  | 0.050076  |
| 7 16  | 0.100630  | 7 17  | -0.050076 | 7 18  | -0.014278 | 7 19  | 0.029181  |
| 7 20  | -0.014903 | 8 8   | 1.062343  | 8 10  | -0.376544 | 8 11  | -0.376544 |
| 8 14  | -0.435901 | 8 15  | -0.435901 | 8 16  | -0.012075 | 8 17  | -0.012075 |
| 8 18  | -0.086546 | 8 19  | 0.042347  | 8 20  | 0.044159  | 9 9   | 1.062345  |
| 9 12  | -0.376545 | 9 13  | -0.376545 | 9 14  | -0.012075 | 9 15  | -0.012075 |
| 9 16  | -0.435904 | 9 17  | -0.435904 | 9 18  | 0.042347  | 9 19  | -0.086545 |
| 9 20  | 0.044199  | 10 10 | 0.570343  | 10 11 | -0.002737 | 10 12 | 0.007460  |
| 10 13 | -0.009091 | 10 14 | 0.168023  | 10 15 | -0.099738 | 10 16 | -0.033031 |
| 10 17 | 0.062311  | 10 18 | 0.032508  | 10 19 | -0.049066 | 10 20 | 0.016558  |
| 11 11 | 0.570343  | 11 12 | -0.009091 | 11 13 | 0.007460  | 11 14 | -0.099738 |
| 11 15 | 0.168023  | 11 16 | 0.062311  | 11 17 | -0.033031 | 11 18 | 0.032508  |
| 11 19 | -0.049066 | 11 20 | 0.016558  | 12 12 | 0.570344  | 12 13 | -0.002736 |
| 12 14 | -0.033030 | 12 15 | 0.062311  | 12 16 | 0.168026  | 12 17 | -0.099738 |
| 12 18 | -0.049066 | 12 19 | 0.032508  | 12 20 | 0.016557  | 13 13 | 0.570344  |
| 13 14 | 0.062311  | 13 15 | -0.033030 | 13 16 | -0.099738 | 13 17 | 0.168026  |
| 13 18 | -0.049066 | 13 19 | 0.032508  | 13 20 | 0.016557  | 14 14 | 0.625854  |
| 14 15 | -0.062504 | 14 16 | -0.126058 | 14 17 | 0.105560  | 14 18 | 0.011411  |
| 14 19 | 0.025339  | 14 20 | -0.036751 | 15 15 | 0.625854  | 15 16 | 0.105560  |
| 15 17 | -0.126058 | 15 18 | 0.011411  | 15 19 | 0.025339  | 15 20 | -0.036751 |
| 16 16 | 0.625854  | 16 17 | -0.062504 | 16 18 | 0.025339  | 16 19 | 0.011411  |
| 16 20 | -0.036750 | 17 17 | 0.625854  | 17 18 | 0.025339  | 17 19 | 0.011411  |
| 17 20 | -0.036750 | 18 18 | 0.086450  | 18 19 | -0.058050 | 18 20 | -0.028400 |
| 19 19 | 0.086450  | 19 20 | -0.028400 | 20 20 | 0.056801  | -1    |           |

## APPENDIX I (continued)

(iii) cis-C<sub>2</sub>D<sub>2</sub>H<sub>2</sub>S

|       |           |       |           |       |           |       |           |
|-------|-----------|-------|-----------|-------|-----------|-------|-----------|
| 1 1   | 0.166667  | 1 2   | 0.033774  | 1 3   | 0.033774  | 1 4   | -0.038911 |
| 1 5   | -0.038911 | 1 6   | -0.038910 | 1 7   | -0.038910 | 1 8   | 0.115402  |
| 1 9   | 0.115402  | 1 10  | -0.002830 | 1 11  | -0.002830 | 1 12  | -0.002831 |
| 1 13  | -0.002831 | 1 14  | -0.068417 | 1 15  | -0.068417 | 1 16  | -0.068417 |
| 1 17  | -0.068417 | 1 18  | -0.041962 | 1 19  | -0.041962 | 1 20  | 0.083925  |
| 2 2   | 0.114611  | 2 3   | 0.021002  | 2 6   | -0.034979 | 2 7   | -0.034979 |
| 2 9   | 0.103741  | 2 10  | -0.004567 | 2 11  | -0.004567 | 2 12  | -0.070223 |
| 2 13  | -0.070223 | 2 14  | -0.014761 | 2 15  | -0.014761 | 2 16  | -0.003551 |
| 2 17  | -0.003551 | 2 18  | 0.064535  | 2 19  | -0.051769 | 2 20  | -0.012766 |
| 3 3   | 0.114611  | 3 4   | -0.034979 | 3 5   | -0.034979 | 3 8   | 0.103741  |
| 3 10  | -0.070223 | 3 11  | -0.070223 | 3 12  | -0.004567 | 3 13  | -0.004567 |
| 3 14  | -0.003550 | 3 15  | -0.003550 | 3 16  | -0.014761 | 3 17  | -0.014761 |
| 3 18  | -0.051769 | 3 19  | 0.064535  | 3 20  | -0.012766 | 4 4   | 1.075427  |
| 4 5   | -0.036401 | 4 8   | -0.069597 | 4 10  | -0.041662 | 4 11  | 0.082409  |
| 4 14  | -0.050076 | 4 15  | 0.100630  | 4 16  | 0.050076  | 4 17  | -0.041933 |
| 4 18  | 0.029181  | 4 19  | -0.014278 | 4 20  | -0.014903 | 5 5   | 0.579833  |
| 5 8   | -0.069597 | 5 10  | 0.082409  | 5 11  | -0.041662 | 5 14  | 0.100630  |
| 5 15  | -0.050076 | 5 16  | -0.041933 | 5 17  | 0.050076  | 5 18  | 0.029181  |
| 5 19  | -0.014278 | 5 20  | -0.014903 | 6 6   | 1.075427  | 6 7   | -0.036401 |
| 6 9   | -0.069597 | 6 12  | -0.041662 | 6 13  | 0.082409  | 6 14  | 0.050076  |
| 6 15  | -0.041933 | 6 16  | -0.050076 | 6 17  | 0.100630  | 6 18  | -0.014278 |
| 6 19  | 0.029181  | 6 20  | -0.014903 | 7 7   | 0.579833  | 7 9   | -0.069597 |
| 7 12  | 0.082409  | 7 13  | -0.041662 | 7 14  | -0.041933 | 7 15  | 0.050076  |
| 7 16  | 0.100630  | 7 17  | -0.050076 | 7 18  | -0.014278 | 7 19  | 0.029181  |
| 7 20  | -0.014903 | 8 8   | 1.489525  | 8 10  | -0.692087 | 8 11  | -0.376544 |
| 8 14  | -0.796177 | 8 15  | -0.435901 | 8 16  | -0.012075 | 8 17  | -0.012075 |
| 8 18  | -0.086546 | 8 19  | 0.042347  | 8 20  | 0.044199  | 9 4   | 1.489529  |
| 9 12  | -0.692089 | 9 13  | -0.376545 | 9 14  | -0.012075 | 9 15  | -0.012075 |
| 9 16  | -0.796181 | 9 17  | -0.435904 | 9 18  | 0.042347  | 9 19  | -0.086545 |
| 9 20  | 0.044199  | 10 10 | 0.997526  | 10 11 | -0.002737 | 10 12 | 0.007460  |
| 10 13 | -0.009091 | 10 14 | 0.279417  | 10 15 | -0.099738 | 10 16 | -0.033031 |
| 10 17 | 0.062311  | 10 18 | 0.032508  | 10 19 | -0.049066 | 10 20 | 0.016558  |
| 11 11 | 0.570343  | 11 12 | -0.009091 | 11 13 | 0.007460  | 11 14 | -0.099738 |
| 11 15 | 0.168023  | 11 16 | 0.062311  | 11 17 | -0.033031 | 11 18 | 0.032508  |
| 11 19 | -0.049066 | 11 20 | 0.016558  | 12 12 | 0.997528  | 12 13 | -0.002736 |
| 12 14 | -0.033030 | 12 15 | 0.062311  | 12 16 | 0.279422  | 12 17 | -0.099738 |
| 12 18 | -0.049066 | 12 19 | 0.032508  | 12 20 | 0.016557  | 13 13 | 0.570344  |
| 13 14 | 0.062311  | 13 15 | -0.033030 | 13 16 | -0.099738 | 13 17 | 0.168026  |
| 13 18 | -0.049066 | 13 19 | 0.032508  | 13 20 | 0.016557  | 14 14 | 1.053038  |
| 14 15 | -0.062504 | 14 16 | -0.126058 | 14 17 | 0.105560  | 14 18 | 0.011411  |
| 14 19 | 0.025339  | 14 20 | -0.036751 | 15 15 | 0.625854  | 15 16 | 0.105560  |
| 15 17 | -0.126058 | 15 18 | 0.011411  | 15 19 | 0.025339  | 15 20 | -0.036751 |
| 16 16 | 1.053039  | 16 17 | -0.062504 | 16 18 | 0.025339  | 16 19 | 0.011411  |
| 16 20 | -0.036750 | 17 17 | 0.625854  | 17 18 | 0.025339  | 17 19 | 0.011411  |
| 17 20 | -0.036750 | 18 18 | 0.086450  | 18 19 | -0.052050 | 18 20 | -0.028400 |
| 19 19 | 0.086450  | 19 20 | -0.028400 | 20 20 | 0.056801  | -1    |           |

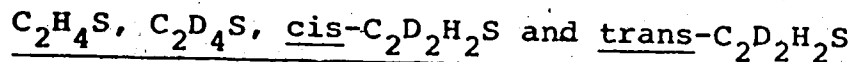
## APPENDIX I (continued)

(iv) trans-C<sub>2</sub>D<sub>2</sub>H<sub>2</sub>S

|       |           |       |           |       |           |       |           |
|-------|-----------|-------|-----------|-------|-----------|-------|-----------|
| 1 1   | 0.166667  | 1 2   | 0.033774  | 1 3   | 0.033774  | 1 4   | -0.038911 |
| 1 5   | -0.038911 | 1 6   | -0.038910 | 1 7   | -0.038910 | 1 8   | 0.115402  |
| 1 9   | 0.115402  | 1 10  | -0.002830 | 1 11  | -0.002830 | 1 12  | -0.002831 |
| 1 13  | -0.002831 | 1 14  | -0.068417 | 1 15  | -0.068417 | 1 16  | -0.068417 |
| 1 17  | -0.068417 | 1 18  | -0.041962 | 1 19  | -0.041962 | 1 20  | 0.083925  |
| 2 2   | 0.114611  | 2 3   | 0.021002  | 2 6   | -0.034979 | 2 7   | -0.034979 |
| 2 9   | 0.103741  | 2 10  | -0.004567 | 2 11  | -0.004567 | 2 12  | -0.070223 |
| 2 13  | -0.070223 | 2 14  | -0.014761 | 2 15  | -0.014761 | 2 16  | -0.003551 |
| 2 17  | -0.003551 | 2 18  | 0.064535  | 2 19  | -0.051769 | 2 20  | -0.012766 |
| 3 3   | 0.114611  | 3 4   | -0.034979 | 3 5   | -0.034979 | 3 8   | 0.103741  |
| 3 10  | -0.070223 | 3 11  | -0.070223 | 3 12  | -0.004567 | 3 13  | -0.004567 |
| 3 14  | -0.003550 | 3 15  | -0.003550 | 3 16  | -0.014761 | 3 17  | -0.014761 |
| 3 18  | -0.051769 | 3 19  | 0.064535  | 3 20  | -0.012766 | 4 4   | 0.579833  |
| 4 5   | -0.036401 | 4 8   | -0.069597 | 4 10  | -0.041662 | 4 11  | 0.082409  |
| 4 14  | -0.050076 | 4 15  | 0.100630  | 4 16  | 0.050076  | 4 17  | -0.041933 |
| 4 18  | 0.029181  | 4 19  | -0.014278 | 4 20  | 0.014903  | 5 5   | 1.075427  |
| 5 8   | -0.069597 | 5 10  | 0.082409  | 5 11  | 0.041662  | 5 14  | 0.100630  |
| 5 15  | -0.050076 | 5 16  | -0.041933 | 5 17  | 0.050076  | 5 18  | 0.029181  |
| 5 19  | -0.014278 | 5 20  | -0.014903 | 6 6   | 1.075427  | 6 7   | -0.036401 |
| 6 9   | -0.069597 | 6 12  | -0.041662 | 6 13  | 0.082409  | 6 14  | 0.050076  |
| 6 15  | -0.041933 | 6 16  | -0.050076 | 6 17  | 0.100630  | 6 18  | -0.014278 |
| 6 19  | 0.029181  | 6 20  | -0.014903 | 7 7   | 0.579833  | 7 9   | -0.069597 |
| 7 12  | 0.082409  | 7 13  | -0.041662 | 7 14  | -0.041933 | 7 15  | 0.050076  |
| 7 16  | 0.100630  | 7 17  | -0.050076 | 7 18  | -0.014278 | 7 19  | 0.029181  |
| 7 20  | -0.014903 | 8 8   | 1.489525  | 8 10  | -0.376544 | 8 11  | -0.692087 |
| 8 14  | -0.435901 | 8 15  | -0.796177 | 8 16  | -0.012075 | 8 17  | -0.012075 |
| 8 18  | -0.086546 | 8 19  | 0.042347  | 8 20  | 0.044199  | 9 9   | 1.489529  |
| 9 12  | -0.692089 | 9 13  | -0.376545 | 9 14  | -0.012075 | 9 15  | -0.012075 |
| 9 16  | -0.796181 | 9 17  | -0.435904 | 9 18  | 0.042347  | 9 19  | -0.086545 |
| 9 20  | 0.044199  | 10 10 | 0.570343  | 10 11 | -0.002737 | 10 12 | 0.007460  |
| 10 13 | -0.009091 | 10 14 | 0.168023  | 10 15 | -0.099738 | 10 16 | -0.033031 |
| 10 17 | 0.062311  | 10 18 | 0.032508  | 10 19 | -0.049066 | 10 20 | 0.016558  |
| 11 11 | 0.997526  | 11 12 | -0.009091 | 11 13 | 0.007460  | 11 14 | -0.099738 |
| 11 15 | 0.279417  | 11 16 | 0.062311  | 11 17 | -0.033031 | 11 18 | 0.032508  |
| 11 19 | -0.049066 | 11 20 | 0.016558  | 12 12 | 0.997528  | 12 13 | -0.002736 |
| 12 14 | -0.033030 | 12 15 | 0.062311  | 12 16 | 0.279422  | 12 17 | -0.099738 |
| 12 18 | -0.049066 | 12 19 | 0.032508  | 12 20 | 0.016557  | 13 13 | 0.570344  |
| 13 14 | 0.062311  | 13 15 | -0.033030 | 13 16 | -0.099738 | 13 17 | 0.168026  |
| 13 18 | -0.049066 | 13 19 | 0.032508  | 13 20 | 0.016557  | 14 14 | 0.625854  |
| 14 15 | -0.062504 | 14 16 | -0.126058 | 14 17 | 0.105560  | 14 18 | 0.011411  |
| 14 19 | 0.025339  | 14 20 | -0.036751 | 15 15 | 1.053038  | 15 16 | 0.105560  |
| 15 17 | -0.126058 | 15 18 | 0.011411  | 15 19 | 0.025339  | 15 20 | -0.036751 |
| 16 16 | 1.053039  | 16 17 | -0.062504 | 16 18 | 0.025339  | 16 19 | 0.011411  |
| 16 20 | -0.036750 | 17 17 | 0.625854  | 17 18 | 0.025339  | 17 19 | 0.011411  |
| 17 20 | -0.036750 | 18 18 | 0.086450  | 18 19 | -0.058050 | 18 20 | -0.028400 |
| 19 19 | 0.086450  | 19 20 | -0.028400 | 20 20 | 0.056801  | -1    |           |

A P P E N D I X I I

POTENTIAL ENERGY DISTRIBUTIONS<sup>a</sup> AND EIGENVECTORS<sup>b</sup> FOR



(i) C<sub>2</sub>H<sub>4</sub>S : Potential Energy Distribution<sup>a</sup>

|                         |         |         |         |         |         |         |         |         |
|-------------------------|---------|---------|---------|---------|---------|---------|---------|---------|
| FREQUENCY = 3018.5 CM-1 |         |         |         |         |         |         |         |         |
| 0.0073                  | 0.0015  | 0.9868  | 0.0024  | 0.0003  | 0.0004  | 0.0000  | 0.0038  | -0.0006 |
| -0.0015                 | -0.0006 | -0.0003 | -0.0000 | 0.0001  | -0.0003 | 0.0006  |         |         |
| FREQUENCY = 1466.0 CM-1 |         |         |         |         |         |         |         |         |
| 0.0828                  | 0.0111  | 0.0032  | 1.1071  | 0.2646  | 0.1377  | 0.0005  | 0.0000  | -0.3095 |
| -0.0976                 | -0.0494 | -0.0946 | -0.0033 | 0.0290  | -0.1604 | 0.0590  |         |         |
| FREQUENCY = 1107.1 CM-1 |         |         |         |         |         |         |         |         |
| 0.8562                  | 0.0904  | 0.0060  | 0.0178  | 0.0487  | 0.0002  | 0.0054  | 0.0000  | 0.0049  |
| -0.0120                 | 0.0584  | -0.0001 | -0.0000 | 0.0000  | 0.0025  | -0.0785 |         |         |
| FREQUENCY = 1023.5 CM-1 |         |         |         |         |         |         |         |         |
| 0.0059                  | 0.0150  | 0.0000  | 0.0877  | 0.2590  | 0.2551  | 0.0003  | 0.0000  | 0.4019  |
| -0.0356                 | -0.0549 | -0.1752 | -0.0062 | 0.0587  | 0.2083  | -0.0151 |         |         |
| FREQUENCY = 635.3 CM-1  |         |         |         |         |         |         |         |         |
| 0.1296                  | 1.0231  | 0.0001  | 0.0363  | 0.0658  | 0.0006  | 0.0155  | 0.0000  | -0.0096 |
| 0.0079                  | -0.2284 | -0.0004 | -0.0000 | 0.0001  | -0.0050 | -0.0355 |         |         |
| FREQUENCY = 3109.2 CM-1 |         |         |         |         |         |         |         |         |
| 0.0                     | 0.0     | 0.9958  | 0.0     | 0.0019  | 0.0043  | 0.0     | -0.0038 | -0.0044 |
| 0.0                     | 0.0     | 0.0030  | 0.0001  | 0.0009  | 0.0023  | 0.0     |         |         |
| FREQUENCY = 1160.2 CM-1 |         |         |         |         |         |         |         |         |
| 0.0                     | 0.0     | 0.0080  | 0.0     | 0.1639  | 0.5485  | 0.0     | -0.0000 | -0.4688 |
| 0.0                     | 0.0     | 0.3768  | 0.0133  | 0.1154  | 0.2430  | 0.0     |         |         |
| FREQUENCY = 890.2 CM-1  |         |         |         |         |         |         |         |         |
| 0.0                     | 0.0     | 0.0000  | 0.0     | 0.9140  | 0.0091  | 0.0     | -0.0000 | 0.1423  |
| 0.0                     | 0.0     | 0.0062  | 0.0002  | 0.0019  | -0.0737 | 0.0     |         |         |
| FREQUENCY = 3010.4 CM-1 |         |         |         |         |         |         |         |         |
| 0.0                     | 0.0013  | 0.9933  | 0.0022  | 0.0003  | 0.0002  | 0.0002  | 0.0038  | -0.0004 |
| 0.0                     | -0.0006 | -0.0001 | 0.0000  | -0.0000 | -0.0002 | 0.0     |         |         |
| FREQUENCY = 1431.9 CM-1 |         |         |         |         |         |         |         |         |
| 0.0                     | 0.0149  | 0.0015  | 1.1196  | 0.3698  | 0.0997  | 0.0028  | 0.0000  | -0.3003 |
| 0.0                     | -0.0653 | -0.0685 | 0.0024  | -0.0210 | -0.1556 | 0.0     |         |         |
| FREQUENCY = 1060.2 CM-1 |         |         |         |         |         |         |         |         |
| 0.0                     | 0.0041  | 0.0002  | 0.1907  | 0.1906  | 0.3308  | 0.0008  | 0.0000  | 0.3927  |
| 0.0                     | -0.0246 | -0.2273 | 0.0080  | -0.0696 | 0.2035  | 0.0     |         |         |
| FREQUENCY = 645.9 CM-1  |         |         |         |         |         |         |         |         |
| 0.0                     | 0.8382  | 0.0012  | 0.0001  | 0.0000  | 0.0308  | 0.1565  | 0.0000  | -0.0001 |
| 0.0                     | 0.0003  | -0.0212 | 0.0007  | -0.0065 | -0.0001 | 0.0     |         |         |
| FREQUENCY = 3100.6 CM-1 |         |         |         |         |         |         |         |         |
| 0.0                     | 0.0     | 1.0023  | 0.0     | 0.0017  | 0.0002  | 0.0     | -0.0038 | -0.0010 |
| 0.0                     | 0.0     | 0.0002  | -0.0000 | -0.0000 | 0.0005  | 0.0     |         |         |
| FREQUENCY = 947.1 CM-1  |         |         |         |         |         |         |         |         |
| 0.0                     | 0.0     | 0.0014  | 0.0     | 1.0447  | 0.0047  | 0.0     | -0.0000 | -0.1098 |
| 0.0                     | 0.0     | 0.0032  | -0.0001 | -0.0010 | 0.0569  | 0.0     |         |         |
| FREQUENCY = 820.5 CM-1  |         |         |         |         |         |         |         |         |
| 0.0                     | 0.0     | 0.0002  | 0.0     | 0.0619  | 0.7581  | 0.0     | -0.0000 | -0.3387 |
| 0.0                     | 0.0     | 0.5208  | -0.0184 | -0.1595 | 0.1755  | 0.0     |         |         |

- a) Entries under each frequency are listed in the order of the sixteen non-zero force constants in the final column of Table 15.
- b) Entries under each frequency are listed in the order of the internal coordinates in Table 5.

1  
APPENDIX II (continued)

(i)  $C_2H_4S$  : Eigenvectors<sup>b</sup>

|                         |         |         |         |         |         |         |         |         |         |
|-------------------------|---------|---------|---------|---------|---------|---------|---------|---------|---------|
| FREQUENCY = 3016.5 CM-1 |         |         |         |         |         |         |         |         |         |
| 0.0906                  | 0.0395  | 0.0395  | -0.5093 | -0.5093 | -0.5093 | -0.5093 | 0.0919  | 0.0919  | -0.0281 |
| -0.0281                 | -0.0281 | -0.0281 | -0.0383 | -0.0383 | -0.0383 | -0.0383 | -0.0177 | -0.0177 | 0.0353  |
| FREQUENCY = 1466.0 CM-1 |         |         |         |         |         |         |         |         |         |
| 0.1491                  | 0.0530  | 0.0530  | 0.0142  | 0.0142  | 0.0142  | 0.0142  | 0.9494  | 0.9494  | -0.3953 |
| -0.3953                 | -0.3953 | -0.3953 | -0.3557 | -0.3557 | -0.3557 | -0.3557 | -0.0317 | -0.0317 | 0.0633  |
| FREQUENCY = 1107.1 CM-1 |         |         |         |         |         |         |         |         |         |
| 0.3597                  | 0.1144  | 0.1144  | 0.0146  | 0.0146  | 0.0146  | 0.0146  | -0.0910 | -0.0910 | 0.1234  |
| 0.1234                  | 0.1234  | 0.1234  | -0.0103 | -0.0103 | -0.0103 | -0.0103 | -0.0804 | -0.0804 | 0.1608  |
| FREQUENCY = 1023.5 CM-1 |         |         |         |         |         |         |         |         |         |
| 0.0277                  | -0.0432 | -0.0432 | -0.0011 | -0.0011 | -0.0011 | -0.0011 | 0.1866  | 0.1866  | 0.2632  |
| 0.2632                  | 0.2632  | 0.2632  | -0.3381 | -0.3381 | -0.3381 | -0.3381 | -0.0189 | -0.0189 | 0.0378  |
| FREQUENCY = 633.3 CM-1  |         |         |         |         |         |         |         |         |         |
| -0.0890                 | 0.2202  | 0.2202  | 0.0008  | 0.0008  | 0.0008  | 0.0008  | 0.0742  | 0.0742  | -0.0821 |
| -0.0821                 | -0.0821 | -0.0821 | -0.0099 | -0.0099 | -0.0099 | -0.0099 | 0.0779  | 0.0779  | -0.1557 |
| FREQUENCY = 3109.2 CM-1 |         |         |         |         |         |         |         |         |         |
| 0.0                     | 0.0     | 0.0     | 0.5269  | -0.5269 | -0.5269 | 0.5269  | 0.0     | 0.0     | -0.0677 |
| 0.0677                  | 0.0677  | -0.0677 | -0.1339 | 0.1339  | 0.1339  | -0.1339 | 0.0     | 0.0     | 0.0     |
| FREQUENCY = 1160.2 CM-1 |         |         |         |         |         |         |         |         |         |
| 0.0                     | 0.0     | 0.0     | 0.0177  | -0.0177 | -0.0177 | 0.0177  | 0.0     | 0.0     | 0.2374  |
| -0.2374                 | -0.2374 | 0.2374  | 0.5620  | -0.5620 | -0.5620 | 0.5620  | 0.0     | 0.0     | 0.0     |
| FREQUENCY = 890.2 CM-1  |         |         |         |         |         |         |         |         |         |
| 0.0                     | 0.0     | 0.0     | 0.0011  | -0.0011 | -0.0011 | 0.0011  | 0.0     | 0.0     | 0.4301  |
| -0.4301                 | -0.4301 | 0.4301  | -0.0554 | 0.0554  | 0.0554  | -0.0554 | 0.0     | 0.0     | 0.0     |
| FREQUENCY = 3010.4 CM-1 |         |         |         |         |         |         |         |         |         |
| 0.0                     | 0.0368  | -0.0368 | 0.5096  | 0.5096  | -0.5096 | -0.5096 | -0.0869 | 0.0869  | 0.0270  |
| 0.0270                  | -0.0270 | -0.0270 | 0.0276  | 0.0276  | -0.0276 | -0.0276 | 0.0458  | -0.0458 | 0.0     |
| FREQUENCY = 1431.9 CM-1 |         |         |         |         |         |         |         |         |         |
| 0.0                     | -0.0600 | 0.0600  | 0.0095  | 0.0095  | -0.0095 | -0.0095 | 0.9325  | -0.9325 | -0.4401 |
| -0.4401                 | 0.4401  | 0.4401  | -0.2957 | -0.2957 | 0.2957  | 0.2957  | -0.0746 | 0.0746  | 0.0     |
| FREQUENCY = 1060.2 CM-1 |         |         |         |         |         |         |         |         |         |
| 0.0                     | 0.0233  | -0.0233 | 0.0024  | 0.0024  | -0.0024 | -0.0024 | 0.2850  | -0.2850 | 0.2339  |
| 0.2339                  | -0.2339 | -0.2339 | -0.3988 | -0.3988 | 0.3988  | 0.3988  | 0.0290  | -0.0290 | 0.0     |
| FREQUENCY = 645.9 CM-1  |         |         |         |         |         |         |         |         |         |
| 0.0                     | 0.2032  | -0.2032 | -0.0038 | -0.0038 | 0.0038  | 0.0038  | 0.0032  | -0.0032 | -0.0001 |
| -0.0001                 | 0.0001  | 0.0001  | -0.0742 | -0.0742 | 0.0742  | 0.0742  | 0.2525  | -0.2525 | 0.0     |
| FREQUENCY = 3100.6 CM-1 |         |         |         |         |         |         |         |         |         |
| 0.0                     | 0.0     | 0.0     | 0.5272  | -0.5272 | -0.5272 | 0.5272  | 0.0     | 0.0     | -0.0648 |
| 0.0648                  | -0.0648 | 0.0648  | -0.0301 | 0.0301  | -0.0301 | 0.0301  | 0.0     | 0.0     | 0.0     |
| FREQUENCY = 947.1 CM-1  |         |         |         |         |         |         |         |         |         |
| 0.0                     | 0.0     | 0.0     | 0.0060  | -0.0060 | 0.0060  | -0.0060 | 0.0     | 0.0     | 0.4893  |
| -0.4893                 | 0.4893  | -0.4893 | 0.0425  | -0.0425 | 0.0425  | -0.0425 | 0.0     | 0.0     | 0.0     |
| FREQUENCY = 820.5 CM-1  |         |         |         |         |         |         |         |         |         |
| 0.0                     | 0.0     | 0.0     | -0.0020 | 0.0020  | -0.0020 | 0.0020  | 0.0     | 0.0     | -0.1032 |
| 0.1032                  | -0.1032 | 0.1032  | -0.4672 | 0.4672  | -0.4672 | 0.4672  | 0.0     | 0.0     | 0.0     |

## APPENDIX II (continued)

(ii)  $C_2D_4S$  : Potential Energy Distribution<sup>a</sup>

|                         |         |         |         |         |         |         |         |         |  |
|-------------------------|---------|---------|---------|---------|---------|---------|---------|---------|--|
| FREQUENCY = 2210.5 CM-1 |         |         |         |         |         |         |         |         |  |
| 0.0355                  | 0.0067  | 0.9517  | 0.0112  | 0.0014  | 0.0018  | 0.0002  | 0.0036  | -0.0025 |  |
| -0.0073                 | -0.0027 | -0.0012 | -0.0000 | 0.0004  | -0.0013 | 0.0027  |         |         |  |
| FREQUENCY = 1186.8 CM-1 |         |         |         |         |         |         |         |         |  |
| 0.5834                  | 0.0648  | 0.0397  | 0.5827  | 0.0871  | 0.0941  | 0.0036  | 0.0002  | -0.1416 |  |
| -0.2141                 | -0.0661 | -0.0646 | -0.0023 | 0.0198  | -0.0734 | 0.0867  |         |         |  |
| FREQUENCY = 949.4 CM-1  |         |         |         |         |         |         |         |         |  |
| 0.3423                  | 0.0203  | 0.0042  | 0.5006  | 0.2943  | 0.0270  | 0.0025  | 0.0000  | -0.1395 |  |
| 0.0879                  | 0.0681  | -0.0186 | -0.0007 | 0.0057  | -0.0723 | -0.1220 |         |         |  |
| FREQUENCY = 764.3 CM-1  |         |         |         |         |         |         |         |         |  |
| 0.0166                  | 0.1951  | 0.0005  | 0.0818  | 0.2675  | 0.2394  | 0.0026  | 0.0000  | 0.3957  |  |
| -0.0577                 | -0.2011 | -0.1645 | -0.0058 | 0.0503  | 0.2051  | -0.0256 |         |         |  |
| FREQUENCY = 610.1 CM-1  |         |         |         |         |         |         |         |         |  |
| 0.1039                  | 0.8543  | 0.0001  | 0.0750  | 0.0081  | 0.0316  | 0.0128  | 0.0000  | -0.0250 |  |
| 0.0524                  | -0.0733 | -0.0217 | -0.0008 | 0.0067  | -0.0130 | -0.0112 |         |         |  |
| FREQUENCY = 2333.4 CM-1 |         |         |         |         |         |         |         |         |  |
| 0.0                     | 0.0     | 0.9768  | 0.0     | 0.0062  | 0.0145  | 0.0     | -0.0037 | -0.0148 |  |
| 0.0                     | 0.0     | 0.0100  | 0.0004  | 0.0030  | 0.0077  | 0.0     |         |         |  |
| FREQUENCY = 522.0 CM-1  |         |         |         |         |         |         |         |         |  |
| 0.0                     | 0.0     | 0.0270  | 0.0     | 0.1861  | 0.5330  | 0.0     | -0.0001 | -0.4926 |  |
| 0.0                     | 0.0     | 0.3662  | 0.0129  | 0.1121  | 0.2553  | 0.0     |         |         |  |
| FREQUENCY = 630.3 CM-1  |         |         |         |         |         |         |         |         |  |
| 0.0                     | 0.0     | 0.0001  | 0.0     | 0.8873  | 0.0144  | 0.0     | -0.0000 | 0.1765  |  |
| 0.0                     | 0.0     | 0.0099  | 0.0003  | 0.0030  | -0.0915 | 0.0     |         |         |  |
| FREQUENCY = 2184.8 CM-1 |         |         |         |         |         |         |         |         |  |
| 0.0                     | 0.0052  | 0.9847  | 0.0085  | 0.0013  | 0.0007  | 0.0010  | 0.0038  | -0.0015 |  |
| 0.0                     | -0.0023 | -0.0005 | 0.0000  | -0.0002 | -0.0008 | 0.0     |         |         |  |
| FREQUENCY = 1066.6 CM-1 |         |         |         |         |         |         |         |         |  |
| 0.0                     | 0.0662  | 0.0073  | 1.0445  | 0.3826  | 0.0675  | 0.0124  | 0.0000  | -0.2513 |  |
| 0.0                     | -0.1401 | -0.0464 | 0.0016  | -0.0142 | -0.1302 | 0.0     |         |         |  |
| FREQUENCY = 827.9 CM-1  |         |         |         |         |         |         |         |         |  |
| 0.0                     | 0.0190  | 0.0006  | 0.2449  | 0.1557  | 0.3664  | 0.0035  | 0.0000  | 0.3782  |  |
| 0.0                     | -0.0485 | -0.2517 | 0.0089  | -0.0771 | 0.1960  | 0.0     |         |         |  |
| FREQUENCY = 607.0 CM-1  |         |         |         |         |         |         |         |         |  |
| 0.0                     | 0.7680  | 0.0036  | 0.0146  | 0.0171  | 0.0269  | 0.1434  | 0.0000  | -0.0336 |  |
| 0.0                     | 0.1008  | -0.0185 | 0.0007  | -0.0057 | -0.0174 | 0.0     |         |         |  |
| FREQUENCY = 2312.1 CM-1 |         |         |         |         |         |         |         |         |  |
| 0.0                     | 0.0     | 0.9987  | 0.0     | 0.0056  | 0.0007  | 0.0     | -0.0038 | -0.0031 |  |
| 0.0                     | 0.0     | 0.0005  | -0.0000 | -0.0002 | 0.0016  | 0.0     |         |         |  |
| FREQUENCY = 707.4 CM-1  |         |         |         |         |         |         |         |         |  |
| 0.0                     | 0.0     | 0.0047  | 0.0     | 1.0744  | 0.0183  | 0.0     | -0.0000 | -0.2195 |  |
| 0.0                     | 0.0     | 0.0126  | -0.0004 | -0.0039 | 0.1138  | 0.0     |         |         |  |
| FREQUENCY = 584.3 CM-1  |         |         |         |         |         |         |         |         |  |
| 0.0                     | 0.0     | 0.0004  | 0.0     | 0.0283  | 0.7440  | 0.0     | -0.0000 | -0.2268 |  |
| 0.0                     | 0.0     | 0.5111  | -0.0181 | -0.1565 | 0.1175  | 0.0     |         |         |  |

## APPENDIX II (continued)

(ii)  $C_2D_4S$  : Eigenvectors<sup>b</sup>

|                         |         |         |         |         |         |         |         |         |         |  |
|-------------------------|---------|---------|---------|---------|---------|---------|---------|---------|---------|--|
| FREQUENCY = 2210.5 CM-1 |         |         |         |         |         |         |         |         |         |  |
| 0.1462                  | 0.0620  | 0.0620  | -0.3662 | -0.3662 | -0.3662 | -0.3662 | 0.1437  | 0.1437  | -0.0415 |  |
| -0.0415                 | -0.0415 | -0.0415 | -0.0616 | -0.0616 | -0.0616 | -0.0616 | -0.0289 | -0.0289 | 0.0578  |  |
| FREQUENCY = 1186.8 CM-1 |         |         |         |         |         |         |         |         |         |  |
| 0.3183                  | 0.1038  | 0.1038  | 0.0402  | 0.0402  | 0.0402  | 0.0402  | 0.5576  | 0.5576  | -0.1770 |  |
| -0.1770                 | -0.1770 | -0.1770 | -0.2380 | -0.2380 | -0.2380 | -0.2380 | -0.0705 | -0.0705 | 0.1411  |  |
| FREQUENCY = 949.4 CM-1  |         |         |         |         |         |         |         |         |         |  |
| 0.1950                  | 0.0465  | 0.0465  | 0.0104  | 0.0104  | 0.0104  | 0.0104  | -0.4134 | -0.4134 | 0.2603  |  |
| 0.2603                  | 0.2603  | 0.2603  | 0.1021  | 0.1021  | 0.1021  | 0.1021  | -0.0474 | -0.0474 | 0.0948  |  |
| FREQUENCY = 764.3 CM-1  |         |         |         |         |         |         |         |         |         |  |
| 0.0346                  | -0.1160 | -0.1160 | -0.0029 | -0.0029 | -0.0029 | -0.0029 | 0.1346  | 0.1346  | 0.1998  |  |
| 0.1998                  | 0.1998  | 0.1998  | -0.2445 | -0.2445 | -0.2445 | -0.2445 | -0.0388 | -0.0388 | 0.0775  |  |
| FREQUENCY = 610.1 CM-1  |         |         |         |         |         |         |         |         |         |  |
| -0.0691                 | 0.1938  | 0.1938  | 0.0011  | 0.0011  | 0.0011  | 0.0011  | 0.1029  | 0.1029  | -0.0278 |  |
| -0.0278                 | -0.0278 | -0.0278 | -0.0709 | -0.0709 | -0.0709 | -0.0709 | 0.0681  | 0.0681  | -0.1363 |  |
| FREQUENCY = 2353.4 CM-1 |         |         |         |         |         |         |         |         |         |  |
| 0.0                     | 0.0     | 0.0     | 0.3917  | -0.3917 | -0.3917 | 0.3917  | 0.0     | 0.0     | -0.0930 |  |
| 0.0930                  | 0.0930  | -0.0930 | -0.1837 | 0.1837  | 0.1837  | -0.1837 | 0.0     | 0.0     | 0.0     |  |
| FREQUENCY = 922.0 CM-1  |         |         |         |         |         |         |         |         |         |  |
| 0.0                     | 0.0     | 0.0     | 0.0257  | -0.0257 | -0.0257 | 0.0257  | 0.0     | 0.0     | 0.2011  |  |
| -0.2011                 | -0.2011 | 0.2011  | 0.4402  | -0.4402 | -0.4402 | 0.4402  | 0.0     | 0.0     | 0.0     |  |
| FREQUENCY = 630.3 CM-1  |         |         |         |         |         |         |         |         |         |  |
| 0.0                     | 0.0     | 0.0     | 0.0008  | -0.0008 | -0.0008 | 0.0008  | 0.0     | 0.0     | 0.3001  |  |
| -0.3001                 | -0.3001 | 0.3001  | -0.0494 | 0.0494  | 0.0494  | -0.0494 | 0.0     | 0.0     | 0.0     |  |
| FREQUENCY = 2184.8 CM-1 |         |         |         |         |         |         |         |         |         |  |
| 0.0                     | 0.0542  | -0.0542 | 0.3682  | 0.3682  | -0.3682 | -0.3682 | -0.1242 | 0.1242  | 0.0395  |  |
| 0.0395                  | -0.0395 | -0.0395 | 0.0383  | 0.0383  | -0.0383 | -0.0383 | 0.0673  | -0.0673 | 0.0     |  |
| FREQUENCY = 1066.6 CM-1 |         |         |         |         |         |         |         |         |         |  |
| 0.0                     | -0.0943 | 0.0943  | 0.0155  | 0.0155  | -0.0155 | -0.0155 | 0.6709  | -0.6709 | -0.3335 |  |
| -0.3335                 | 0.3335  | 0.3335  | -0.1812 | 0.1812  | 0.1812  | -0.1812 | -0.1172 | 0.1172  | 0.0     |  |
| FREQUENCY = 827.9 CM-1  |         |         |         |         |         |         |         |         |         |  |
| 0.0                     | 0.0392  | -0.0392 | 0.0033  | 0.0033  | -0.0033 | -0.0033 | 0.2522  | -0.2522 | 0.1672  |  |
| 0.1672                  | -0.1672 | -0.1672 | -0.3277 | 0.3277  | 0.3277  | -0.3277 | 0.0487  | -0.0487 | 0.0     |  |
| FREQUENCY = 607.0 CM-1  |         |         |         |         |         |         |         |         |         |  |
| 0.0                     | 0.1828  | -0.1828 | -0.0062 | -0.0062 | 0.0062  | 0.0062  | 0.0452  | -0.0452 | -0.0401 |  |
| -0.0401                 | 0.0401  | 0.0401  | -0.0652 | 0.0652  | 0.0652  | -0.0652 | 0.2272  | -0.2272 | 0.0     |  |
| FREQUENCY = 2312.1 CM-1 |         |         |         |         |         |         |         |         |         |  |
| 0.0                     | 0.0     | 0.0     | 0.3924  | -0.3924 | 0.3924  | -0.3924 | 0.0     | 0.0     | -0.0871 |  |
| 0.0871                  | -0.0871 | 0.0871  | -0.0404 | 0.0404  | -0.0404 | 0.0404  | 0.0     | 0.0     | 0.0     |  |
| FREQUENCY = 707.4 CM-1  |         |         |         |         |         |         |         |         |         |  |
| 0.0                     | 0.0     | 0.0     | 0.0082  | -0.0082 | 0.0082  | -0.0082 | 0.0     | 0.0     | 0.3706  |  |
| -0.3706                 | 0.3706  | -0.3706 | 0.0627  | -0.0627 | 0.0627  | -0.0627 | 0.0     | 0.0     | 0.0     |  |
| FREQUENCY = 584.3 CM-1  |         |         |         |         |         |         |         |         |         |  |
| 0.0                     | 0.0     | 0.0     | -0.0020 | 0.0020  | -0.0020 | 0.0020  | 0.0     | 0.0     | -0.0497 |  |
| 0.0497                  | -0.0497 | 0.0497  | -0.3296 | 0.3296  | -0.3296 | 0.3296  | 0.0     | 0.0     | 0.0     |  |



## APPENDIX II (continued)

(iii) cis-C<sub>2</sub>D<sub>2</sub>H<sub>2</sub>S : Potential Energy Distribution<sup>a</sup>

|                         |         |         |         |         |         |         |         |         |
|-------------------------|---------|---------|---------|---------|---------|---------|---------|---------|
| FREQUENCY = 3062.1 CM-1 |         |         |         |         |         |         |         |         |
| 0.0030                  | 0.0006  | 0.9958  | 0.0009  | 0.0010  | 0.0003  | 0.0000  | -0.0005 | -0.0007 |
| -0.0006                 | -0.0002 | -0.0000 | -0.0000 | 0.0000  | 0.0002  | 0.0002  |         |         |
| FREQUENCY = 2259.1 CM-1 |         |         |         |         |         |         |         |         |
| 0.0179                  | 0.0034  | 0.9730  | 0.0072  | 0.0044  | 0.0015  | 0.0001  | 0.0004  | -0.0036 |
| -0.0040                 | -0.0017 | -0.0004 | -0.0000 | 0.0001  | 0.0001  | 0.0017  |         |         |
| FREQUENCY = 1329.1 CM-1 |         |         |         |         |         |         |         |         |
| 0.1704                  | 0.0214  | 0.0162  | 0.9741  | 0.2776  | 0.1385  | 0.0010  | 0.0000  | -0.3056 |
| -0.1332                 | -0.0623 | -0.0761 | -0.0034 | 0.0233  | -0.1188 | 0.0768  |         |         |
| FREQUENCY = 1080.0 CM-1 |         |         |         |         |         |         |         |         |
| 0.7449                  | 0.0697  | 0.0108  | 0.0448  | 0.1603  | 0.0118  | 0.0049  | 0.0000  | -0.0357 |
| -0.0126                 | 0.0712  | 0.0077  | -0.0003 | -0.0024 | 0.0264  | -0.1016 |         |         |
| FREQUENCY = 967.5 CM-1  |         |         |         |         |         |         |         |         |
| 0.0004                  | 0.0233  | 0.0009  | 0.1046  | 0.2455  | 0.2695  | 0.0001  | 0.0000  | 0.3965  |
| 0.0084                  | -0.0503 | -0.0859 | -0.0065 | 0.0263  | 0.0643  | 0.0030  |         |         |
| FREQUENCY = 760.2 CM-1  |         |         |         |         |         |         |         |         |
| 0.0325                  | 0.0297  | 0.0026  | 0.0252  | 0.9901  | 0.0111  | 0.0012  | -0.0000 | -0.2574 |
| -0.0178                 | -0.0566 | 0.0259  | -0.0015 | -0.0079 | 0.1989  | -0.0259 |         |         |
| FREQUENCY = 657.6 CM-1  |         |         |         |         |         |         |         |         |
| 0.0317                  | 0.4135  | 0.0006  | 0.0101  | 0.0788  | 0.4527  | 0.0054  | -0.0000 | -0.1478 |
| -0.0262                 | -0.1146 | 0.2755  | -0.0110 | -0.0843 | 0.1294  | -0.0139 |         |         |
| FREQUENCY = 608.2 CM-1  |         |         |         |         |         |         |         |         |
| 0.0809                  | 0.5797  | 0.0000  | 0.0845  | 0.0088  | 0.2215  | 0.0090  | 0.0000  | -0.0080 |
| 0.0472                  | -0.0604 | 0.1070  | -0.0054 | -0.0328 | -0.0224 | -0.0099 |         |         |
| FREQUENCY = 3063.7 CM-1 |         |         |         |         |         |         |         |         |
| 0.0                     | 0.0005  | 0.9950  | 0.0006  | 0.0011  | 0.0025  | 0.0001  | -0.0006 | -0.0026 |
| 0.0                     | -0.0002 | 0.0017  | 0.0001  | 0.0005  | 0.0013  | 0.0     |         |         |
| FREQUENCY = 2257.4 CM-1 |         |         |         |         |         |         |         |         |
| 0.0                     | 0.0026  | 0.9756  | 0.0068  | 0.0049  | 0.0094  | 0.0005  | 0.0006  | -0.0104 |
| 0.0                     | -0.0014 | 0.0055  | 0.0002  | 0.0017  | 0.0040  | 0.0     |         |         |
| FREQUENCY = 1302.7 CM-1 |         |         |         |         |         |         |         |         |
| 0.0                     | 0.0176  | 0.0122  | 0.9695  | 0.3870  | 0.1437  | 0.0033  | 0.0000  | -0.3620 |
| 0.0                     | -0.0646 | -0.0233 | 0.0035  | -0.0071 | -0.0797 | 0.0     |         |         |
| FREQUENCY = 1068.1 CM-1 |         |         |         |         |         |         |         |         |
| 0.0                     | 0.0138  | 0.0094  | 0.0002  | 0.3898  | 0.3838  | 0.0026  | -0.0000 | 0.1358  |
| 0.0                     | -0.0422 | 0.1533  | 0.0093  | 0.0469  | 0.1173  | 0.0     |         |         |
| FREQUENCY = 517.8 CM-1  |         |         |         |         |         |         |         |         |
| 0.0                     | 0.0034  | 0.0047  | 0.3290  | 0.2906  | 0.3919  | 0.0006  | -0.0000 | -0.2276 |
| 0.0                     | 0.0077  | -0.0314 | 0.0095  | -0.0096 | 0.2313  | 0.0     |         |         |
| FREQUENCY = 719.2 CM-1  |         |         |         |         |         |         |         |         |
| 0.0                     | -0.1347 | 0.0003  | 0.0020  | 0.6578  | 0.0757  | 0.0251  | 0.0000  | 0.2529  |
| 0.0                     | -0.0729 | -0.0255 | 0.0018  | -0.0078 | -0.0442 | 0.0     |         |         |
| FREQUENCY = 615.8 CM-1  |         |         |         |         |         |         |         |         |
| 0.0                     | 0.6859  | 0.0027  | 0.0045  | 0.1292  | 0.0166  | 0.1280  | 0.0000  | -0.0251 |
| 0.0                     | 0.0836  | -0.0113 | 0.0004  | -0.0035 | -0.0109 | 0.0     |         |         |

## APPENDIX II (continued)

(iii) cis-C<sub>2</sub>D<sub>2</sub>H<sub>2</sub>S : Eigenvectors<sup>b</sup>

|                         |         |         |         |         |         |         |         |         |         |
|-------------------------|---------|---------|---------|---------|---------|---------|---------|---------|---------|
| FREQUENCY = 3062.1 CM-1 |         |         |         |         |         |         |         |         |         |
| -0.0590                 | -0.0258 | -0.0258 | 0.7325  | -0.0457 | 0.7325  | -0.0457 | -0.0553 | -0.0553 | -0.0312 |
| 0.0631                  | -0.0312 | 0.0631  | 0.0018  | 0.0455  | 0.0018  | 0.0455  | 0.0115  | 0.0115  | -0.0230 |
| FREQUENCY = 2259.1 CM-1 |         |         |         |         |         |         |         |         |         |
| 0.1060                  | 0.0450  | 0.0450  | -0.0271 | -0.5345 | -0.0271 | -0.5345 | 0.1181  | 0.1181  | -0.1037 |
| 0.0286                  | -0.1037 | 0.0286  | -0.0797 | -0.0176 | -0.0797 | -0.0176 | -0.0209 | -0.0209 | 0.0419  |
| FREQUENCY = 1329.1 CM-1 |         |         |         |         |         |         |         |         |         |
| 0.1926                  | 0.0668  | 0.0668  | 0.0132  | 0.0385  | 0.0132  | 0.0385  | 0.8074  | 0.8074  | -0.4647 |
| -0.1860                 | -0.4647 | -0.1860 | -0.4093 | -0.2045 | -0.4093 | -0.2045 | -0.0417 | -0.0417 | 0.0834  |
| FREQUENCY = 1080.0 CM-1 |         |         |         |         |         |         |         |         |         |
| 0.3273                  | 0.0980  | 0.0980  | 0.0148  | 0.0225  | 0.0148  | 0.0225  | -0.1406 | -0.1406 | 0.3080  |
| 0.0263                  | 0.3080  | 0.0263  | 0.0645  | -0.0870 | 0.0645  | -0.0870 | -0.0747 | -0.0747 | 0.1493  |
| FREQUENCY = 967.5 CM-1  |         |         |         |         |         |         |         |         |         |
| -0.0070                 | -0.0507 | -0.0507 | -0.0003 | -0.0072 | -0.0003 | -0.0072 | 0.1926  | 0.1926  | 0.3417  |
| 0.0248                  | 0.3417  | 0.0248  | -0.4511 | -0.1110 | -0.4511 | -0.1110 | -0.0103 | -0.0103 | 0.0205  |
| FREQUENCY = 760.2 CM-1  |         |         |         |         |         |         |         |         |         |
| -0.0481                 | 0.0451  | 0.0451  | 0.0043  | -0.0082 | 0.0043  | -0.0082 | 0.0743  | 0.0743  | 0.2110  |
| -0.4978                 | 0.2110  | -0.4978 | 0.1643  | -0.0567 | 0.1643  | -0.0567 | 0.0255  | 0.0255  | -0.0510 |
| FREQUENCY = 657.6 CM-1  |         |         |         |         |         |         |         |         |         |
| -0.0411                 | 0.1453  | 0.1453  | -0.0003 | 0.0039  | -0.0003 | 0.0039  | -0.0407 | -0.0407 | -0.1320 |
| -0.0027                 | -0.1320 | -0.0027 | -0.2118 | 0.3502  | -0.2118 | 0.3502  | 0.0479  | 0.0479  | -0.0958 |
| FREQUENCY = 608.2 CM-1  |         |         |         |         |         |         |         |         |         |
| -0.0608                 | 0.1591  | 0.1591  | 0.0006  | 0.0004  | 0.0006  | 0.0004  | 0.1088  | 0.1088  | -0.0357 |
| -0.0197                 | -0.0357 | -0.0197 | 0.1006  | -0.2449 | 0.1006  | -0.2449 | 0.0572  | 0.0572  | -0.1143 |
| FREQUENCY = 3063.7 CM-1 |         |         |         |         |         |         |         |         |         |
| 0.0                     | -0.0235 | 0.0235  | -0.7320 | 0.0542  | 0.7320  | -0.0542 | 0.0473  | -0.0473 | 0.0354  |
| -0.0650                 | -0.0354 | 0.0650  | 0.0859  | -0.1133 | -0.0859 | 0.1133  | -0.0292 | 0.0292  | 0.0     |
| FREQUENCY = 2257.4 CM-1 |         |         |         |         |         |         |         |         |         |
| 0.0                     | 0.0397  | -0.0397 | 0.0408  | 0.5340  | -0.0408 | -0.5340 | -0.1148 | 0.1148  | 0.1070  |
| -0.0346                 | -0.1070 | 0.0346  | 0.1770  | -0.0983 | -0.1770 | 0.0983  | 0.0493  | -0.0493 | 0.0     |
| FREQUENCY = 1302.7 CM-1 |         |         |         |         |         |         |         |         |         |
| 0.0                     | 0.0594  | -0.0594 | -0.0013 | -0.0346 | 0.0013  | 0.0346  | -0.7895 | 0.7895  | 0.5515  |
| 0.1771                  | -0.5515 | -0.1771 | 0.4535  | 0.0543  | -0.4535 | -0.0543 | 0.0738  | -0.0738 | 0.0     |
| FREQUENCY = 1068.1 CM-1 |         |         |         |         |         |         |         |         |         |
| 0.0                     | -0.0431 | 0.0431  | 0.0109  | -0.0223 | -0.0109 | 0.0223  | -0.0095 | 0.0095  | -0.1922 |
| -0.2490                 | 0.1922  | 0.2490  | 0.5827  | -0.1869 | -0.5827 | 0.1869  | -0.0535 | 0.0535  | 0.0     |
| FREQUENCY = 917.8 CM-1  |         |         |         |         |         |         |         |         |         |
| 0.0                     | -0.0184 | 0.0184  | 0.0112  | -0.0101 | -0.0112 | 0.0101  | 0.3240  | -0.3240 | 0.3096  |
| -0.1709                 | -0.3096 | 0.1709  | -0.0311 | -0.5305 | 0.0311  | 0.5305  | -0.0229 | 0.0229  | 0.0     |
| FREQUENCY = 719.2 CM-1  |         |         |         |         |         |         |         |         |         |
| 0.0                     | -0.0907 | 0.0907  | 0.0014  | 0.0029  | -0.0014 | -0.0029 | -0.0198 | 0.0198  | 0.2011  |
| -0.3652                 | -0.2011 | 0.3652  | 0.0464  | 0.1770  | -0.0464 | -0.1770 | -0.1127 | 0.1127  | 0.0     |
| FREQUENCY = 615.8 CM-1  |         |         |         |         |         |         |         |         |         |
| 0.0                     | -0.1753 | 0.1753  | 0.0026  | 0.0073  | -0.0026 | -0.0073 | -0.0253 | 0.0253  | -0.0704 |
| 0.1417                  | 0.0704  | -0.1417 | 0.0502  | 0.0534  | -0.0502 | -0.0534 | -0.2178 | 0.2178  | 0.0     |

## APPENDIX II (continued)

(iv) trans-C<sub>2</sub>H<sub>2</sub> : Potential Energy Distribution<sup>a</sup>

|                         |         |         |         |         |         |         |         |         |  |
|-------------------------|---------|---------|---------|---------|---------|---------|---------|---------|--|
| FREQUENCY = 3067.0 CM-1 |         |         |         |         |         |         |         |         |  |
| 0.0029                  | 0.0066  | 0.9923  | 0.0007  | 0.0001  | 0.0026  | 0.0000  | -0.0005 | -0.0026 |  |
| -0.0005                 | -0.0002 | 0.0016  | 0.0001  | 0.0005  | 0.0012  | 0.0002  |         |         |  |
| FREQUENCY = 2270.2 CM-1 |         |         |         |         |         |         |         |         |  |
| 0.0176                  | 0.0033  | 0.9601  | 0.0083  | 0.0050  | 0.0097  | 0.0001  | 0.0005  | -0.0108 |  |
| -0.0045                 | -0.0017 | 0.0048  | 0.0002  | 0.0027  | 0.0036  | 0.0017  |         |         |  |
| FREQUENCY = 1338.3 CM-1 |         |         |         |         |         |         |         |         |  |
| 0.1389                  | 0.0170  | 0.0213  | 0.9521  | 0.2735  | 0.1644  | 0.0008  | 0.0000  | -0.3314 |  |
| -0.1215                 | -0.0537 | -0.0619 | -0.0022 | 0.0346  | -0.0990 | 0.0671  |         |         |  |
| FREQUENCY = 1118.8 CM-1 |         |         |         |         |         |         |         |         |  |
| 0.5313                  | 0.0668  | 0.0075  | 0.0045  | 0.0588  | 0.2006  | 0.0031  | 0.0000  | -0.1697 |  |
| 0.0321                  | 0.0078  | 0.1346  | 0.0048  | 0.0422  | 0.0852  | -0.0096 |         |         |  |
| FREQUENCY = 1026.1 CM-1 |         |         |         |         |         |         |         |         |  |
| 0.2369                  | 0.0041  | 0.0101  | 0.0097  | 0.2702  | 0.2075  | 0.0022  | -0.0000 | 0.2530  |  |
| -0.1001                 | 0.0286  | 0.0730  | 0.0026  | 0.0437  | 0.0532  | -0.0946 |         |         |  |
| FREQUENCY = 876.5 CM-1  |         |         |         |         |         |         |         |         |  |
| 0.0196                  | 0.0371  | 0.0086  | 0.2311  | 0.3244  | 0.3116  | 0.0000  | -0.0000 | -0.2288 |  |
| 0.0529                  | -0.0247 | -0.0206 | -0.0007 | 0.0655  | 0.2163  | 0.0079  |         |         |  |
| FREQUENCY = 698.7 CM-1  |         |         |         |         |         |         |         |         |  |
| 0.0391                  | 0.1822  | 0.0001  | 0.0046  | 0.7168  | 0.0473  | 0.0033  | 0.0000  | 0.2371  |  |
| -0.0302                 | -0.1447 | -0.0099 | -0.0004 | 0.0087  | -0.0186 | -0.0293 |         |         |  |
| FREQUENCY = 616.7 CM-1  |         |         |         |         |         |         |         |         |  |
| 0.0954                  | 0.8301  | 0.0001  | 0.0404  | 0.0884  | 0.0181  | 0.0122  | 0.0000  | 0.0095  |  |
| 0.0329                  | -0.0864 | -0.0062 | -0.0002 | 0.0038  | -0.0253 | -0.0128 |         |         |  |
| FREQUENCY = 3958.8 CM-1 |         |         |         |         |         |         |         |         |  |
| 0.0                     | 0.0005  | 0.9986  | 0.0007  | 0.0010  | 0.0002  | 0.0001  | -0.0005 | -0.0006 |  |
| 0.0                     | -0.0002 | 0.0000  | -0.0000 | -0.0000 | 0.0002  | 0.0     |         |         |  |
| FREQUENCY = 2245.9 CM-1 |         |         |         |         |         |         |         |         |  |
| 0.0                     | 0.0026  | 0.9895  | 0.0058  | 0.0043  | 0.0010  | 0.0005  | 0.0005  | -0.0031 |  |
| 0.0                     | -0.0014 | -0.0000 | 0.0000  | -0.0002 | 0.0005  | 0.0     |         |         |  |
| FREQUENCY = 1288.7 CM-1 |         |         |         |         |         |         |         |         |  |
| 0.0                     | 0.0218  | 0.0063  | 1.0154  | 0.4232  | 0.0583  | 0.0041  | 0.0000  | -0.3189 |  |
| 0.0                     | -0.0774 | -0.0441 | 0.0016  | -0.0207 | -0.1096 | 0.0     |         |         |  |
| FREQUENCY = 1000.9 CM-1 |         |         |         |         |         |         |         |         |  |
| 0.0                     | 0.0026  | 0.0003  | 0.2048  | 0.1975  | 0.3380  | 0.0005  | 0.0000  | 0.3929  |  |
| 0.0                     | -0.0158 | -0.1581 | 0.0056  | -0.0711 | 0.1029  | 0.0     |         |         |  |
| FREQUENCY = 784.8 CM-1  |         |         |         |         |         |         |         |         |  |
| 0.0                     | 0.0878  | 0.0019  | 0.0099  | 0.9440  | 0.0633  | 0.0164  | -0.0000 | -0.2437 |  |
| 0.0                     | -0.0664 | 0.0146  | -0.0005 | -0.0133 | 0.1861  | 0.0     |         |         |  |
| FREQUENCY = 659.1 CM-1  |         |         |         |         |         |         |         |         |  |
| 0.0                     | 0.0235  | 0.0003  | 0.0614  | 0.0154  | 0.6463  | 0.0044  | 0.0000  | -0.0726 |  |
| 0.0                     | 0.0125  | 0.3914  | -0.0138 | -0.1359 | 0.0670  | 0.0     |         |         |  |
| FREQUENCY = 618.2 CM-1  |         |         |         |         |         |         |         |         |  |
| 0.0                     | 0.7196  | 0.0031  | 0.0146  | 0.0835  | 0.0776  | 0.1343  | 0.0000  | -0.1116 |  |
| 0.0                     | 0.0585  | 0.0032  | -0.0001 | -0.0163 | 0.0335  | 0.0     |         |         |  |

## APPENDIX II (continued)

(iv) trans-C<sub>2</sub>D<sub>2</sub>H<sub>2</sub>S : Eigenvectors<sup>b</sup>

|                         |         |         |         |         |         |         |         |         |         |
|-------------------------|---------|---------|---------|---------|---------|---------|---------|---------|---------|
| FREQUENCY = 3067.0 CM-1 |         |         |         |         |         |         |         |         |         |
| -0.0583                 | -0.0255 | -0.0255 | -0.0502 | 0.7321  | 0.7321  | -0.0502 | -0.0513 | -0.0513 | 0.0653  |
| -0.0342                 | -0.0242 | 0.0653  | 0.1205  | -0.0782 | -0.0782 | 0.1205  | 0.0113  | 0.0113  | -0.0227 |
| FREQUENCY = 2270.2 CM-1 |         |         |         |         |         |         |         |         |         |
| 0.1059                  | 0.0449  | 0.0449  | -0.5332 | -0.0341 | -0.0341 | -0.5332 | 0.1273  | 0.1273  | 0.0329  |
| -0.1094                 | -0.1094 | 0.0329  | 0.0812  | -0.1906 | -0.1906 | 0.0812  | -0.0209 | -0.0209 | 0.0419  |
| FREQUENCY = 1338.3 CM-1 |         |         |         |         |         |         |         |         |         |
| 0.1751                  | 0.0599  | 0.0599  | 0.0462  | 0.0084  | 0.0084  | 0.0462  | 0.8037  | 0.8037  | -0.1592 |
| -0.4742                 | -0.4742 | -0.1592 | -0.1435 | -0.4810 | -0.4810 | -0.1435 | -0.0381 | -0.0381 | 0.0762  |
| FREQUENCY = 1118.8 CM-1 |         |         |         |         |         |         |         |         |         |
| 0.2863                  | 0.0994  | 0.0994  | 0.0952  | 0.0227  | 0.0227  | 0.0952  | -0.0462 | -0.0462 | -0.1162 |
| 0.1551                  | 0.1551  | -0.1162 | -0.2905 | 0.3611  | 0.3611  | -0.2905 | -0.0620 | -0.0620 | 0.1240  |
| FREQUENCY = 1026.1 CM-1 |         |         |         |         |         |         |         |         |         |
| -0.1753                 | -0.0227 | -0.0227 | -0.0247 | 0.0017  | 0.0017  | -0.0247 | 0.0621  | 0.0621  | -0.1992 |
| -0.3250                 | -0.3250 | -0.1992 | -0.1148 | 0.4168  | 0.4168  | -0.1148 | 0.0473  | 0.0473  | -0.0946 |
| FREQUENCY = 876.5 CM-1  |         |         |         |         |         |         |         |         |         |
| 0.0431                  | 0.0580  | 0.0580  | 0.0189  | -0.0047 | -0.0047 | 0.0189  | -0.2593 | -0.2593 | 0.1793  |
| -0.3085                 | -0.3085 | 0.1793  | 0.4519  | 0.0218  | 0.0218  | 0.4519  | 0.0012  | 0.0012  | -0.0024 |
| FREQUENCY = 698.7 CM-1  |         |         |         |         |         |         |         |         |         |
| -0.0485                 | 0.1025  | 0.1025  | 0.0010  | 0.0008  | 0.0008  | 0.0010  | 0.0291  | 0.0291  | -0.4023 |
| 0.1302                  | 0.1302  | -0.4023 | 0.1292  | 0.0234  | 0.0234  | 0.1292  | 0.0396  | 0.0396  | -0.0793 |
| FREQUENCY = 616.7 CM-1  |         |         |         |         |         |         |         |         |         |
| 0.0669                  | -0.1931 | -0.1931 | -0.0007 | -0.0008 | -0.0008 | -0.0007 | -0.0763 | -0.0763 | -0.0528 |
| 0.1199                  | 0.1199  | -0.0528 | 0.0742  | 0.0199  | 0.0199  | 0.0742  | -0.0673 | -0.0673 | 0.1346  |
| FREQUENCY = 3058.8 CM-1 |         |         |         |         |         |         |         |         |         |
| 0.0                     | -0.0238 | 0.0238  | 0.0497  | -0.7324 | 0.7324  | -0.0497 | 0.0512  | -0.0512 | -0.0628 |
| 0.0324                  | -0.0324 | 0.0628  | -0.0377 | 0.0054  | -0.0054 | 0.0377  | -0.0296 | 0.0296  | 0.0     |
| FREQUENCY = 2245.9 CM-1 |         |         |         |         |         |         |         |         |         |
| 0.0                     | -0.0397 | 0.0397  | -0.5355 | -0.0337 | 0.0337  | 0.5355  | 0.1053  | -0.1053 | 0.0301  |
| -0.1011                 | 0.1011  | -0.0301 | -0.0007 | -0.0654 | 0.0654  | 0.0007  | -0.0493 | 0.0493  | 0.0     |
| FREQUENCY = 1288.7 CM-1 |         |         |         |         |         |         |         |         |         |
| 0.0                     | -0.0654 | 0.0654  | 0.0238  | 0.0060  | -0.0060 | -0.0238 | 0.7992  | -0.7992 | -0.2165 |
| -0.5587                 | 0.5587  | 0.2165  | -0.1301 | -0.3503 | 0.3503  | 0.1301  | -0.0813 | 0.0813  | 0.0     |
| FREQUENCY = 1000.9 CM-1 |         |         |         |         |         |         |         |         |         |
| 0.0                     | 0.0174  | -0.0174 | 0.0020  | 0.0038  | -0.0038 | -0.0020 | 0.2788  | -0.2788 | 0.0441  |
| 0.3148                  | -0.3148 | -0.0441 | -0.1968 | -0.5009 | 0.5009  | 0.1968  | 0.0216  | -0.0216 | 0.0     |
| FREQUENCY = 784.8 CM-1  |         |         |         |         |         |         |         |         |         |
| 0.0                     | 0.0799  | -0.0799 | 0.0055  | -0.0061 | 0.0061  | -0.0055 | -0.0480 | 0.0480  | 0.4729  |
| -0.2710                 | 0.2710  | -0.4729 | 0.0311  | -0.1799 | 0.1799  | -0.0311 | 0.0993  | 0.0993  | 0.0     |
| FREQUENCY = 659.1 CM-1  |         |         |         |         |         |         |         |         |         |
| 0.0                     | 0.0347  | -0.0347 | -0.0013 | -0.0024 | 0.0024  | 0.0013  | -0.1005 | 0.1005  | -0.0033 |
| -0.0585                 | 0.0585  | 0.0033  | 0.4204  | -0.2518 | 0.2518  | -0.4204 | 0.0431  | -0.0431 | 0.0     |
| FREQUENCY = 618.2 CM-1  |         |         |         |         |         |         |         |         |         |
| 0.0                     | 0.1803  | -0.1803 | -0.0080 | -0.0021 | 0.0021  | 0.0080  | 0.0459  | -0.0459 | -0.1114 |
| 0.0624                  | -0.0624 | 0.1114  | -0.1592 | 0.0047  | -0.0047 | 0.1592  | 0.2240  | -0.2240 | 0.0     |

A P P E N D I X . I I I

POTENTIAL ENERGY DISTRIBUTIONS FOR C<sub>2</sub>H<sub>4</sub>S, C<sub>2</sub>D<sub>4</sub>S, cis-C<sub>2</sub>D<sub>2</sub>H<sub>2</sub>S AND trans-C<sub>2</sub>D<sub>2</sub>H<sub>2</sub>S AMONG THE DIAGONAL ELEMENTS OF THE SYMMETRIZED F MATRIX

The entries in the following tables for C<sub>2</sub>H<sub>4</sub>S and C<sub>2</sub>D<sub>4</sub>S are listed, under each frequency, in the order of the symmetry coordinates listed in Table 6 with the exception that certain symmetry coordinates, S<sub>i</sub>, were re-defined to yield the symmetry coordinates, S<sub>i</sub>', as shown below.

$$S'_4 = \frac{1}{\sqrt{6}} \{2S_4 + S_5 + S_6\} \quad (\text{redundant})$$

$$S'_5 = \frac{1}{\sqrt{6}} \{2S_4 - S_5 - S_6\} \quad (\text{CH}_2 \text{ deformation})$$

$$S'_6 = \frac{1}{\sqrt{2}} \{S_5 - S_6\} \quad (\text{CH}_2 \text{ wag})$$

$$S'_{10} = \frac{1}{\sqrt{2}} \{S_{10} + S_{11}\} \quad (\text{CH}_2 \text{ rock})$$

$$S'_{11} = \frac{1}{\sqrt{2}} \{S_{10} - S_{11}\} \quad (\text{CH}_2 \text{ twist})$$

$$S'_{14} = \frac{1}{\sqrt{6}} \{2S_{14} + S_{15} + S_{16}\} \quad (\text{redundant})$$

$$S'_{15} = \frac{1}{\sqrt{6}} \{2S_{14} - S_{15} - S_{16}\} \quad (\text{CH}_2 \text{ deformation})$$

$$S'_{16} = \frac{1}{\sqrt{2}} \{S_{15} - S_{16}\} \quad (\text{CH}_2 \text{ wag})$$

$$S'_{19} = \frac{1}{\sqrt{2}} \{S_{19} + S_{20}\} \quad (\text{CH}_2 \text{ rock})$$

$$S'_{20} = \frac{1}{\sqrt{2}} \{S_{19} - S_{20}\} \quad (\text{CH}_2 \text{ twist})$$

Appendix III (continued)

The entries in the tables for cis-C<sub>2</sub>D<sub>2</sub>H<sub>2</sub>S and trans-C<sub>2</sub>D<sub>2</sub>H<sub>2</sub>S are listed, under each frequency, in the order of the symmetry coordinates listed in Tables 7 and 8, respectively.

(i) C<sub>2</sub>H<sub>4</sub>S

|                         |        |        |        |        |        |        |        |        |        |
|-------------------------|--------|--------|--------|--------|--------|--------|--------|--------|--------|
| FREQUENCY = 3018.5 CM-1 |        |        |        |        |        |        |        |        |        |
| 0.0073                  | 0.0015 | 0.9906 | 0.0000 | 0.0015 | 0.0000 | 0.0000 | 0.0    | 0.0    | 0.0    |
| 0.0                     | 0.0    | 0.0    | 0.0    | 0.0    | 0.0    | 0.0    | 0.0    | 0.0    | 0.0    |
| FREQUENCY = 1466.0 CM-1 |        |        |        |        |        |        |        |        |        |
| 0.0820                  | 0.0111 | 0.0032 | 0.0097 | 0.7112 | 0.0022 | 0.0005 | 0.0    | 0.0    | 0.0    |
| 0.0                     | 0.0    | 0.0    | 0.0    | 0.0    | 0.0    | 0.0    | 0.0    | 0.0    | 0.0    |
| FREQUENCY = 1107.1 CM-1 |        |        |        |        |        |        |        |        |        |
| 0.8562                  | 0.0904 | 0.0061 | 0.0002 | 0.0180 | 0.0447 | 0.0054 | 0.0    | 0.0    | 0.0    |
| 0.0                     | 0.0    | 0.0    | 0.0    | 0.0    | 0.0    | 0.0    | 0.0    | 0.0    | 0.0    |
| FREQUENCY = 1023.5 CM-1 |        |        |        |        |        |        |        |        |        |
| 0.0059                  | 0.0150 | 0.0000 | 0.0063 | 0.0345 | 1.0583 | 0.0003 | 0.0    | 0.0    | 0.0    |
| 0.0                     | 0.0    | 0.0    | 0.0    | 0.0    | 0.0    | 0.0    | 0.0    | 0.0    | 0.0    |
| FREQUENCY = 633.3 CM-1  |        |        |        |        |        |        |        |        |        |
| 0.1296                  | 1.0231 | 0.0001 | 0.0004 | 0.0364 | 0.0390 | 0.0155 | 0.0    | 0.0    | 0.0    |
| 0.0                     | 0.0    | 0.0    | 0.0    | 0.0    | 0.0    | 0.0    | 0.0    | 0.0    | 0.0    |
| FREQUENCY = 3109.2 CM-1 |        |        |        |        |        |        |        |        |        |
| 0.0                     | 0.0    | 0.0    | 0.0    | 0.0    | 0.0    | 0.0    | 0.0    | 0.9919 | 0.0064 |
| 0.0012                  | 0.0    | 0.0    | 0.0    | 0.0    | 0.0    | 0.0    | 0.0    | 0.0    | 0.0    |
| FREQUENCY = 1160.2 CM-1 |        |        |        |        |        |        |        |        |        |
| 0.0                     | 0.0    | 0.0    | 0.0    | 0.0    | 0.0    | 0.0    | 0.0    | 0.0080 | 0.7272 |
| 0.2091                  | 0.0    | 0.0    | 0.0    | 0.0    | 0.0    | 0.0    | 0.0    | 0.0    | 0.0    |
| FREQUENCY = 890.2 CM-1  |        |        |        |        |        |        |        |        |        |
| 0.0                     | 0.0    | 0.0    | 0.0    | 0.0    | 0.0    | 0.0    | 0.0    | 0.0000 | 0.2715 |
| 0.7948                  | 0.0    | 0.0    | 0.0    | 0.0    | 0.0    | 0.0    | 0.0    | 0.0    | 0.0    |
| FREQUENCY = 3010.4 CM-1 |        |        |        |        |        |        |        |        |        |
| 0.0                     | 0.0    | 0.0    | 0.0    | 0.0    | 0.0    | 0.0    | 0.0    | 0.0    | 0.0    |
| 0.0                     | 0.0013 | 0.9971 | 0.0001 | 0.0010 | 0.0000 | 0.0002 | 0.0    | 0.0    | 0.0    |
| FREQUENCY = 1431.9 CM-1 |        |        |        |        |        |        |        |        |        |
| 0.0                     | 0.0    | 0.0    | 0.0    | 0.0    | 0.0    | 0.0    | 0.0    | 0.0    | 0.0    |
| 0.0                     | 0.0149 | 0.0015 | 0.0090 | 0.5438 | 0.0289 | 0.0028 | 0.0    | 0.0    | 0.0    |
| FREQUENCY = 1060.2 CM-1 |        |        |        |        |        |        |        |        |        |
| 0.0                     | 0.0    | 0.0    | 0.0    | 0.0    | 0.0    | 0.0    | 0.0    | 0.0    | 0.0    |
| 0.0                     | 0.0041 | 0.0002 | 0.0061 | 0.0854 | 1.0147 | 0.0008 | 0.0    | 0.0    | 0.0    |
| FREQUENCY = 645.9 CM-1  |        |        |        |        |        |        |        |        |        |
| 0.0                     | 0.0    | 0.0    | 0.0    | 0.0    | 0.0    | 0.0    | 0.0    | 0.0    | 0.0    |
| 0.0                     | 0.8382 | 0.0012 | 0.0058 | 0.0060 | 0.0374 | 0.1565 | 0.0    | 0.0    | 0.0    |
| FREQUENCY = 3100.6 CM-1 |        |        |        |        |        |        |        |        |        |
| 0.0                     | 0.0    | 0.0    | 0.0    | 0.0    | 0.0    | 0.0    | 0.0    | 0.0    | 0.0    |
| 0.0                     | 0.0    | 0.0    | 0.0    | 0.0    | 0.0    | 0.0    | 0.9984 | 0.0012 | 0.0001 |
| FREQUENCY = 947.1 CM-1  |        |        |        |        |        |        |        |        |        |
| 0.0                     | 0.0    | 0.0    | 0.0    | 0.0    | 0.0    | 0.0    | 0.0    | 0.0    | 0.0    |
| 0.0                     | 0.0    | 0.0    | 0.0    | 0.0    | 0.0    | 0.0    | 0.0014 | 0.3966 | 0.5333 |
| FREQUENCY = 820.5 CM-1  |        |        |        |        |        |        |        |        |        |
| 0.0                     | 0.0    | 0.0    | 0.0    | 0.0    | 0.0    | 0.0    | 0.0    | 0.0    | 0.0    |
| 0.0                     | 0.0    | 0.0    | 0.0    | 0.0    | 0.0    | 0.0    | 0.0002 | 0.6078 | 0.4720 |

## APPENDIX III (continued)

(ii)  $C_2D_4S$ 

|                         |        |        |        |        |        |        |     |        |        |        |
|-------------------------|--------|--------|--------|--------|--------|--------|-----|--------|--------|--------|
| FREQUENCY = 2210.5 CM-1 |        |        |        |        |        |        |     |        |        |        |
| 0.0355                  | 0.0067 | 0.9553 | 0.0002 | 0.0066 | 0.0003 | 0.0002 | 0.0 | 0.0    | 0.0    | 0.0    |
| 0.0                     | 0.0    | 0.0    | 0.0    | 0.0    | 0.0    | 0.0    | 0.0 | 0.0    | 0.0    | 0.0    |
| FREQUENCY = 1186.8 CM-1 |        |        |        |        |        |        |     |        |        |        |
| 0.5834                  | 0.0648 | 0.0399 | 0.0076 | 0.3551 | 0.0081 | 0.0036 | 0.0 | 0.0    | 0.0    | 0.0    |
| 0.0                     | 0.0    | 0.0    | 0.0    | 0.0    | 0.0    | 0.0    | 0.0 | 0.0    | 0.0    | 0.0    |
| FREQUENCY = 949.4 CM-1  |        |        |        |        |        |        |     |        |        |        |
| 0.3423                  | 0.0203 | 0.0042 | 0.0015 | 0.3530 | 0.0851 | 0.0025 | 0.0 | 0.0    | 0.0    | 0.0    |
| 0.0                     | 0.0    | 0.0    | 0.0    | 0.0    | 0.0    | 0.0    | 0.0 | 0.0    | 0.0    | 0.0    |
| FREQUENCY = 764.3 CM-1  |        |        |        |        |        |        |     |        |        |        |
| 0.0166                  | 0.1951 | 0.0005 | 0.0073 | 0.0291 | 1.0363 | 0.0026 | 0.0 | 0.0    | 0.0    | 0.0    |
| 0.0                     | 0.0    | 0.0    | 0.0    | 0.0    | 0.0    | 0.0    | 0.0 | 0.0    | 0.0    | 0.0    |
| FREQUENCY = 610.1 CM-1  |        |        |        |        |        |        |     |        |        |        |
| 0.1039                  | 0.8543 | 0.0001 | 0.0000 | 0.0577 | 0.0154 | 0.0128 | 0.0 | 0.0    | 0.0    | 0.0    |
| 0.0                     | 0.0    | 0.0    | 0.0    | 0.0    | 0.0    | 0.0    | 0.0 | 0.0    | 0.0    | 0.0    |
| FREQUENCY = 2333.4 CM-1 |        |        |        |        |        |        |     |        |        |        |
| 0.0                     | 0.0    | 0.0    | 0.0    | 0.0    | 0.0    | 0.0    | 0.0 | 0.9731 | 0.0216 | 0.0    |
| 0.0040                  | 0.0    | 0.0    | 0.0    | 0.0    | 0.0    | 0.0    | 0.0 | 0.0    | 0.0    | 0.0    |
| FREQUENCY = 922.0 CM-1  |        |        |        |        |        |        |     |        |        |        |
| 0.0                     | 0.0    | 0.0    | 0.0    | 0.0    | 0.0    | 0.0    | 0.0 | 0.0269 | 0.7412 | 0.0    |
| 0.1798                  | 0.0    | 0.0    | 0.0    | 0.0    | 0.0    | 0.0    | 0.0 | 0.0    | 0.0    | 0.0    |
| FREQUENCY = 630.3 CM-1  |        |        |        |        |        |        |     |        |        |        |
| 0.0                     | 0.0    | 0.0    | 0.0    | 0.0    | 0.0    | 0.0    | 0.0 | 0.0001 | 0.2424 | 0.0    |
| 0.8213                  | 0.0    | 0.0    | 0.0    | 0.0    | 0.0    | 0.0    | 0.0 | 0.0    | 0.0    | 0.0    |
| FREQUENCY = 2184.8 CM-1 |        |        |        |        |        |        |     |        |        |        |
| 0.0                     | 0.0    | 0.0    | 0.0    | 0.0    | 0.0    | 0.0    | 0.0 | 0.0    | 0.0    | 0.0    |
| 0.0                     | 0.052  | 0.9885 | 0.0002 | 0.0041 | 0.0000 | 0.0010 | 0.0 | 0.0    | 0.0    | 0.0    |
| FREQUENCY = 1066.6 CM-1 |        |        |        |        |        |        |     |        |        |        |
| 0.0                     | 0.0    | 0.0    | 0.0    | 0.0    | 0.0    | 0.0    | 0.0 | 0.0    | 0.0    | 0.0    |
| 0.0                     | 0.0662 | 0.0073 | 0.0102 | 0.5860 | 0.0580 | 0.0124 | 0.0 | 0.0    | 0.0    | 0.0    |
| FREQUENCY = 827.9 CM-1  |        |        |        |        |        |        |     |        |        |        |
| 0.0                     | 0.0    | 0.0    | 0.0    | 0.0    | 0.0    | 0.0    | 0.0 | 0.0    | 0.0    | 0.0    |
| 0.0                     | 0.0190 | 0.0006 | 0.0058 | 0.1179 | 1.0181 | 0.0035 | 0.0 | 0.0    | 0.0    | 0.0    |
| FREQUENCY = 607.0 CM-1  |        |        |        |        |        |        |     |        |        |        |
| 0.0                     | 0.0    | 0.0    | 0.0    | 0.0    | 0.0    | 0.0    | 0.0 | 0.0    | 0.0    | 0.0    |
| 0.0                     | 0.7680 | 0.0037 | 0.0046 | 0.0291 | 0.0049 | 0.1434 | 0.0 | 0.0    | 0.0    | 0.0    |
| FREQUENCY = 2312.1 CM-1 |        |        |        |        |        |        |     |        |        |        |
| 0.0                     | 0.0    | 0.0    | 0.0    | 0.0    | 0.0    | 0.0    | 0.0 | 0.9949 | 0.0038 | 0.0010 |
| 0.0                     | 0.0    | 0.0    | 0.0    | 0.0    | 0.0    | 0.0    | 0.0 | 0.0    | 0.0    | 0.0    |
| FREQUENCY = 707.4 CM-1  |        |        |        |        |        |        |     |        |        |        |
| 0.0                     | 0.0    | 0.0    | 0.0    | 0.0    | 0.0    | 0.0    | 0.0 | 0.0047 | 0.4718 | 0.4543 |
| 0.0                     | 0.0    | 0.0    | 0.0    | 0.0    | 0.0    | 0.0    | 0.0 | 0.0    | 0.0    | 0.0    |
| FREQUENCY = 584.3 CM-1  |        |        |        |        |        |        |     |        |        |        |
| 0.0                     | 0.0    | 0.0    | 0.0    | 0.0    | 0.0    | 0.0    | 0.0 | 0.0    | 0.0    | 0.0    |
| 0.0                     | 0.0    | 0.0    | 0.0    | 0.0    | 0.0    | 0.0    | 0.0 | 0.0004 | 0.5300 | 0.5503 |

## APPENDIX III (continued)

(iii) cis-C<sub>2</sub>D<sub>2</sub>H<sub>2</sub>S

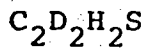
|                         |        |        |        |        |        |        |        |        |        |
|-------------------------|--------|--------|--------|--------|--------|--------|--------|--------|--------|
| FREQUENCY = 3062.1 CM-1 |        |        |        |        |        |        |        |        |        |
| 0.0030                  | 0.0006 | 0.9920 | 0.0039 | 0.0009 | 0.0002 | 0.0008 | 0.0000 | 0.0003 | 0.0000 |
| 0.0                     | 0.0    | 0.0    | 0.0    | 0.0    | 0.0    | 0.0    | 0.0    | 0.0    | 0.0    |
| FREQUENCY = 2259.1 CM-1 |        |        |        |        |        |        |        |        |        |
| 0.0179                  | 0.0034 | 0.0025 | 0.9705 | 0.0072 | 0.0041 | 0.0003 | 0.0014 | 0.0001 | 0.0001 |
| 0.0                     | 0.0    | 0.0    | 0.0    | 0.0    | 0.0    | 0.0    | 0.0    | 0.0    | 0.0    |
| FREQUENCY = 1329.1 CM-1 |        |        |        |        |        |        |        |        |        |
| 0.1704                  | 0.0214 | 0.0017 | 0.0145 | 0.9741 | 0.2393 | 0.0363 | 0.1082 | 0.0270 | 0.0010 |
| 0.0                     | 0.0    | 0.0    | 0.0    | 0.0    | 0.0    | 0.0    | 0.0    | 0.0    | 0.0    |
| FREQUENCY = 1080.0 CM-1 |        |        |        |        |        |        |        |        |        |
| 0.7449                  | 0.0697 | 0.0032 | 0.0075 | 0.0448 | 0.1592 | 0.0012 | 0.0041 | 0.0074 | 0.0049 |
| 0.0                     | 0.0    | 0.0    | 0.0    | 0.0    | 0.0    | 0.0    | 0.0    | 0.0    | 0.0    |
| FREQUENCY = 967.5 CM-1  |        |        |        |        |        |        |        |        |        |
| 0.0004                  | 0.0233 | 0.0000 | 0.0009 | 0.1046 | 0.2442 | 0.0013 | 0.2479 | 0.0150 | 0.0001 |
| 0.0                     | 0.0    | 0.0    | 0.0    | 0.0    | 0.0    | 0.0    | 0.0    | 0.0    | 0.0    |
| FREQUENCY = 760.2 CM-1  |        |        |        |        |        |        |        |        |        |
| 0.0325                  | 0.0297 | 0.0005 | 0.0020 | 0.0252 | 0.1508 | 0.8393 | 0.0533 | 0.0063 | 0.0012 |
| 0.0                     | 0.0    | 0.0    | 0.0    | 0.0    | 0.0    | 0.0    | 0.0    | 0.0    | 0.0    |
| FREQUENCY = 657.6 CM-1  |        |        |        |        |        |        |        |        |        |
| 0.0317                  | 0.4135 | 0.0000 | 0.0006 | 0.0101 | 0.0788 | 0.0000 | 0.1184 | 0.3234 | 0.0054 |
| 0.0                     | 0.0    | 0.0    | 0.0    | 0.0    | 0.0    | 0.0    | 0.0    | 0.0    | 0.0    |
| FREQUENCY = 608.2 CM-1  |        |        |        |        |        |        |        |        |        |
| 0.0809                  | 0.5797 | 0.0000 | 0.0000 | 0.0845 | 0.0067 | 0.0021 | 0.0312 | 0.1850 | 0.0090 |
| 0.0                     | 0.0    | 0.0    | 0.0    | 0.0    | 0.0    | 0.0    | 0.0    | 0.0    | 0.0    |
| FREQUENCY = 3063.7 CM-1 |        |        |        |        |        |        |        |        |        |
| 0.0                     | 0.0    | 0.0    | 0.0    | 0.0    | 0.0    | 0.0    | 0.0    | 0.0    | 0.0    |
| 0.0                     | 0.0005 | 0.9896 | 0.0054 | 0.0006 | 0.0003 | 0.0009 | 0.0009 | 0.0016 | 0.0001 |
| FREQUENCY = 2257.4 CM-1 |        |        |        |        |        |        |        |        |        |
| 0.0                     | 0.0    | 0.0    | 0.0    | 0.0    | 0.0    | 0.0    | 0.0    | 0.0    | 0.0    |
| 0.0                     | 0.0026 | 0.0057 | 0.9700 | 0.0068 | 0.0044 | 0.0005 | 0.0074 | 0.0023 | 0.0005 |
| FREQUENCY = 1302.7 CM-1 |        |        |        |        |        |        |        |        |        |
| 0.0                     | 0.0    | 0.0    | 0.0    | 0.0    | 0.0    | 0.0    | 0.0    | 0.0    | 0.0    |
| 0.0                     | 0.0176 | 0.0000 | 0.0122 | 0.9695 | 0.3508 | 0.0362 | 0.1451 | 0.0021 | 0.0033 |
| FREQUENCY = 1068.1 CM-1 |        |        |        |        |        |        |        |        |        |
| 0.0                     | 0.0    | 0.0    | 0.0    | 0.0    | 0.0    | 0.0    | 0.0    | 0.0    | 0.0    |
| 0.0                     | 0.0138 | 0.0018 | 0.0076 | 0.0002 | 0.0634 | 0.1064 | 0.3548 | 0.0367 | 0.0026 |
| FREQUENCY = 917.8 CM-1  |        |        |        |        |        |        |        |        |        |
| 0.0                     | 0.0    | 0.0    | 0.0    | 0.0    | 0.0    | 0.0    | 0.0    | 0.0    | 0.0    |
| 0.0                     | 0.0034 | 0.0026 | 0.0021 | 0.3250 | 0.2227 | 0.0679 | 0.0014 | 0.4000 | 0.0006 |
| FREQUENCY = 719.2 CM-1  |        |        |        |        |        |        |        |        |        |
| 0.0                     | 0.0    | 0.0    | 0.0    | 0.0    | 0.0    | 0.0    | 0.0    | 0.0    | 0.0    |
| 0.0                     | 0.1347 | 0.0001 | 0.0003 | 0.0020 | 0.1531 | 0.5048 | 0.0050 | 0.0725 | 0.0251 |
| FREQUENCY = 615.8 CM-1  |        |        |        |        |        |        |        |        |        |
| 0.0                     | 0.0    | 0.0    | 0.0    | 0.0    | 0.0    | 0.0    | 0.0    | 0.0    | 0.0    |
| 0.0                     | 0.6859 | 0.0003 | 0.0024 | 0.0045 | 0.0255 | 0.1036 | 0.0080 | 0.0090 | 0.1280 |



## APPENDIX III (continued)

(iv) trans-C<sub>2</sub>D<sub>2</sub>H<sub>2</sub>S

|                         |        |        |        |        |        |        |        |        |        |        |
|-------------------------|--------|--------|--------|--------|--------|--------|--------|--------|--------|--------|
| FREQUENCY = 3067.0 CM-1 |        |        |        |        |        |        |        |        |        |        |
| 0.0029                  | 0.0006 | 0.0047 | 0.9877 | 0.0007 | 0.0009 | 0.0002 | 0.0022 | 0.0009 | 0.0000 | 0.0000 |
| 0.0                     | 0.0    | 0.0    | 0.0    | 0.0    | 0.0    | 0.0    | 0.0    | 0.0    | 0.0    | 0.0    |
| FREQUENCY = 2270.2 CM-1 |        |        |        |        |        |        |        |        |        |        |
| 0.0176                  | 0.0033 | 0.9562 | 0.0039 | 0.0083 | 0.0004 | 0.0045 | 0.0018 | 0.0100 | 0.0001 | 0.0001 |
| 0.0                     | 0.0    | 0.0    | 0.0    | 0.0    | 0.0    | 0.0    | 0.0    | 0.0    | 0.0    | 0.0    |
| FREQUENCY = 1338.3 CM-1 |        |        |        |        |        |        |        |        |        |        |
| 0.1389                  | 0.0170 | 0.0206 | 0.0007 | 0.9521 | 0.0277 | 0.2458 | 0.0163 | 0.1827 | 0.0008 | 0.0008 |
| 0.0                     | 0.0    | 0.0    | 0.0    | 0.0    | 0.0    | 0.0    | 0.0    | 0.0    | 0.0    | 0.0    |
| FREQUENCY = 1111.4 CM-1 |        |        |        |        |        |        |        |        |        |        |
| 0.5313                  | 0.0668 | 0.0004 | 0.0071 | 0.0045 | 0.0211 | 0.0376 | 0.0054 | 0.1474 | 0.0031 | 0.0031 |
| 0.0                     | 0.0    | 0.0    | 0.0    | 0.0    | 0.0    | 0.0    | 0.0    | 0.0    | 0.0    | 0.0    |
| FREQUENCY = 1026.1 CM-1 |        |        |        |        |        |        |        |        |        |        |
| 0.2369                  | 0.0041 | 0.0101 | 0.0000 | 0.0097 | 0.0738 | 0.1964 | 0.0177 | 0.2335 | 0.0022 | 0.0022 |
| 0.0                     | 0.0    | 0.0    | 0.0    | 0.0    | 0.0    | 0.0    | 0.0    | 0.0    | 0.0    | 0.0    |
| FREQUENCY = 876.5 CM-1  |        |        |        |        |        |        |        |        |        |        |
| 0.0196                  | 0.0371 | 0.0081 | 0.0005 | 0.2311 | 0.0819 | 0.2425 | 0.3762 | 0.0009 | 0.0009 | 0.0009 |
| 0.0                     | 0.0    | 0.0    | 0.0    | 0.0    | 0.0    | 0.0    | 0.0    | 0.0    | 0.0    | 0.0    |
| FREQUENCY = 698.7 CM-1  |        |        |        |        |        |        |        |        |        |        |
| 0.0391                  | 0.1822 | 0.0000 | 0.0000 | 0.0046 | 0.6484 | 0.0680 | 0.0484 | 0.0016 | 0.0033 | 0.0033 |
| 0.0                     | 0.0    | 0.0    | 0.0    | 0.0    | 0.0    | 0.0    | 0.0    | 0.0    | 0.0    | 0.0    |
| FREQUENCY = 616.7 CM-1  |        |        |        |        |        |        |        |        |        |        |
| 0.0954                  | 0.8301 | 0.0000 | 0.0000 | 0.0404 | 0.0143 | 0.0740 | 0.0205 | 0.0015 | 0.0122 | 0.0122 |
| 0.0                     | 0.0    | 0.0    | 0.0    | 0.0    | 0.0    | 0.0    | 0.0    | 0.0    | 0.0    | 0.0    |
| FREQUENCY = 3058.8 CM-1 |        |        |        |        |        |        |        |        |        |        |
| 0.0                     | 0.0    | 0.0    | 0.0    | 0.0    | 0.0    | 0.0    | 0.0    | 0.0    | 0.0    | 0.0    |
| 0.0                     | 0.0005 | 0.0046 | 0.9940 | 0.0007 | 0.0008 | 0.0002 | 0.0001 | 0.0000 | 0.0000 | 0.0000 |
| FREQUENCY = 2245.9 CM-1 |        |        |        |        |        |        |        |        |        |        |
| 0.0                     | 0.0    | 0.0    | 0.0    | 0.0    | 0.0    | 0.0    | 0.0    | 0.0    | 0.0    | 0.0    |
| 0.0                     | 0.0026 | 0.9856 | 0.0039 | 0.0058 | 0.0004 | 0.0040 | 0.0000 | 0.0008 | 0.0005 | 0.0005 |
| FREQUENCY = 1288.7 CM-1 |        |        |        |        |        |        |        |        |        |        |
| 0.0                     | 0.0    | 0.0    | 0.0    | 0.0    | 0.0    | 0.0    | 0.0    | 0.0    | 0.0    | 0.0    |
| 0.0                     | 0.0218 | 0.0059 | 0.0004 | 1.0154 | 0.0553 | 0.3679 | 0.0094 | 0.0682 | 0.0041 | 0.0041 |
| FREQUENCY = 1000.9 CM-1 |        |        |        |        |        |        |        |        |        |        |
| 0.0                     | 0.0    | 0.0    | 0.0    | 0.0    | 0.0    | 0.0    | 0.0    | 0.0    | 0.0    | 0.0    |
| 0.0                     | 0.0026 | 0.0001 | 0.0002 | 0.2048 | 0.0038 | 0.1936 | 0.0357 | 0.2312 | 0.0005 | 0.0005 |
| FREQUENCY = 784.8 CM-1  |        |        |        |        |        |        |        |        |        |        |
| 0.0                     | 0.0    | 0.0    | 0.0    | 0.0    | 0.0    | 0.0    | 0.0    | 0.0    | 0.0    | 0.0    |
| 0.0                     | 0.0878 | 0.0008 | 0.0011 | 0.0099 | 0.7106 | 0.2334 | 0.0014 | 0.0485 | 0.0164 | 0.0164 |
| FREQUENCY = 659.1 CM-1  |        |        |        |        |        |        |        |        |        |        |
| 0.0                     | 0.0    | 0.0    | 0.0    | 0.0    | 0.0    | 0.0    | 0.0    | 0.0    | 0.0    | 0.0    |
| 0.0                     | 0.0235 | 0.0001 | 0.0002 | 0.0614 | 0.0000 | 0.0154 | 0.3756 | 0.1347 | 0.0044 | 0.0044 |
| FREQUENCY = 618.2 CM-1  |        |        |        |        |        |        |        |        |        |        |
| 0.0                     | 0.0    | 0.0    | 0.0    | 0.0    | 0.0    | 0.0    | 0.0    | 0.0    | 0.0    | 0.0    |
| 0.0                     | 0.7196 | 0.0029 | 0.0002 | 0.0146 | 0.0635 | 0.0199 | 0.0612 | 0.0001 | 0.1343 | 0.1343 |

INFRARED SPECTRA OF GASEOUS  $C_2D_4S$ , cis- $C_2D_2H_2S$  AND trans-Preparation and Handling of Samples

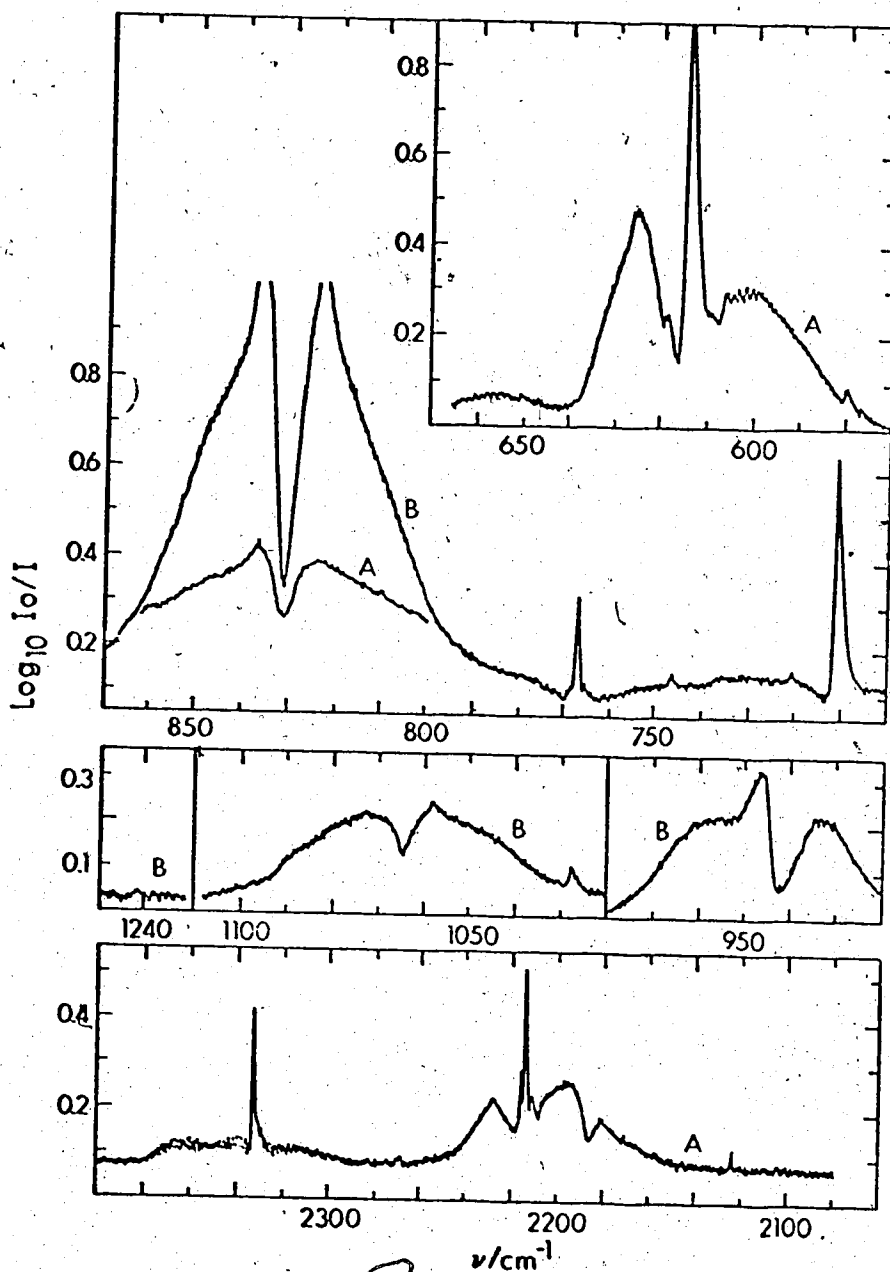
The deuterated forms of ethylene sulphide were supplied by Dr. O. P. Strausz of this department. The  $C_2D_4S$  was prepared by the reaction of the carbonate ester of 1,1,2,2-ethylene- $d_4$  glycol (prepared by the method of W. H. Carothers and F. J. Van Natta, J. Amer. Chem. Soc. 52, 314 (1930)) with potassium thiocyanate (S. Seakles and E. F. Lutz, J. Amer. Chem. Soc. 80, 3168 (1958)). The product was purified by gas-liquid chromatography using a 10 ft. long 20% tricresyl phosphate column at 46°C, with a helium flow rate of 60 cc/min. Mass spectroscopy of the product indicated that it contained 9% or less of  $C_2D_3HS$ .

The cis- and trans-1,2-dideuterioethylene sulphides were prepared by the photolytic reaction of cis- or trans-1,2-dideuterioethylene with carbonyl sulphide in the presence of carbon dioxide. The reaction is, with care, stereo-specific (A. Jackson and O. P. Strausz, to be published) but varying amounts of the cis- isomer existed as impurities in the trans- isomer, and vice versa. Except for traces of water and carbon dioxide in some samples, no other impurities

Appendix IV (continued)

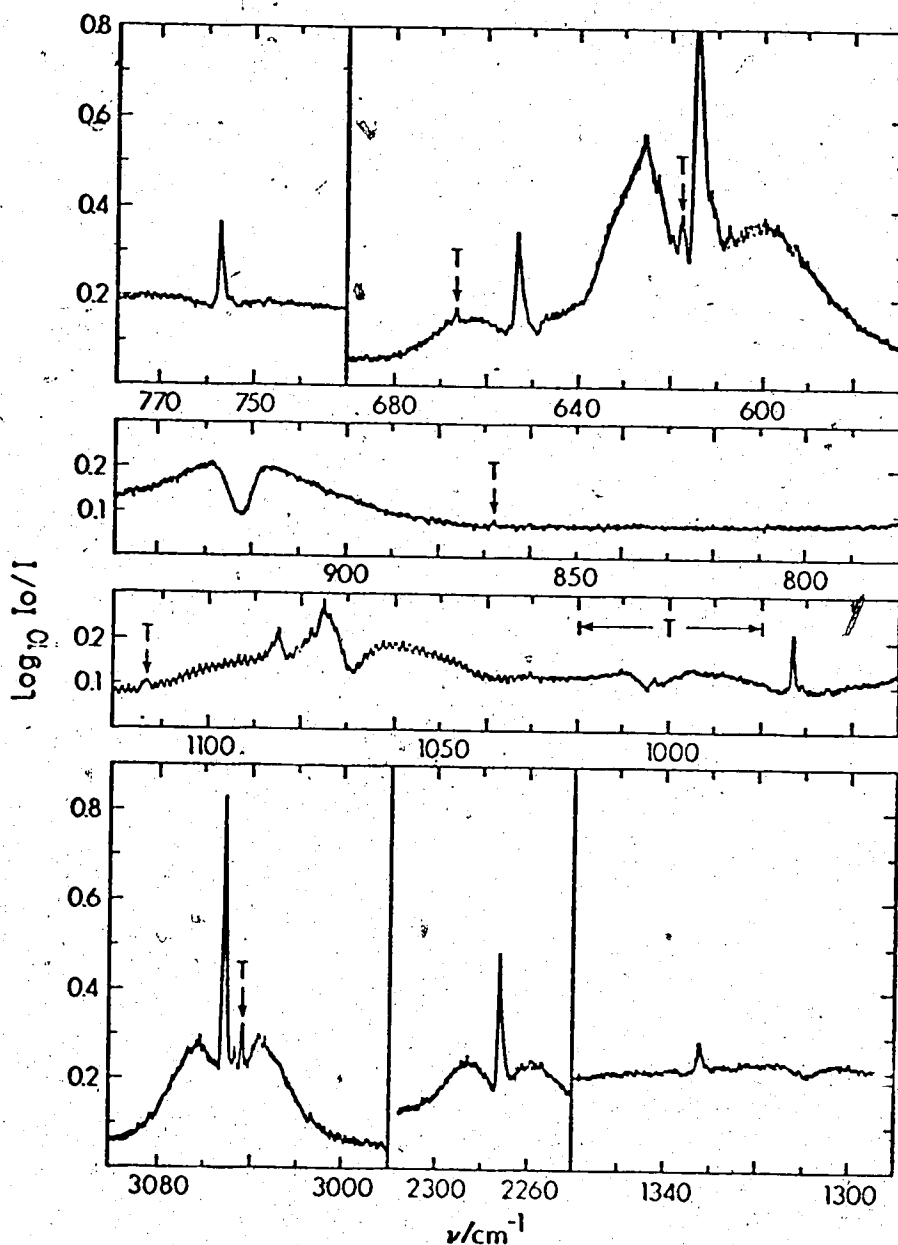
were detected.

The infrared spectra were recorded by D. A. Othen of this laboratory on a Beckman IR-12 spectrophotometer, operated at a resolution of about  $1 \text{ cm}^{-1}$ . The gases were contained in a 9.5 cm. long Pyrex microcell which was fitted with cesium iodide windows and a standard taper, greaseless Teflon stop-cock. The pressure of gas within the cell was not known accurately but was probably between 10 and 60 Torr in all cases.



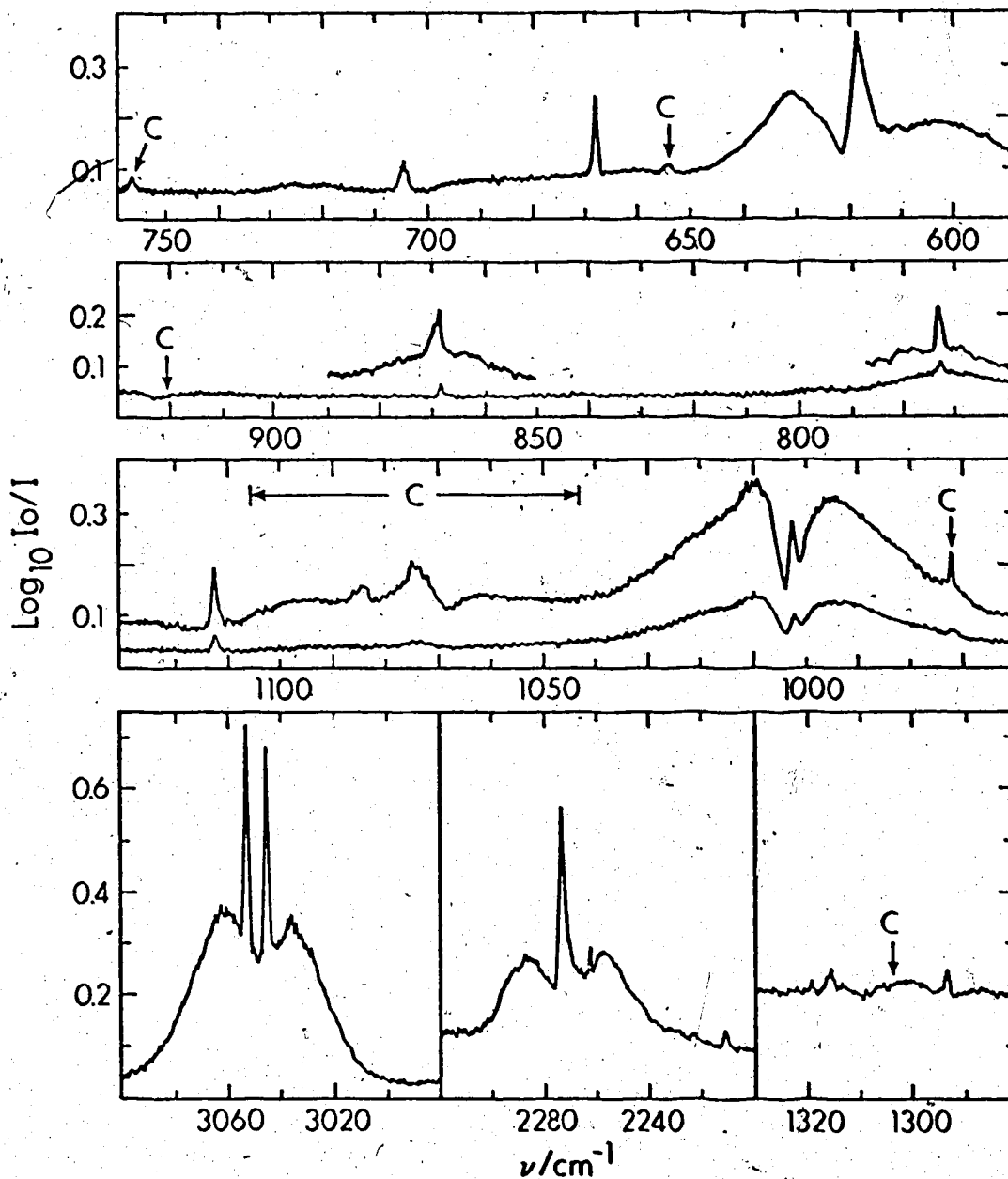
Infrared spectrum of gaseous  $C_2D_4S$  at  $+25^\circ$ . The curves labelled A show the spectrum of one sample; those labelled B show the spectrum of a second sample. The frequency scale is the same for all spectra below  $2000\text{ cm}^{-1}$ .

## Appendix IV (continued)



Infrared spectrum of gaseous cis- $\text{C}_2\text{D}_2\text{H}_2\text{S}$  at  $+25^\circ\text{C}$ . All curves show the spectrum of a single sample. The features labelled T arise from trans- $\text{C}_2\text{D}_2\text{H}_2\text{S}$  which was present as an impurity.

## Appendix IV (continued)



Infrared spectrum of gaseous trans- $\text{C}_2\text{D}_2\text{H}_2\text{S}$  at  $+25^\circ\text{C}$ . The bottom curves in the upper three boxes show the spectrum of one sample and the other curves show the spectrum of a second sample. The features labelled C arise from cis- $\text{C}_2\text{D}_2\text{H}_2\text{S}$  which was present as an impurity.